The Role of T-cadherin in Regulating Skeletal Muscle Myogenesis

Submitted by

Lauren Taylor

In fulfilment of the requirement for the degree of

Doctor of Philosophy

College of Public Health, Medical and Veterinary Sciences

James Cook University

February 2024

Acknowledgements

This piece of work would not have been possible without the contributions and support of every single person in my life. Whether it was reading and editing my written work, assisting me with my lab work, listening to me complaining about lab work, distracting me from failed lab work or accompanying me on a much-needed coffee break (from lab work) – everyone played a small part in getting me to the end.

I surely would not have gotten through this project without the support and guidance of my advisory panel. Lionel – thank you for bringing me on to this project, reading and editing page after page and for always making time for a chat. Ira – thank you for introducing me to the world of bioinformatics and for guiding me through failed code and statistics. Craig – thank you for everything you have taught me about muscles, cell culture and research. You always believed in me, and I cannot thank-you enough for your mentorship and support.

My lab work also would not have been so successful without the help and guidance of Miriam. Thank you for sharing your wealth of knowledge, infallible shortcuts, and your passion for a clean laboratory. I would also like to acknowledge the hardworking staff in CPHMVS and the JCU animal research facility.

I am so thankful to my entire network of friends for their continuous support and encouragement. I wish I could express how much I appreciated those coffee dates, lab chats and after work drinks. Your friendship made it possible to get through the tough times. A big thank you to Rhys who was always willing to listen to my problems, help me mourn failed assays, and keep me company in the lab.

I especially could not have made it this far without the love and support of my parents and sisters who have been there since the beginning. I cannot tell you how thankful I am to you for constantly inspiring me to achieve great things, listening to me talk about my research and making my day a little bit brighter when things didn’t go to plan.

Finally, to my partner Tim – thank you for giving me the freedom, support, and love that I needed to push through to the end. Thank you for always believing in me and pushing me whenever I started to doubt myself. Words cannot express how grateful I am for all that you do and have done.

Statement of the Contribution of Others

This thesis project was supported by the James Cook University's 'Research Training Program Scholarship and Stipend'.

I would like to thank and acknowledge the following people for their contribution to data collection, analysis, and editorial support.

Nature of Assistance	Contribution	Names, Titles, and Affiliations
Intellectual support	Proposal writing Editorial assistance Data analysis Statistical support	A/Prof. Lionel Hebbard (JCU) Dr. Craig McFarlane (JCU) Dr. Ira Cooke (JCU)
Financial support	Fee offset/waiver Research costs Stipend	JCU Research Training Program Scholarship and Stipend JCU 'My Research Rules' Competition winner research grant JCU Sandpit to Seed (S2S) Funding; New ways to grow Muscle
Laboratory assistance	Data collection Data processing Support with analyses	A/Prof. Lionel Hebbard (JCU) Dr. Craig McFarlane (JCU) Dr. Miriam Wankell (JCU) AGRF Sequencing Facility (Melbourne)
Animal welfare	Animal breeding Husbandry	Ms Serrin Rowarth (JCU) Ms Kylie Robertson (JCU)

Any specific assistance with data collection or analysis have been included in the footnotes.

Abstract

Skeletal muscles are the largest tissue type in the human body. They make up approximately 40% of total body weight and are responsible for maintaining posture, stability, and strength for everyday movements. Muscles are formed in the early stages of embryonic development during which the precursor cells fuse together to form large, multinucleated muscle fibres. This process, known as myogenesis, is tightly controlled by myogenic regulatory factors (MRFs), which regulate both the proliferation and fusion of these cells. Due to the crucial role that muscles play in our bodies, any dysregulation of their developmental or regenerative processes can be detrimental to our health. Muscle atrophy, or a loss of muscle mass, can often be reversed in healthy individuals through an active lifestyle, but can be a serious problem for the elderly or individuals with chronic illness. Thus, research to prolong muscle life and regenerative ability is critical. Fortunately, muscles can maintain their mass, and even build upon it due to complex mechanisms of regeneration and a population of self-renewing stem cells known as satellite cells. Of interest to this study is the role that cell adhesion molecules (CAMs), known as cadherins, play in regulating and facilitating differentiation. Truncated cadherin (T-cadherin) is found abundantly on the skeletal muscle, but it's role in development and regeneration is still poorly understood. This thesis aimed to uncover the mechanisms by which T-cadherin negatively regulates skeletal muscle myogenesis.

Our results show that that T-cadherin and adiponectin double knockout (DKO) muscle, but not T-cadherin knockout (T-cad KO) muscle, have enhanced regenerative ability *in vivo*. RNA sequencing studies show many differentially expressed genes between wild-type (WT) and DKO differentiating myoblasts, but there are very limited differences for T-cad KO versus WT. Many of the up-regulated pathways in the DKO cells were related to muscle differentiation and cell adhesion. This was further exemplified through injury regeneration studies where our findings show that DKO muscles have increased numbers of activated satellite cells and macrophages at day three of regeneration and more centrally located nuclei in newly formed muscle fibres at day 7 of regeneration. Moreover, and in addition, we find that DKO muscle cells have increased mitochondrial content and function.

Furthermore, to assign modus of operation, we find that T-cadherin and M-cadherin interact in differentiating C2C12 murine muscle cells. Given that M-cadherin forms part of the myogenic cell adhesion complex and is an important regulator of skeletal muscle myogenesis, we suggest that T-cadherin may negatively regulate skeletal muscle fusion by interfering with this complex through M-cadherin binding.

Taken together our data implicate T-cadherin and adiponectin as potential negative regulators of skeletal muscle regeneration. Ongoing research into the role of these molecules will not only improve our understanding of myogenesis but may lead to the identification of targets that can be used to improve muscle regeneration and growth. This will have significant ramifications for strength building and muscle disease and may help in the treatment and recovery of muscle atrophy commonly associated with chronic conditions and ageing. In summary, this thesis provides a detailed insight into the role of T-cadherin and adiponectin in skeletal muscle regeneration.

Table of Contents

List of Tables

List of Figures

List of Abbreviations

Abbreviation	Meaning
ABC	Active β-catenin
ACC	Acetyl Co-A carboxylase
AdipoR1/2	Adiponectin receptor 1/2
ADP	Adenosine diphosphate
AGRF	Australian Genome Research Facility
AMP	Adenosine monophosphate
AMPK	AMP-activated protein kinase
APN[i]	Adiponectin
APPL1	Adaptor protein, phosphotyrosine interacting with PH domain and leucine zipper 1
APS	Ammonium persulfate
ATP	Adenosine triphosphate
bHLH	Basic helix-loop-helix
BMP4	Bone morphogenic protein 4
BOC	Brother of CDO
BSA	Bovine serum albumin
CAM	Cell adhesion molecule
CaMKKβ	Calcium/Calmodulin Dependent Protein Kinase Kinase 2
CDO	Cell adhesion molecule, downregulated by oncogenes
CEE	Chicken embryo extract
ChIP-seq	chromatin immunoprecipitation sequencing
CK1α	Casein kinase 1 alpha
COPD	Chronic obstructive pulmonary disease
db/db	Mouse model for type 2 diabetes
DKO	Double knockout
DM1/2	Myotonic dystrophy 1/2

[i] While adiponectin has been abbreviated to ‘APN’ in this thesis, it is also commonly referred to as ADIPOQ, ACRP30 (adipocyte complement-related protein of 30 kDa) and APN1.

DMD	Duchenne muscular dystrophy
DMEM	Dulbecco’s modified eagle medium
DMSO	Dimethyl sulfoxide
DNA	Deoxyribonucleic acid
DRM	Detergent resistance membrane
DSHB	Developmental studies hybridoma bank
DTSSP	3,3'-Dithiobis(sulfosuccinimidylpropionate)
DTT	Dithiothreitol
EC	Extracellular cadherin
ECL	Enhanced chemiluminescence
ECM	Extracellular matrix
EDTA	Ethylenediaminetetraacetic acid
ETC	Electron transport chain
FA	Fatty acid
FACS	Fluorescence-activated cell sorting
fAPN	Full-length APN
FBS	Foetal bovine serum
FCCP	Carbonyl cyanide-p-trifluoromethoxyphenylhydrazone
FG	Fast glycolytic
FO	Fast oxidative
GAPDH	Glyceraldehyde-3-phosphate dehydrogenase
gAPN	Globular APN
GO	Gene ontology
GORILLA	Gene Ontology enRIchment anaLysis and visuaLizAtion tool
GSK-3β	Glycogen synthase kinase-3 beta
GWAS	Genome wide association study
H&E	Hematoxylin and eosin
HEPES	(N-2-hydroxyethylpiperazine-N'-2-ethanesulfonic acid
HMW	High molecular weight
hr	Hour
HRP	Horseradish peroxidase
HS	Horse serum

IgG	Immunoglobulin G
KO	Knockout
LDL	Low-density lipoprotein
LKB1	Liver kinase B1
LMW	Low molecular weight
M-cad	M-cadherin
mdx	Mouse model for DMD
MFI	Median fluorescence intensity
MHC	Myosin heavy chain
MMW	Medium molecular weight
MPC	Myogenic progenitor cell
MRF	Myogenic regulatory factor
Mrf4	Muscle specific regulatory factor 4
mtDNA	Mitochondrial DNA
Myf5	Myogenic regulatory factor 5
MYOD	Myoblast determination protein 1
MyoG	Myogenin
NADH	Nicotinamide adenine dinucleotide
OCR	Oxygen consumption rate
OCT	Optimum cutting temperature
OXPHOS	Oxidative phosphorylation
p38-MAPK	P38 mitogen-activated protein kinase
PAX7	Paired box 7
PBS	Phosphate-buffered saline
PGC-1α	Peroxisome proliferator-activated receptor gamma coactivator 1-alph
Pi	Inorganic phosphate
PMSF	Phenylmethylsulfonyl fluoride
PPAR	Peroxisome proliferator-activated receptors
p-β-catenin	Phosphorylation β-catenin
RIPA	Radioimmunoprecipitation assay
RNA	Ribonucleic acid

SC	Satellite cell
SDS	Sodium dodecyl-sulphate
SDS-PAGE	Sodium dodecyl-sulphate polyacrylamide gel electrophoresis
SNP	Single nucleotide polymorphism
TA	Tibialis anterior
TBST	TBS with Tween 20 detergent
T-cad	T-cadherin
TCF/LEF	T-cell factor/lymphoid enhancer factor
TEMED	Tetramethylethylenediamine
VCAM-1	Vascular cell adhesion molecule
VLA-4	Integrin α4β1 (very late antigen 4)
WT	Wild type

1 Introduction

1.1 Introduction to the Thesis Outline

Each chapter in this thesis has been written as a traditional research chapter. Any works originating from papers or manuscripts have been reformatted for detail and clarity (original copies can be found in the appendix).

Chapter 1 introduces the relevant literature and includes, in part, a review article published in Biochemica et Biophyscia Acta (BBA) in 2021. The literature review has been modified to include further information not featured in the paper. A full copy of the published review can be found in appendix 1 (see section 9.1). This chapter also includes currently unpublished, preliminary data essential for understanding the rationale behind this work. This is summarised at the beginning of subsequent chapters for clarity. This chapter concludes with a summary of the rationale, an overarching hypothesis as well as specific aims.

Chapter 2 describes the materials and methods used throughout this work. Detailed company/lot information is included where possible. Relevant methods are also summarized at the beginning of each chapter.

Chapter 3 details the results obtained from the *in-silico* analysis of the genetic mechanism of T-cadherin and is written as a traditional research chapter. Chapter 4 is written as a traditional research chapter outlining the results of T-cadherin's role in muscle growth and regeneration. Chapter 5 is written as a traditional research chapter and details the results of the metabolic comparison between wild-type (WT) and T-cadherin/adiponectin (APN) double knockout (DKO) muscle cells. The final data chapter, chapter 6, is written as a traditional research chapter which describes T-cadherin's interactions in the cell adhesion complex.

Chapter 7 includes the final discussion and any concluding remarks, followed by the references and appendices.

1.2 Introduction to Skeletal Muscles

Muscles are the largest tissue in the human body and account for 40% of the total body weight. They are a complex ensemble of heterogeneous tissue responsible for maintaining posture, strength and controlling movements. The viability of muscles is dependent on a well-maintained arrangement of muscles fibres, blood vessels and connective tissues.

1.2.1 Skeletal muscle structure

The term skeletal muscle is generally used to refer to the overall collection of parallel muscle cells surrounded by connective tissue and connected to the bone. This connective tissue, termed epimysium, encloses cylindrical bundles of muscle fibres (myofibers) also known as fascicles (**Figure 1.1**). The fascicles themselves are surrounded by a layer of connective tissue known as the perimysium and contain many parallel myofibers interspersed with blood vessels that are essential for oxygen supply [4]. The parallel muscle fibres are the primary component of skeletal muscle. These multinucleated myofibers are surrounded by a plasma membrane (sarcolemma) and can contain several hundred nuclei within a single fibre [5]. The myofibers contain hundreds of striated muscle organelles known as myofibrils. These myofibrils are comprised of sarcomeres – the smallest functional contractile unit of muscle. The sarcomeres are organized into thin actin filaments which come together to form the Z-line, and thick myosin filaments which connect at the M-line (**Figure 1.1**) [4]. A thick myosin filament consists of a pair of myosin heavy chains, essential light chains, regulatory light chains, myosin heads, and myosin tails [4].

1.2.2 Skeletal muscle contraction

The myosin head is an important binding site that facilitates the interaction of myosin with actin. The actin, which acts as a binding site for myosin, is blocked by troponin and tropomyosin during the relaxed state (**Figure 1.1**). The interaction of these proteins is responsible for the contraction of muscles, a process known as ‘cross-bridge cycling’. Initiated by signals to ‘move’ an influx of calcium binds to troponin and displaces the tropomyosin from the myosin binding site, allowing the ADP/Pi-bound

myosin to form a ‘cross-bridge’ with the actin filament [6, 7]. Next, the inorganic phosphate is released, causing the ‘power stroke’ - a movement by which the myosin pulls the actin filament towards the M-line. Following the power stroke, the ADP is released and the myosin remains connected to the actin until bound by ATP [6]. The cycle continues until the calcium disappears and the muscles re-enter their resting state.

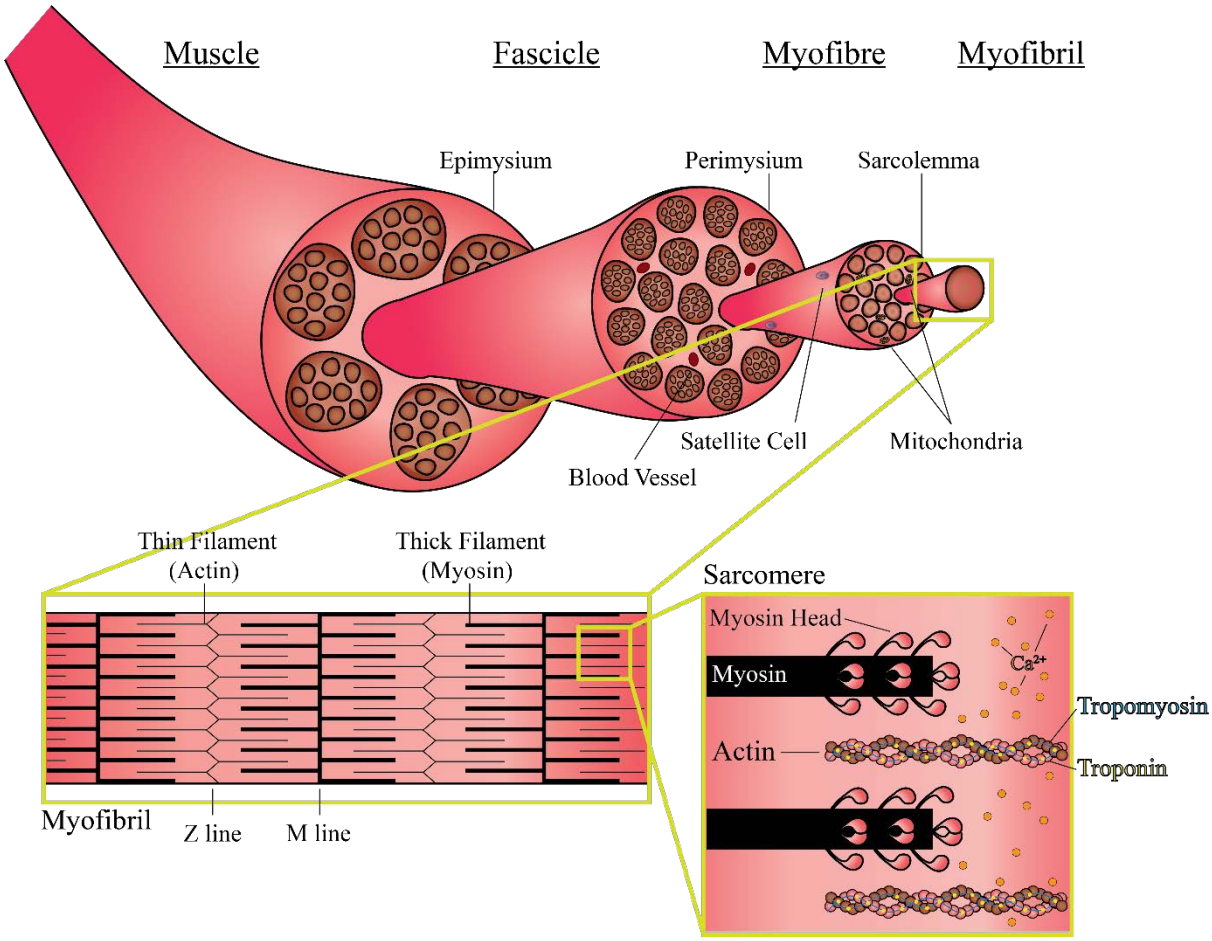

Figure 1.1. Structure of skeletal muscle. The skeletal muscles are made up of fascicles that house hundreds of myofibers, surrounding by the epimysium. The myofibers consist of bundles of myofibrils surrounded by the basal lamina. Within the myofibrils are the myofilaments actin, and myosin, which are responsible for contraction of the fibres. The binding sites on the actin filament are covered by tropomyosin until calcium binds the troponin. The subsequent binding of the myosin head to actin is known as ‘cross bridge cycling’ and is responsible for contraction.

1.2.3 Muscle fibre types

The speed with which contraction occurs is often attributed to the difference in muscle fibre type. The four fibre types, classified by their myosin heavy chain (MHC) isoforms, can be subdivided into two categories: fast twitch (type IIA, IIX and IIB (not present in humans)) and slow twitch (type I) [8-10]. The ratio of fibre types can vary greatly between individuals and are mainly controlled by genetics, but it is also possible to remodel muscle phenotypes through exercise and training to adapt to different uses. The physiological and metabolic diversity provided allows for a range of functions but can also alter someone's susceptibility to certain muscle diseases (see section 1.8).

1.2.3.1 Type I – Slow oxidative (SO)

Slow twitch fibres are useful for endurance activities (long-distance running and maintaining posture) with small movements that occur often but don't require a lot of energy. The ATP generated by these fibres comes primarily from aerobic respiration which is slower but more efficient that anaerobic methods. Due to the oxygen requirements of these fibres they generally have a rich capillary supply, numerous mitochondria and a high concentration of myoglobin (a protein that helps move oxygen around the muscle) [11].

1.2.3.2 Type II – Fast oxidative (FO)/fast glycolytic (FG)

Fast-twitch fibres are used for rapid movements (jumping or sprinting) that require fast muscle contractions of short duration. These fibres generally rely on anaerobic respiration, which can produce ATP relatively quickly, but only in short bursts. The fast twitch muscles can be further separated into fast oxidative (type IIA) and fast glycolytic (type IIX) fibres. Type IIA muscle fibres are often referred to as intermediate fibres. They produce ATP relatively quickly through aerobic respiration and do not fatigue as quickly as the glycolytic fibres. These fibres are useful for walking but not explosive movements. Type IIX fibres primarily utilize anaerobic glycolysis as their ATP source. These fibres have a large diameter and possess a high amount of glycogen that they use to generate ATP [11]. Type IIX fibres can generate energy very quickly and are therefore useful for rapid, forceful contractions to make quick, powerful movements such as sprinting or jumping. Unfortunately, due to this method of ATP production, these muscles fatigue quickly, thus can only be used for short periods.

1.3 Skeletal Muscle Development

The formation of skeletal muscle begins during embryonic development when the myogenic precursor cells migrate out from the somites. During gestation, the future positions and identities of cells are determined by their designations into one of the three germ layers, the ectoderm, mesoderm, and endoderm [12]. The muscle cells originate from the somites, which segment out from the paraxial mesoderm on either side of the neural tube and notochord [13, 14]. The dorsal section of these somites, known as the dermomyotome, ultimately supplies the body with the cells of the skeletal muscles [13, 14]. Specification of these cells occurs following the expression of external signalling molecules, such as wingless (Wnt) and sonic hedgehog (Shh), secreted from the notochord and neural tube [15, 16]. Canonical Wnt signalling is essential for myogenesis and is important for the activation of many downstream molecules, including the myogenic regulatory factors and β-catenin [15, 17, 18]. Both *WNT1* and *WNT3a* are first expressed in the dorsal neural tube and affect gene expression through the activation of β-catenin [15, 19]. β-catenin plays a dual role in myogenesis, participating in both gene expression and cell-adhesion (see section 1.6 and 1.7.2). Manipulation of β-catenin levels in cultured mouse cell lines can both inhibit and promote myogenic differentiation. Studies have been conducted to investigate the importance of β-catenin in cultured mouse cells and Cui, et. al. has recently shown that β-catenin/Wnt signalling is vital for the timely activation of the myogenic gene program [20]. Prior to this, the somites are not yet committed to a specific lineage and will adopt alternative fates in the absence of Wnt signalling [21]. The cells from the somites will split into two lineages: the sclerotome, that forms the tendons, ribs and vertebrae, and the dermomyotome, that forms the dermis and skeletal muscles [14].

1.3.1 Paired box transcription factors

The paired box, or Pax, genes also play an essential role in the formation of muscle fibres. Cells within the dermomyotome express *PAX3* and *PAX7* as they continually proliferate to increase the cell population before specification [22, 23]. PAX3 (which is expressed prior to the myogenic regulatory factors (MRFs)) recruits and guides undifferentiated cells toward a myogenic lineage before assisting in the activation of MRFs [24]. A small population of these cells will then migrate out to form

the limbs before switching from *PAX3* expression to MRF expression [25]. The Pax protein levels generally decline following the expression of the MRFs, except in the case of the muscle cells capable of regeneration [22, 25]. *PAX7* expression is vital for the formation and renewal of muscle-specific stem cells and is upregulated in a subset of precursor cells within the central dermomyotome that will become the muscle stem cells (satellite cells) (see section 1.4). Following segmentation into somites, the cells then begin expressing the myogenic regulatory factors.

1.3.2 Myogenic regulatory factors

Myogenic regulatory factors (MRFs) are transcription factors that regulate the process of myogenesis. The MRFs, despite displaying a slight variation in length, are proteins that contain three structural domains: a basic helix-loop-helix (bHLH) domain, cysteine/histidine domain (N-terminal), and a serine/threonine-rich domain (C-terminal) [26]. It is the bHLH domain that is the main contributor to myogenesis. Using this domain, the MRFs can bind specific sequences known as E-Box (enhancer box) domains found in the regulatory sequences of target genes to alter their expression [27]. The first MRF to be expressed is myogenic regulatory factor-5 (*MYF5*) and

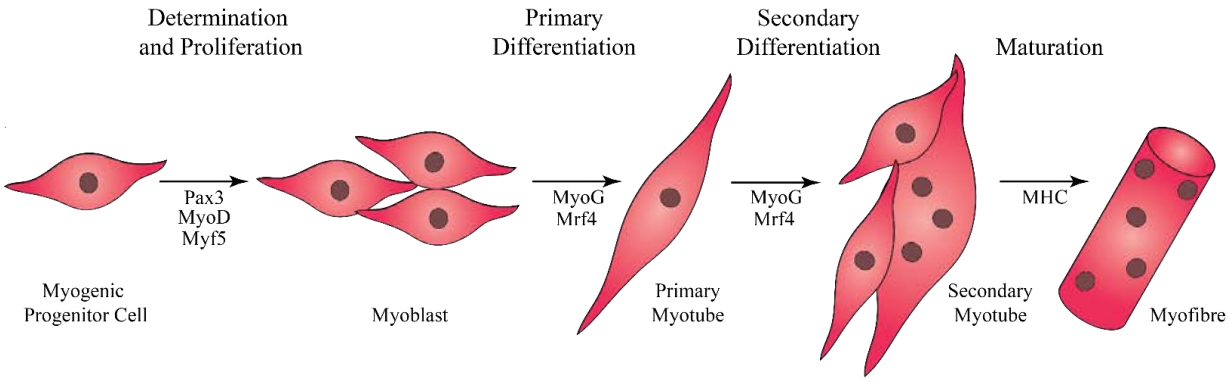

Figure 1.2. Skeletal muscle myogenesis. Following migration out from the dermomyotome the progenitor cells will begin to express MRFs (myoblast determination protein 1 (MyoD) and myogenic regulatory factor-5 (Myf5)), initiating differentiation into myoblasts. These myoblasts will enter the cell cycle to increase the population of available muscle cells before switching expression to differentiation proteins: myogenin (MyoG) and muscle specific regulatory factor-4 (Mrf4). These MRFs promote the fusion of myoblasts into myotubes and their maturation into multinucleated muscle fibres.

signifies the switch from myogenic progenitor cells (MPC) to muscle cells (myoblasts) [28, 29]. *MYF5* expression can be initiated by WNT1, WNT3 and SHH or directly through PAX3 [30-32]. This in turn can activate myoblast determination protein 1 (*MYOD*) [32]. First discovered in 1987, MYOD is able to convert cultured fibroblasts into skeletal myocytes and plays an important role in myogenesis [29]. Along with MYF5, WNT7 is also able to induce the expression of *MYOD* but can be blocked by bone morphogenic protein 4 (BMP4) to inhibit premature expression [33]. Furthermore, the loss of MYOD or MYF5 individually are compensated by the overexpression of the other, and double mutant mice fail to form muscle cells [34-36].

Following specification to myoblasts, the cells exit the cell cycle to begin fusing (differentiating) into muscle fibres (**Figure 1.2**). The first wave of myofibers are formed when myoblasts begin to elongate and form mononucleated primary myofibers. These primary fibres provide a scaffold for the next wave of muscle fibres to attach, forming larger multinucleated myofibers. This process begins with the expression of additional MRFs: *MYOG* (myogenin) and *MYF4* (muscle specific regulatory factor-4) [14, 37]. Myogenin has been shown to be essential for myotube formation as muscle cells lacking myogenin fail to form myotubes, even in the presence of normally committed myoblasts [38]. On the other hand, the presence of myogenin alone can compensate for a lack of MYF4 [39]. Initially thought to be expressed in waves, the expression of MRFs overlaps throughout myogenesis. In fact, MRF4 can rescue myogenesis in the early stages of commitment even in the absence of MYF5 and MYOD [40].

1.3.3 Mechanism of fusion

Although the expression of MRFs has been relatively well established, there is still a large gap in our knowledge regarding the specific mechanism of myoblast fusion. Fusion is a complex process that involves many proteins for cell recognition, adhesion, and fusion pore formation. Many of these proteins have been well characterised for drosophila and zebrafish but are largely unknown in mice and humans. In contrast, the role of the actin cytoskeleton in cell fusion appears to be well conversed between species and is therefore better understood (reviewed Kim, et al., 2015) [41].

It is only in the past decade that we have begun to identify the major players in the fusion process including two fusion factors: myomaker (or TMEM8C) and myomerger

(or ESPG). Myomaker, the first to be discovered, was initially identified through an *in silico* analysis and confirmed by its ability to induce fusion between fibroblasts and muscle cells [42]. Interestingly, myomaker was not able to induce fusion between fibroblasts themselves, indicating the requirement for another myogenic fusion protein. Myomerger, also known as myomixer and minion, can induce fusion between fibroblasts when co-expressed with myomaker [43-45]. Both factors are expressed in the myotome beginning at mouse embryonic day 10 (E10) but are not detectable following postnatal day 21 (P21) or in healthy adult myofibers [46]. Interestingly, E-Box elements have been found upstream of both genes, indicating a role for MRFs in their activation [47]. Mouse loss of function studies for both proteins, separately, resulted in death at birth due to a complete lack of skeletal muscle formation [46]. Although there is still evidence of differentiated cells (i.e., myosin positive cells) they are not able to fuse and form multinucleated myofibers. In the future, gain of function studies may shed more light on the function of these proteins *in vivo*.

1.4 Skeletal Muscle Regeneration

Not only do our muscles undergo constant damage due to everyday wear and tear, but they can also be damaged following severe injuries, strength building and disease [48]. Muscle regeneration is highly dependent on a synchronised process of pro- and anti-inflammatory factors that determine how the damage will be repaired. This regenerative cycle can be split into two specific processes: degeneration and regeneration. Degeneration describes the rapid inflammation of tissue and the removal of damaged cells to make room for new fibres [49, 50]. Breakdown of these fibres can be characterized by an increase in muscle specific proteins, such as creatine kinase, and an influx of calcium ions important for activating calcium-dependent proteolysis and assisting in tissue degeneration [51]. The muscle necrosis also activates an inflammatory response leading to an influx of neutrophils and macrophages [52]. Neutrophils, which first appear within 2 hours of injury, begin to clear away the damaged tissue and release inflammatory cytokines to promote inflammation [53]. These are then followed by monocyte-derived macrophages, which peak at day three of regeneration and are classified into two subsets: M1 and M2 [54]. The M1 macrophages are typically pro-inflammatory, while the M2 macrophages are anti-

inflammatory and pro-regenerative [53] The induction of the pro-inflammatory macrophages promotes myoblast proliferation and inhibits differentiation while the anti-inflammatory macrophages encourage regeneration by inhibiting proliferation and promoting differentiation [54, 55]. Although originally thought to infiltrate the muscle tissue sequentially, recent studies have shown that there is no clear-cut M1 to M2 phenotype switch during the early stages of repair [56]. M1 and M2 stimuli often co-exist in the muscle microenvironment and macrophages can display mixed phenotypes throughout regeneration. Following the removal of the debris, the regenerative cells then begin the repair process.

1.4.1 Satellite cells

Skeletal muscles maintain a resident community of stem cells, known as satellite cells (SCs), that have the ability to fuse into new skeletal muscles to repair injuries [57]. These self-repairing cells were first discovered through electron microscopy by Mauro (1961) who identified the cell ‘wedged’ between the plasma membrane and the basement membrane of a muscle fibre from a frog [58]. These cells are located within a niche against the sarcolemma and beneath the basal lamina [59]. The microenvironment of this niche undergoes dramatic changes during muscle regeneration and provides all the necessary signals required for SC activation and proliferation. While these cells account for nearly 30% of all nuclei during early life, their abundance decreases to approximately 5% in adults [60]. Most of these cells are present to support postnatal development and only a small proportion of them will persist in adult muscle. Since their discovery, the role of SCs has been studied and extensively reviewed elsewhere [57, 61].

The SCs themselves appear to present as a heterogeneous population varying in MRF expression levels, their ability to differentiate and self-renew, and their mitotic rate. The number of SCs also differs with location and fibre type; there are more SCs present on type I fibres than on type II fibres [62, 63]. These SCs originate in the somites, like the precursor myoblasts, but express a high ratio of PAX7 to MYOD, forcing them to adopt a quiescent state beneath the basal lamina [64]. These quiescent cells will continue expressing PAX7, and in some cases PAX3, and low levels of MRF5, until activation (**Figure 1.3**) [65].

Following injury, the muscle microenvironment releases signals to allow the translation of *MYF5* and *MYOD*. SCs are highly polarised and express different adhesion molecules on their basal and apical surfaces [59]. SCs express high levels of integrin α7 and β1 on their basal surface and M-cadherin (muscle cadherin) and NCAM (neural cell adhesion molecule) on the apical surface (see section 1.6 for review on adhesion molecules) [66].

The SCs then begin proliferating and enter the cycle of myogenesis. The majority of the SCs (80-90%) quickly enter into the cell cycle to increase availability of MPCs, while a small portion of the SCs are much slower to enter into the cell cycle - perhaps only to replenish this population of cells rather than for fusion [67]. Although SCs uniformly express *PAX7*, activated SCs can generate both $MYF5^{+}$ and $MYF5^{-}$ cells through asymmetric apical-basal division [68]. The $MYF5^{+}$ cells that lose contact with

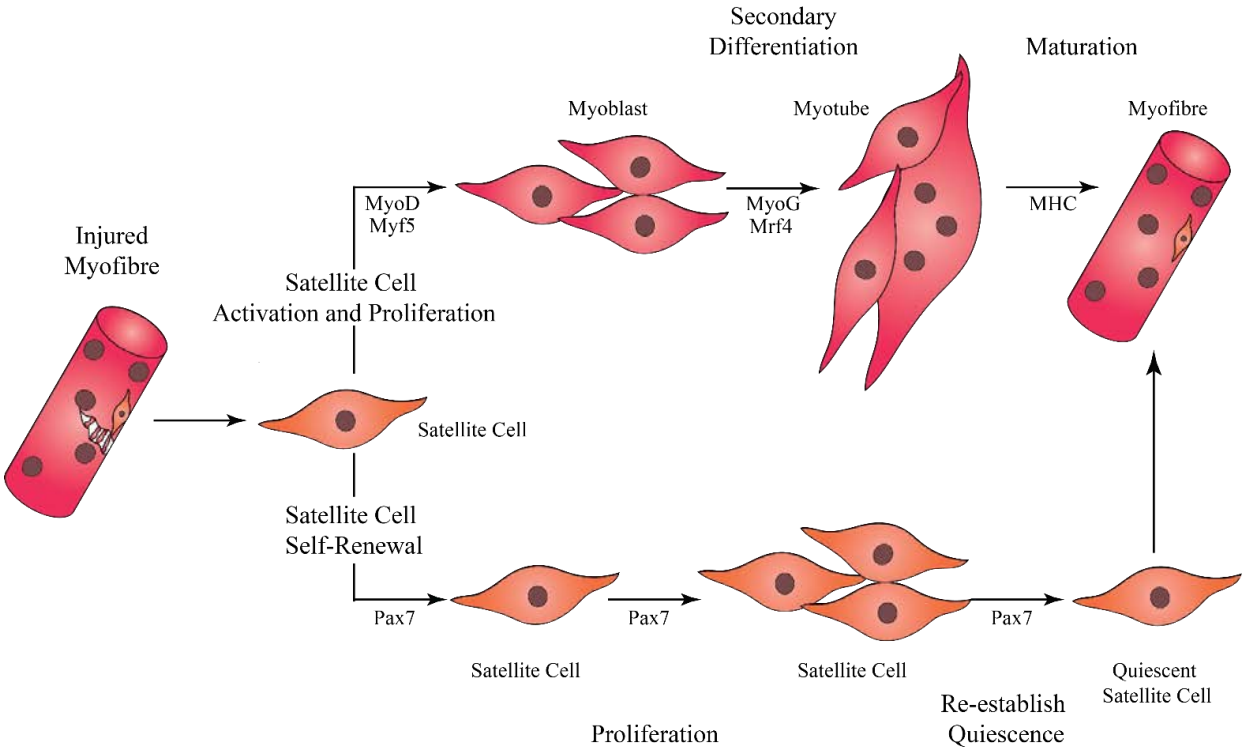

Figure 1.3. Skeletal muscle fibre regeneration following SC activation. Once injury occurs most SCs upregulate expression of MYOD and MYF5 and decrease their expression of PAX7. These cells, now myoblasts, will enter the cell cycle to increase the population of cells before continuing through the conventional path of myogenesis to fuse into regenerated muscle fibres. A small population of these SCs will maintain their expression of PAX7, increase their population size and provide the next generation of quiescent SCs.

the basal surface preferentially differentiate, while the MYF5$^-$ cells remain connected with the basal surface and contribute to SC renewal. Following proliferation, most of these cells will downregulate *PAX7* expression and begin to fuse into new myofibers, while a small population of these cells will suppress *MYOD* and maintain *PAX7* expression to return to quiescence [69]. While SCs have been shown to express *MYOD* at as early as 12 hours post-injury, most cells will express either *MYF5* or *MYOD* by 24 hours and both MRFs by 48 hours [70, 71]. During regeneration, MYOD knockout mice produce an increased population of myoblasts around the site of injury but these fail to differentiate and fuse [72]. In contrast the MYF5 knockout mice appear to struggle with proliferation but possess a hypertrophic phenotype [73]. From this, it is likely that MYF5 is important for proliferation and MYOD for initiating differentiation.

Terminal differentiation then begins with the expression of other MRFs, *MYOG* and *MRF4*. The induction of these MRFs is primarily dependent on MYOD [74]. Following the expression of *MYOG* and *MRF4*, the myoblasts enter the myogenic differentiation program and begin to fuse to one another or to damaged myofibers This balance between quiescence, activation and differentiation is crucial to maintaining a healthy pool of SCs and regenerative capacity. Due to the changing energy requirements of muscle, it is important that the SCs can adapt their metabolic profiles during regeneration.

1.5 Skeletal Muscle Metabolism

For everyday movement and explosive exercise, energy availability is vital for muscle functions, including crossbridge cycling (see section 1.2.2). Muscles are a major metabolic organ and will utilize available glucose, through insulin-mediated glucose uptake, for ATP production and store the remaining glucose as glycogen. As muscles constantly require a source of energy, they have a store of readily available ATP that can be utilized immediately. For short bursts of high intensity exercise, like those utilising type IIB fibres, the muscle cells will mainly derive their energy through anaerobic respiratory pathways relying on the conversion of phosphocreatine to creatine and glycogen to lactate [75].

During prolonged exercise the slow type I fibres utilize oxidative phosphorylation pathways to produce energy from intramuscular glycogen stores, blood glucose and

free fatty acids from adipose tissue [75]. The five complexes in the electron transport chain (ETC) essential for oxidative phosphorylation are found within the inner mitochondrial membrane: complex I (NADH: ubiquinone oxidoreductase), complex II (succinate dehydrogenase), complex III (cytochrome bc1 complex), complex IV (cytochrome C oxidase) and complex V (ATP synthase). The ETC receives electrons from electron carriers and passes them down the chain to combine with oxygen to form water, which results in a proton gradient that powers ATP synthase. The electrons that pass through the ETC can originate from the breakdown of glucose through glycolysis, or free fatty acids via β-oxidation [76].

Quiescent SCs primarily rely on fatty acid and pyruvate oxidation for energy needs but will switch to aerobic glycolysis following activation [77, 78]. During differentiation there is an increase in mitochondrial biogenesis to accommodate the increased demand for oxidative phosphorylation [77, 79, 80]. One of the methods by which mitochondrial biogenesis is promoted is through the interaction of the adipokine (a cytokine secreted by adipose tissue), adiponectin (APN), with skeletal muscle [77, 79, 80].

1.5.1 Adiponectin

Adiponectin is released from the adipocytes following energy deficient conditions and has been well studied for its role as an anti-inflammatory and insulin-sensitizing adipokine. APN is encoded by *ADIPOQ* located at chromosome 3q27 and is comprised of three exons and two introns. The full-length structure of APN is a monomeric subunit (fAPN) that associates with other monomers to form low molecular weight (LMW), medium molecular weight (MMW), and high molecular weight (HMW) oligomers (**Figure 1.4**) [81, 82]. The fAPN monomer is usually not detected in the circulation and the HMW forms appear to be the most biologically active [83]. Alternatively, the fAPN can undergo proteolytic cleavage and form trimers only with its globular head (gAPN) [84].

1.5.1.1 Adiponectin receptors

There are three known receptors for APN: adiponectin receptor 1 (AdipoR1), adiponectin receptor 2 (AdipoR2), and T-cadherin (T-cad) [85-87]. Each receptor can bind different isoforms of APN with different affinities. AdipoR1 and AdipoR2 are integral membrane proteins with seven transmembrane domains, expressed within the

liver (AdipoR1, and R2) and on skeletal muscle (AdipoR1) [87]. AdipoR1 was the first described receptor and binds predominantly to gAPN on skeletal muscle [86, 88]. AdipoR2 is commonly expressed in the liver and binds fAPN [89].

These receptors are important in regulating normal glucose metabolism and insulin sensitivity. This has been confirmed in mouse studies where AdipoR1 and -R2 double knockout mice show glucose intolerance and high levels of circulating insulin [89]. Furthermore, there is reduced expression of both AdipoR1 and -R2 in the livers of obese mice [90]. T-cadherin's functions will be considered in later sections of this chapter.

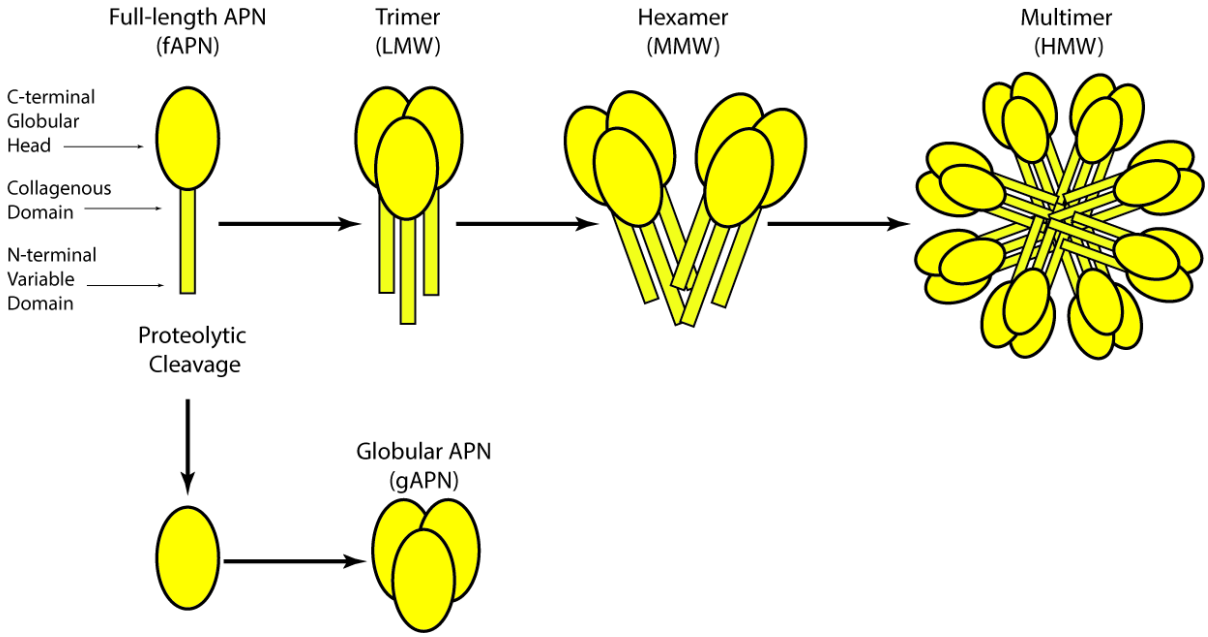

Figure 1.4. Structures of adiponectin (APN). Full-length adiponectin (fAPN) consists of a variable N-terminal domain, a collagenous domain, and a C-terminal globular domain. fAPN exists as a low molecular weight trimer (LMW) and can form both medium molecular weight hexamers (MMW) and high molecular weight multimers (HMW) in plasma. Alternatively, fAPN can undergo proteolytic cleavage and form trimers with only its globular head (gAPN).

1.5.1.2 Adiponectin and metabolic syndromes

Adiponectin has a well-established role in balancing glucose and lipid metabolism and has been shown to have insulin-sensitizing properties [91]. In contrast to other adipokines, decreased APN levels are associated with metabolic syndromes including obesity and type 2 diabetes that are usually accompanied by elevated triglyceride

content [92]. Various studies have found the presence of genetic mutations in or surrounding the *ADIPOQ* gene that are associated with obesity, type 2 diabetes and aberrant APN levels [93-95]. Furthermore, APN knockout mice have reduced mitochondrial content, and decreased electron transport chain and kreb's cycle activity [96].

Interestingly, the administration of APN leads to an improvement in insulin sensitivity in insulin resistant subjects [97]. APN can improve metabolic health through the activation of many pathways including 5' adenosine monophosphate-activated protein kinase (AMPK).

1.5.1.3 Metabolic pathways effected by adiponectin

AMPK is considered an 'energy sensor' and is activated in times of energy depletion. As the name suggests it is activated by a high AMP:ATP ratio, as well as exercise and other causes of energy depletion. Within the skeletal muscle, this pathway works to increase glucose uptake, fatty acid oxidation and mitochondrial biogenesis [98]. APN mediated activation of AMPK is achieved through the binding of an adapter protein, containing pleckstrin homology domain phosphotyrosine binding domain and leucine zipper motif (APPL1) to AdipoR1/R2 (**Figure 1.5**). Like APN, APPL1 expression is reduced in obese models and complete oblation can lead to insulin resistance [88, 99]. Both APPL1 and AdipoR1 are highly expressed within the skeletal muscle allowing the rapid activation of energy generation in times of need [100].

APPL1 induces the translocation of a protein kinase, LKB1 (serine-threonine liver kinase B1) into the cytosol that increases AMPK activation [101]. Furthermore, APN can also activate AMPK through increasing the influx of calcium into skeletal muscle. This not only affects contractile force but also activates calcium/calmodulin-dependent protein kinase kinase beta (CaMKKβ), which can increase AMPK activation [101].

CaMKKβ also contributes to the increased expression of peroxisome proliferator-activated receptor gamma coactivator 1-alpha (PGC-1α). PGC-1α is important for activating many transcription factors, including nuclear respiratory factors (NRF-1 and -2) and peroxisome proliferator-activated receptors (PPARs) that have roles in regulating mitochondrial biogenesis and function [102]. Furthermore, AMPK itself is also responsible for the activation of PGC-1α in the muscle.

Adiponectin signalling also influences the activation of p38 mitogen-activated protein kinase (p38-MAPK) through AMPK [103]. This enhances fatty acid oxidation through the transcriptional activation of PPARα, which increases the expression of genes involved in fatty acid transport and breakdown [103]. AMPK also inhibits acetyl-CoA carboxylase (ACC) that catalyses the committed step in fatty acid synthesis to further enhance fatty acid oxidation. The increase in β-oxidation results in reduced triglyceride content and assists in improving insulin sensitivity. Furthermore, the interaction between AMPK and p38-MAPK results in the translocation of GLUT4 to the plasma membrane to increase glucose uptake [104]. Together the upregulated pathways reduce the AMP:ATP ratio and increase energy utilization of cells (**Figure 1.5**).

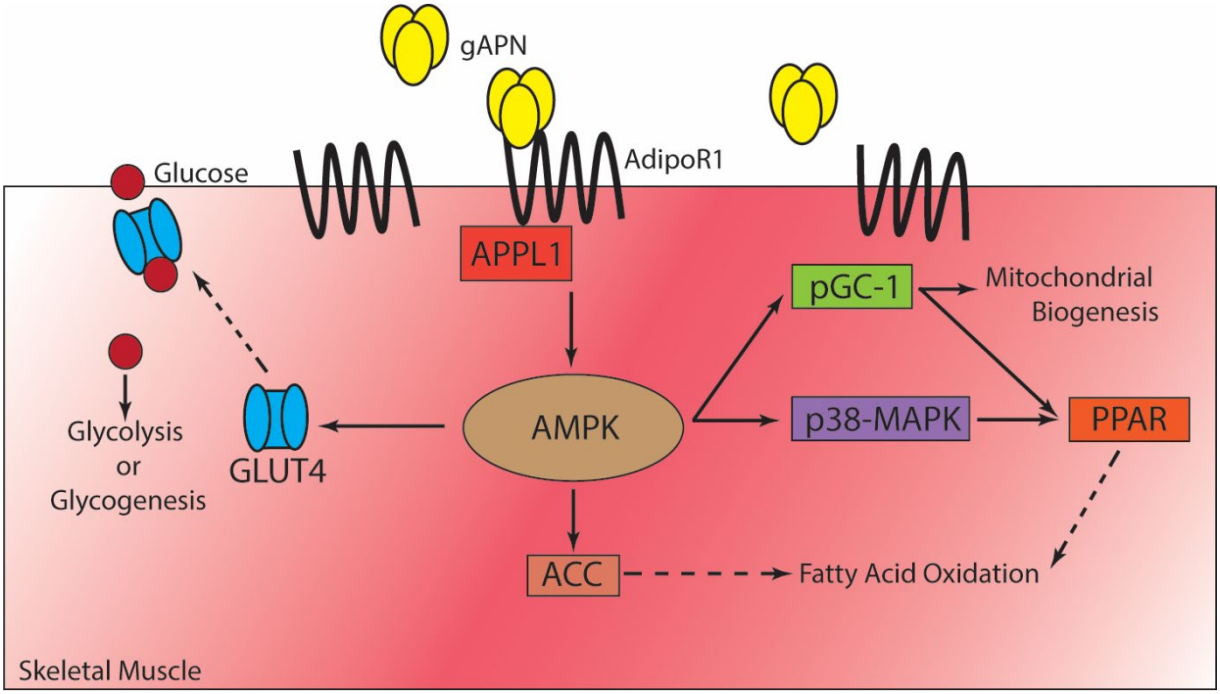

Figure 1.5. gAPN exhibits its metabolic effects on skeletal muscles through binding to AdipoR1. This receptor interacts with the adaptor protein APPL1 that signals to AMPK. AMPK interacts with PPARα through PGC-1 and p38-MAPK. Along with the inhibition of ACC, this leads to increased fatty acid oxidation and improves glucose uptake by increasing the number of GLUT4 transporters on the cell surface.

1.5.1.4 Adiponectin's effects on insulin sensitivity

Adiponectin has been well studied for its insulin sensitizing effects. Although APN levels are reduced in obese and diabetic subjects, administration of APN can lower blood sugar levels and reduce insulin resistance. In the muscles, APN can regulate

insulin sensitivity by increasing fatty acid oxidation, glucose uptake and activating insulin signalling pathways. AMPK assists in the activation of the insulin receptor substrate 1 (IRS-1) to enhance insulin signalling in the muscle [105].

1.5.1.5 Adiponectin in skeletal muscle myogenesis

Initially thought to be expressed exclusively by the adipose tissue, APN can also be expressed by the skeletal muscle [106]. Given that APN is expressed by muscle and can improve metabolism, it may play an important role in muscle function and repair [106-108]. Fiaschi and colleagues (2009 & 2012) demonstrated that gAPN activates SCs, promotes motility and induces the expression of *Mrf4* and *Myog* that in turn promote a switch from proliferation to differentiation [109, 110]. It is possible that APN promotes exit from the cell cycle through the activation of p38-MAPK [111].

The third receptor for APN, the cell adhesion molecule T-cadherin (truncated cadherin), is, in the field of muscle biology, poorly studied. The role of cell adhesion in muscle function was the focus of the literature review published in 2021 and can be found in the following pages (section 1.6) and appendix one (section 9.1).

1.6 PUBLICATION: Cell adhesion an important determinant of myogenesis and satellite cell activity

Published in Biochemica et Biophysica Acta (BBA), 2021. 1869(2)
Available online 8 November 2021: https://doi.org/10.1016/j.bbamcr.2021.119170

Lauren Taylor [a], Miriam Wankell [a], Pankaj Saxena [b,c], Craig McFarlane [a], Lionel Hebbard [a,d]

[a] Department of Molecular and Cell Biology, College of Public Health, Medical and Veterinary Sciences, Centre for Molecular Therapeutics, Centre for Tropical Bioinformatics and Molecular Biology, Australian Institute of Tropical Medicine and Health, James Cook University, Townsville, Queensland, Australia

[b] Department of Cardiothoracic Surgery, The Townsville University Hospital, Townsville, Queensland, Australia

[c] College of Medicine, Dentistry, James Cook University, Townsville, Queensland, Australia

[d] Storr Liver Centre, Westmead Institute for Medical Research, Westmead Hospital and University of Sydney, Sydney, New South Wales, Australia

Keywords: myogenesis, cell adhesion molecules, satellite cells

1.6.1 Abstract

Skeletal muscles represent a complex and highly organised tissue responsible for all voluntary body movements. Developed through an intricate and tightly controlled process known as myogenesis, muscles form early in development and are maintained throughout life. Due to the constant stresses that muscles are subjected to, skeletal muscles maintain a complex course of regeneration to both replace and repair damaged myofibers and to form new functional myofibers. This process, made possible by a pool of resident muscle stem cells, termed satellite cells, and controlled by an array of transcription factors, is additionally reliant on a diverse range of cell adhesion molecules and the numerous signalling cascades that they initiate. This

article will review the literature surrounding adhesion molecules and their roles in skeletal muscle myogenesis and repair.

1.6.2 Introduction

The largest tissue type in the human body is the skeletal muscles. They make up approximately 40% of the total body weight and are responsible for imparting strength, stability, and support to facilitate voluntary movement. Skeletal muscle development, or myogenesis, begins early during embryonic development and is made possible through the formation, growth, differentiation and fusion of committed myogenic progenitor cells present in the myotome compartment of somites [13, 14]. Myogenesis is tightly controlled by a group of transcription factors known as myogenic regulatory factors (MRFs), which regulate myogenic commitment, muscle cell (myoblast) proliferation, fusion and eventual differentiation of myoblasts into multinucleated myotubes [112]. The MRF myogenic regulatory factor-5 (Myf5), which is initially expressed in the somite, together with myogenic determination factor (MyoD), commit cells to adopt a myogenic fate [28]. These MRFs act in concert with one another and can be overexpressed to compensate for each other in knockout cells and in mice [34, 35]. Following the formation of a pool of myogenic progenitor cells, these cells give rise to myoblasts, or skeletal muscle cells, which during primary myogenesis differentiate and fuse together to form multinucleated myotubes. Myoblast fusion requires cell movement, the apposition of membranes and reorganisation of the cytoskeleton to form fusion pores and ultimately the merging of membranes. Recent research has shown critical roles for two muscle proteins, Myomaker and Myomixer in myoblast fusion, and a contemporary review has been published [42, 43, 113]. During secondary myogenesis, mononucleated myoblasts align along these primary myotubes, and through further fusion form secondary myotubes [114]. This fusion process, otherwise referred to as myogenic differentiation, is controlled by the expression of additional MRFs, known as myogenin and MRF-4 (muscle specific regulatory factor-4) [14, 37].

Importantly, skeletal muscles are able to maintain their mass postnatally, and even build upon it, thanks to a resident population of muscle specific stem cells, termed satellite cells (SCs), that reside between the sarcolemma and basal lamina of muscle fibres [58, 115]. SCs originate in the somites, similar to the precursor myoblasts, but

adopt a quiescent state beneath the basal lamina [116]. However, in response to muscle injury or damage, SCs are able to activate, re-enter the cell cycle, and undertake myogenesis similar to what is observed during embryonic growth, fuse to form new multinucleated myotubes, and facilitate the replacement of damaged or defective muscle fibres. Consistent with their stem cell nature, sub-populations of SCs are then able to return to a quiescent state and have the ability to self-renew, so as to maintain their population throughout adult life [69].

Given the importance of SCs in maintaining skeletal muscle mass, any defects in SC function, and the associated regenerative processes of skeletal muscle can have detrimental downstream consequences on human health. Most notably, reduced SC numbers and defective SC function has been linked to the loss of muscle mass and impaired muscle function associated with chronic diseases, including type 2 diabetes and sarcopenia [117, 118]. Recent evidence suggests that specific cell adhesion molecules (CAMs), including the calcium-dependent cadherins M-cadherin and N-cadherin, have pivotal roles in maintaining SC quiescence and activation [119, 120], which suggests CAMs may have roles in muscle disease. Hence, the role of CAMs in skeletal muscle myogenesis is of particular interest to the field, with a better understanding of these complex processes providing a potential avenue for developing therapeutic approaches for improving muscle growth and chronic disease outcomes. Thus, this review will consider myogenic CAMs and will discuss their known function in skeletal muscle growth and maintenance and highlight potential avenues for further research.

1.6.3 Cell adhesion molecules (CAMS)

The formation of myofibers during development not only depends on the complex expression of myogenic transcription factors, but also on the select expression of adhesion molecules. CAMs are proteins, located on the cell surface, that are involved in binding cells to one another or to the extracellular matrix (ECM). CAMs have diverse functions within the body and are not only important for adhesion but also for signalling in development, proliferation and in cancer progression. CAMs are often divided into four superfamilies: the immunoglobulin superfamily of adhesion molecules (IgCAMs), cadherins, integrins and selectins. The various groups of CAMs and their role in myogenesis will now be considered. Selectins are typically responsible for

binding carbohydrates and are important for leukocyte trafficking to expose leukocytes to signalling molecules [121]. Although studies have revealed potential roles for selectins in facilitating skeletal muscle regeneration [122], selectins have not been shown to play a major role in myogenesis, as such will not be discussed in this review. The remaining groups of CAMs and their role in myogenesis will now be considered.

1.6.3.1 Integrins

Integrins are a family of cell adhesion molecules that are responsible for both cell-cell and cell-matrix interactions as well as acting as receptors for extracellular ligands and binding to the cytoskeleton. As these proteins are the principal tools used for binding and communicating with the ECM, they are abundantly present on the cell surface. These heterodimeric glycoproteins consist of noncovalently bound α and β subunits; forming up to 24 unique integrins based on the varying complexity of the subunits [123-125]. Integrins influence cell behaviour as bi-directional cell signalling molecules. In the resting state they exist in a bent-over inactive conformation and become activated through the binding of agonists such as chemokines and growth factors to G-protein receptors, and extracellular force. This in turn leads to molecules such as paxillin, talin and kindlin binding to the β subunit to promote an open and activated integrin, allowing binding to ECM components (collagen, laminin, fibronectin). Subsequently, this promotes integrin clustering and the recruitment of signalling molecules including, integrin linked tyrosine (ILK) and focal adhesion kinases (FAK), and the modulation of downstream signalling including Akt, extracellular signal-related kinase (ERK), Rho guanine nucleotide binding proteins (Rho GTPases) and mammalian target of rapamycin (mTOR). The nature of signalling is dependent on the integrin, cell type and ECM. During developmental myogenesis specific integrins are expressed and their presence coincides with that of their extracellular ligands laminin and fibronectin [126, 127].

The dystrophin-glycoprotein complex (DGC) and integrin α7β1, serve as the two primary laminin receptors in skeletal muscle, binding the muscle fibres to the basal lamina [128, 129]. Mutations in nearly all the DGC associated proteins result in skeletal muscle pathologies; with mutations in the major DGC protein, dystrophin, resulting in Duchenne and Becker muscle dystrophies (DMD and BMD), and in dystroglycans and sarcoglycans associating with a wide range of limb-girdle muscular dystrophies and other pathological changes [130]. Integrin α7 was postulated to play a major role in

secondary myogenesis due to observations that α7 and its ligand laminin are expressed on primary myotubes following primary myogenesis [131]. In this regard, patients with congenital myopathy were observed to possess a mutated α7 gene, and this was supported by experiments showing that α7 null mice develop mild muscular dystrophy [132, 133]. Significantly, endogenous α7β1 integrin mRNA and protein, is upregulated in DMD patients and in *mdx* mice (a mouse model of human DMD) and was suggested to be a compensatory action between the two laminin ligands [134, 135]. In agreement, the over-expression of α7β1 in *mdx*/*utr*$^{-/-}$ mice that lack both dystrophin and utrophin, led to an extension in life, a reduction in muscular dystrophy pathology and an increase in satellite cell number [134, 136]. These data suggested that α7 was protective, and as a consequence double knock-out mice lacking both α7 and dystrophin (*mdx* mice) had a much more severe and progressive muscular dystrophy than that observed in mice with the individual loss of each gene alone [137]. Together, these reports suggested that the re-expression of α7 could be a therapeutic strategy for treatment of DMD patients. Subsequent studies using adeno-associated virus (AAV) delivery methods in *mdx* and *mdx*/ *utr*$^{-/-}$ mice resulted in improved muscle fibre size and lifespan [138, 139]. Further studies using the small molecule SU9516 reduced the phosphorylation of pro-inflammatory p65-nuclear factor-κβ (NF-κβ) and activity of Ste20-related proline alanine rich kinase (SPAK) and oxidative stress response 1 (OSR1) kinase pathways, promoted α7β1 expression in myogenic cell lines, and reduced disease progression in *mdx* mice [140]. As a consequence, therapies targeting α7 could be an avenue to treat muscular dystrophies.

β1 integrin itself appears to be essential for the development of myofibers, as defects in myoblast fusion, observed through the accumulation of unfused cells and the formation of short muscle fibres, are observed in *in vitro* studies and in mice with muscle-specific inactivation of the β1 integrin. Importantly, the muscle-specific inactivation of the integrin β1 gene in mice leads to death at birth with non-inflated lungs, and poorly developed muscle fibres [141, 142]. At the signalling level β1 can interact with transmembrane 182 (TMEM182) to regulate FAK, ERK and Akt myogenic signalling, and additionally co-operate with fibroblast growth factor (FGF) signalling to maintain SC proliferation and renewal [143, 144]. Another β integrin, β3 has been found to be transiently expressed in activated SCs during mouse muscle regeneration, mediates myogenic gene expression and SC migration, and β3 integrin gene absence

in vivo leads to impaired muscle regeneration. Mechanistically, it was found that β3 is required for maintaining Rac1 GTPase activity (a Rho GTPase family member), myogenic gene expression and focal adhesion complexes in differentiating myoblasts [145].

In addition to α7β1, *in vitro* studies in rodent and avian cells indicate that integrins α4β1, α4β7 and α5β1 which bind fibronectin, and α6β1 and laminin, respectively, may also play a role in cell adhesion and communication during skeletal muscle myogenesis. The α4 integrins, found on multinucleated myotubes, were as well thought to be of importance during secondary myogenesis through interactions with a counter receptor, vascular cell adhesion protein-1 (VCAM-1), found on the proliferating myoblasts [146]. However chimeric mice with a high percentage of α4-deficient embryonic stem cells developed normal muscle and displayed uninhibited myotube formation *in vitro* [147]. The exact role for α5β1 in muscle development is poorly understood notwithstanding studies have shown that α5 absence in chimeric mice results in changes in muscle structure resembling muscular dystrophy [148]. The loss of α6 in mice does not lead to a muscle phenotype [149]. However *in vitro* studies inhibiting α6 have presented unexpected results, as blocking antibodies and siRNA treatment limited differentiation of porcine primary muscle cells, whereas treatment with blocking antibodies in murine explants activated the myogenic programme in dermomyotomal cells [150, 151]. These data suggest that α6β1 may have alternate functions during distinct myogenic stages.

1.6.3.2 Immunoglobulin superfamily of adhesion molecules

The cell adhesion molecules of the IgCAM family function in diverse cell types and are involved in a variety of biological processes. This family includes the neural cell adhesion molecule (*NCAM*), vascular adhesion protein-1 (*VCAM-1*), CAM-related/down-regulated by oncogenes (*CDO*), brother of CDO (*BOC*) and neogenin.

1.6.3.2.1 NCAM

NCAM was the first IgCAM implicated in myogenesis in the somites and the myotome compartment during development [152]. *In vitro* overexpression studies in murine C2C12 myoblasts, revealed that increased NCAM enhances myoblast fusion [153, 154]. Further studies have revealed that myoblasts express transmembrane isoforms of NCAM, that then switch to an alternate GPI-anchored form in myotubes, which is

suggested to be essential for the fusion of myoblasts to myotubes [152, 155, 156]. Additionally, NCAM is found expressed on both quiescent and activated satellite cells from the proliferative stages through to fusion, which suggest a role for NCAM in postnatal myogenesis [63, 157]. Despite these studies, NCAM null mice do not have any apparent defects in skeletal muscle development, and NCAM knock-out primary myoblasts differentiate *in vitro* at the same rate as wild-type cells, suggesting that other cell adhesion molecules can compensate for NCAM loss [158].

1.6.3.2.2 VCAM-1

VCAM-1 is expressed by proliferating myoblasts and on SCs and has a high affinity for integrin α4β1 (also known as VLA-4), which is present on the surface of multinucleated myofibers [146]. The inhibition of VCAM-1, or its ligands, in C2C12 cells, results in a reduced number of nuclei within the myotubes, when compared to controls, suggesting an inhibition of myoblast fusion [146]. The selective deletion of VCAM-1 from SCs in mice, during regeneration resulted in SCs with premature lineage progression to a more differentiated state, a robust influx of immune cells expressing integrin α4β1 and apoptosis, leading to a transient delay in myofiber growth. However, 30 days post-injury no defects were noted in myofiber cross-sectional area, suggesting that VCAM-1 is not required at later stages of regeneration, or that perhaps there is compensation by other cell-cell adhesion molecules. Interestingly, in uninjured VCAM-1 null mice, the basal fusion of the SCs was reduced, and this corresponded with reduced myofiber cross-sectional area [159]. Taken together, these reports suggest that the role of VCAM-1 in myogenesis and myofiber growth is contingent on the inflammatory state of the SC niche.

1.6.3.2.3 CDO

CAM-related/down-regulated by oncogenes (CDO), also known as CDON, is a further member of the Ig/FNIII (Fibronectin type III) family of cell surface receptors and possesses five Ig-like domains, with three FNIII like repeats in the extracellular region, a transmembrane domain and a cytoplasmic tail [160]. CDO is initially expressed in the central nervous system as early as E7.5, however expression is also seen in the skeletal muscle precursors, but is absent in the adult muscle [161, 162]. CDO exhibits a promyogenic role *in vivo* and *in vitro* and appears to be an integral component of the link between the cell surface and nuclear transcription factors, that positively regulates myogenic differentiation. In this manner, CDO overexpression enhances differentiation

and the expression of muscle-specific proteins, while the expression of anti-sense CDO limits myotube formation [162]. Moreover, CDO null mice show delayed muscle development, and knock-out primary myoblasts derived from the CDO null mice display defective differentiation in culture [163]. Mechanistically, CDO, through interactions with promyogenic cadherins, N-cadherin and M-cadherin, positively regulate the differentiation of myogenic cell lines by post-translationally activating MyoD [164]. Further intricate studies illustrated that CDO can complex to the scaffold proteins JLP (JNK-associated leucine zipper protein) and Bnip-2 (BCL2/ adenovirus E1B 19 kDa protein-interacting protein 2), and the adaptor protein APPL1 (adaptor protein containing PH [pleckstrin homology]) domain, PTB [phosphotyrosine binding] domain, and leucine zipper motif to respectively activate p38 mitogen activated protein kinase (p38MAPK) and Akt, two key myogenic signalling pathways [165, 166]. Studies by the same group then found that TGF-β-activated kinase 1 (TAK1) and apoptosis signal-regulating kinase 1 (ASK1) interacted with CDO to promote myogenesis through activation of p38MAPK [167]. Further placing CDO in an influential position in myogenesis, recent data shows that the specific deletion of CDO from muscle SCs impairs muscle regeneration, fibroblast growth factor (FGF) and integrin signalling. Specifically, the loss of CDO in SCs resulted in impaired muscle regeneration and increased fibrotic deposition. Further analysis showed that CDO loss decreased β1-integrin expression, reduced extracellular signal-regulated kinase (ERK) levels, and impaired SC response to FGF, resulting in reduced proliferation and self-renewal capacity of SCs [168].

1.6.3.2.4 BOC

Brother of CDO (BOC), is an additional member of the Ig/FNIII family of receptor proteins and has four Ig repeats and three FNIII structures in its ectodomain. The expression of BOC during both embryonic development and in C2C12 myoblasts overlap significantly with CDO [169, 170]. Immunoprecipitation studies show strong binding between CDO and BOC and shows that the two CAMs function together as components of an adhesion complex that acts to regulate myogenic differentiation [169]. Notably, oncogenic forms of Ras, a family of GTPases that act as crucial members of a signalling network controlling cell cycle growth, migration, and apoptosis, can block differentiation in C2C12 cells through transcriptional downregulation of MyoD, myogenin, CDO and BOC. Significantly, the forced re-expression of either CDO

or BOC in Ras expressing C2C12 cells leads to the induction of endogenous MyoD and myogenin, and thus myogenesis [169]. Moreover, it was observed that the forced expression of BOC or CDO in the human rhabdomyosarcoma cell line RD promoted muscle-cell like differentiation [171]. Together, these data suggest a positive link for BOC and CDO between the cell surface and MRFs.

1.6.3.2.5 Neogenin

Neogenin is a multifunctional transmembrane receptor that is a part of the immunoglobulin superfamily and is composed of an extracellular domain containing four Ig-like loops and six FNIII repeats, a transmembrane region, and a cytoplasmic tail. As a homologue of DCC (deleted in colorectal cancer), the primary function of neogenin was predicted to be similar to DCC to facilitate axon guidance through the binding of netrins, which represent a small family of laminin-related proteins, that associate with cell membranes and the ECM [172, 173]. In C2C12 cells, neogenin overexpression enhanced myotube formation by promoting myoblast differentiation [174]. Subsequent studies revealed that despite normal myotome development, neogenin-null mice display smaller myofibers at E18.5 and postnatally from 3 weeks of age [175]. Mechanistically, it was found that neogenin can complex with CDO, and bind Netrin-3, a laminin related protein, which *via* CDO stimulated the Nuclear factor of activated T-cells (NFAT) pathway, to regulate muscle differentiation [174, 176]. An interesting aspect of the binding of netrin and neogenin on myoblasts, is that it does not lead to alterations in muscle-specific gene products, including MyoD, myogenin, and MHC, suggesting an alternative pro-myogenic mechanism is in play.

1.6.3.3 Cadherins

Cadherins exist in multiple tissue-specific isoforms and promote both homophilic (binding between cells of the same type) and heterophilic (binding between cells of different types) interactions. Cadherins typically express a C-terminal cytoplasmic domain, a transmembrane domain, and an N-terminal variable extracellular domain, often used to classify the cadherin into subgroups. Each of these subgroups are responsible for a variety of functions between cells, and by example, the classic cadherins express 5 extracellular domains between which reside three calcium binding sites that are necessary for correct conformation and intercellular binding [177, 178]. The binding of calcium brings rigidity to the ectodomain so that it adopts a crescent shape necessary for bonding between adjacent cells [179]. Cadherins are primarily

located at adherens junctions, which are protein structures along the plasma membrane that mediate adhesion between cells [180]. The cadherins facilitate adhesion through the formation of trans bonds between the N-terminal β-strands of the EC1 domains, bridging the intermembrane space through their ectodomains [181, 182]. Furthermore, cadherins, along with conferring adhesion between cells, are essential for intracellular and intercellular signalling and communication, which is achieved through the interaction of their cytoplasmic tails with catenin proteins [183].

The most abundant cadherins in skeletal muscle are muscle (M-), neuronal (N-), retinal (R-), and truncated (T-) cadherins [184-187]. M- and N-cadherin are best described in myogenesis, and cadherin control of the Rho family of guanine triphosphate hydrolases (GTPases) has been studied due to the dependence of fusion on the recognition, adherence and alignment between myoblasts [188]. Rho is a subgroup of the Ras superfamily of GTPases and are major contributors to morphogenic and migratory properties of cells [189, 190]. Through the activation of muscle specific promoters, RhoA is expressed and is crucial for the accumulation of β-catenin at sites of cell-cell contact. Similarly, the GTPases Rac1 and Cdc42 are essential for myoblast fusion *in vivo* and *in vitro*, as their loss impairs muscle formation [191-193].

1.6.3.3.1 N-cadherin

The first cadherin to appear during myogenesis is N-cadherin, where it is expressed in the myotome compartment of somites and in embryonic muscle during development [194]. First described in neurons, N-cadherin plays a significant role in the development of many tissues within the body. N-cadherin signalling, which is important for cell cycle exit, occurs in-part through the regulation of RhoA and Rac1. N-cadherin negatively regulates Rac1 function and increases the activity of RhoA, thereby initiating myogenic progression [193]. N-cadherin is down-regulated in secondary myogenesis during the point in embryonic development where myoblasts switch the expression of their primary adhesion proteins from N- to M- cadherin [195, 196]. Due to the vital role N-cadherin plays in heart muscle development, N-cadherin-null mice are embryonically lethal and are unable to be studied [197]. Studies blocking N-cadherin function in C2C12 myoblasts inhibited myogenesis [198, 199]. Nevertheless, the subsequent isolation of N-cadherin null myoblasts revealed that their fusion competence was equivalent to wild-type and suggested that other CAMs could compensate for N-cadherin myogenic function [200]. Despite these findings, subsequent signalling

studies found that N-cadherin ligation between opposing myoblasts stimulated CDO-dependent activation of p38MAPK, that in turn promotes muscle differentiation [201]. In sum, these data suggest N-cadherin is a key signalling CAM in myogenesis.

1.6.3.3.2 M-cadherin

M-cadherin is abundantly expressed in the developing skeletal muscle but is downregulated in adult muscle fibres, where it is only found in muscle SCs at low levels [202, 203]. M-cadherin expression is activated through the binding of MRFs to transcription sites close to the M-cadherin gene. Initial M-cadherin knockdown studies in muscle cell lines indicated that reduced M-cadherin leads to a reduction in myoblast adhesion and differentiation [204]. Nevertheless, M-cadherin knockout mice have normal muscle development with no obvious defects in growth or repair, suggesting that *in vivo* M-cadherin loss could be compensated by other cadherins like N- and R-cadherin [205]. Subsequent cell biology studies show M-cadherin stabilises β-catenin, and regulates β-catenin/Wnt signalling to promote myogenesis independent of T-cell specific transcription factor/lymphoid enhancer binding factor (TCF/LEF) [206].

Recent studies have shown that CAMs occupy an important role in readying SCs for activation. The study by Goel et al. [119] showed that M-and N-cadherin mediated adhesion between SCs and myofibers is necessary for promoting SC quiescence, while the genetic removal of both M-cadherin and N-cadherin diminishes cell-to-cell binding, leading to partial SC activation, without injury. A contemporary cell biology study has also linked M-cadherin to metabolism, where it was shown that insulin stimulated phosphorylation of β-catenin on Serine 552 was critical for GLUT4 translocation to the cell membrane, and subsequent binding of β-catenin to M-cadherin [207]. These studies suggest a plausible molecular link between insulin resistance and SC activity, *via* the interactions of M-cadherin and β-catenin.

1.6.3.3.3 R-cadherin

Retinal cadherin (R-cadherin) is another classical cadherin, originally discovered in the retina, but is also expressed in the heart, kidney, thymus and on the skeletal muscle [208, 209]. R-cadherin is detected in the somites and localises to the cell-cell contacts of primary myoblasts but is diminished in normal adult muscle. Interestingly, R-cadherin is present in rhabdomyosarcomas (RMS), a cancer of the muscle tissue, but is absent in normal myoblasts. Moreover, it has been shown that R-cadherin can

promote tumorigenesis in C2C12 myoblasts by inhibiting myogenic induction through impairing cell cycle exit and promoting cell motility. Furthermore, R-cadherin can upregulate the activity of Rac1, leading to the inhibition of the cell cycle and hence muscle myogenesis, and additionally downregulate M- and N-cadherin function to disrupt muscle development [208, 210].

1.6.3.3.4 T-cadherin

In contrast to the classical cadherins, T-cadherin does not express a transmembrane, or cytoplasmic domain, and is instead attached to the cell membrane through a glycosylphosphatidylinositol (GPI) moiety that localises to lipid rafts [187]. Another key difference between T-cadherin and the classical cadherins is that T-cadherin executes homophilic binding through a different mechanism. While classical cadherins bind one another through a strand-swapping mechanism, T-cadherin engages in intracellular recognition through a homophilic interface between the EC1 and EC2 domains – referred to as the X-dimer [211]. T-cadherin is expressed on developing and mature skeletal muscle, but limited studies have been performed to identify the role of this cadherin in skeletal muscle growth. Nonetheless, a recent study considering skeletal muscle regeneration in mice suggests T-cadherin may play a role by acting as a receptor for adiponectin [212]. Here the genetic loss of adiponectin or T-cadherin had no effect on muscle regeneration. Muscle regeneration improved only when adiponectin was adenovirally expressed to supra physiological levels (10- to 30-fold above normal) together with infused angiotensin II to partially mimic muscle ageing. Thus, further studies are required to consider T-cadherin's molecular functions in myogenesis and SC activity.

1.6.4 The myogenic cell adhesion complex

The many years of study by numerous investigators has led to the development of an elegant model for myogenic cell adhesion molecules in how they communicate and interact with one another to regulate skeletal muscle myogenesis. Some of these molecules have been found to participate in the formation of an integrated promyogenic cell adhesion complex with other CAMs. CDO and BOC form a cis complex through an association of their ectodomains and cytoplasmic tails [213]. Both CDO and BOC can as well bind to cadherins, which can communicate with the cytoplasmic catenins, and importantly, studies indicate that this cadherin interaction is

necessary for the promyogenic effects of CDO [164, 214]. This cell adhesion complex also interacts with other members of the immunoglobulin superfamily, namely neogenin and netrin [174, 213]. Data suggests that neogenin mediates most of its role through selective binding with CDO, which in turn regulates netrin signalling (**Figure 1.6** and **Table 1.1**). These reports indicate that there is a promyogenic effect associated with the formation of this complex. Nevertheless, there is still much to be understood about how they mediate these effects, and how this complex regulates muscle development, regeneration, and SC activation. Moreover, in this light recent research by the Rudnicki group has shown that the DGC plays a necessary role in regulating SCs cell polarity and epigenetic activation of SC commitment. The absence of dystrophin causes a dramatic reduction in asymmetric division, and hence the number of myogenic progenitors to support regeneration [215-217]. Significantly, in regard to the information presented in this review concerning α7β1, VCAM-1, CDO, M-

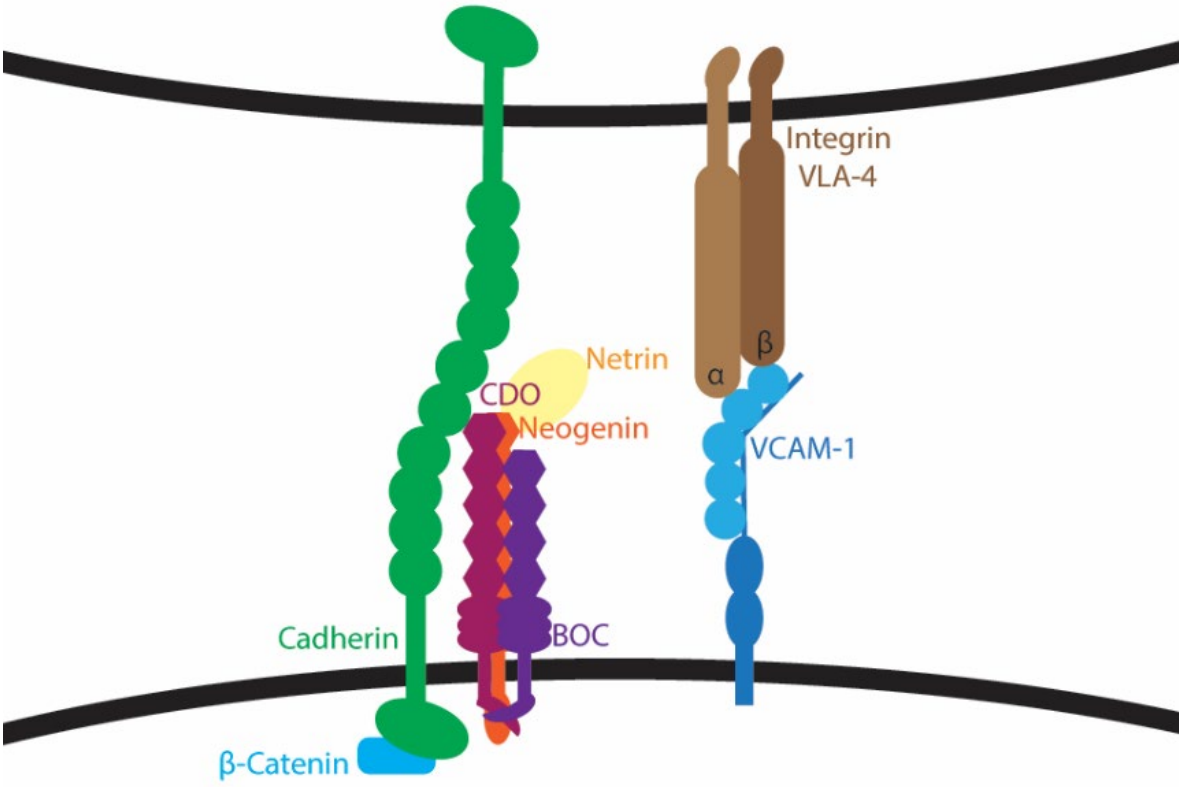

Figure 1.6. Cartoon depicting the major cell adhesion molecules in the promyogenic cell adhesion complex. Research from the last 20 years shows the presence and interaction of N- and M-cadherin (green), CDO (rouge), Neogenin (orange), and BOC (purple) in the complex; and neogenin binds netrins. VCAM-1 (blue) and VLA-4 (brown; integrin α4β1) bind independently of the other CAMs.

and N-cadherin, it is likely that other CAMs could regulate SCs division and differentiation. These CAMs and/or their downstream signalling could possibly be used to counter the negative influence of a dysfunctional DGC in muscular dystrophy or muscle wasting diseases and provide a therapeutic approach.

Table 1.1. Lists the major myogenic CAMs, their function and expression.

Family	***CAM***	***Function***	***Expression***	***Reference***
Integrin	α7β1	Binding of the muscle fibres to the basal lamina to assist adhesion of myoblasts	Myoblasts and myotubes	[129]
	α4β1	Assists secondary myogenesis through adhesion with counter receptor VCAM-1	Myoblasts and myotubes	[125, 146]
	α4β7	Assists secondary myogenesis through adhesion with counter receptor VCAM-1	Myoblasts and myotubes	[125, 146]
	α5β1	Maintaining a proliferative state, and thus sustaining growth	Myoblasts and myotubes	[125, 148]
	α6β1	Helps to facilitate the transition of myoblasts from proliferation to differentiation	Myoblasts and myotubes	[125]
IgCAM	NCAM	Enhances myoblast fusion	Myoblasts, myotubes, and satellite cells	[154]
	VCAM-1	Assists secondary myogenesis through adhesion to integrin subunit alpha 4	Myoblasts and satellite cells	[146]
	CDO	Enhances differentiation	Myoblasts and satellite cells	[163]
	BOC	Enhances differentiation	Myoblasts and satellite cells	[169]
	Neogenin	Enhances differentiation	Myoblasts and myotubes	[163, 174]
Cadherins	N-cadherin	Initiates myogenic differentiation through cell cycle exit	Myoblasts and satellite cells	[193]

M-cadherin	Enhances myoblast adhesion and differentiation	Myoblasts, myotubes and satellite cells	[184]
R-cadherin	Enhances differentiation through cell cycle exit	Myoblasts	[208]
T-cadherin	Binds adiponectin, role in myogenesis largely unknown	Myoblasts and myotubes	[187, 212]

1.6.5 Conclusion

In conclusion, cell adhesion molecules play a significant role in the formation and maintenance of skeletal muscle cells. The formation of an intricate ‘adhesion complex’ at cell-cell contacts throughout muscle development and regeneration signifies the importance of improving our understanding of this process. Publications suggest that SC phenotype and function is regulated through cell adhesion and offer a potential window to develop more cogent therapeutic strategies. Hence CAMs and their downstream signalling could become therapeutic targets to alleviate the effects of dystrophin loss or reduced expression, and to promote SC expansion and differentiation to treat muscle wasting diseases. Better understanding the mechanisms that regulate degeneration, and repair, could play a dynamic role in assisting patients to maintain muscle mass, increasing life expectancy, and reducing disease morbidity.

End of Publication

1.7 Cell adhesion molecules

The following provides information in addition to the published literature review regarding cadherins and their roles in skeletal muscle development and regeneration.

1.7.1 T-cadherin

The T-cadherin protein is coded by the *CDH13* gene on chromosome 16q24 and has described roles in initiating signalling for proliferation, differentiation and migration rather than just simple cell adhesion [218]. T-cadherin is expressed on many tissues and cell types including endothelium, smooth muscle cells, cardiomyocytes, skeletal muscles, retina, pancreas, and epithelium. In addition, T-cadherin plays an important role in the guidance of neurons during development and regulating angiogenesis [1, 187]. Homophilic interactions between T-cadherin molecules results in cellular deadhesion through the activation of Rho GTPases [219].

1.7.1.1 T-cadherin and adiponectin

T-cadherin is a receptor for the hexameric and HMW species of APN, as well as low-density lipoproteins (LDL) [220, 221]. The colocalization of T-cadherin and APN has been demonstrated on both the skeletal muscles and cardiomyocytes. Moreover, native APN appears to bind specifically to cells expressing T-cadherin independently of AdipoR1, and -R2 [222]. In the heart, T-cadherin is essential for APN-mediated revascularization and cardio protection, and T-cadherin loss results in increased serum APN and a lack of APN binding on cardiac tissue [223, 224]. The absence of APN binding in T-cadherin knockout (T-cad KO) mice is also seen for the skeletal muscle and suggests and important role for T-cadherin in muscle regeneration [212].

1.7.1.2 T-cadherin in muscle regeneration

During muscle regeneration, T-cadherin and APN expression initially decreases before returning to normal levels by day 7 [212]. A recent study by Tanaka et al. suggests that T-cadherin plays an important role in muscle regeneration by acting as a receptor for APN [212]. The study showed that the overexpression of APN to supranormal levels, in aged APN null mice, increased regenerating fibres and decreased necrotic areas. However, these effects were not seen in T-cadherin null mice, suggesting T-cadherin is important for APN signalling in muscle fibres. Nonetheless, studies have not

examined T-cadherin's APN-independent functions in myogenesis, and this is the major focus of this thesis.

1.7.2 M-cadherin and β-catenin

An important element of the myogenic adhesion complex is the interaction with β-catenin and the actin cytoskeleton. During myogenesis, M-cadherin accumulates at areas of cell-cell contact between myoblasts and co-localizes with β-catenin [225]. Following cell adhesion, M-cadherin interacts with β-catenin and links with the actin cytoskeleton to provide mechanical stability throughout the fusion process and assist in actin reorganization. There is still much to be understood regarding this complex and its function during skeletal muscle myogenesis.

In the presence of Wnt signalling, β-catenin translocates to the nucleus where it associates with TCF/LEF (T-cell factor/lymphoid enhancer factor) to regulate gene expression. Importantly, during myoblast proliferation β-catenin interacts with MYOD and enhances its transcriptional activation of downstream MRFs, including myomaker and myomixer [20, 226]. As Wnt signalling decreases, β-catenin remains in the cytoplasm where it localises to regions of cell-to-cell contact and assists in myoblast fusion [227].

In the absence of Wnt signalling or cadherin interaction, β-catenin is phosphorylated and marked for degradation by glycogen synthase kinase-3 beta (GSK3-β) [228]. Both gain- and loss- of β-catenin function studies in mice show impaired myogenesis and suggest β-catenin expression must be tightly regulated during myogenesis [226, 227]. Of interest, M-cadherin contributes to the regulation of β-catenin as M-cadherin knockdown studies show significant increases in β-catenin phosphorylation, leading to its degradation [206].

1.8 Skeletal Muscle Disease

Given that the first results chapter of this thesis considers the association of T-cadherin (*CDH13*) with muscle disease through bioinformatic analyses, the following section provides an overview of the major muscle disease types and possible links to T-cadherin.

Muscle diseases commonly associate with other debilitating chronic illnesses and can be devastating to a patient and their family. A loss of muscle mass, commonly referred to as muscle atrophy, can lead to movement difficulties and can seriously reduce quality of life. Muscle diseases and muscle loss can occur because of chronic illness, severe trauma, age, poor nutrition, or genetics. For individuals with chronic illnesses, atrophy is a result of functional and metabolic alterations that lead to poor muscle performance. Many people suffering from muscle wasting, particularly those suffering because of trauma or poor nutrition, can reverse this atrophy through proper nutrition, and physiotherapy. However, for those suffering from muscle atrophy associated with chronic illness, ageing or with genetic causes, there are few solutions.

1.8.1 Muscular dystrophies

A group of diseases that effects the muscle repair system are muscular dystrophies. Muscular dystrophies are a group of inherited disorders that are typically characterised by a progressive degeneration of skeletal muscles. The following section provides a brief overview of these disorders as an extensive review has been published elsewhere [229]. Duchenne muscular dystrophy (DMD), the most common genetic muscular disorder, is an X-linked genetic disorder that has a worldwide incidence of 1:5000 male births [230]. Although this disease commonly affects males, female carriers may also present with mild, moderate, or severe DMD due to skewed X-inactivation, or in rare cases, an inherited mutation from the mother and a de novo mutation from the father [231]. Patients suffering from this disease have a genetic mutation within the DMD gene on the X-chromosome that precludes the production of the muscle protein ‘dystrophin’ – a protein essential for maintaining muscle structure and function [232, 233]. Dystrophin is a vital protein for skeletal muscles that helps to strengthen and protect them from contractile stress. Without dystrophin, muscles are unable to handle mechanical stress, and undergo necrosis [234]. Webster et al., demonstrated that in patients with DMD, type II fibres are the first to degenerate and are eventually lost, while type I fibres are affected relatively late in the disease process [235]. Although muscles with dystrophin-deficiency retain their ability to repair fibres, the new muscles are ineffective, and are condemned to a cycle of necrosis and repair, leading to the muscle being ultimately replaced with adipose and connective tissue [234-236].

Although the mutations behind dystrophin disease-causing variants have been researched for decades it is still unclear what role SCs play in this disease. Originally, it was theorized that the SCs simply become exhausted and are unable to continue repairing the fibres. Nonetheless, studies have since shown that muscle fibres isolated from mdx mice and DMD patients possess elevated numbers of SCs, particularly in type I muscle fibres [237, 238]. Hence, a more recent model argues that the SCs themselves become dysfunctional and are unable to efficiently repair the muscle. Given that SCs have been shown to express dystrophin, it is likely that they may not retain full regenerative functionality [216].

During regeneration it is important that metabolic capacity is maintained. This is in part resolved by removing damaged mitochondria and replacing them with new mitochondria from the fusing SCs. Indeed, mitochondrial dysfunction is one of the many complications associated with mdx dystrophic muscle [239, 240]. Importantly, the absence of dystrophin in the muscle results in an increase in cytosolic calcium and oxidative stress that creates a pro-inflammatory environment leading to mitochondrial dysfunction [211, 241]. Interestingly, mdx mice that overexpress APN actually show reduced inflammation, oxidative stress and an increase in expression of *MRF4* and *MYOG* [242]. Thus, the emerging genetic therapies that aim to repair the dystrophin gene [243] may benefit from altering the metabolic function of SCs to assist in repair.

Myotonic dystrophies, type I (DM1) and type 2 (DM2) are one of the most common adult-onset dystrophies. Both types are caused by microsatellite expansions in different genes, *DMPK* (DM1 protein kinase) for DM1, and *CNBP* (CCHC-type zing finger nucleic acid binding protein) for DM2, and share a range of clinical symptoms but differ in fibre type phenotypes [244]. DM1 shows atrophy and a high frequency of central nuclei in type I fibres, and DM2 shows atrophy and central nuclei in type II fibres [245, 246]. For these reasons, manipulation of the muscle fibre type to replace deficient fibres is a candidate therapeutic approach for some dystrophies.

1.8.2 Sarcopenia

Another common cause of muscle atrophy is ageing. Sarcopenia, characterised by a progressive and generalised loss of muscle mass, affects a large majority of elderly patients, and correlates with poor life quality, physical disability and shortened

life expectancy [247, 248]. Sarcopenia can be categorised into primary, or age-related, sarcopenia and secondary sarcopenia, which is caused by factors other than, or in addition to, ageing [249]. Specifically, sarcopenia is characterized by reduced size and atrophy of type II fibres [250]. Although the potential for regeneration remains, the functionality and overall number of SCs is greatly reduced in aged muscle and is likely responsible for this altered regenerative capability [251, 252]. It is possible that the increased atrophy of type II fibres is due to the reduced expression of PGC-1 that promotes oxidative metabolism and represses atrophy [253-255]. The atrophic phenotype of type II muscles can be serious for people suffering from chronic illnesses, who due to their disease, are unable for retain muscle mass. For example, 80% of cancer patients experience cachexia (an overall loss of body fat and muscle mass), and near 30% of these will die as a direct result of muscle loss [256]. In this light, improving our understanding of the mechanisms that modulate degeneration and repair, could play a role in assisting these patients in maintaining muscle mass, and increasing their life expectancy.

Age-related sarcopenia has also been shown to be more prevalent in obese patients [257]. Although the association with sarcopenia and obesity could simply be a result of decreased motility and exercise, studies have shown that sarcopenic patients have lower serum APN levels than in non-sarcopenic individuals [258].

1.8.3 Obesity and type 2 diabetes

The presence of both carbohydrates and free fatty acids are important components of skeletal muscle metabolism, particularly during prolonged exercise. However, hyper-nutrition commonly associated with western diets and the increased consumption of sugar and fats, as well as the resulting adipose tissue can drive human disease. According to the 2017-2018 Australian National Health Survey, approximately 67% of adults, and 25% of children, were overweight or obese and 4.5% had type 2 diabetes [259]. Obesity is a well-established risk factor for several other chronic disorders including type 2 diabetes, cardiovascular diseases, arthritis, and some types of cancer.

More recently, obesity has been suggested to increase a patient's risk of developing cognitive disorders later in life and is often associated with depression and bipolar

disorder. Obese individuals, and those with type 2 diabetes appear to have reduced proportions of type I fibres and increased proportions of type IIX fibres [11, 260]. The proportion of type I fibres is associated with insulin responsiveness [261]. Consistent with a shift to type IIX fibres, biopsies from these individuals show reduced expression of PGC-1 and less oxidative metabolism [262, 263].

The association between APN and the metabolic syndrome is well established and extensively studied. Low levels of circulating APN in individuals correlate with metabolic abnormalities such as obesity, diabetes, and hypertension. Increased circulating APN negatively associates with insulin resistance and diabetes. Of note to this section, individuals with these clinical conditions also have reduced muscle regenerative capacity because of decreased APN and subsequent AMPK activity [264, 265].

1.8.4 Heart failure and COPD

Muscle atrophy occurs in many individuals with chronic illnesses, such as chronic heart failure and chronic obstructive pulmonary disease (COPD). This comorbidity can have serious effects on the quality of life and survival of affected individuals. Adiponectin may play a role in the dysregulation of muscle metabolism in patients with chronic heart failure and studies suggest an association between APN levels and COPD in mice [266, 267]. There has been limited research in patients.

1.8.5 T-cadherin SNPs associated with disease

Genetic studies are an important method of understanding the underlying mechanism of many diseases. Given T-cadherin's association with APN, studies have assessed potential genetic links between T-cadherin and metabolic disease. To date, multiple single nucleotide polymorphisms (SNPs) have been identified within the T-cadherin gene that associate with the metabolic syndrome (**Table 1.2**). Korean genome wide association studies (GWAS) show reduced HMW APN levels associated with SNPs in the *CDH13* gene, and separate studies based on French cohorts have identified the same SNP, along with another, that associate with type 2 diabetes. These GWAS also show an association between *CDH13* promoter methylation and a decrease in plasma APN levels [268]. Despite these studies, there is little data

published on *CDH13* function or linkage with human muscle disease, hence the first results chapter will use bioinformatic analyses to explore these links.

Table 1.2. Known single nucleotide polymorphism and their documented effects in or around the *CDH13* gene.

SNP	Known Associations	Publications
rs3865188	Decreased HMW APN in Asian populations and Type 2 diabetes in French population	[268-272]
rs11646213	Type 2 diabetes in French population and metabolic syndrome in Swedish population	[270]
rs8060301	Promoter methylation associated with 4.5-fold decrease in plasma APN levels	[268]
cg09415485	Promoter methylation associated with 4.5-fold decrease in plasma APN levels	[268]
rs4783244	Higher APN levels and linked with a higher susceptibility to COPD in the Chinese population	[271, 273, 274]
rs12051272	Increased APN levels	[271]
rs12922394	Linked with an increased susceptibility to COPD in the Chinese population	[273]
rs12596316	Associated with type 2 diabetes	[275]
rs7193788	APN levels, diabetes, and ischemic stroke	[275]

1.9 Conclusion

Although APN has been implicated in having a role in muscle regeneration, important regulators of myogenesis are the myoblast cell adhesion molecules. These proteins sense their surroundings, have various ligands and form signalling complexes with each other to modulate the speed and extent of muscle formation. Despite T-cadherin being a receptor for APN, there are few published reports exploring T-cadherin's function in myogenesis and muscle repair, independently of its APN binding function. T-cadherin, through homophilic binding, has been implicated as a negative regulator of axon growth and endothelial migration. Thus, in view of the following preliminary data, the overarching aim of this thesis was to explore how T-cadherin binding could regulate myogenesis and muscle regeneration.

1.10 Preliminary Data

Preliminary work for this project has been performed by Dr. Hebbard and myself as part of my Honours thesis, which aimed to examine the effects of T-cadherin and APN loss on muscle growth in mice. The following is an introduction to these results and assists in providing a rationale for this project.

To determine the function of T-cadherin in skeletal muscle myogenesis, the Hebbard lab overexpressed T-cadherin in murine C2C12 myoblasts (pLTcad) and evaluated differences in myogenic proteins and fusion index (the number of nuclei present inside the myotubes as a percentage of the total number of nuclei in the field of vision) (**Figure 1.7**). These results showed that overexpressing T-cadherin led to reduced levels of myosin heavy chain (MHC), a marker of muscle maturity, and myogenin, a marker of muscle fibre differentiation. Furthermore, pLTcad cells had reduced fusion as evident in their significantly lower fusion index. Overall, this demonstrates that T-cadherin negatively regulates myogenesis in C2C12 cells.

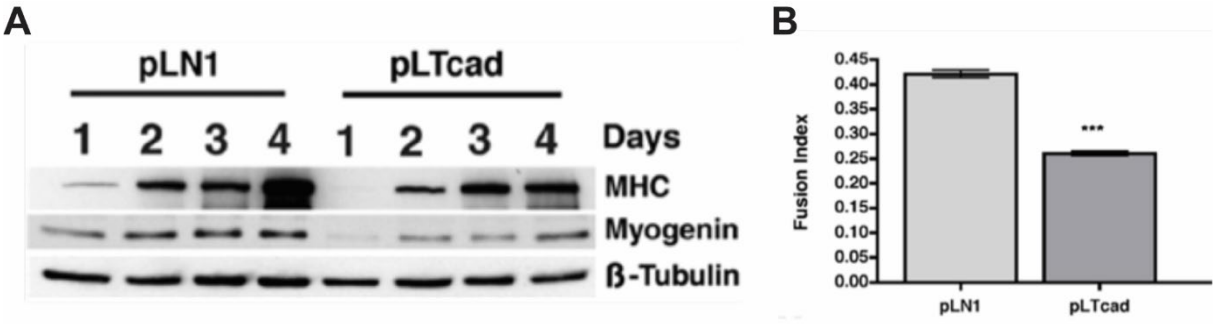

Figure 1.7. T-cadherin overexpression in myoblasts impairs myogenesis. **A.** Western blot of pLN1 (control) and pLTcad C2C12 cells differentiated for 1-4 days and probed for MHC, myogenin and β-tubulin loading control. **B.** Graph showing myoblast fusion index of differentiated C2C12 pLN1 and pLTcad cells. *** = $p<0.001$.

Given this and the established relationship between T-cadherin and APN on the skeletal muscle, my Honours research focused on the difference in muscle growth and differentiation between primary myoblasts isolated from wild-type (WT) and T-cadherin/APN double knockout (DKO) mice. Initial body weight comparison showed little difference between the WT and DKO mice at 5, 6 and 7 weeks of age (**Figure 1.8** A). Although statistical testing showed a significant difference between the body

weights of 5- and 6-week-old mice, this study only had a small sample size and hence exhibited variability within the genotypes. Moreover, there was no significant difference in the ratio of *tibialis anterior* (TA), *quadriceps* (QUAD), or *gastrocnemius* (GAS) muscle versus body weights of the individually isolated hindlimb muscles (**Figure 1.8** B). These results suggest that there were no observable differences in primary muscle development between WT and DKO mice.

Following these results, primary myoblasts were used to investigate if there were differences in post-natal muscle myogenesis. Interestingly, muscle cells isolated from the DKO mice fused more rapidly and grew to a larger size than those from WT mice (**Figure 1.9** A-E). Furthermore, protein analysis showed that DKO muscle cells expressed MYOG and MHC at earlier time points than WT fibres (**Figure 1.9** F). These results demonstrated that myoblasts isolated from DKO murine hindlimbs possess enhanced differentiation *ex vivo*.

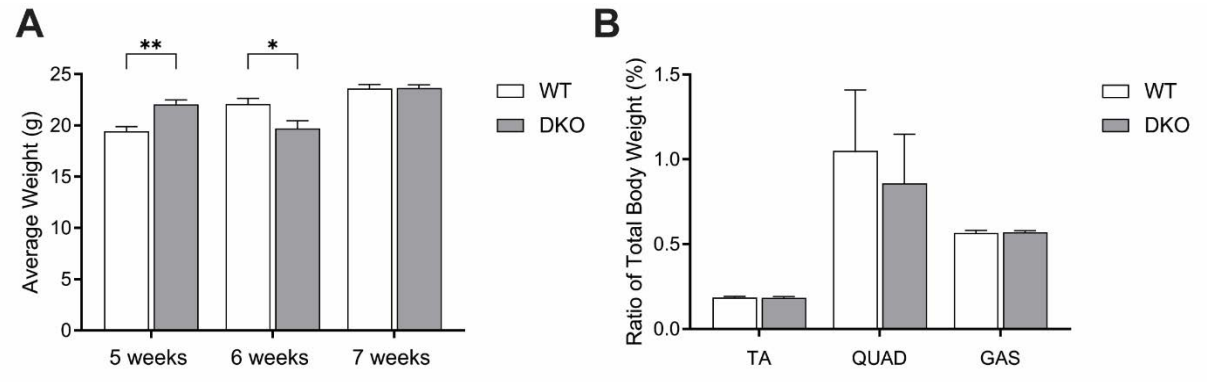

Figure 1.8. **A.** Average body weight comparison of WT and DKO mice between 5-7 weeks of age (n=4). **B.** Average hindlimb *tibialis anterior* (TA), *quadriceps* (QUAD), *gastrocnemius* (GAS) muscle versus body weight ratio comparison of WT and DKO mice. Statistical significance determined by Bonferroni multiple comparisons. * = $p<0.05$, ** = $p<0.01$.

However, it was not clear if the differences in myogenesis were due to the lack of T-cadherin, APN, or a combination of both. This thesis is a thorough interrogation and continuation of these studies.

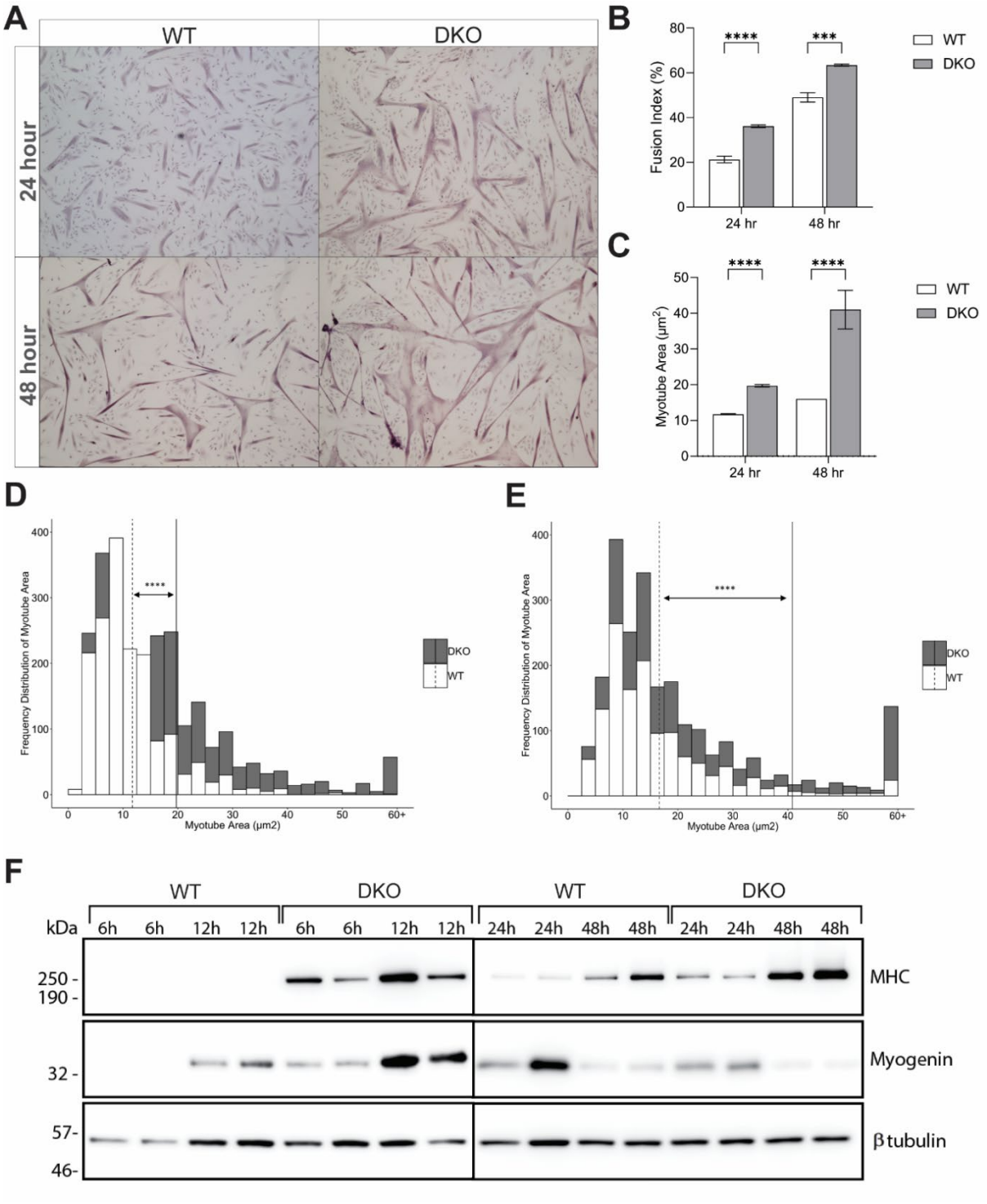
A
WT
DKO
24 hour
48 hour
B
Fusion Index (%)
****
***
WT
DKO
24 hr
48 hr
C
Myotube Area (μm²)
****
****
WT
DKO
24 hr
48 hr
D
Frequency Distribution of Myotube Area
****
DKO
WT
Myotube Area (μm2)
E
Frequency Distribution of Myotube Area
****
DKO
WT
Myotube Area (μm2)
F
WT
DKO
WT
DKO
kDa
6h 6h 12h 12h 6h 6h 12h 12h 24h 24h 48h 48h 24h 24h 48h 48h
250 -
190 -
MHC
32 -
Myogenin
57-
46-
βtubulin

Figure 1.9. T-cadherin/APN double knockout (DKO) primary myoblasts show enhanced differentiation compared to WT myoblasts. **A.** Representative images of differentiating WT and DKO primary myoblasts at 24- and 48-hours differentiation. **B.** Fusion index of WT and DKO myoblasts at 24- and 48-hours differentiation. **C.** Average myotube area of WT and DKO myofibers at 24- and 48-hours differentiation. Overlapped frequency distribution of myotube area of WT and DKO myotubes at **D.** 24- and **E**. 48-hours differentiation. Vertical lines represent average values. **F.** Protein expression of differentiating WT and DKO myoblasts between 6-48 hours. Multiple t-tests were used to determine significance. *** = $p<0.001$, **** = $p<0.0001$.

1.11 Project Rationale, Hypothesis and Aims

Given the preliminary results, this thesis aimed to understand the specific mechanisms by which T-cadherin regulates skeletal muscle myogenesis. This thesis utilized *in silico* genome wide association studies (GWAS) and RNA-sequencing studies to identify potential polymorphisms and downstream genetic targets of T-cadherin. Following this, both *ex vivo* and *in vivo* studies were performed to examine the effects of T-cadherin loss on myogenesis and regeneration. Primary myoblasts were also used to understand how APN and T-cadherin affect muscle metabolism during myogenesis. Finally, *in vitro* studies with C2C12 muscle cells were used to understand T-cadherin's interactions with the myogenic adhesion complex.

1.11.1 Project hypothesis

The overarching hypothesis of this thesis was that T-cadherin acts as a negative regulator of skeletal muscle regeneration.

1.11.2 Project aims

The aims of this project were:

1. To examine T-cadherin's association with muscle disease (chapter 3).
2. Investigate the role of T-cadherin and APN in muscle regeneration and repair (chapter 4).
3. Understand the metabolic effects of T-cadherin and APN loss during regeneration of skeletal muscles *ex vivo* (chapter 5).
4. To elucidate T-cadherin's involvement with the myogenic adhesion complex during myogenesis (chapter 6).

2 Materials and Methods

2.1 Materials

The following section provides details about the specific materials used throughout this study and details, where available, the company and product numbers to assist repeatability.

2.1.1 Primary and secondary antibodies

The following tables list the primary and secondary antibodies that were used in the experiments.

Table 2.1. List of primary antibodies used for protein analysis. All antibodies were prepared in 5% milk in TBST except those marked with '*' which were prepared in 5% BSA in TBST.

Antibody	Dilution	Company	Catalogue Number	Host
Anti-Myogenin	1:500	BD Pharmingen	556358	Mouse
Anti-Myogenin[ii]	1:500	DSHB	F5D-c	Mouse
Anti-MyHC[iii]	1:1000	DSHB	MF20-c	Mouse
Anti-β-tubulin[iv]	1:1000	DSHB	E7-c	Mouse
Anti-N-cadherin	1:1000	BD Biosciences	610820	Mouse
Anti-M-cadherin	1:1000	Cell Signalling	40491	Rabbit
Anti-Pan-cadherin	1:1000	Cell Signalling	4068	Rabbit
OXPHOS Cocktail	1:250	Abcam	110413	Mouse
Anti-β-catenin*	1:1000	SIGMA	2206	Rabbit
Anti-p-β-catenin*	1:1000	Cell Signalling	9564	Rabbit

[ii] F5D was deposited to the DSHB by Wright, W.E. (DSHB Hybridoma Product F5D)

[iii] MF 20 was deposited to the DSHB by Fischman, D.A. (DSHB Hybridoma Product MF 20)

[iv] E7 was deposited to the DSHB by Klymkowsky, M. (DSHB Hybridoma Product E7)

Table 2.2. List of primary antibodies used for immunoprecipitation analysis. All antibodies were prepared in 5% milk in TBST.

Antibody	Dilution	Company	Catalogue Number	Host
Anti-T-cadherin[v]	1:10	Hebbard, et al. [1]		Rabbit
Anti-M-cadherin	1:20	Cell Signalling	40491	Rabbit
Anti-N-cadherin	1:20	BD Transduction Laboratories	610920	Mouse
Anti-CDO	1:10	Life Technologies	PA5-47315	Goat
Rabbit IgG	1:50	Sigma Aldrich	I8140	Rabbit
Mouse IgG	1:50	Sigma Aldrich	I8765	Mouse
Goat IgG	1:50	Sigma Aldrich	I5256	Goat

Table 2.3. List of secondary antibodies used for protein analysis. All antibodies were prepared in 5% milk in TBST.

Antibody	Dilution	Company	Catalogue Number	Host
Anti-mouse IgG HRP	1:1000	Cell Signalling Technologies	7076S	Horse
Anti-rabbit IgG HRP	1:1000	Cell Signalling Technologies	7074S	Goat
Anti-goat IgG HRP	1:1000	Sigma Aldrich	A8918	Rabbit
Anti-sheep IgG HRP	1:1000	Sigma Aldrich	SAB3700723	Donkey

[v] Generated against a fusion protein in the lab of Barbara Ranscht

Table 2.4. List of primary antibodies used for immunohistochemical staining. All antibodies were prepared in 5% BSA in PBS.

Antibody	Dilution	Company	Catalogue Number	Host
Anti-Laminin	1:500	ICN Biomedicals	69-610	Rat
Anti-MyoD	1:100	BD Biosciences	554130	Mouse
DAPI	1:1000	Sigma Aldrich	D9542	
Anti-Pax7[vi]	1:50	DSHB	PAX7	Mouse
Anti-CD68	1:100	BioLegend	137001	Rat
Anti-Type I MHC[vii]	1:25	DSHB	A4.840	Mouse
Anti-Type IIB[viii]	1:25	DSHB	10F5	Mouse
Anti-Type IIA[ix]	1:25	DSHB	2F7	Mouse
Anti-Type IIX[x]	1:25	DSHB	6H1	Mouse

Table 2.5. List of secondary antibodies used for immunohistochemistry. All antibodies were prepared in 5% BSA in PBS.

Antibody	Dilution	Company	Catalogue Number	Host
Goat α-rat 544	1:500	Jackson Immuno Research	112-585-062	Goat
Sheep α-mouse 488	1:400	Jackson Immuno Research	515-545-062	Sheep

[vi] PAX7 was deposited to the DSHB by Kawakami, A. (DSHB Hybridoma Product PAX7)

[vii] A4.840 was deposited to the DSHB by Blau, H.M. (DSHB Hybridoma Product A4.840)

[viii] 10F5 was deposited to the DSHB by Lucas, C. (DSHB Hybridoma Product 10F5)

[ix] 2F7 was deposited to the DSHB by Lucas, C. (DSHB Hybridoma Product 2F7)

[x] 6H1 was deposited to the DSHB by Lucas, C. (DSHB Hybridoma Product 6H1)

2.1.2 List of all reagents

The following table lists the reagents used in this thesis in alphabetical order. The table includes the company and catalogue number where possible.

Table 2.6. List of reagents used in this thesis.

Reagent	Company	Catalogue Number
3-aminopropyltrimethoxysilane	Sigma-Aldrich	281778
4iPBA	Sigma-Aldrich	471933
Acetic Acid	Chem Supply	64197
Affinipure Fab Fragments Donkey anti-mouse IgG	Jackson Immuno Research	715-007
Ammonium persulfate	Sigma-Aldrich	A3678
Antimycin	Sigma-Aldrich	A8674
Bovine serum albumin (BSA)	Sigma-Aldrich	A7906
Brij 97	Sigma-Aldrich	P6136
BSA Fatty-acid free	Sigma-Aldrich	A8806
Carbonyl cyanide 4-(trifluoromethoxy)phenylhydrazone	Sigma-Aldrich	C2959
Chicken Embryo Extract	Made in-house (see section 2.1.4)	
Collagenase type IA	Sigma-Aldrich	9891
DC Protein Assay	Bio-Rad	5000111
D-Glucose	Sigma-Aldrich	G8270
Direct Red 80	Sigma-Aldrich	365548
DPX Mountant	Sigma-Aldrich	06522
DTT	AG Scientific	C-1029
Dulbeccos Modified Eagle Media	Sigma-Aldrich Gibco	D6429 10569-101
ECM Gel from Engelbreth-Holm-Swarm murine sarcoma	Sigma-Aldrich	E1270
Eosin-Y	BDH	34197
Foetal Bovine Serum	Serana OR Bovogen OR Corning	S-FBS-AU-015 SFBS-AU 35-076 CV
Fluoroshield	Sigma-Aldrich	F6182
Formaldehyde	Sigma-Aldrich	F8775
Glutamine	Sigma-Aldrich	59202C
Glycine	Sigma-Aldrich	G5417
Ham’s Nutrient Mixture F12	Merck	51651C
Hematoxylin	ProSciTech	AMH-1L
HEPES	Gibco	15630-080
Horse Serum	Thermo Fisher	16050122
Luminol	Sigma-Aldrich	48511
Magnesium Sulphate	Sigma-Aldrich	F90327
NP20	Sigma-Aldrich	NP40S

OCT Compound	Tissue-Tek	IA018
Oligomycin	Sigma-Aldrich	04876
OptiMEM	Gibco	31985
PBS – Tablet	Sigma-Aldrich	P4417
Penicillin-Streptomycin (10,000 U/ml)	Thermo Fisher Scientific	15140122
PMSF	Merck	10837091001
Ponceau Stain	Sigma-Aldrich	P3504
Protease Inhibitor Cocktail	Sigma-Aldrich	P8340
Protein G- Sepharose	BioVision	6511
Rotenone	Sigma-Aldrich	R8875
SDS	Sigma-Aldrich	L3771
Seahorse Base Media	Agilent Technologies	103193-100
Seahorse Calibrant	Agilent	103059-000
Seahorse Calibrant	Agilent Technologies	103059-000
Seahorse Mito Stress Test Kit	Agilent Technologies	103270
Seahorse XFp Base Media	Agilent	103193-100
Seahorse XFp Calibrant	Agilent	103059-000
Sodium Bicarbonate	Sigma-Aldrich	S5761
Sodium Chloride	Sigma-Aldrich	S7653
Sodium fluoride	Sigma-Aldrich	201154
Sodium molybdate	Sigma-Aldrich	243655
Sodium orthovanadate	Sigma-Aldrich	S6508
Sodium Pyruvate	Sigma-Aldrich	P2256
Sodium Pyruvate	Sigma-Aldrich	P2256
Sterile PBS	Thermo Fisher Scientific	14190-144
TEMED	Sigma-Aldrich	T7024
Tricine	Sigma-Aldrich	T0377
Triethanolamine	Sigma-Aldrich	90279
Tris-HCL	Astral Scientific	BIOSD8127
Triton X-100	Sigma-Aldrich	T8787
Triton X-100	Sigma-Aldrich	9002-93-1
Trizma	Sigma-Aldrich	RDD008
Trypan Blue	Gibco	15250-061
Trypsin	Thermo Fisher	15400054
Tween 20	Sigma-Aldrich	P1379
XF Base Medium	Agilent	103334
Xylene	Sigma-Aldrich	214736
β-glycerophosphate	Sigma-Adrich	G9422
β-mercaptoethanol	Sigma-Aldrich	M3148

2.1.3 Chicken embryo extract

Chicken embryos (9–12-day) were macerated through a 20 ml syringe and collected in DMEM at a 1:1 ratio. The tissue was shaken at 80 rpm at room temperature for 2 hours before being frozen at -80 °C overnight. Following thawing, the tissue was centrifuged at 15,000 *g* for 10 minutes, the liquid supernatant removed and filtered through a 0.45 µM filter, a 0.22 µM filter and frozen at -80 °C in aliquots until use.

2.1.4 Primary satellite cell isolation

The following tables list the reagents used for the isolation of muscle SCs from murine muscle.

Table 2.7. Satellite cell proliferation media.

Satellite Cell Proliferation Media	Concentration/Volume
Foetal bovine serum	20% (v/v)
Horse serum	10% (v/v)
Penicillin/streptomycin	1% (v/v)
Chicken embryo extract	0.5% (v/v)
DMEM to desired volume	

Table 2.8. Satellite cell differentiation media.

Differentiation Media	Concentration/Volume
Horse serum	2% (v/v)
Penicillin/streptomycin	1% (v/v)
DMEM to desired volume	

Table 2.9. 10% ECM gel from Engelbreth-Holm-Swarm Murine Sarcoma.

10% ECM gel	Concentration/Volume
ECM gel	10% (v/v)
DMEM to desired volume	

Table 2.10. 10x Phosphate-buffered solution (PBS).

Phosphate-buffered saline (10x solution)	Concentration/Volume
Sodium chloride	80 g
Potassium chloride	2 g
Disodium phosphate	14.4 g
Potassium phosphate	2.4 g
MilliQ water to total volume	1 L
Adjust pH to 7.4	
Dilute to 1x with MilliQ water before use	

Table 2.11. 1x trypsin EDTA solution

1x Trypsin Solution	Concentration/Volume
10x Trypsin EDTA	1 ml
1x PBS	9 ml

2.1.5 Gel electrophoresis and western blotting

The following tables list the reagents used for protein validation, SDS-PAGE gel electrophoresis, western blotting, and immunoprecipitation.

Table 2.12. 5x SDS-PAGE separating buffer.

5x Separating Buffer	Concentration/Volume
Tris	46 g
SDS	1 g
MilliQ water to total volume	200 ml
Adjust pH to 8.8 with HCl	

Table 2.13. 40% acrylamide for SDS-PAGE gel.

40% Acrylamide	Concentration/Volume
Acrylamide/bis-acrylamide	38% (v/v)
N,N'-methylbisacrylamide	2% (w/v)
MilliQ water to desired volume	

Table 2.14. SDS-PAGE for 8%, 12% and 15% separating gel.

Separating Gel	Concentration/Volume		
	8% Gel	12% Gel	15% Gel
40% Acrylamide (**Table 2.13**)	1 ml	1.5 ml	1.875 ml
5x Separating buffer (**Table 2.12**)		1 ml	
MilliQ Water	3 ml	2.5 ml	2.125 ml
10% APS		50 µl	
TEMED		5 µl	

Table 2.15. 5x SDS-PAGE stacking buffer.

5x Stacking Buffer	Concentration/Volume
Tris	30.25 g
SDS	1 g
MilliQ water to total volume	200 ml
Adjust pH to 6.8 with HCl	

Table 2.16. SDS-PAGE stacking gel.

Stacking Gel	Concentration/Volume
40% Acrylamide (**Table 2.13**)	250 µl
5x Separating buffer (**Table 2.12**)	500 µl
MilliQ Water	1.75 ml
10% APS	25 µl
TEMED	5 µl

Table 2.17. 20x TruPAGE TEA-Tricine SDS running buffer.

20x Running Buffer	Concentration/Volume
Triethanolamine	179.0 g
Tricine	143.3 g
SDS	20 g
MilliQ water to total volume	1 L
Adjust pH to 8.2-8.3	

Table 2.18. 5x SDS sample buffer with DTT.

5x SDS Sample Buffer	Concentration/Volume
Glycerol	50% (v/v)
1 M Tris-HCl (pH 6.5)	300 mM
SDS	10% (w/v)
Bromophenol blue	0.5% (w/v)
DTT	~500 mM
MilliQ water to desired volume	

Table 2.19. 20x TruPAGE transfer buffer.

20x Transfer Buffer	Concentration/Volume
Trizma	30.3 g
Glycine	144.1 g
MilliQ water to total volume	1 L

Table 2.20. 10x Tris-buffered saline (TBS) diluted to 1x with Tween 20.

10x TBST	Concentration/Volume
Tris-HCl (pH 7.6)	250 mM
NaCl	1.5 M
Dilute to 1x before adding:	
Tween-20	0.05% (v/v)

Table 2.21. 5% Skim milk blocking solution.

5% Milk Blocking Solution	Concentration/Volume
Skim milk powder	5% (w/v)
1x TBST (**Table 2.20**) to desired volume	

Table 2.22. 10% BSA blocking solution.

10% BSA Blocking Solution	Concentration/Volume
BSA	10% (w/v)
TBST (**Table 2.20**) to desired volume	

Table 2.23. Radioimmunoprecipitation assay (RIPA) lysis buffer.

RIPA Buffer	Concentration/Volume
Tris (pH 7.5)	50 mM
Sodium chloride	150 mM
NP40	1% (w/v)
Sodium deoxycholate	0.5% (w/v)
SDS	0.1% (w/v)
MilliQ water to desired volume	

Table 2.24. Brij 97 lysis buffer without inhibitors.

Brij 97 Buffer	Concentration/Volume
Tris-HCl (pH7.5)	10 mM
NaCl	150 mM
$CaCl_2$	1 mM
Brij 97	1% (v/v)
MilliQ water to desired volume	

Table 2.25. Triton X-100 lysis buffer without inhibitors.

Triton X-100 Buffer	Concentration/Volume
Tris-HCl (pH 7.5)	50 mM
NaCl	100 mM
$CaCl_2$	0.5 mM
Triton X-100	1% (v/v)
MilliQ water to desired volume	

Table 2.26. Triton X-114 lysis buffer without inhibitors.

Triton X-114 Buffer	Concentration/Volume
Tris-HCl (pH 7.5)	50 mM
NaCl	100 mM
$CaCl_2$	0.5 mM
Triton X-114	1% (v/v)
MilliQ water to desired volume	

Table 2.27. Complete lysis buffer. All protease inhibitors added to lysis buffer.

Complete Lysis Buffer	Concentration/Volume
Sodium orthovanadate	2 mM
NaFl	50 mM
Sodium molybdate	1 mM
β-glycero-phosphate	40 mM
PMSF	1 mM
Protease inhibitor cocktail	1/100
Lysis buffer to desired volume	

Table 2.28. Homemade enhanced chemiluminescence reagent for western blot detections [276].

Homemade ECL reagent	Concentration/Volume
100 mM Tri-HCl pH 8.8	1 ml
1.25 mM Luminol (in DMSO)	5 µl
2 mM 4iPBA (in DMSO)	22.2 µl
Hydrogen peroxide	0.54 µl

Table 2.29. Amido black staining solution.

Amido Black Staining Solution	Concentration/Volume
Amido black 10B powder dye	0.1 g
Methanol	40 ml
Glacial acetic acid	10 ml
MilliQ Water to total volume	1 L

Table 2.30. Amido black de-staining solution.

Amido Black De-Staining Solution	Concentration/Volume
MilliQ Water	50 ml
Methanol	20 ml
Glacial acetic acid	7.5 ml
Adjust volume to 100 ml with MilliQ water	

Table 2.31. Ponceau S staining solution.

Ponceau S Solution	Concentration/Volume
Ponceau S	0.1% (w/v)
Acetic acid	5% (v/v)
MilliQ water to total volume	

2.1.6 Hematoxylin and eosin staining

The following tables list the reagents used for hematoxylin[xi] and eosin staining of myoblasts and muscle sections.

Table 2.32. 20:2:1 ethanol: formaldehyde: acetic acid cell fixative.

Fixative 20:2:1	Concentration/Volume
70% Ethanol	20 ml
37% Formaldehyde	2 ml
Acetic acid	1 ml

Table 2.33. Scott's tap water.

Scott's Tap Water	Concentration/Volume
Sodium bicarbonate	3.5 g
Magnesium Sulphate	20 g
MilliQ water	1 L

Table 2.34. Eosin (yellowish) solution.

Eosin-Y	Concentration/Volume
Eosin-Y	0.5% (w/v)
MilliQ water	100 ml
Acetic acid	200 µl
Filtered through Whatman paper	

[xi] Pre-made Hematoxylin (ProSciTech AMH-1L) was filtered through Whatman paper prior to use.

2.1.7 Muscle cross section staining

The following tables list the reagents used for the staining of tibialis anterior muscle cross sections.

Table 2.35. Picrosirius red solution.

Picrosirius Red	Concentration/Volume
Direct red 80	0.1 g
Picric acid	100 ml

Table 2.36. Acidified water for de-staining picrosirius red.

Acidified Water	Concentration/Volume
Acetic acid (glacial)	0.5% (v/v)
Water to desired volume	

Table 2.37. 10% buffered formalin solution for fixing tissue.

Buffered Formalin	Concentration/Volume
Formaldehyde (37%)	100 ml
Sodium phosphate (monobasic)	4 g
Sodium phosphate (dibasic)	6.5 g
MilliQ water	900 ml
Adjust pH to 7.2	

2.1.8 Myoblast metabolism

The following tables list the reagents and concentrations used for the metabolic analyses of myoblasts.

Table 2.38. C2C12 cell growth medium.

C2C12 Growth Medium	Concentration/Volume
Foetal bovine serum	10% (v/v)
Penicillin/streptomycin	1% (v/v)
DMEM to desired volume	

Table 2.39. Assay medium for seahorse XFp mitochondrial stress test assay.

Seahorse XFp Assay Medium	Concentration/Volume
D-Glucose	10 mM
Glutamine	2 mM
Sodium pyruvate	1 mM
Agilent Base Medium to desired volume	
Adjust pH to 7.4	

Table 2.40. Concentrations used for mitochondrial complex inhibitors.

Inhibitor	10x Concentration	Volume to load
Oligomycin	10 µM	20 µl
FCCP	15 µM	22 µl
Rotenone and antimycin A	5 µm each	25 µl

2.1.8.1 Preparing BSA conjugated palmitate

To conjugate BSA with palmitate, both fatty acid free BSA and sodium palmitate were first dissolved separately in 150 mM NaCl. The BSA solution was created by combining fatty acid free BSA with NaCl (**Table 2.41**) in a 37 °C water bath, stirring constantly until dissolved. The BSA solution was filtered, and half of the solution was diluted 1:1 with 150 mM NaCl to create a 0.17 mM stock while the other half was combined with the palmitate solution. The palmitate solution was created by combining sodium palmitate with 150 mM NaCl in a water bath with constant stirring while the temperature was raised to 70 °C (**Table 2.42**). The palmitate solution was then added to the remaining BSA solution at 37 °C, at constant temperature and with stirring for one hour (**Table 2.43**). The volume was increased with additional 150 mM NaCl solution, and pH adjusted to 7.4. The BSA-conjugated palmitate and BSA stock solution aliquots were stored in glass vials at -20 °C until use.

Table 2.41. BSA solution for BSA-conjugated palmitate preparation

Fatty Acid Free BSA solution	Concentration/Volume
Fatty acid free BSA	0.45 g
150 mM NaCl	20 ml
Prepare at 37 °C	
Dilute 1:1 with 150 mM NaCl for 0.17 mM stock or conjugate with palmitate	

Table 2.42. Palmitate solution for BSA-conjugated palmitate preparation

Palmitate solution	Concentration/Volume
Sodium palmitate	6.12 mg
150 mM NaCl	8.8 ml
Heat to 70 °C	

Table 2.43. BSA conjugated palmitate for fatty oxidation assay

BSA Conjugated Palmitate	Concentration/Volume
BSA solution (**Table 2.41**)	10 ml
Palmitate solution (**Table 2.42**)	8 ml
Prepare at 37 ° C.	
Adjust final volume to 20 ml with 150 mM NaCl	

Table 2.44. Substrate-limited medium for Seahorse palmitate oxidation stress test.

Seahorse Substrate-Limited Medium	Concentration/Volume
D-Glucose	0.5 mM
Glutamine	1 mM
L-Carnitine	0.5 mM
Horse Serum	2% (v/v)
Agilent Base Medium to desired volume	

Table 2.45. Assay medium for seahorse fatty acid oxidation assay.

Seahorse XFp Assay Medium	Concentration/Volume
D-Glucose	2.5 mM
Carnitine	0.5 mM
Agilent Base Medium to desired volume	

Table 2.46. Mitochondrial isolation buffer.

Mitochondrial Isolation buffer	Concentration/Volume
Sucrose	250 mM
EDTA	1 mM
HEPES	10 mM

Table 2.47. Buffered Formalin (v/v).

10% Buffered formalin	Concentration/Volume
Sodium phosphate, monobasic	4 g
Sodium phosphate, dibasic	6.5 g
37% formaldehyde	100 ml
MilliQ water	900 ml

2.1.9 Immunofluorescent staining

The following tables list reagents and concentrations used for immunofluorescent staining of muscle fibres.

Table 2.48. Auto fluorescence blocking mixture for immunofluorescent staining.

Blocking mixture	Concentration/Volume
Triton X-100	0.5% (v/v)
BSA	0.2% (v/v)
Normal goat serum	10% (v/v)
1x PBS to desired volume	

Table 2.49. Primary antibody diluent for immunofluorescent fibre typing.

Primary antibody diluent	Concentration/Volume
BSA	0.2% (v/v)
Normal goat serum	5% (v/v)
Tween-20	0.1% (v/v)
1x PBS to desired volume	

2.1.10 T-cadherin's interactions in vitro

The following tables list the reagents and concentrations used for investigating the interactions of T-cadherin *in vitro*.

Table 2.50. CHO cell growth media.

CHO Growth Media	Concentration/Volume
Foetal bovine serum	10% (v/v)
Penicillin/streptomycin	1% (v/v)
Ham's Nutrient Mixture F12	

Table 2.51. HEPES buffer, calcium, and magnesium free (HCMF).

HCMF Buffer	Concentration/Volume
NaCl	137 mM
KCl	5.4 mM
Na2HPO4.12H2O	0.34 mM
Glucose	0.1% (w/v)
HEPES	10 mM
MilliQ Water to desired volume	
Adjust pH to 7.4 with NaOH	

Table 2.52. HEPES buffer, magnesium free (HMF).

HMF Buffer	Concentration/Volume
HCMF (**Table 2.51**)	1 L
$CaCl_2$	1 mM

Table 2.53. Trypsin calcium (TC) solution, EDTA free, to maintain cadherins on cells.

TC Solution	Concentration/Volume
10x trypsin solution (EDTA-free) (see section 2.1.11)	2% (v/v)
$CaCl_2$	1 mM
HCMF to desired volume	

2.1.11 Trypsin-EDTA dialysis

10 ml of 10x Trypsin-EDTA solution was placed into dialysis tubing with ties at each end. The tubing was placed into 1x PBS (refreshed daily) with a stir bar overnight at 4 °C for three days.

2.1.12 Methylene blue staining

The following tables are a list of the reagents used for methylene blue staining of cells.

Table 2.54. 10x borate buffer.

10x Borate Buffer	Concentration/Volume
Boric Acid	6.8 g
MilliQ Water to total volume	1 L
Adjust pH to 8.3	
Dilute to 1x before use	

Table 2.55. Formal saline.

Formal Saline	Concentration/Volume
Sodium Chloride	0.87 g
MilliQ Water	75 ml
37% Formaldehyde	25 ml

Table 2.56. 1% methylene blue for cell staining.

Methylene Blue	Concentration/Volume
Methylene blue	1 g
1x borate buffer (**Table 2.54**)	100 ml

2.2 Methods

2.3 Primary Myoblast Isolation

2.3.1 Animal studies

C57BL/6 wild-type (WT), C57BL/6 T-cadherin knockout (T-cad KO) and C57BL/6 T-cadherin/APN double knockout (DKO) mice were housed in the Immunogenetics Small Animal House at James Cook University, building 86. The T-cad KO and DKO mice were provided by the Ranscht group and have been previously described [1, 224]. All animal procedures were conducted as approved by the James Cook University Animal Ethics committee (approval ID: A2497).

2.3.2 Isolating primary satellite cells

Four- to six-week-old mice of each strain were euthanized with CO_2 and the hindlimb muscle excised, collected, and placed in a tube with 30 ml of sterile PBS (**Table 2.10**) and 1% penicillin/streptomycin. Each tube contained the muscles of approximately 2 mice, and 4-6 mice of each strain were used for each experiment. These muscles were then finely minced in a 10 cm dish with a number 22 scalpel blade and then transferred to a falcon tube filled to 50 ml with PBS. The muscles were centrifuged at 1,500 *g* for ten minutes and the supernatant discarded. Freshly made, filter sterilised, 0.2% collagenase solution (made in warm DMEM) was used to resuspend the muscle pellet, which was subsequently shaken at 37 °C on an orbital shaker for 60-90 minutes. This tube was filled to 50 ml with PBS and centrifuged again for ten minutes at 1,500 *g*. The supernatant was removed and replaced with 50 ml of PBS and the solution triturated for three minutes with a 10 ml pipette. This suspension was passed through a 100 µM filter into a new tube, filled to 50 ml with sterile PBS and centrifuged at 1,500 *g*. Following this, most of the supernatant was removed, leaving approximately 5 ml of solution, that was then supplied with 10 ml of warm satellite cell proliferation media (**Table 2.7**). To remove contaminating fibroblasts, the solution was then subjected to pre-plating steps and left for three hours in a cell culture incubator at 37 °C, with 5% CO_2 [277].

After three hours, the cell suspension was transferred to a new 10 cm dish, coated with 10% ECM gel dissolved in ice-cold DMEM (**Table 2.9**) and incubated for 24 hours in a cell culture incubator. Following this time, the cells were either split by trypsinisation to propagate more growth or plated immediately for subsequent experiments.

To split the cells the media was removed and replaced with 2 ml of trypsin (**Table 2.11**). This trypsin was removed immediately, and the plate placed in the 37 °C incubator for approximately one minute, until the cells came off the plate. The plates were tapped three times to dislodge the cells and checked under the microscope. 10 ml of warm satellite cell proliferation media (**Table 2.7**) was then supplied to the plates to resuspend the cells and inhibit trypsin activity, and then split between two ECM coated (**Table 2.9**) plates with an additional 5 ml proliferation media per plate. The cells were then returned to the cell culture incubator and allowed to attach.

Following this incubation time, the plates were trypsinised and counted with 1:1 trypan blue. The cells were plated at the required density.

2.3.3 Cells for protein extraction and H&E staining

6-well and 24-well plates were coated with 10% ECM gel dissolved in ice-cold DMEM (**Table 2.9**) and plated at 25,000 cells/cm^2 for protein extraction and H&E staining, respectively. For H&E staining, cells were plated on top of ECM coated (**Table 2.9**) glass coverslips (ThermoFisher Scientific – Thermanox Coverslips, cat: 174950). After the cells had adhered to the plate, the proliferation media was replaced with warm differentiation media (**Table 2.8**) and the cells were left to differentiate for 6, 12, 24 and 48 hours for protein analysis (see section 2.5.3) and 0, 24 and 48 hours for H&E (see sections 2.5.1-2.5.2).

2.4 RNA Isolation and Analysis

2.4.1 Cells for RNA isolation

To collect RNA from cells, 10 cm plates were plated at 25 000 cells/cm^2. After the cells had adhered to the plate, the proliferation media (**Table 2.7**) was replaced with the warm differentiation media (**Table 2.8**) and left to differentiate for 12- and 24-hours. At this time, the cells were washed once with PBS and trypsinised with 2 ml of warm trypsin, which was immediately removed from the cells. After the cells had dissociated, they were then collected in 5 ml of warm PBS and centrifuged at 1500 *g*. After this, the supernatant was removed from the cells and resuspended with 350 µl of RLY buffer (Meridian Isolate II RNA Mini Kit BIO-52072) and 3.5 µl of β-mercaptoethanol, and snap frozen on dry ice and stored at -80 °C until RNA isolation.

2.4.2 RNA isolation

RNA was isolated using the Meridian Bioscience ISOLATE II RNA Mini Kit (BIO-52072). Following isolation, the RNA yield and purity was checked using the Agilent RNA ScreenTape Analysis (5067-5576) on the Agilent TapeStation.

2.4.3 RNA sequencing and analysis

RNA sequencing was performed on samples by the Australian Genome Research Facility Ltd (AGRF). Sequencing was performed following TruSeq mRNA library prep, on the Illumina NovaSeq 6000 with 100 bp paired end reads, and 20 million read pairs. Primary analysis by AGRF included real time image analysis using NovaSeq Control Software (NCS) (v 1.7.0) and Real Time Analysis (RTA) (v 3.4.4). They then used the Illumina bcl2fastq 2.20.0.422 pipeline to generate the sequence data. Following this, each sample had approximately 50 million reads and an average length of 100 bp. Upon receiving the sequencing results from AGRF, the samples were run through FastQC (v 0.11.7) and MultiQC (v 1.8) to check the raw sequencing data [278, 279].

The reference genome was prepared using the GRCm39 mouse reference genome from the NCBI database. The reads were then aligned to the reference mouse genome GRCm39 (NCBI) using RSEM (v 1.3.3) [280].

Gene differential expression analysis was performed using the Bioconductor package DESeq2 (v 3.16) and results were filtered to include genes with an adjusted p-value of <0.05 [281]. Fold change is a measure that describes how much a quantity changes between two measurements and the FDR (false discovery rate) helps to eliminates potential false positives. RNA from DKO and T-cad KO cells were compared with those from the WT group to determine differentially expressed genes.

The lists of differentially expressed genes were then analysed with the **G**ene **O**ntology en**RI**chment ana**L**ysis and visua**L**is**A**tion tool (GORILLA[xii]) for Gene Ontology (GO) terms using ranked lists [282]. Ranking was performed using the Wald test statistic generated by DESeq2 that accounts for both significance values (p-value) and the direction of change (fold-change value) as this is the default statistic used for hypothesis testing when comparing two groups. This enrichment analysis used human gene nomenclature to identify the genes in these lists. The enriched terms were then further filtered for redundancy using the **RE**duce and **VI**sualise **G**ene **O**ntology (REVIGO) (v 1.8.1) tool [283].

2.4.4 Genome wide association study

A genome wide association analysis was performed using data obtained from the NCBI database of genotypes and phenotypes (dbGaP). Two separate datasets were used for this analysis (**Table 2.58**) and downloaded using Aspera Connect. Data files were extracted into usable file formats using VCFTools (v0.1.13) [284]. Further information about the study description, patient selection and data collection can be found on the NCBI dbGaP website using the accession numbers (**Table 2.58**).

[xii] GORILLA database was last updated on 6th March 2021.

Table 2.57. NCBI dbGaP datasets used in the GWAS.

Study Name	Accession Number	Samples	Study Description	Date Downloaded
Genetics of Inherited Muscle Disease[xiii]	phs000655.v3.p1	420	Patients with severe neuromuscular disease or immediate relatives of those with diseases	March 2019
Genetic Epidemiology of COPD[xiv]	phs000951.v5.p5	10355	Patients aged 45 – 80 years old with smoking history of 10+ years and with/without a diagnosis of COPD	March 2019

The association analysis was run using PLINK [v 1.9]: an open-source whole genome association toolset [285]. Sample sizes were significantly reduced due to the presence of multiallelic samples found during PLINK analysis. The analysis focused specifically on the region encompassing and directly surrounding the T-cadherin gene (82.6 Mbp – 83.8 Mbp) including any recognized promoter and enhancer regions as well as the gene itself. The output file was exported to RStudio and filtered to include SNPs with an adjusted p-value less than or equal to 0.05. Bonferroni multiple testing correction was applied and adjusted p values <0.05 deemed significant.

[xiii] We thank the Broad Institute for generating high-quality sequence data supported by NHGRI funds (grant # U54 HG003067) with Eric Lander as PI. The datasets used in this manuscript were obtained from dbGaP at http://www.ncbi.nlm.nih.gov/gap through dbGaP accession number phs000655.
[xiv] This study is part of the NHLBI Grand Opportunity Exome Sequencing Project (GO-ESP). Funding for GO-ESP was provided by NHLBI grants RC2 HL103010 (HeartGO), RC2 HL102923 (LungGO) and RC2 HL102924 (WHISP). The exome sequencing was performed through NHLBI grants RC2 HL102925 (BroadGO) and RC2 HL102926 (SeattleGO). The datasets used in this manuscript were obtained from dbGaP at http://www.ncbi.nlm.nih.gov/gap through dbGaP accession number phs000179.

2.5 Primary Myoblast Growth Analysis

Continued from section 2.3.

2.5.1 Fixing the cells prior to staining

To fix the cells for staining, the differentiation media was removed, and the wells were washed with 1 ml of PBS. Following two washes, 500 µl of fixative (**Table 2.32**) was added to each well and left for 30 seconds. After removing the fixative, the wells were washed three times with PBS and the final wash was left in the wells. The plate was sealed and stored at 4 °C for H&E staining.

2.5.2 Hematoxylin and eosin staining of coverslips

For hematoxylin and eosin (H&E) staining, PBS was removed and replaced with Mayer's Hematoxylin (ProSciTech, cat: AMH-1L) for four minutes. The hematoxylin was removed, and the wells covered with 0.1% HCl for a few seconds, and then washed with Scott's Tap Water (**Table 2.33**) five times for one minute. Counter staining was performed with 0.5% Eosin-Y (**Table 2.34**) for 30 seconds and washed with 70% ethanol for five minutes. Following the 70% ethanol wash, the wells were washed with 100% ethanol, twice, for five minutes each. The glass coverslips were then removed from the wells, placed into a glass container of xylene, and left to dehydrate for ten minutes prior to mounting with DPX mountant onto a glass slide.

2.5.3 Protein extraction

To extract protein from the cells, the cells were washed twice with ice-cold PBS and then lysed with 50-100 µl/well ice-cold complete RIPA buffer (**Table 2.27**). The plates were left on ice for 5 minutes and the lysate scraped with a rubber policeman and transferred to an Eppendorf tube. The DNA was sheared by passing the lysate through an insulin syringe, centrifuged at 4 °C, 19,000 *g* for ten minutes, and the supernatant transferred to another Eppendorf tube and stored at -80 °C.

2.5.4 SDS-PAGE gel electrophoresis

The protein concentration of the cell lysates was quantified using the Bio-Rad DC protein assay (Bio-Rad cat: 500-0116), as per the company protocol for a microtiter plate and was used to ensure equal protein loading throughout the wells. The lysates were diluted to 5 µg per 25 µl with RIPA buffer (**Table 2.23**), and 5µl of 5x SDS sample loading buffer (**Table 2.18**). For a broad size range of proteins of interest, lysates were separated using SDS polyacrylamide gel electrophoresis with a 12 well TruPAGE precast gel (4-12%, 10 x 8 cm) from Sigma-Aldrich (cat: PCG2011) and 1x running buffer (**Table 2.17**).

For a narrow size range of proteins, lysates were separated using in-house prepared SDS-PAGE gels and 1x running buffer (**Table 2.17**). Briefly, the separating gel solution (**Table 2.12** & **Table 2.14**) was made fresh and added to the space between a 1 mm BioRad spacer plate and a BioRad short glass plate. Once set, the stacking gel (**Table 2.15** & **Table 2.16**) was made fresh and added on top of the separating gel, a 10-well comb inserted and the gel allowed to set.

2.5.5 Western blotting

Following electrophoresis, the proteins were transferred onto a PVDF membrane using a wet transfer system with 1x transfer buffer (**Table 2.19**) (diluted in MilliQ water, with 10% methanol). Wet transfer was performed at 30 volts, 4 °C overnight, with constant stirring. To confirm equal loading of the proteins, the membranes were stained with Ponceau S solution (**Table 2.31**). The Ponceau staining was then removed with TBST (**Table 2.20**) and membranes blocked with 5% skim milk (**Table 2.21**) at room temperature for one hour. The membrane was then cut into strips based on the size of the protein and probed with specific primary antibodies overnight at 4 °C (**Table 2.1**). The membranes were then washed with TBST, three times, for 10 minutes each and re-blocked with 5% milk for another 15 minutes before being incubated with species specific secondary antibodies (**Table 2.3**) for one hour at room temperature. The membranes were then washed with TBST, 5 times, for 5 minutes each. The proteins of interest were detected using a homemade enhanced chemiluminescence (ECL) method (**Table 2.28**), and the Syngene detection system

[276]. To confirm equal loading in the absence of ponceau S and a loading control, the membranes were stained with Amido Black 10B (section 2.5.6).

2.5.6 Amido black staining

PVDF membranes were rinsed three times with water and placed into amido black solution (**Table 2.29**) for 5 mins. The membrane was then transferred to the de-staining solution (**Table 2.30**) and de-stained for 5 mins, three times. Finally, the membranes were rinsed with water and dried overnight.

2.6 T-cadherin's interactions *in vitro*

2.6.1 Preparation of T-cadherin overexpressing C2C12 cells

The pLN1 and T-cadherin over-expressing C2C12 (pLTcad) cells were previously derived by the Hebbard lab. Briefly, the pLEGFP-N1 vector (Clontech), was treated with Not1/BamH1 to remove EGFP, then the Klenow Fragment, and a blunt ligation performed. The T-cadherin murine cDNA (identical sequence to GenBank accession number AB022100) was used as the template to amplify DNA encoding EC1 through EC4 using forward and reverse primers with BamH1 and EcoR1 sites, respectively at the 5' ends. The cDNA was sequentially restricted with Sal1/BamH1 (Sal1 site filled using Klenow) and pLEGFP-N1 sequentially restricted with Not1/BamH1 (Not1 site filled using Klenow) to remove EGFP. The T-cadherin fragment and cut vector were ligated and colonies sequenced. Virus was produced by transfecting 293GP packaging cells with CMV-G (VSV-G envelope gene construct), pLN1 or pLTcad and Polyfect (Qiagen) for 24 hours. The medium was renewed and supernatant containing virus collected 24 and 48 hours later, filtered and stored at -80 °C. C2C12 cells were treated with virus and Polybrene (SIGMA) for 24 hours after which 400 µg/ml Geneticin (G418) was applied to select cells expressing pLN1 and pLTcad. T-cadherin expression was confirmed by western blot and pooled cells were used for all experiments.

2.6.2 Co-immunoprecipitation

1.64 x 10^6 C2C12 or pLTcad cells were seeded onto 0.5% porcine gelatine pre-coated 10 cm cell culture plates and grown for 24 hours in C1C12 growth medium (**Table 2.38**). To promote *in vitro* myogenesis the media was replaced with differentiation media (**Table 2.8**) and left to differentiate for 72 hours. Cells were then lysed in either Brij 97 lysis buffer (**Table 2.24**) or Triton X-114 lysis buffer (**Table 2.25**) as per the protocol in 2.5.3. The lysates were pooled, and DNA sheared through an insulin syringe before preclearing by centrifugation at 19,000 *g* for 10 minutes at 4 °C. To prepare the beads, protein G-sepharose beads were pre-blocked with 1% BSA in PBS and bound to appropriate antibodies (**Table 2.2**) for 2 hours at 4 °C with slow rotation. For immunoprecipitation, the lysate was incubated with the prepared protein

G-sepharose beads for four hours at 4 °C, with slow rotation. Following incubation, the beads were washed four times with lysis buffer, the final lysate was removed with a Hamilton syringe, and the beads resuspended in 1x SDS sample loading buffer (1:5 diluted 5x SDS sample loading buffer **Table 2.18**), diluted in PBS and frozen at -20 °C.

2.6.3 Stable transfection of CHO cells

Cadherin constructs were previously developed by the Hebbard lab. Briefly, the pLEGFP-N1 vector and cadherin cDNA were treated with either Sa1I/NotI (M-cadherin insert) or Not1/BamH1 (T-cadherin insert to remove GFP) and ligated with T4 DNA ligase (Promega cat: M179A).

Chinese Hamster Ovary (CHO) cells were grown in CHO growth media (**Table 2.50**), until 70-90% confluent. Following the protocol for the lipofectamine 3000 reagent (Thermo Fisher Scientific cat: L3000015), CHO cells were stably transfected with empty pLN1, T-cadherin or M-cadherin cDNA. Briefly, 5 µg of plasmid DNA was diluted in OPTI-MEM media, with 1 µl/µg lipofectamine, and 2 µl/µg of the p3000 reagent. The cells were incubated with the plasmid for 48 hours at 37 °C. The cells were washed and given fresh CHO growth media with 500 µl/µg of Geneticin (G418) antibiotic to allow for selection of transfected cells. The cells were then grown in the presence of the antibiotic until confluent and split to a new 10cm dish. From this, single colonies were isolated and transferred to a 24 well plate to grow. Expression of each cadherin was checked using western blotting.

2.6.4 Dissociation of cells to single cell culture

CHO cells overexpressing pLN1, pLTcad, and pEMcad.GFP were plated on 10 cm plates and allowed to reach 90% confluency. The cultures were rinsed twice with HMF buffer (**Table 2.52**) and treated with TC solution (**Table 2.53**) for 30 minutes on a rotary shaker (150 rpm). The cells were then collected in a 15 ml tube and centrifuged at 4 °C, 215 *g* to remove the trypsin solution. Kept on ice, the cells were then resuspended in ice-cold HCMF buffer (**Table 2.51**) and adjusted to a concentration of 10,000 cells/ml.

2.6.5 Short term aggregation assay

The CHO cells were then plated at 5,000 cell/well with 1mM calcium chloride in a 24-well plate coated with 5% BSA in PBS in the following combinations: pLN1, pLTcad, pEMcad.GFP, pLN1 and pEMcad.GFP, and pLTcad and pEMcad.GFP. The plates were then placed on a gyrating shaker at 80 rpm for 20 minutes at 37 °C. Following aggregation, each well was given an equal volume of 8% paraformaldehyde (PFA) and kept at 4 °C for imaging. Images of the entire well were taken, and aggregates were counted as small (<5 cell aggregates), medium (5-10 cell aggregates) and large (> 10 cell aggregates).

2.7 Muscle Metabolism

2.7.1 Mitochondrial respiratory capacity

These experiments were performed with C2C12 cells (pLN1 and pLTcad cells prepared as per section 2.6.1) and primary myoblasts, grown as per section 2.3.

C2C12 Cells: C2C12 cells were suspended in C2C12 growth media (**Table 2.38**) and plated into an 8-well Seahorse XFp cell culture miniplate at a density of 2500 cells/well.

Primary Myoblasts: Following the second pre-plate step, the cells were trypsinised and seeded into an 8-well Seahorse XFp cell culture miniplate, pre-coated with 10% ECM gel (**Table 2.9**), at a density of 15,000 cells/well.

Plates were prepared as per the Agilent 'Seahorse XFp Mito Stress Test Protocol', with 400 µl of PBS added to each of the moats surrounding the wells. Cells were either changed to differentiation media (**Table 2.8**) 4 hours after plating and left for 24 or 48 hours or used immediately for the 0 hours differentiation time point. Seahorse XFp sensor cartridges (Agilent Technologies, cat: 103193-100) were hydrated overnight at 37 °C in a humid, non-CO_2 incubator by adding 200 µl of MilliQ water to each of the wells and 400 µl to each of the moats surrounding the wells. One hour prior to the test the media was replaced with 180 µl of assay medium (**Table 2.39**) and the plates were incubated in a 37 °C, non-CO_2, humid incubator. The water was removed from the wells of the cartridge and replaced with 200 µl Agilent Seahorse Calibrant (Agilent Technologies, cat 103059-000) one hour prior to the assay. The hydrated cartridge and utility plate were placed into the Seahorse XFp Flux Extracellular Analyser 20 minutes prior to running the assay to calibrate the sensor probes. The utility plate was then replaced with the cell culture miniplate, and the assay was set to run as per Agilent Technologies standard 'Mitochondrial Stress test Protocol' for the XFp device. Three oxygen consumption rate (OCR) measurements were recorded prior to any injections and then after each subsequent injection of 1 µM Oligomycin, 1.5 µM FCCP and 0.5 µM antimycin/rotenone solutions (**Table 2.40**), dissolved in assay media (**Table 2.39**).

Following the assay, the assay media was removed from the cells and the cells were fixed with formal saline (**Table 2.55**) for 30 minutes. For normalization, the cells were stained with methylene blue (**Table 2.56**) for 30 minutes and washed five times with

1x borate buffer (**Table 2.54**). Once washed, the cells were then leached with 1:1 solution of ethanol: HCl and absorbance was measured at OD 655 nm. OCR readings were normalized within the Agilent WAVE software.

Figure 2.1 depicts the typical schematic representation of real time oxygen consumption rate (OCR) measurements following inhibitor injection for the Mitochondrial Stress Test. These values are used to calculate basal respiration, ATP production, proton leak, non-mitochondrial respiration, maximal respiration, and spare capacity.

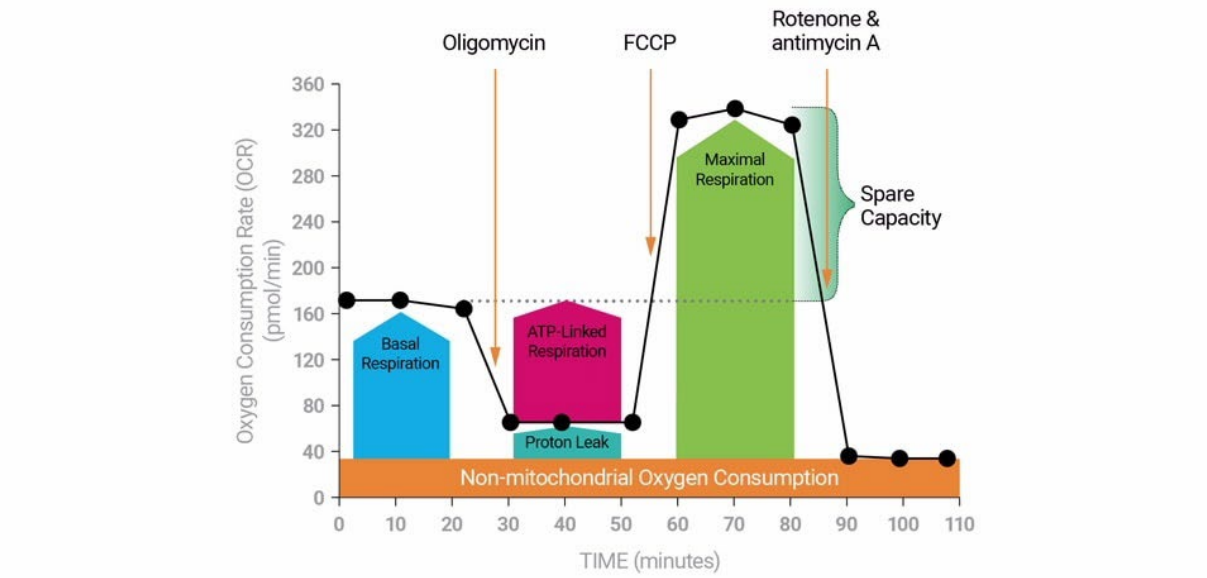

Figure 2.1. Agilent seahorse XFp Cell Mito Stress Test profile of the key parameters of mitochondrial respiration. Sequential compound injections measure basal respiration, ATP production, proton leak, maximal respiration, spare respiratory capacity, and non-mitochondrial respiration. Image taken from 'Seahorse XF Cell Mito Stress Test Kit User Guide' [3].

2.7.2 Palmitate oxidative stress test

C2C12 cells were harvested, suspended in C2C12 growth medium (**Table 2.38**) and plated into an 8-well Seahorse XFp cell culture miniplate at a density of 2,500 cells/well. Growth media was replaced four hours after plating with C2C12 differentiation media (**Table 2.8**) and the cells allowed to differentiate for 48 hours. The cell culture miniplate and Agilent Seahorse sensor cartridge were prepared as per

section 2.7.1. On the day of the assay, the differentiation media was replaced with 100 µl of substrate-limited growth medium (**Table 2.44**) and the plates were incubated in a 37 °C, 5% CO_2 incubator. Following 6 hours incubation, the media was replaced with 150 µl of assay medium (**Table 2.45**) and the plates were incubated in a 37 °C, non-CO_2 incubator for one hour. Just prior to the assay, the cells were provided with either 30 µl of BSA (**Table 2.41**) or BSA-conjugated palmitate (**Table 2.43**) and the Seahorse XFp analyser was set to run as per the Agilent Technologies standard 'Mitochondrial Stress test Protocol' for the XFp device. Six OCR measurements were recorded prior to any injections and three measurements were taken after each subsequent injection of 1 µM Oligomycin, 1.5 µM FCCP and 0.5 µM antimycin/rotenone solutions (**Table 2.40**), dissolved in assay media (**Table 2.45**).

2.7.3 Mitochondrial isolation from cells

C2C12 cells, isolated from approximately 20 confluent plates, were scraped using a rubber policeman in 5 ml of mitochondrial isolation buffer (**Table 2.46**) with protease inhibitors (**Table 2.27**). Cells were then mechanically disrupted by passing through a 26-gauge needle and centrifuged at 600 g for 5 minutes. The pellet (nuclear fraction) was discarded, and the supernatant fraction (cytosolic and mitochondrial proteins) was collected and centrifuged again at 8,000 *g* for 15 minutes to pellet the mitochondria. The pellet was then washed once by resuspending in mitochondrial isolation buffer and centrifuging at 8,000 *g* for 15 minutes. Finally, the pellet (mitochondrial fraction) was lysed in RIPA buffer containing protease inhibitors (**Table 2.27**). The lysates were then run through a 12% SDS-PAGE gel and probed with the abcam OXPHOS antibody cocktail (**Table 2.1**), followed by a secondary HRP-linked antibody for visualization (see section 2.5.4 and 2.5.5)

2.7.4 FACS analysis of mitotracker green FM-stained myoblasts

C2C12 and murine myoblasts were seeded at a density of 15,000 cells/cm^2 onto 6-well plates. The next day, myoblasts were stained with 150 nM MitoTracker Green FM for 20 minutes at 37 °C in the dark, trypsinised and collected in conical tubes. Cell pellets from three biological replicates were resuspended in PBS and FACS analysis was performed immediately using the FITC channel of a FACS Fortessa flow cytometry

system (BD Biosciences). The FITC signal was recorded from the unstained cells to obtain a background signal and a total of 10,000 events from each of the three technical replicates per experimental group was detected. The background signal was subtracted from the average of each group and the mean was represented as mean fluorescence intensity (MFI).

2.8 Mouse Muscle Injury and Regeneration

2.8.1 Intramuscular injection

Mice were anaesthetised with isoflurane and their left-hand side hind limb was shaved and cleaned with 70% ethanol. Using a clean long Hamilton Syringe 0.15 µg (10 µl @ 15 µg/ml) of Notexin (Latoxan Laboratory, France) was injected longitudinally through the entire tibialis anterior (TA) muscle. The incision was then sealed with a 'liquid skin' skin glue. The mice were then allowed to recover from the anaesthesia and monitored daily until sacrifice. Following a recovery time of 2, 3, 7, and 10 days, the mice were euthanized by CO_2 asphyxiation, and both hind limb TA muscles embedded in optimum cutting temperature (OCT) compound using liquid nitrogen cooled isopentane for myofiber cross-sectional area analysis. Transverse serial sections (6 µm) were cut from the mid region of the embedded TA muscles were dissected using a Cryotome (Thermo Fisher Scientific), mounted on glass microscope slides and stored at -80 °C for staining.

2.9 Cross Sectional Analysis of Muscle Fibres

2.9.1 Immunofluorescence

Cryosections of muscle tissue, frozen on glass microscope slides, were thawed at room temperature for 30 minutes. Using a wax pen, a border was drawn around each of the sections before fixing with either 4% paraformaldehyde solution in PBS for 10 minutes, or ice-cold acetone (for CD68 staining) for 30 minutes. The sections were washed three times in PBS and blocked and permeabilised with 0.1% Triton X-100, 1% sucrose, 5% BSA, and 3/100 Fab Donkey anti-mouse fragments (Jackson ImmunoResearch) in PBS for one hour. The sections were washed three times in PBS and probed with the appropriate antibodies (**Table 2.4**) in 5% BSA/PBS overnight in a light protected container. Following the removal of the primary antibody, the sections were washed three times in PBS and probed with the appropriate fluorescent conjugated secondary antibody and DAPI (1:1,000) for one hour at room temperature in a light protected container (**Table 2.5**). The secondary antibody was removed, and the sections washed three times with PBS, and once with water, before being allowed to dry. The sections were mounted with anti-fade mounting media and a glass coverslip.

2.9.2 Muscle fibre typing

Once thawed, the muscle sections were incubated with 1:25 dilutions of each of the myosin heavy chain antibodies (**Table 2.4**) overnight at 4 °C. The sections were then washed three times with 1x PBS to remove the non-specifically bound primary antibody and were then fixed with 10% buffered formalin (**Table 2.47**) for 5 minutes and washed three times with 1x PBS. The biotinylated secondary anti-mouse IgG antibody, diluted 1:200 in diluent (**Table 2.49**), was then applied to the sections for one hour at room temperature. The sections were washed three times in 1x PBS and incubated with streptavidin Alexa Fluor 488 conjugate tertiary antibody, diluted 1:400 in 0.2% BSA and 0.1% PBS-Tween 20, for one hour at room temperature in the dark. The sections were washed with 1x PBS, incubated with DAPI diluted 1:1,000 in PBS for 5 minutes and washed again with 1x PBS. After completely drying the sections,

they were mounted with ProLong Gold Antifade mounting solution. The fluorescent stained sections were kept in a dark box following experiment end.

2.9.3 Sirius red staining protocol

The muscle sections were thawed at room temperature for 30 minutes, and then fixed in 4% paraformaldehyde/PBS solution for 10 minutes. The sections were then stained with picrosirius red (**Table 2.35**) for one hour at room temperature, then washed in two changes of acidified water (**Table 2.36**) and dehydrated in three changes of 100% ethanol. The stained sections were cleared in xylene and mounted with DPX mounting media.

2.9.4 H&E staining of muscle sections

For H&E staining of the TA muscle sections the glass slides were 'dipped' into each of the reagents as follows. The slides were stained with hematoxylin for one minute, Scott's tap water (**Table 2.33**) for two minutes, and Eosin-Y (**Table 2.34**) for two minutes. The slides were rinsed with tap water following each stain. Using increasing concentrations of ethanol (50%, 70%, 95% and 100%) the slides were then dehydrated before being cleared with Xylene and mounted with DPX mounting media.

2.10 Statistical Analysis

Statistical analyses were performed with GraphPad Prism 9 (GraphPad Software Inc). Students two-tailed t-test were conducted for statistical analyses to assess the differences between two experimental groups. A one-way ANOVA and Bonferroni's correction for multiple comparisons was applied for analyses of more than two statistical groups. Error bars represent standard error of the mean (SEM) unless otherwise stated. *$p<0.05$, **$p<0.01$, ***$p<0.001$, ****$p<0.0001$ denote significance levels used within the analysis.

3 *In silico* analysis of T-cadherin in Skeletal Muscle Disease

3.1 Introduction

The advancement of sequencing technologies in the last decade has vastly improved the value of performing genetic studies when researching diseases. Genome wide association studies (GWAS) involve scanning for markers across the genome of subjects with and without a specific disease to locate genetic variations associated with disease. This can lead to the discovery of genetic markers that can be used to detect, treat, or even to prevent disease.

To date SNPs have been identified within the T-cadherin gene (*CDH13*) that associate with various metabolic diseases (see section 1.8.5). In many populations, SNPs within this gene are associated with decreased levels of APN and metabolic syndrome. The purpose of part one of this chapter was to analyse the genomes of patients with genetically inherited muscle disorders to uncover disease causing variants within *CDH13*.

The development of high throughput sequencing has revolutionized our understanding of transcriptomics. Sequencing the genome can provide a more detailed and quantitative view of gene expression, alternative splicing, and allele specific expression. RNA sequencing is a technique used to examine the quantity and sequences of RNA and can be used to identify genes, or groups of genes, that are differently expressed between different experimental groups.

Researchers can identify strongly associated genes and investigate them as potential drug targets, or targets for genetic manipulation. This form of research lays the groundwork for personalized medicine. The second part of this chapter utilises RNA sequencing to identify genes affected by the absence of T-cadherin signalling that may be involved in muscle hypertrophy. The identification of such genes may provide downstream targets that could be manipulated to increase muscle regeneration in patients with muscle atrophy.

3.2 Preliminary data and aims

Initial studies showed a significant difference in growth and differentiation between wild-type (WT) and T-cadherin/Adiponectin double knockout (DKO) myoblasts (see chapter one section 1.10). These results show that the DKO myoblasts are committing to myogenesis sooner and fusing to form myotubes more rapidly than WT myoblasts. Initial RNA sequencing experiments performed as a part of my Honours research focussed on discovering any genetic differences between adult muscle tissue isolated from WT and DKO mice (data not shown). The analysis showed only 35 differentially expressed genes between the two groups. Furthermore, initial findings regarding mouse body weight and individual hindlimb muscle weight indicated that there is no phenotypic difference between the overall weight or muscle weight of the mice (see section 1.10). These findings suggest that any differences seen in primary myoblast growth do not affect healthy adult muscle tissue. In addition, studies examining mutations within the T-cadherin gene suggested a correlation with diseases such as type 2 diabetes and obesity. However, in the context of myopathies, there is limited research examining the role of T-cadherin. The studies described in this chapter intended to achieve the following:

1. Perform a genome wide association study (GWAS) to determine the relationship between T-cadherin mutations and disease.
2. Understand the differences in gene expression between WT and DKO differentiating myoblasts.

3.3 Methods

For complete methods please see chapter 2 section 2.4.

3.3.1 Searching for disease variant associations within the T-cadherin gene

Briefly, a genome wide association analysis was performed using data obtained from the NCBI database of genotypes and phenotypes (dbGaP). The analysis focused solely on the region encompassing and surrounding the T-cadherin gene (82.6 Mbp – 83.8 Mbp) and included promoter and enhancer regions. Two separate datasets were used for this analysis: 'Genetics of Inherited Muscle Disease' (phs000655.v3.p1), and 'Genetic Epidemiology of COPD (COPDGene)' (phs000179.v6.p2.c1). The association analysis was run using PLINK [v 1.9], an open-source whole genome association toolset.

3.3.2 RNA sequencing and differential expression analysis

For RNA sequencing analysis, total RNA was isolated from murine myotubes differentiated for 12- and 24-hours from WT, DKO, and T-cad KO mice. This study was conducted separately to the RNA sequencing from my honours research (mentioned in section 3.2) which focussed on RNA isolated from adult murine muscle tissue rather than differentiating primary myoblasts. This RNA was checked for purity and sent to the Australian Genomic Research Facility (ARGF) for RNA sequencing. The results generated from the RNA sequencing of the three genotypes were used to perform a differential expression analysis. This analysis was performed using RSEM (v 1.3.3) [280] and DESeq2 (v 1.38.1) [281]. This list of genes was then run through GORILLA[xv] [282] and REVIGO (v 1.8.1) [283] to identify enriched GO terms.

[xv] GORILLA database was last updated on 6th March 2021.

3.4 Results

3.4.1 Genome wide association study

A GWAS was conducted on two datasets: one focusing on patients with inherited muscle diseases and the other on patients with COPD. The analysis for the dataset 'Genetics of Inherited Muscle Disease' was based on a comparison of 33 cases and 18 controls and found 2 SNPs with a p-value <0.05, but no significant SNPs following a Bonferroni correction for multiple testing (**Figure 3.1**). Bonferroni correction is used when multiple tests are conducted simultaneously and only deems a score significant if the corresponding p-value is less than or equal to 0.05 divided by the number of tests performed [286]. Unfortunately, many of the samples from the original dataset were removed during PLINK analysis as they did not pass quality assurance checks. The two SNPs with an uncorrected p-value < 0.05 were not variants of any

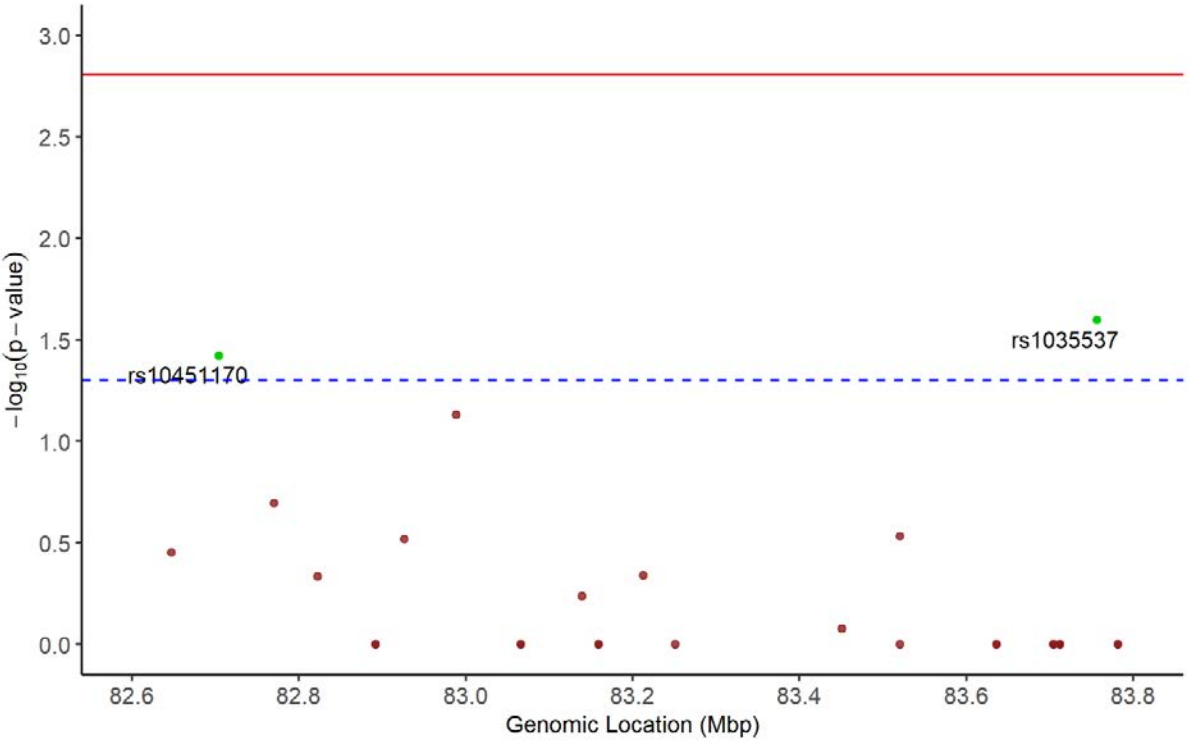

Figure 3.1. Association analysis for single nucleotide polymorphisms within the T-cadherin gene (*CDH13*) for inherited muscle disease. Each point represents a SNP and its corresponding chi-squared calculated p-value, green points show SNPs that had a p-value greater than 0.05. The two lines indicate significance values; the blue line is an uncorrected significance value of 0.05, while the red line indicates the significance line after Bonferroni correction for multiple testing.

known clinical significance when searched through the NCBI database of SNPs (dbSNP).

The same analysis was performed on the dataset obtained for COPD patients which included 501 cases and 493 controls. This analysis found 71 SNPs with a p-value < 0.05, and 1 SNP (rs7206590) with a Bonferroni corrected p-value <0.05 (**Figure 3.2**). These SNPs did not present as variants of any known clinical significance when searched through the NCBI database 'dbSNP'. A region of interest, surrounded by the dashed lines, is located at the far end of the T-cadherin gene, and features many SNPs with an uncorrected p-value < 0.05. Although there was only one SNP that passed Bonferroni correction, the fact that there is a peak of SNPs here suggests that variants in this region may associate with the muscular phenotypes present in COPD patients. As there are currently no publications linking these SNPs with any clinical significance, further research is required.

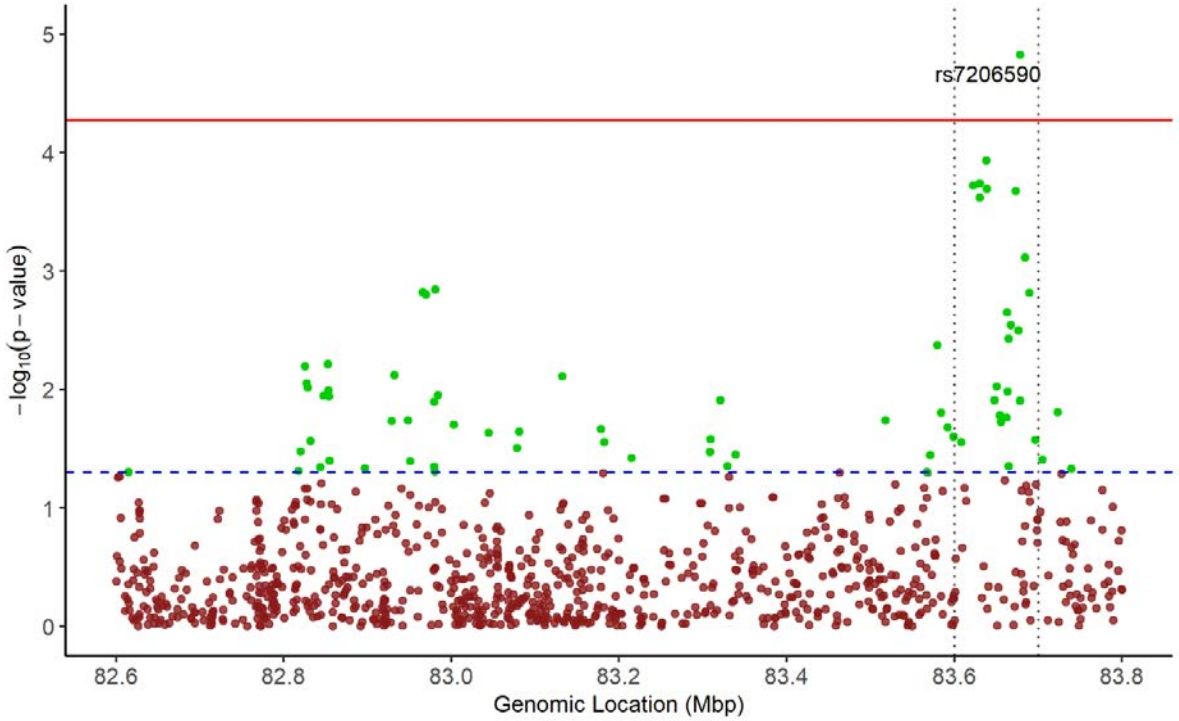

Figure 3.2. Association analysis for SNPs within the T-cadherin gene (*CDH13*) for COPD. Each point represents a SNP and its corresponding chi-squared calculated p-value, green points show SNPs that had a p-value greater than 0.05. The two-coloured lines indicate significance values; the blue dashed line is an uncorrected significance value of 0.05, while the red line indicates the significance line after Bonferroni correction for multiple testing. The vertical dotted lines border a region of interest.

3.4.2 Differential gene expression

The following sections describes the results obtained from RNA sequencing and differential gene expression analysis on WT, DKO and T-cadherin (T-cad) KO primary myoblasts at 12- and 24-hours differentiation.

3.4.2.1 Principal component analysis

Gene expression was quantified for two replicates of the three genotypes (WT, DKO and T-cad KO) from primary myoblasts 12- and 24-hours post differentiation. Principal component analysis of the gene expression data showed two distinct groups for the 12- and 24-hour samples (**Figure 3.3**). Most of the 12-hour samples were in a tight formation, except one WT 12-hour sample that appeared distinct from the others. This, along with data from a quality control check, suggested that this sample represented a failed library prep and could not be used for further analysis (quality control data not shown). As a result of removing this sample, the bioinformatic analysis could not be completed for the 12-hour RNA sequencing due to insufficient controls.

Focusing only on the 24-hour data set, the DKO samples are distinct from the other genotypes. The duplicate samples were all situated together, indicating little variation

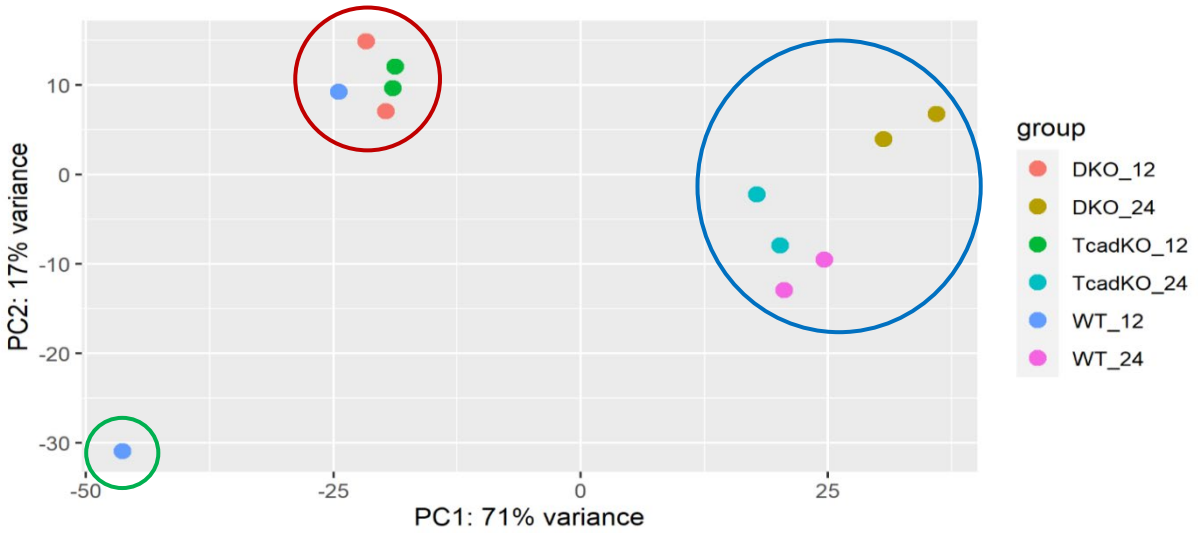

Figure 3.3. Principal component analysis of reads from each of the samples processed for RNA-sequencing. The red and blue circled groups highlight the 12- and 24-hours post-differentiation groups, respectively, and the green circled group highlights the 12-hour WT sample identified as an outlier.

between the replicate samples. The WT and T-cad KO samples also clustered together and were likely to have little difference between them.

3.4.3 Differentially expressed genes

A Venn diagram was generated of differentially expressed genes (DEGs) for each comparison: T-cad KO versus WT, DKO versus WT, and DKO versus T-cad KO (**Figure 3.4**). The majority of the differentially expressed genes were found between the WT and T-cad KO samples compared with the DKO. This analysis revealed 3908 significant DEGs in the DKO versus WT samples, 3556 genes in the DKO versus T-cad KO samples, and just 31 DEGs between the T-cad KO and WT samples. A total of 57.48% (2725) of the DEGs were shared between the DKO versus WT and the T-cad KO versus DKO comparison, and 0.23% of these were common to all

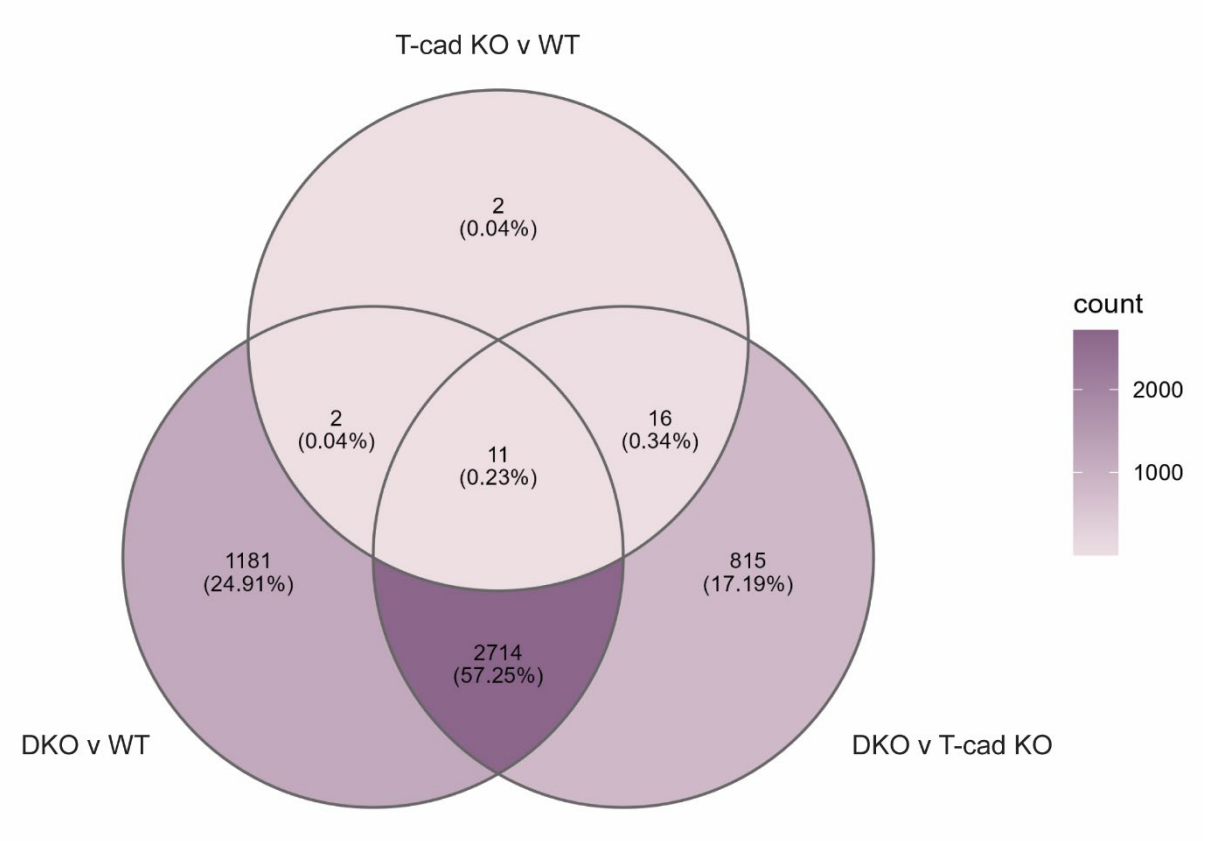

Figure 3.4. Venn diagram of differentially expressed genes between each of the genotypes. Significantly differentially expressed genes ($p < 0.05$) were extracted using DESeq2 for T-cad KO versus WT (top), DKO versus WT (left) and DKO versus T-cad KO (right).

comparisons. Out of the 31 DEGs in the T-cad KO versus WT comparison, only two were unique. The top 10 up- and down-regulated genes for each comparison are listed in **Table 3.1**, **Table 3.2** and **Table 3.3** below.

3.4.3.1 DKO versus WT myoblasts

Fold-change, DESeq2's wald statistic ('Stat') and significance of the top 10 up- and down-regulated genes for the DKO versus WT comparison are listed in **Table 3.1**. Of the 10 upregulated genes in the DKO, many are involved in muscle structure (*Col2a1, Acta1, Pcyt2, Hspg2* and *Zyx*) and metabolism (*Mvd* and *Isyna1*). Most of the down-regulated genes were either guanylate-binding proteins (GBPs) or interferon-induced very large GTPases – two of the four families of interferon-induced GTPases vital for autonomous immunity.

Table 3.1. Top 10 up- and down-regulated genes in DKO versus WT myoblasts. Results have been sorted by the wald statistic ("Stat") given by DESeq2. The 'Log2 FC' represents the log-ratio of a gene's expression value. The p-value (adj) represents the adjusted p-value for significance testing. 'Up' and 'Down' represent genes up- and down-regulated in the DKO cells.

		Gene ID	Gene Name	Log2 FC	Stat	P-value (adj)
Up	1	*Mvd*	Mevalonate Diphosphate Decarboxylase	1.927	8.735	3.10E-14
	2	*Hspg2*	Heparan Sulphate Proteoglycan 2	1.707	8.629	3.92E-14
	3	*Isyna1*	Inositol-3-phosphate synthase enzyme	1.759	8.450	9.24E-14
	4	*Ptov1*	Prostate tumour-overexpressed gene 1	1.981	8.247	4.12E-13
	5	*Zyx*	Zyxin	1.554	8.091	1.25E-12
	6	*Col2a1*	Collagen type II alpha 1 chain	1.557	7.991	2.43E-12
	7	*Acta1*	Skeletal alpha (α)-actin	1.602	7.916	3.88E-12
	8	*Pcyt2*	CTP: Phosphoethanolamine Cytidylyltransferase	1.138	7.809	8.15E-12
	9	*Tmem132a*	Transmembrane Protein 132A	1.791	7.676	2.05E-11
	10	*Rpl28*	Ribosomal Protein L28	1.584	7.666	2.05E-11
Down	1	*Gbp9*	Guanylate-binding protein 9	-1.625	-8.543	5.55E-14
	2	*Gbp6*	Guanylate-binding protein 8	-1.650	-5.838	5.25E-07
	3	*Adamts12*	ADAM metallopeptidase with thrombospondin type 1 motif 12	-0.980	-5.479	2.64E-06
	4	*Rbfox1*	RNA binding Fox-1 homolog 1	-1.081	-5.444	3.11E-06

	5	*Kitl*	KIT ligand	-1.187	-5.404	3.69E-06
	6	*Gvin1*	Interferon-induced very large GTPase 1	-1.506	-5.353	4.58E-06
	7	*Cd93*	CD93 protein	-0.935	-5.279	6.30E-06
	8	*Samd9l*	Sterile alpha motif domain containing 9 like	-1.273	-5.213	8.49E-06
	9	*Gvin2*	Interferon-induced very large GTPase 2	-1.351	-5.085	1.42E-05
	10	*Gbp4*	Guanylate-binding protein 4	-1.116	-5.044	1.70E-05

3.4.3.2 T-cad KO versus WT myoblasts

The list of the top 10 up- and down-regulated genes, the log2 fold change, DESeq2 stat value and adjusted p-value found in the T-cad KO versus WT comparison are listed in **Table 3.2**.

Table 3.2. Top 10 up and all 8 down-regulated genes in T-cad KO versus WT differentiating cells. Results have been sorted by the wald statistic ("Stat") given by DESeq2. The 'Log2 FC' represents the log-ratio of a gene's expression value. The p-value (adj) represents the adjusted p-value for significance testing. 'Up' and 'Down' represent genes up- and down-regulated in the T-cad KO cells.

		Gene ID	**Gene Name**	**Log2 FC**	**Stat**	**P-value (adj)**
Up	1	*Angpt2*	Angiopoietin 2	0.847	6.095	1.44E-05
	2	*Egr1*	Early growth response 1	1.235	5.538	2.01E-04
	3	*Fabp4*	Fatty acid binding protein	1.109	5.310	4.80E-04
	4	*Emcn*	Endomucin	1.048	5.117	8.48E-04
	5	*Cd93*	CD93	0.877	5.110	8.48E-04
	6	*Pecam1*	Platelet and endothelial cell adhesion molecule 1	0.945	4.894	0.002
	7	*Crim1*	Cysteine rich transmembrane BMP regulator 1	0.671	4.731	0.004
	8	*Adgrf5*	Adhesion G-protein-coupled receptor F5	0.807	4.713	0.004
	9	*Edn1*	Endothelin 1	0.850	4.641	0.005
	10	*Cdh5*	Cadherin 5	0.842	4.554	0.006
Down	1	*Loc118568103*	Gm53826 predicted gene	-5.867	-4.587	0.006
	2	*Csrp3*	Cysteine and glycine rich protein 3	-0.633	-4.415	0.008

3	*Loc118568417*	Rho-related BTB domain-containing protein 1	-6.213	-4.147	0.019
4	*Loc118568335*	Unknown	-6.034	-4.056	0.027
5	*Cemip*	Cell migration inducing hyaluronidase 1	-0.715	-3.972	0.034
6	*Gm33198*	PPP4r3b protein phosphatase 4	-5.146	-3.966	0.034
7	*Gm6958*	Gm6958 predicted gene	-5.360	-3.927	0.039
8	*Gm52090*	Unknown	-6.308	-3.905	0.041

Given that there were only 31 DEGs between the T-cad KO versus WT myoblasts, there was minimal fold change of the up-regulated genes in this dataset. A total of 23 genes were up-regulated, and 8 genes down-regulated in the T-cad KO samples. Of the up-regulated genes, two are involved in muscle growth and differentiation (*Angtp2* and *Egr1*), and three in angiogenesis (*Emcn, Edn1,* and *Adgrf5*). Most of the down-regulated genes were predicted genes and have limited published information available, except *Csrp3* and *Cemip* that function within the cytoskeleton and ECM, respectively.

3.4.3.3 DKO versus T-cad KO myoblasts

Fold-change, DESeq2's wald statistic ('Stat') and the significance value of the top 10 up- and down-regulated genes for the DKO versus T-cad KO comparison are listed in **Table 3.3**. Of the top 10 genes up-regulated in the DKO, four were also found up-regulated in the DKO myoblasts in the DKO versus WT comparison (*Acta1, Isyna1, Hspg2* and *Mvd*). There were also three additional genes up regulated that were involved in muscle structure and function (*Ckm, Flnc* and *Obscn*). Of the top 10 down-regulated genes, five were up-regulated in the T-cad KO versus WT comparison (*Angpt2, Cd93, Adgrf5, Fabp4* and *Emcn*) and two were also found down-regulated in the DKO versus WT sample (*Gvin1* and *Cd93*).

Table 3.3. Top 10 up- and down-regulated genes in the DKO cells versus the T-cad KO differentiating cells. Results have been sorted by the wald statistic ("Stat") given by DESeq2. The 'Log2 FC' represents the log-ratio of a gene's expression value. The p-value (adj) represents the adjusted p-value for significance testing. 'Up' and 'Down' represent genes up- and down-regulated in the DKO cells.

		Gene ID	Gene Name	Log2 FC	Stat	P-value (adj)
Up	1	*Acta1*	Skeletal alpha (α)-actin	1.829	9.036	5.33E-16
	2	*Thop1*	Thimet oligopeptidase 1	1.874	8.968	7.92E-16
	3	*Isyna1*	Inositol-3-phosphate synthase enzyme	1.861	8.942	8.35E-16
	4	*Ckm*	Creatine kinase M-type	2.003	8.768	3.42E-15
	5	*Hspg2*	Heparan Sulphate Proteoglycan 2	1.730	8.744	3.71E-15
	6	*Rab3il1*	RAB3A interacting protein like 1	1.527	8.710	4.01E-15
	7	*Mvd*	Mevalonate Diphosphate Decarboxylase	1.822	8.300	8.59E-14
	8	*Flnc*	Filamin C	1.383	8.077	5.12E-13
	9	*Obscn*	Obscurin	1.464	8.059	5.62E-13
	10	*Ptov1*	Prostate tumour-overexpressed gene 1	1.927	8.052	5.63E-13
Down	1	*Angpt2*	Angiopoietin 2	-1.455	-10.351	2.74E-21
	2	*Cd93*	CD93 protein	-1.812	-10.350	2.74E-21
	3	*Adgrf5*	Adhesion G-protein-coupled receptor F5	-1.656	-9.490	1.01E-17
	4	*Fabp4*	Fatty acid binding protein 4	-1.857	-8.723	3.95E-15
	5	*Apln*	Apelin	-1.725	-8.698	4.05E-15
	6	*Flt1*	Fms related receptor tyrosine kinase 1	-1.650	-8.587	9.79E-15
	7	*Gvin1*	Interferon-induced very large GTPase 1	-2.354	-8.484	2.20E-14
	8	*Adamts12*	ADAM metallopeptidase with thrombospondin type 1 motif 12	-1.508	-8.466	2.38E-14
	9	*Emcn*	Endomucin	-1.748	-8.410	3.59E-14
	10	*Mylk*	Myosin light chain kinase	-1.321	-7.988	9.02E-13

3.4.3.4 Differentially expressed genes common to all genotypes

There were 11 common DEG shared between the three comparisons (**Table 3.4** and **Figure 3.4**). They are involved in angiogenesis and cell adhesion. Generating a heat map for visualisation and using WT as the control, all 11 genes are upregulated in the T-cad KO cells and downregulated in the DKO cells. Interestingly, the angiogenic and cell adhesion genes are down-regulated in the DKO but are up-regulated in T-cad KO cells (**Figure 3.5**).

Table 3.4. The 11 genes differentially expressed between all three genotypes and the biological processes with which they are involved.

	Gene ID	Gene Name	Biological Process
1	*Adgrf5*	Adhesion G protein-coupled receptor F5	Angiogenesis
2	*Adgrl4*	Adhesion G protein-coupled receptor L4	Angiogenesis
3	*Angpt2*	Angiopoietin 2	Angiogenesis Cell adhesion
4	*Apln*	Apelin	Angiogenesis
5	*Cd24a*	CD24 molecule	Cell adhesion
6	*Cd93*	CD93 molecule	Cell adhesion
7	*Crim1*	Cysteine rich transmembrane BMP regulator 1	Motor neuron differentiation Angiogenesis
8	*Emnc*	Endomucin	Angiogenesis Cell adhesion
9	*Fabp4*	Fatty acid binding protein 4	Metabolism
10	*Flt1*	Fms related receptor tyrosine kinase 1	Angiogenesis
11	*Itga1*	Integrin subunit alpha 1	Cell adhesion

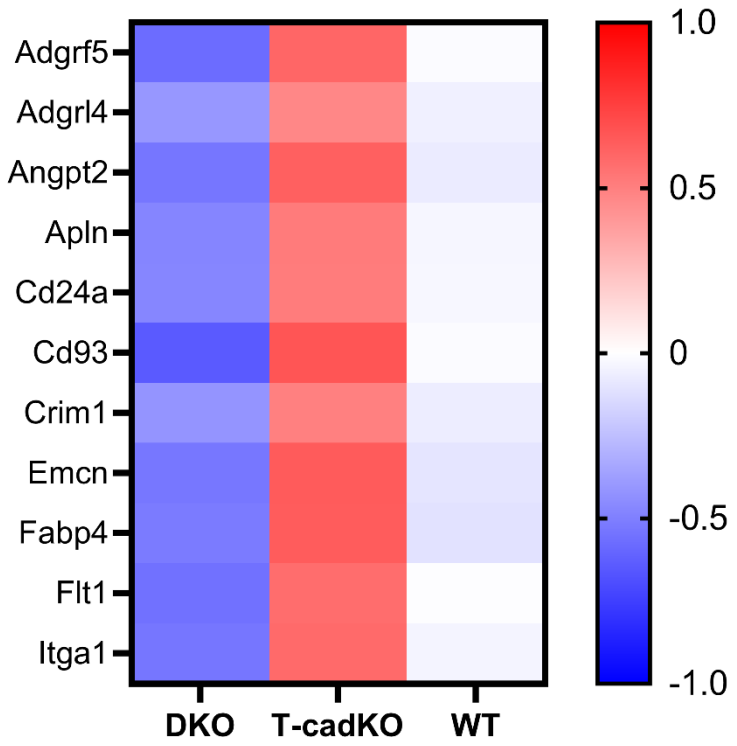

Figure 3.5. Heatmap of the 11 common differentially expressed genes between WT, DKO and T-cad KO myoblasts. Values are log2 fold-changes from the mean and were normalised with variance stabilising transformation. Each row represents a separate gene, sorted in alphabetical order.

3.4.4 Gene ontology

To visualise the differentially expressed genes identified by these analyses, multiple enrichment steps were performed. For each of the genotype comparisons, the significantly expressed genes were analysed with the GORILLA tool for Gene Ontology (GO) 'biological processes', 'molecular function', and 'cellular components' terms. The enriched terms were then further filtered for redundancy using the REVIGO tool.

The first comparison of GO terms considered differences between DKO and WT cells (**Figure 3.6**). In considering the biological processes GO terms, the DKO cells had altered expression of genes involved in three main areas: metabolic pathways, muscle system pathways and adhesion pathways. The metabolic pathways involved the GO terms 'respiratory chain pathways', 'pyruvate synthesis', 'NADH metabolism and regeneration', and 'generation of precursor metabolites' (**Figure 3.6** A). The enriched

biological processes GO terms also included ‘muscle system processes’, ‘muscle contraction’ and ‘active filament-based movement’. Aside from the broad ‘animal organ development’ term, the next most enriched biological processes term, with over 4% of the DEGs, was ‘cell adhesion’. Similarly, the enriched molecular function GO terms included ‘structural constituent of muscle’ and ‘cell adhesion molecule binding’ (**Figure 3.6** B). The main enriched cellular components in the DKO were like the enriched biological processes terms and included genes involved in the ‘respiratory chain complex’, ‘NADH dehydrogenase complex’ and ‘cytoskeleton’. Interestingly, there were also a high percentage of genes (> 5%) involved in ‘cell junction’, ‘anchoring junction’, and ‘adherens junction components’ (**Figure 3.6** C).

The second comparison of GO terms considered differences between DKO and T-cad KO cells. This revealed enriched biological processes terms like ‘respiratory electron transport chain’, ‘pyruvate synthesis’, ‘creatine metabolic processes’, ‘ATP metabolic processes’ and ‘NADH metabolic processes’ (**Figure 3.7** A). This analysis also shows biological processes terms involved in ‘muscle system processes’, ‘muscle contraction’, ‘actin filament-based movement and sliding’, and ‘regulation of myotube differentiation’. For the molecular function terms, ‘actin binding’, ‘NADH dehydrogenase activity’ and ‘creatine kinase activity’ were all enriched in this analysis (**Figure 3.7** B). Enriched cellular component terms included ‘sarcolemma’, ‘z-disc’ and ‘contractile fibres’, and metabolic components like ‘respiratory chain complex’ and ‘NADH dehydrogenase complex’ (**Figure 3.7** C).

There was an insufficient number of DEGs between the T-cad KO and WT genotypes to identify enriched GO terms.

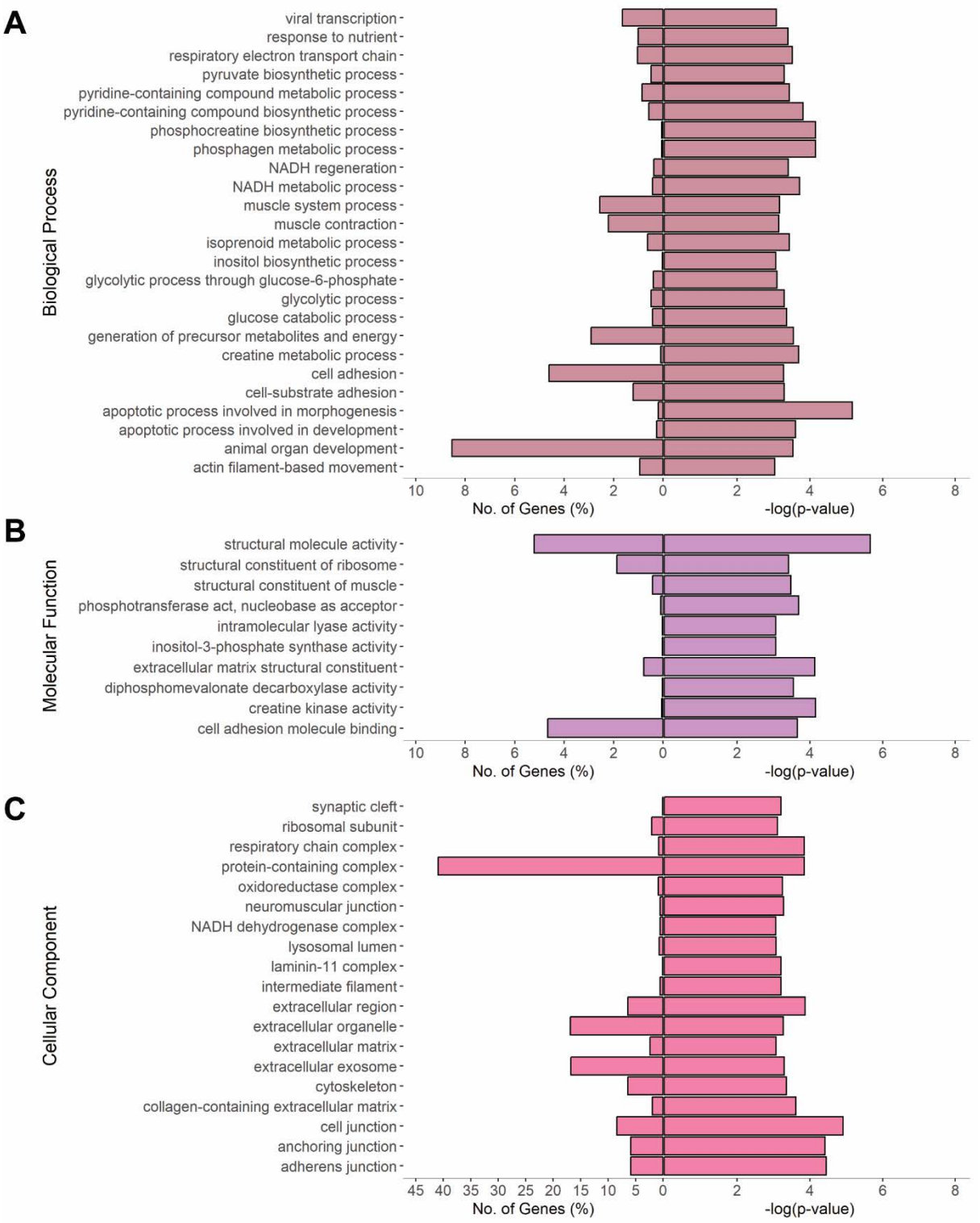

Figure 3.6. Enriched GO terms in the DKO versus WT comparison. **A.** Biological Processes, **B.** Molecular Function and **C.** Cellular Components. "No. of Genes (%)" represents the number of genes found enriched in the GO term as a percentage of the total number of differentially regulated genes. The -log(p-value) is the negative log of the enrichment p-value computed by REVIGO.

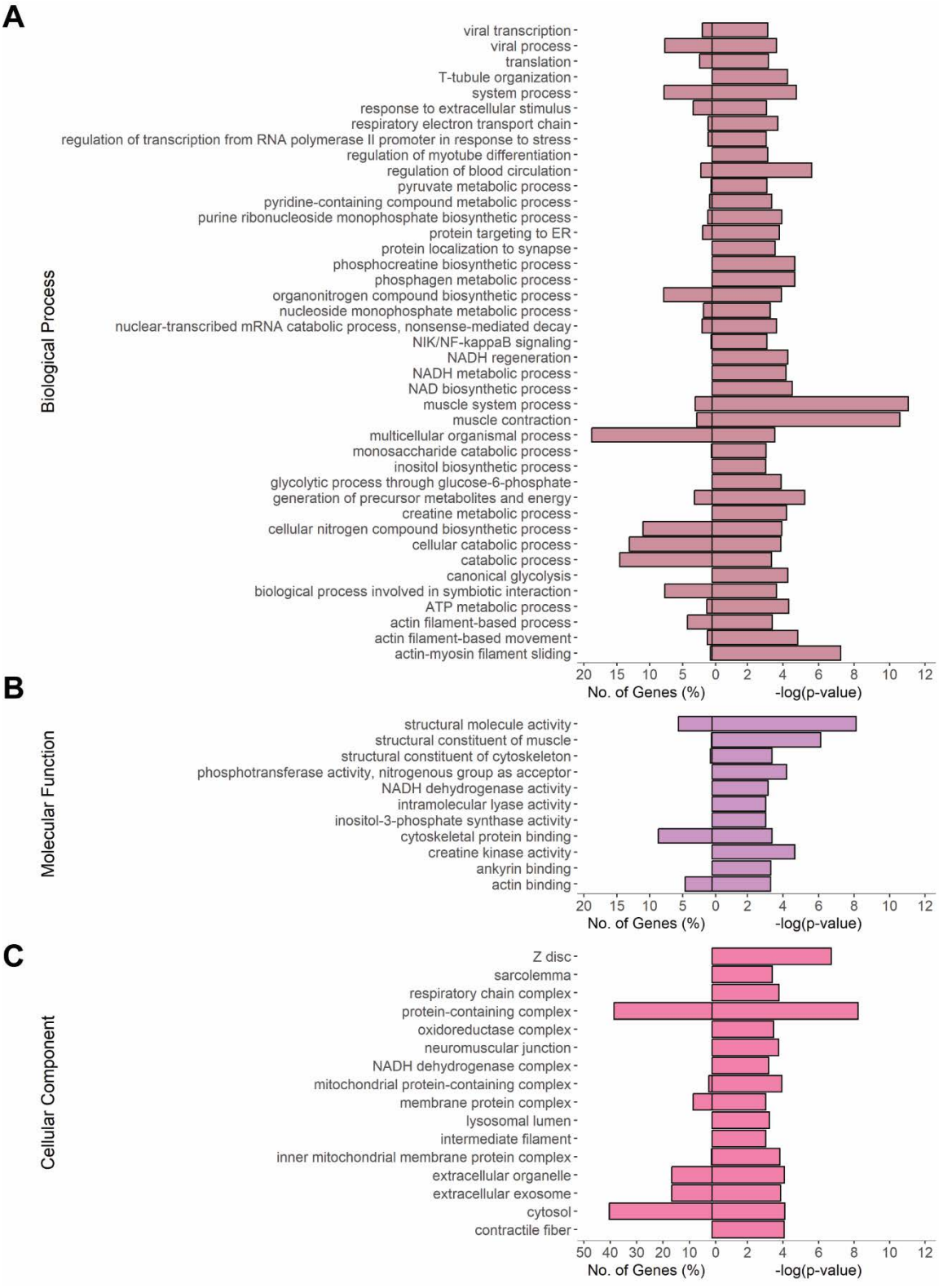

Figure 3.7. Enriched GO terms in the DKO versus T-cad KO comparison. **A.** Biological Processes, **B.** Molecular Function and **C.** Cellular Components. "No. of Genes (%)" represents the number of genes found enriched in the GO term as a percentage of the total number of differentially regulated genes. -log(p-value) is the negative log of the enrichment p-value computed by REVIGO.

3.4.5 Enriched GO terms

Based on the results of the GO analysis, it was important to isolate these terms to determine specifically which genes are involved and how they were differently expressed between each genotype. To do this, heatmaps were generated based on the genes involved in relevant biological processes GO terms for this study. Gene lists for each GO term were sourced from the list of annotations from the Jackson Laboratory 'Mouse Genome Informatics'.

3.4.5.1 Enriched metabolic terms

Heatmaps were generated for two metabolic pathways: 'NADH regeneration' (GO term ID: 0006735) and 'APN-activated signalling pathway' (GO term ID: 0033211) (**Figure 3.8**). All genes classed with the 'NADH regeneration' GO term appeared to be upregulated in the DKO myoblasts compared to the other genotypes. They include glycolytic enzymes such as aldolase, enolase, glyceraldehyde-3-phosphate dehydrogenase, glucose-6-phosphatase, phosphofructokinase, and pyruvate kinase (**Figure 3.8** A).

For the 'APN-activated signalling pathway', both *Adipor1* and *-r2* (adiponectin-receptor 1 and 2) were upregulated in the DKO along with long-chain fatty acid CoA ligase1 (*Acsl1*), casein kinase 2 beta (*Csnk2b*) and solute carrier family 27 member 1 (*Slc27a1*) (**Figure 3.8** B). *Appl1* and *Appl2* (adaptor protein, phosphotyrosine interacting with PH domain and leucine zipper 1 and 2) were downregulated in the DKO cells and upregulated in the WT samples relative to the mean. The expression of these genes in the T-cad KO samples was intermediate between the WT and the DKO cells.

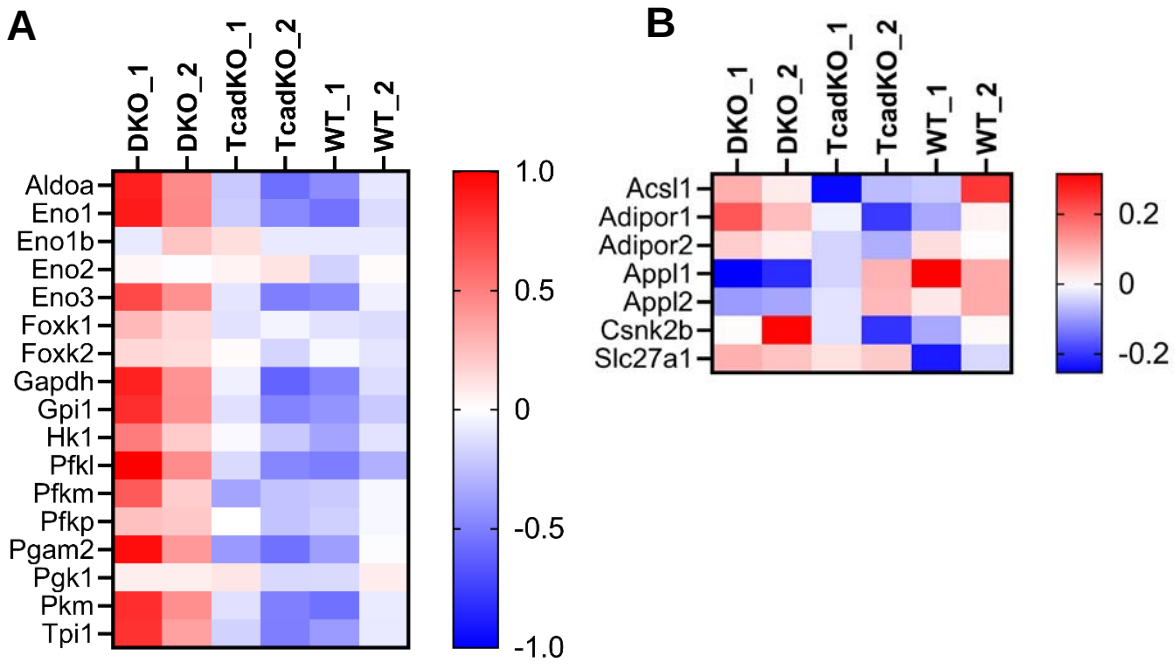

Figure 3.8. Heatmaps of the gene expression of metabolic pathways in WT, T-cad KO and DKO cells. **A.** 'NADH regeneration' (GO:0006735), or **B. '**APN-activated signalling pathway' (GO:0033211). Values are log2 fold-changes from the mean and were normalised with variance stabilising transformation. Each row represents a separate gene, sorted in alphabetical order.

3.4.5.2 Enriched cell adhesion terms

There was minimal difference in the expression of genes involved in 'cadherin mediated cell-cell adhesion' (GO:0044331), (**Figure 3.9** A) and 'integrin mediated cell-cell adhesion' (GO:0033631) (**Figure 3.9** B). The notable exceptions are *Cdh15* (M-cadherin), *Cdh5* (VE-cadherin), *Notch1* (neurogenic locus notch homolog protein 1), Wnt5a (Wnt family member 5A), *Cd24a* (cluster of differentiation 24), *Itga4* (integrin subunit alpha 4), *Itga5* (integrin subunit alpha 5) and *Piezo1* (piezo type mechanosensitive ion channel component 1). *Cdh15* and *Cdh5* are members of the calcium-dependent cadherin superfamily. M-cadherin is involved in muscle adhesion and VE-cadherin is expressed by endothelial cells. *Itga4* (integrin subunit alpha 4) was up-regulated in the T-cad KO and down-regulated in the DKO. In contrast, *ITGA5* (integrin subunit alpha 5) was up-regulated in the DKO and T-cad KO cells but more so in the DKO myoblasts. *Piezo1* is up regulated in the DKO myoblasts. There is some variability in gene expression within the genotype samples.

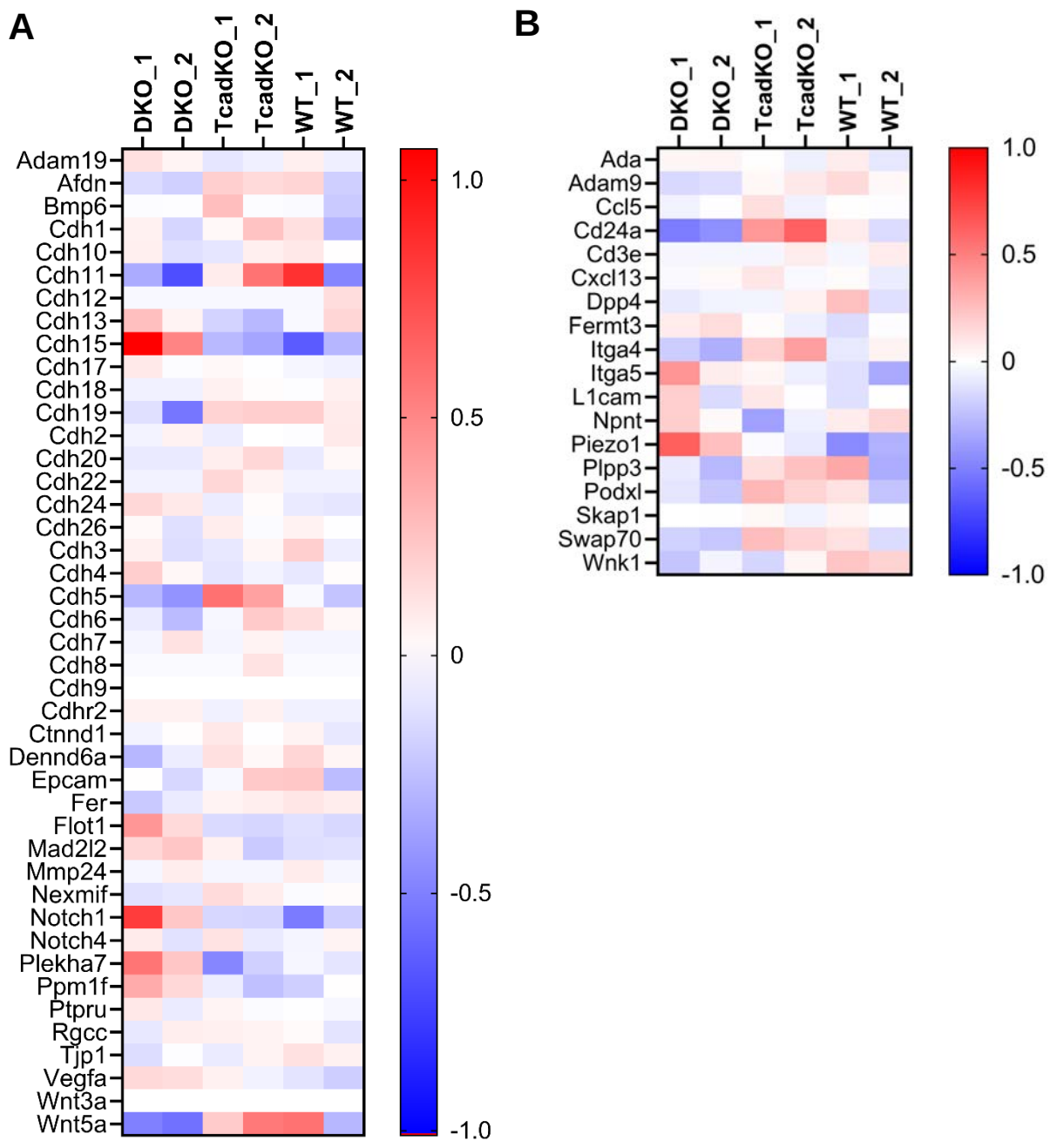

Figure 3.9. Heatmaps of the gene expression of cell-cell adhesion in WT, T-cad KO and DKO cells. **A.** 'Cadherin-mediated' (GO:0044331), or **B.** 'integrin-mediated' (GO:0033631) cell-cell adhesion. Values are log2 fold-changes from the mean and were normalised with variance stabilising transformation. Each row represents a separate gene, sorted in alphabetical order.

3.4.5.3 Enriched muscle development and function terms

Finally, muscle pathways were considered under the GO terms ‘myoblast fusion’ (GO:0007520) and ‘skeletal muscle contraction’ (GO:003009). As expected, the DKO myoblasts have increased expression of genes associated with myoblast fusion (**Figure 3.10** A) and these include *Ehd1* (EH domain containing 1), *Mymk* (myomaker), *Mymx* (myomixer), *Myod1* (myogenic differentiation 1), *Myog* (myogenin) and pleckstrin homology domain containing family o member 1 (*Plekho1)*. Additionally, C*acna1s* (calcium voltage-gated channel subunit alpha1 S), a calcium channel in skeletal muscle cells, and *Cav3* (caveolin 3), which plays a role in sarcolemma repair in muscle, are up-regulated in the DKO cells. Like the cell-cell adhesion GO terms, there is variability between the duplicate genotype samples.

The genes listed in the GO term ‘skeletal muscle contraction’ were almost entirely upregulated in the DKO except for *Dmd* (dystrophin), a major component of the dystrophin glycoprotein complex, *Homer1* (homer scaffold protein 1), *Rcsd1* (RCSD domain containing 1), and *Stac* (SH3 and cysteine rich domain) (**Figure 3.10** B). Many of the genes that code for structural proteins including actinin alpha 3 (*Actn3*), caveolin 3 (*Cav3*), myosin heavy chain 14, 3, 7 and 7 (*Myh14, Myh3, Myh7* and *Myh8* respectively), myosin light chain kinase 2 (*Mylk2*) and troponin C1, C2, I1-3, T1 and T3 (*Tnnc1, Tnnc2, Tnni1, Tnni2, Tnni3, Tnnt1,* and *Tnnt3* respectively) were up-regulated in the DKO cells.

In summary, the bioinformatic GO analyses of the next generation sequencing data identified, in DKO primary myoblasts, up-regulated expression of genes involved with metabolism, myogenesis and muscle contraction, together with specific genes involved in cell-cell adhesion.

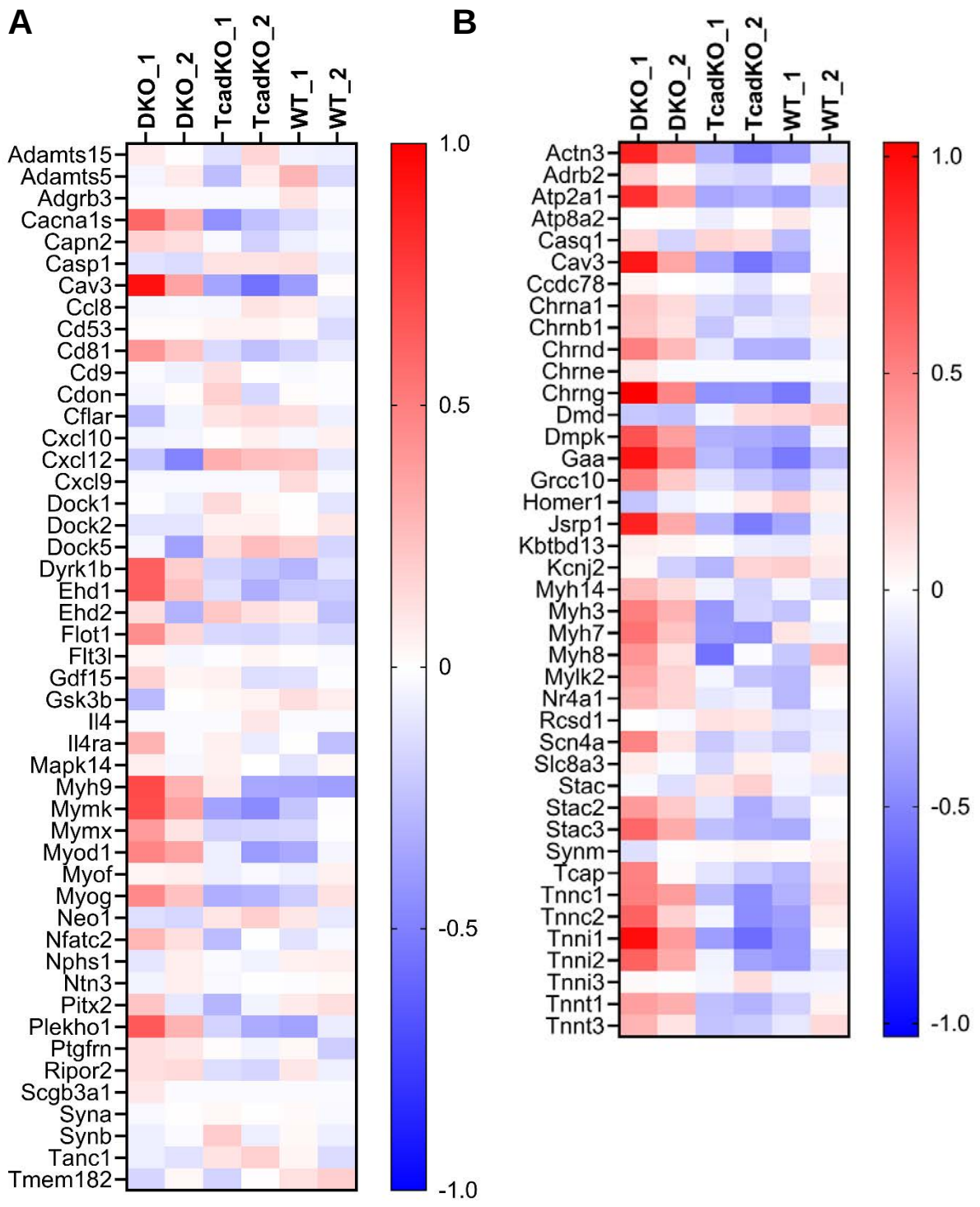

Figure 3.10. Heatmaps of the gene expression of muscle pathways in WT, T-cad KO and DKO cells. **A.** 'Myoblast fusion' (GO:0007520), and **B.** 'skeletal muscle contraction' (GO:003009). Values are log2 fold-changes from the mean and were normalised with variance stabilising transformation. Each row represents a separate gene and is sorted by alphabetical order.

Discussion

In this chapter the role of T-cadherin in muscle disease and COPD was investigated using public genomic databases and bioinformatic analyses. Additionally, using RNA from primary myoblasts of WT, T-cad KO and DKO mice, next generation sequencing was performed and interrogated using advanced bioinformatic approaches. The results of this chapter are discussed below.

3.4.6 Genome wide association studies

GWAS identify SNPs that associate with a particular phenotype and allelic frequency that in the future could be targeted for therapeutics. A GWAS approach was used to identify *CDH13* SNPs that associate with muscle disease and COPD. Studies of this type require many subjects to establish significance and are costly and time consuming to perform. Therefore, this study utilised previously established online databases. Due to the number of samples that are available in these muscle related datasets, the analysis did not have the statistical power required for this in-depth analysis. Although there were hundreds of samples available in this dataset, many were not compatible with the software and were removed. The analysis was still completed expecting that it would highlight a previously identified SNP, however, none of the identified SNPs had sufficient statistical significance after correction for multiple testing.

Skeletal muscle dysfunction is a serious comorbidity for patients with COPD and population-based studies have shown that genetic variants can affect a person's susceptibility to this disease. Thus, it is possible that patients may also have genetic variants that increase their vulnerability for skeletal muscle dysfunction. The genetic epidemiology of the COPD database contained 501 cases and 493 controls that were analysed for genetic markers of skeletal muscle function within the T-cadherin gene. After correction for multiple testing, one SNP (rs7206590) in *CDH13* was found. This SNP is an intron variant within the T-cadherin gene but is not mentioned in any publications or associated with any clinical significance at this time. Given the emerging importance of non-coding SNPs as significant modifiers of disease, this SNP requires further investigation. Interestingly, there is a cluster of SNPs in this area with

high significance, but not above the threshold (**Figure 3.2**: Area of interest). This suggests that this area within *CDH13* may be worth investigating, rather than the individual SNPs themselves which are not currently known to have any clinical significance.

3.4.7 Next generation sequencing of primary myoblasts

Results show that DKO myoblasts commit to fusion sooner than the WT cells and the RNA sequencing agrees with these observations. Compared to WT control, the DKO myoblasts had the greatest number of differentially expressed genes (3908 genes). Of these genes, 69% (2725 genes) were also differentially expressed in the DKO compared to T-cad KO, suggesting the T-cad KO expression profile was more like the WT. Moreover, when the T-cad KO was compared to the WT, only 31 differentially expressed genes were found.

3.4.7.1 DKO murine myoblasts have a unique genetic signature

The top three up-regulated DEGs in the DKO versus WT comparison were *Mvd* (mevalonate diphosphate decarboxylase), *Hspg2* (heparan sulphate proteoglycan 2) and *Isyna1* (inositol-3-phosphate synthase 1). MVD is a key enzyme in the mevalonate pathway that synthesizes sterol isoprenoids, such as cholesterol, and disruptions within this pathway can result in abnormal glucose and lipid metabolism [287-289]. The change to MVD is likely linked to reduced APN signalling in the DKO myoblasts.

HSPG2 encodes the proteoglycan perlecan, a component of the basal lamina that binds laminin and α-dystroglycan [290, 291]. Perlecan is expressed by C2C12 myoblasts and is downregulated upon differentiation and upregulated following muscle injury [292, 293]. Increased HSPG2 expression may coincide with the enhanced differentiation of the DKO myoblasts.

Isyna1 was highly up-regulated in the DKO myoblasts and converts glucose-6-phosphate to myo-inositol-1-phosphate. Myo-inositol is a component of membrane phospholipids and depletion of intracellular myo-inositol is commonly observed in diabetic animal models in primary sites for the development of diabetic microvascular complications [294]. Inositol supplements are useful in the management of diabetes because they decrease blood glucose levels and increase insulin secretion [294, 295]. There are limited reports on the role of ISYNA1 in myogenesis.

Other genes in the top 10 up-regulated gene list in the DKO versus WT comparison include collagen type II alpha I chain (*Col2a1*) and actin alpha 1 (*Acta1*), which encodes collagen and actin, respectively, and are both important components of the contractile apparatus in skeletal muscles. Zyxin (*Zyx*) modulates mechano-transduction by influencing cytoskeletal structure and signalling pathways in smooth muscle cells [296]. Phosphate cytidylyltransferase 2 ethanolamine (*Pcyt2*) is important in membrane function by structurally stabilising membrane-anchored proteins [297]. Finally, prostate-tumour-overexpressed 1 (*Ptov1*) that shows increased expression in prostate cancer, regulates gene expression and is also found expressed in normal tissues such as the brain, heart, liver, kidney and skeletal muscle, but its function is yet to be determined [298].

Of the down-regulated genes, many GTPases, a family of genes important in cell-autonomous immunity, were also down-regulated in the DKO cells, however their role in myogenesis in unclear. Of interest and downregulated in the DKO, CD93 is involved in enhancing angiogenesis, and RBFOX1 encodes for a member of the Rbfox family that regulates RNA splicing required to maintain muscle physiology [299, 300].

3.4.7.2 T-cad KO mice display similar genetic characteristics to WT mice

Although only 31 DEGs were identified, many of the up-regulated DEGs in the T-cad KO versus WT comparison play a role in angiogenesis. Angiopoietin 2 (*Angpt2)* regulates angiogenesis, is up regulated during differentiation and may enhance myoblast fusion [301]. Endomucin (*Emcn*) loss impairs angiogenesis [302] and endothelin (*Edn1*) and adhesion G-protein-coupled receptor F5 (*Agrf5*) regulate angiogenesis [303-305]. *Fabp4* (fatty acid binding protein 4) encodes for a fat binding protein that acts as a carrier for fatty acids and can regulate the accumulation of fat within the muscle [306].

Only 8 down-regulated genes were noted, and most have little published information, except for *Csrp3* (Cysteine and glycine rich protein 3) and *Cemip* (Cell migration inducing hyaluronidase 1). CSRP3 regulates glucose homeostasis and CEMIP is involved in multiple cancers as an oncogene [307, 308].

3.4.7.3 DKO versus T-cad KO differentially expressed genes

Many of the DEGs in this comparison where also present in the DKO versus WT comparison, by example, *Acta1, Isyna1, Hspg2, Mvd* and *Ptov1*. Additionally, structural

genes *Flnc* (filamin C) and *Obscn* (obscurin) were up regulated in the DKO. Filamins are a group of filaments that cross-link with actin filaments. Obscurin is a giant myofibril-associated protein that interacts with titin at the M-band and the Z-disc and is linked with distal myopathies [309].

Ckm (creatine kinase M-type) *and Rab3il1* (RAB3A interacting protein like 1) were up-regulated in the DKO. CKM encodes for a subunit of creatine kinase that catalyses the phosphorylation of creatine to phosphocreatine to generate ATP from ADP. RAB3IL1 functions as a guanine nucleotide exchange factor for the Rab3A small GTPase and has been identified as a MAPK (mitogen-activated protein kinases)-phosphatase regulated substrate with a possible role in enhancing muscle regeneration [310, 311].

Interestingly, many of the genes that were down-regulated in the DKO versus T-cad KO comparison were up-regulated in the T-cad KO versus WT comparison, including *Angpt2, Adgrf5, Fabp4, Apln* and *Emcn.* Of the 11 DEGs common to all comparisons, angiogenic genes *Adgrf5*, *Adgrl4* and *Angpt2* were upregulated in the T-cad KO, suggesting a relationship to APN over-expression in this genotype.

3.4.8 Pathways identified by gene ontology comparisons

Gene ontology showed enriched terms associated with metabolic pathways, cell adhesion, myoblast fusion and muscle contraction.

3.4.8.1 Muscle Metabolism

Many of the genes involved in the NADH regeneration pathway (see **Figure 3.8**) including glycolytic enzymes such as *Aldoa* (aldolase A), *Hk1* (hexokinase 1), *Eno1*, *Eno1b, Eno2* and *Eno3* (enolase isoenzymes) were up regulated in the DKO group. This suggests that the DKO myoblasts were actively producing energy at an increased rate. This counters APN's normal role in regulating skeletal muscle metabolism, where APN application stimulates glucose uptake. These data suggest that T-cadherin itself may regulate metabolism and that the increase in glycolytic enzymes is a result of the increase in differentiation.

Adipor1 and -r2 were upregulated and the receptor-binding proteins APPL1 and APPL2 were down-regulated in the DKO cells, suggesting the dysregulation of APN signalling. ACSL1 and SLC27A1 (also known as FATP1), which are essential for the

activation, transportation, and degradation of fatty acids, were up regulated in the DKO cells, and point towards increased ability of the DKO cells to uptake fatty acids.

3.4.8.2 Cell adhesion

The most notable differences in gene expression for cadherin mediated cell-cell adhesion and integrin mediated cell-cell adhesion were *Cdh15, Cdh5, Notch1 Wnt5a, Cd24a, Itga4, Itga5* and *Piezo1* (see **Figure 3.9**). CDH15 known as M-cadherin, and CDH5 (VE-cadherin) are members of the cadherin superfamily. M-cadherin was up regulated and is involved in muscle adhesion and SC function, and VE-cadherin was down regulated and is exclusive to endothelial cells. NOTCH1 was up regulated and is a highly conserved transmembrane protein that is involved in muscle development and has roles in the development of most tissues [312]. WNT5A was down-regulated and can regulate muscle development [15]. CD24A was down regulated and is a signal transducing molecule commonly used as a marker of regenerating muscle [313]. *Itga4* (integrin subunit alpha 4) was up-regulated in the T-cad KO cells and down-regulated in the DKO cells. In contrast, *Itga5* (integrin subunit alpha 5) was up regulated in the DKO. Both integrins play roles in skeletal muscle development and were discussed in chapter 1 (see section 1.6). Finally, *Piezo1* (piezo type mechanosensitive ion channel component 1) was up regulated in the DKO myoblasts, and is a mechanical transducer that controls intracellular signalling for the development and regeneration of muscle fibres [314].

3.4.8.3 Myoblast fusion

Genes involved in regulating myoblast fusion were also increased in the DKO myoblasts. Myomaker, myomixer, MYOD and myogenin were all upregulated in DKO, consistent with the results showing increased differentiation and fusion (see section 1.10). Up regulated in the DKO was caveolin 3 (*Cav3*), which associates with components of the dystrophin glycoprotein complex (DGC) and is necessary for efficient myoblast fusion [315]. Additionally, EH domain containing 1 (*Ehd1*) which regulates myoblast fusion by binding through myoferlin, and pleckstrin homology domain containing family o member 1 (*Plekho1*), which is suspected to regulate myoblast fusion were up regulated in the DKO samples [316]. Loss of EHD1 leads to smaller muscle *in vivo* and PLEKHO1 promotes proliferation and stimulates the expression of myogenin through the PI3K (phosphoinositide 3-kinases) pathway [316, 317].

3.4.8.4 Muscle contraction

The GO terms ‘muscle contraction’ and ‘muscle system process’ were enriched in the gene ontology study. This indicated that many other structural proteins including actinin alpha 3, caveolin 3, myosin heavy chain 14, 3, 7 and 7 (*Myh14, Myh3, Myh7* and *Myh8,* respectively), myosin light chain kinase 2 (*Mylk2*) and troponin C1, C2, I1-3, T1 and T3 (*Tnnc1, Tnnc2, Tnni1, Tnni2, Tnni3, Tnnt1,* and *Tnnt3,* respectively) were up-regulated in the DKO. This likely represents the accelerated myoblast fusion and resulting increase in muscle cell mass *ex vivo*.

3.4.9 Limitations and future recommendations

qPCR was used to validate the up-regulated genes with the highest fold-change in the DKO versus WT analysis[xvi]. Unexpectedly, we could not record any differences. However, on further investigation of this genotype in chapter 5, we found that the DKO cells had a metabolic advantage and likewise many of the metabolic genes commonly used as housekeeper genes such as *Gapdh, Rpl41, Rpl27* and *Aldoa* were strongly upregulated in the DKO, as per the next generation sequencing data. Moving forward, repeat qPCR experiments could be used to validate this sequencing data provided that suitable controls can be identified. At the time of the thesis writing, studies are underway in the group to perform western blots on the primary myoblasts for some of the strongly up-regulated genes such as M-cadherin, MYOD, myomixer and myomaker to assist in data validation.

The findings in this chapter agree with the preliminary results showing the DKO myoblasts are committing to fusion sooner and developing myotubes more rapidly than the WT. Unfortunately, due to some quality issues with the 12-hour control samples, RNA sequencing analysis could not be performed with the earlier timepoint. Moving forward, repeat RNA sequencing studies should be conducted with a minimum of three samples per timepoint to avoid this complication. Furthermore, future studies may also benefit from the inclusion of myoblast RNA from earlier differentiation timepoints. For example, 3- and 6-hour differentiation studies may reveal differences in genes involved in activating and expanding the pool of SCs.

[xvi] qPCR validation was performed by Dr. Miriam Wankell.

3.5 Conclusion

These data strongly support the concept that the DKO cells have accelerated differentiation. In support, we find the up regulation of genes representing the myogenic transcriptional programme and cell adhesion. Interestingly, we also observed that the DKO cells have a genetic signature that reflects increased metabolism and the likely ability to take up fatty acids more readily. Both genetic attributes counter the loss of APN and its expected functions and suggest that T-cadherin has APN independent functions in myogenesis. These attributes are explored in the later chapters of this thesis.

4 T-cadherin's Function in Muscle Regeneration and Repair

4.1 Introduction

Skeletal muscle injury occurs constantly throughout life. To counterbalance this, muscles possess an inherent restorative process driven by myogenic transcription factors to facilitate regeneration and repair. This is supported by skeletal muscles maintaining a small population of muscle specific stem cells known as satellite cells (SCs). These self-renewing cells are activated following injury and begin the process of myogenesis to repair injured tissue. Prior to regenerating, the muscle fibres first exhibit rapid inflammation as characterised by the presence of neutrophils and macrophages, after which the damaged cells are removed to allow growth of new fibres [52]. The SCs are activated and begin proliferating to provide self-renewing cells and myoblasts to repair the damaged fibres. On injury, SCs increase the expression of *Myf5* and *Myod* transcription factors and enter a regenerative cycle of myogenesis. This process will continue until the muscle fibres have been repaired and a small population of SCs re-enter quiescence just below the basement membrane. Although it can take up to one month to fully repair the damaged fibres, the majority of the muscle architecture is fully restored after 10 days of regeneration [318]. Both T-cadherin and APN are decreased following injury, and increase around day three of regeneration [212]. Although the presence of both proteins during regeneration has been established, it is not yet clear what roles they play in muscle repair.

4.2 Preliminary data and aims

The Hebbard lab previously examined T-cadherin's role in myogenesis by overexpressing T-cadherin in C2C12 myoblasts (pLTcad cells) and evaluating myogenic protein expression and fusion index (**Figure 4.1**[xvii]). They showed that overexpressing T-cadherin in C2C12 cells led to reduced levels of myosin heavy chain

[xvii] **Figure 4.1** is identical to **Figure 1.7** in section 1.10 and has been duplicated here for convenience.

(MHC), myogenin and decreased the fusion index (the number of nuclei present inside the myotubes as a percentage of the total number of nuclei in the field of vision).

Studies performed for my Honours thesis in the Hebbard Lab showed a significant difference in the growth and fusion of DKO myoblasts compared to WT controls. These results illustrated that the DKO myoblasts commit to myogenesis sooner, fuse faster and form myotubes earlier than WT myoblasts (**Figure 4.2**[xviii]).

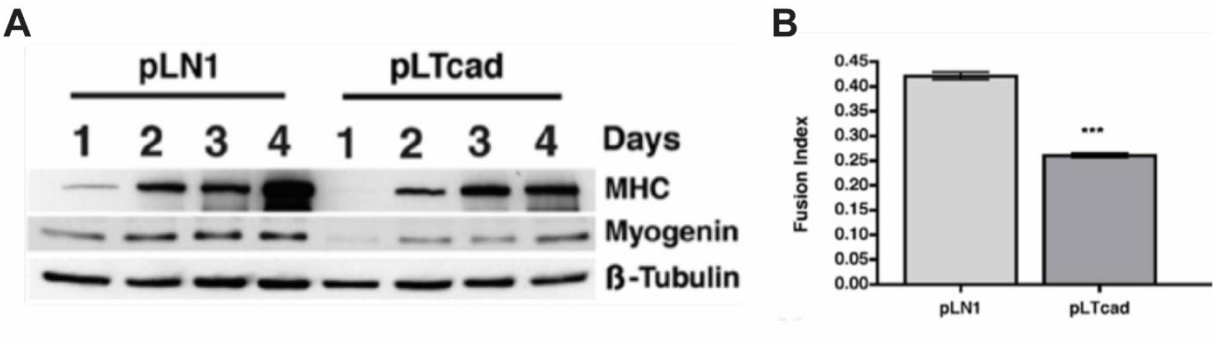

Figure 4.1. T-cadherin overexpression in myoblasts impairs myogenesis. **A.** Western blot of pLN1 (control) and pLTcad C2C12 cells differentiated for 1-4 days and probed for MHC, Myogenin and β-tubulin as loading control. **B.** Graph showing myoblast fusion index of differentiated C2C12 pLN1 and pLTcad cells. *** = $p<0.001$

[xviii] **Figure 4.2** is a condensed version of the data in **Figure 1.9** in section 1.10 and has been duplicated here for convenience.

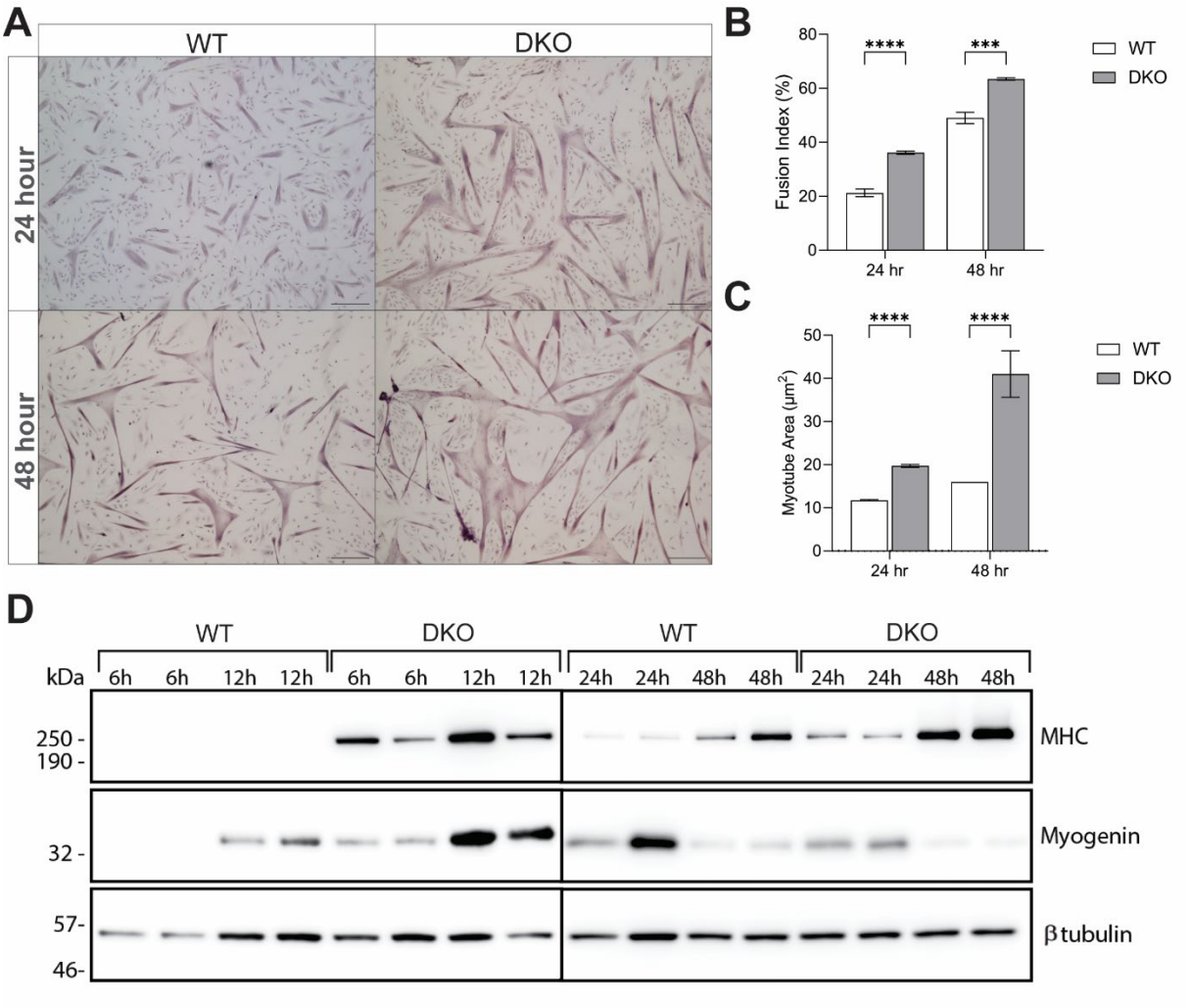

Figure 4.2. T-cadherin/APN double knockout (DKO) primary myoblasts show enhanced differentiation compared to WT myoblasts. **A.** Representative images of differentiating WT and DKO primary myoblasts at 24- and 48-hours differentiation. Scale bar 500 μm. **B.** Fusion index of WT and DKO myoblasts at 24- and 48-hours differentiation (mean ± SEM). **C.** Average myotube area of WT and DKO myofibers at 24- and 48-hours differentiation (mean ± SEM). **D.** Western blot showing protein expression of MHC, myogenin and β-tubulin as loading control in differentiating WT and DKO myoblasts between 6-48 hours. *** = $p<0.001$, **** = $p<0.0001$.

In terms of developmental myogenesis, there was no notable difference between the overall weights of the young adult mice or of their individual muscles (**Figure 4.3**[xix]), and limited differences were observed in gene expression as shown through RNA sequencing of adult murine WT and DKO tissue (data not shown). Taken together, these results suggest that the myogenic enhancement observed in the DKO murine muscle may occur within the muscle SCs during regeneration and repair rather than during muscle development.

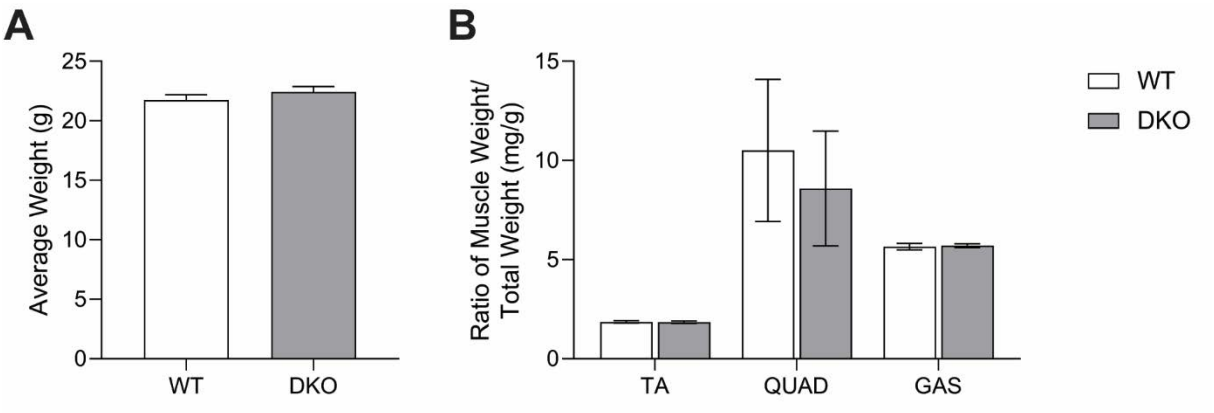

Figure 4.3. **A.** Average body weights of WT and DKO mice between the age of 5-7 weeks. (WT n=25, DKO n=18, mean ± SEM). **B.** Average tibialis anterior (TA), quadriceps (QUAD) and gastrocnemius (GAS) hindlimb muscle weight of 7-week-old WT and DKO mice (n=4, mean ± SEM).

As a result of these findings, the studies described in this chapter aimed to achieve the following:

1. To investigate differences in differentiation between WT and single T-cadherin knockout (T-cad KO) primary myoblasts.
2. Evaluate differences between WT, DKO and T-cad KO mouse myofibers.
3. Determine differences in the regeneration and repair capacity of WT, DKO and T-cad KO muscles *in vivo*.

[xix] **Figure 4.3** is identical to **Figure 1.8** in section 1.10 and has been duplicated here for convenience.

4.3 Methods

For complete materials and methods please see chapter 2 section 2.3, 2.5 and 2.8.

4.3.1 Ex vivo examination of myoblast growth

Briefly, myoblasts were isolated from the hind limbs of 4-6 male mice aged 4-6 weeks, cultured, and plated as per chapter 2 section 2.3 and differentiated for 0-, 6-, 12-, 24-, or 48-hours prior to being fixed or lysed for protein analysis. The fixed cells were then stained with hematoxylin and eosin and examined for myotube area, fusion index (the number of nuclei present inside the myotubes as a percentage of the total number of nuclei in the field of vision) and myotube number and the lysates separated by SDS-PAGE and examined via western blotting.

4.3.2 Regeneration and repair following injury

Mice were injected with 0.15 µg of Notexin (10 µl of 15 µg/ml diluted with PBS) longitudinally through the left TA muscle and then left for 2, 3, 7, and 10 days[xx], at which time, the mice were euthanised with CO_2 and both their left (injured) and right (control) TA muscles were removed and embedded in optimum cutting temperature (OCT) compound for cross-sectional analysis. Transverse serial sections were cut from the mid region of the embedded muscle and mounted on glass microscope slides[xxi]. The sections were subsequently stained for quiescent SCs (Pax7), activated SCs (MYOD), fibrosis (sirius red), macrophage infiltration (CD68) and with hematoxylin and eosin (pathology and fibre size).

Analyses were performed using ImageJ software and statistical analyses using GraphPad Prism. * = $p<0.05$, ** = $p<0.01$, *** = $p<0.001$, **** = $p<0.0001$ denote the significance values used throughout this chapter. Errors bars on graphs represent standard error of the mean (SEM) unless stated otherwise.

[xx] Notexin injections were performed by Dr. Craig McFarlane.
[xxi] Cross sections were obtained by Dr. Lionel Hebbard.

4.4 Results

Given the differences seen between the growth and differentiation of WT and DKO myoblasts, further analyses were performed to understand the role of T-cadherin on SCs and in myogenesis. Immunofluorescence was used to establish the presence of T-cadherin on SCs through DAPI and Pax7 co-staining in uninjured WT muscle tissue. T-cadherin was visible on the muscle cell membranes and co-localised with Pax7 positive nuclei (**Figure 4.4**).

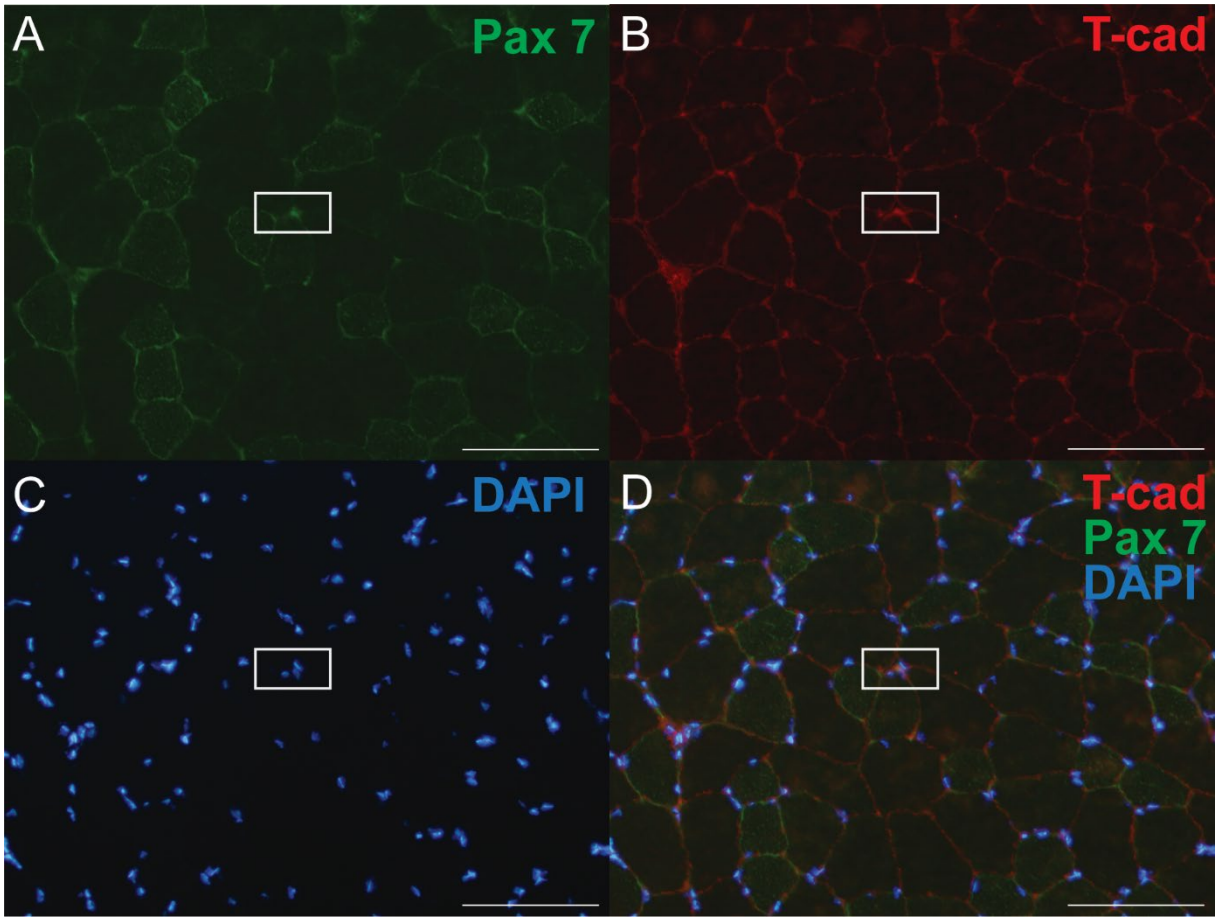

Figure 4.4. Immunofluorescence staining of an uninjured WT murine TA muscle section. Sections were stained for **A.** Pax7 (green), **B.** T-cadherin (red), **C.** DAPI (blue), and **D.** Merged. Scale bar 100 µm.

4.4.1 Differentiation of WT and T-cadherin KO primary myoblasts

To differentiate between the effects of T-cadherin and APN in myogenesis, the primary myoblast experiments reported in the preliminary results were repeated using myoblasts isolated from WT and T-cadherin single knockout (T-cad KO) mice. Each biological replicate represents cells pooled from at least 4 mice.

Following the isolation of primary myoblasts, the cells were allowed to differentiate for 24- and 48-hours and stained with hematoxylin and eosin (**Figure 4.5** A). Unlike the comparison with the DKO myofibers (see preliminary data **Figure 4.2**), there were no differences in the growth and differentiation of WT versus T-cad KO fibres. Using H&E stained myotubes, analyses were performed to evaluate the fusion index and myotube area. Assessment revealed no differences between the genotypes in fusion index or myotube area (**Figure 4.5** B-D). The fusion index, or percentage of total nuclei present in myofibers, was 19.6% for WT and 23.6% for T-cad KO at 24 hours and increased to 68.4% for WT and 65.9% for T-cad KO at 48 hours (**Figure 4.5** B). At 24- and 48-hours respectively, the average size of the WT myofibers was 2.078 μm^2 and 4.159 μm^2, and the T-cad KO 2.297 μm^2 and 4.304 μm^2 (**Figure 4.5** C). The increase in fusion index and average size for each genotype from 24- to 48-hours was significant ($p < 0.0001$) (**Figure 4.5** B-C). The maximum fibre size at 24 and 48 hours increased from 6 μm^2 to 49 μm^2 for WT from 7 μm^2 to 56 μm^2 for the T-cad KO and there was no difference between genotypes (**Figure 4.5** D-E).

Following differentiation, whole cell lysates were collected from cultures of each genotype at 6-, 12-, 24- and 48-hours differentiation and used for western blot analysis with the myogenic markers myogenin, myosin heavy chain and β-tubulin (loading control). Myogenin, a marker of commitment to differentiation, was expressed as early as 6 hours into differentiation of both the WT and T-cad KO cultures (**Figure 4.6** A). As the loading controls appeared uneven for each sample, a densitometry analysis was performed to compare the protein of interest versus loading control (**Figure 4.6** B-C).

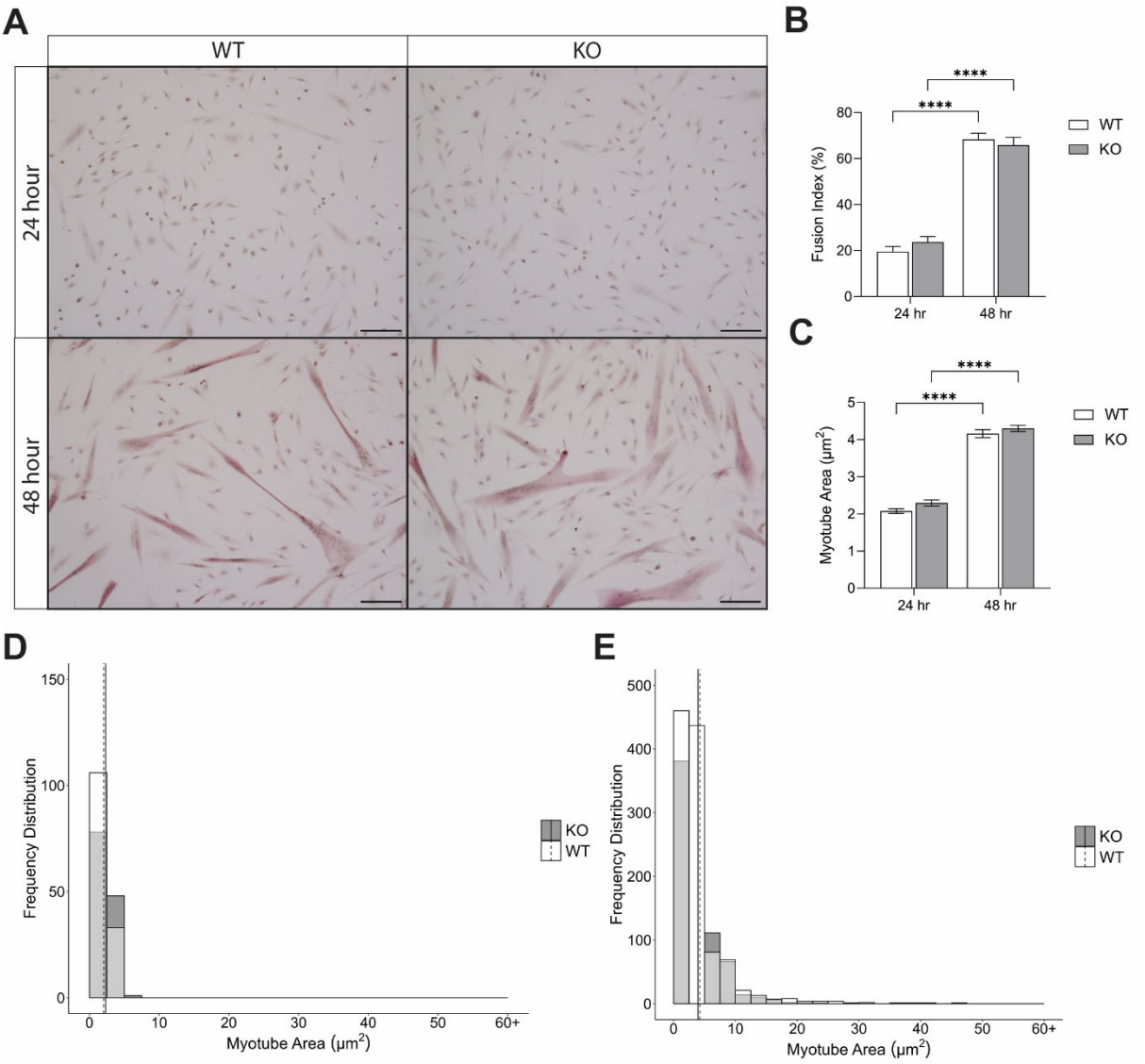

Figure 4.5. Comparison between differentiating WT and T-cad KO (KO) primary myoblasts (n=2). These results represent multiple experiments conducted with similar results. **A.** Examples of hematoxylin and eosin-stained myoblasts/myotubes after 24- and 48-hours differentiation. Scale bar 100 μm. Any cell with 3 or more nuclei are considered to be myotubes. **B.** Myoblast fusion index at 24- and 48-hours differentiation (mean ± SEM). T-tests indicate no significant difference between either group. **C.** Primary myotube area at 24- and 48-hours differentiation (mean ± SEM). T-tests indicate no significant difference between either group. Overlapped frequency distribution graph of myotubes at **D.** 24- and **E.** 48- hours differentiation. The light grey areas show the overlap between the WT and T-cad KO bars and the solid and dashed lines represent the average myotube area for T-cad KO and WT cells, respectively.

This indicated that the T-cad KO samples expressed more myogenin at 6- and 12-hours, but the differences were not significant. WT myoblasts had higher myogenin expression at 24 hours but similar levels at 48 hours. MHC, a marker of mature myofibers, did not appear in the lysates until 48 hours. Densitometry showed a low level of MHC expression at 24 hours, but this was not visible by western blot.

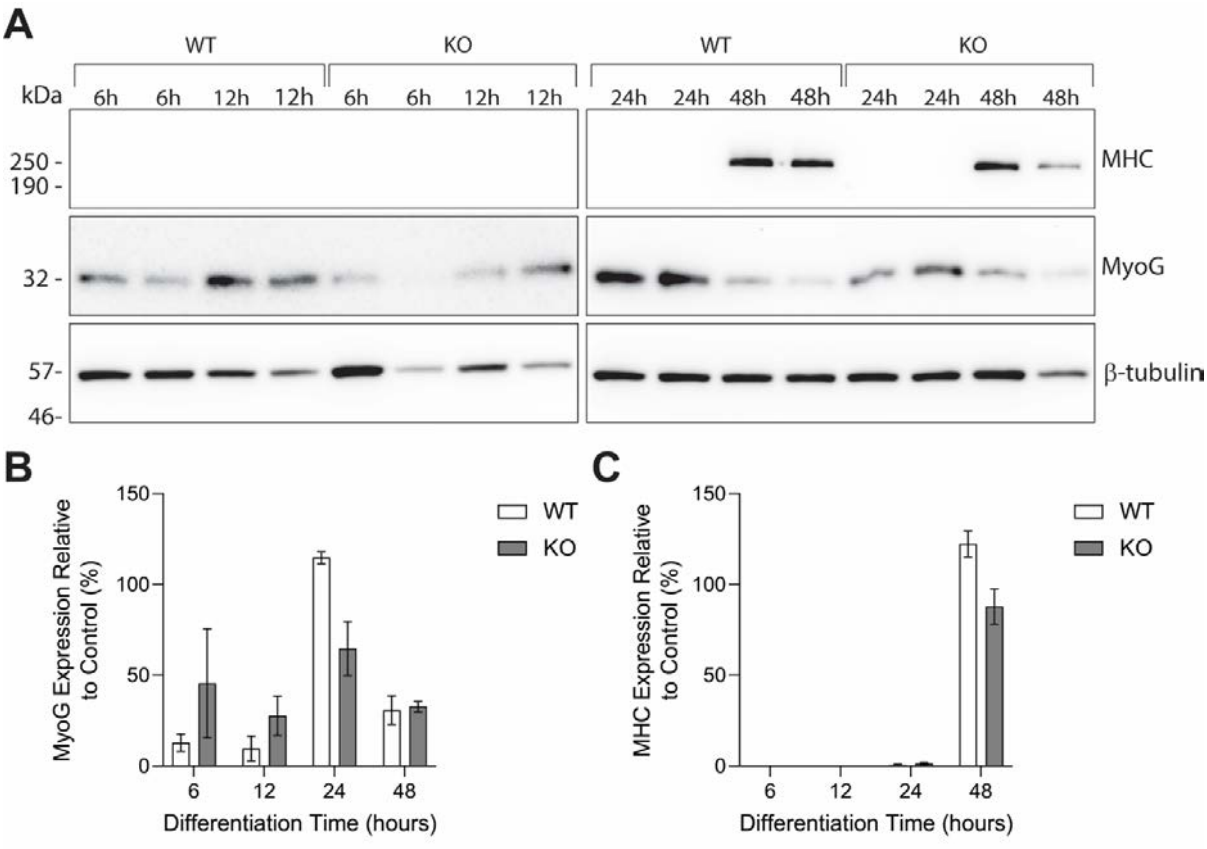

Figure 4.6. Protein expression analysis of primary WT and T-cad KO (KO) myoblasts at during differentiation. **A.** Western blot of primary cell lysates at 6-, 12-, 24-, and 48-hours differentiation. The 6- and 12-hour lysates and 24- and 48-hour lysates were collected from separate experiments. Blots were probed for MHC, myogenin (MyoG), and β-tubulin as loading control. Relative expression was then calculated from the β-tubulin control for both **B.** MyoG and **C.** MHC (mean ± SEM). Multiple t-tests indicate no significant differences between the genotypes.

After 48-hours differentiation, the MHC expression was 1.4-fold greater in the WT cells than in the T-cad KO cells. In addition, there was a decrease in the expression of myogenin (WT: 3.7-fold and T-cad KO: 2-fold) and an increase in the expression of MHC (WT: 230-fold and T-cad KO: 64-fold) between 24- and 48-hours. However, none of these differences were significant.

4.4.2 Examining differences in muscle development

The results from my Honours studies showed a significant increase in the *ex vivo* growth of muscle from DKO versus WT mice. Using mice from this study, the mouse body weight analysis for WT, DKO and T-cad KO mice was expanded (**Figure 4.3** A analysis expanded in **Figure 4.7**). The updated comparison of body weights further separates the mice by age to account for differences in body weight over time. The analysis shows no differences between the weights of the mice at any time point. Given this information, this project focussed on examining whether there were differences in the *in vivo* regeneration of injured muscle fibres. To do this, TA muscles from each genotype were injured and allowed to repair for 2, 3, 7, and 10-days prior to isolation and histological evaluation.

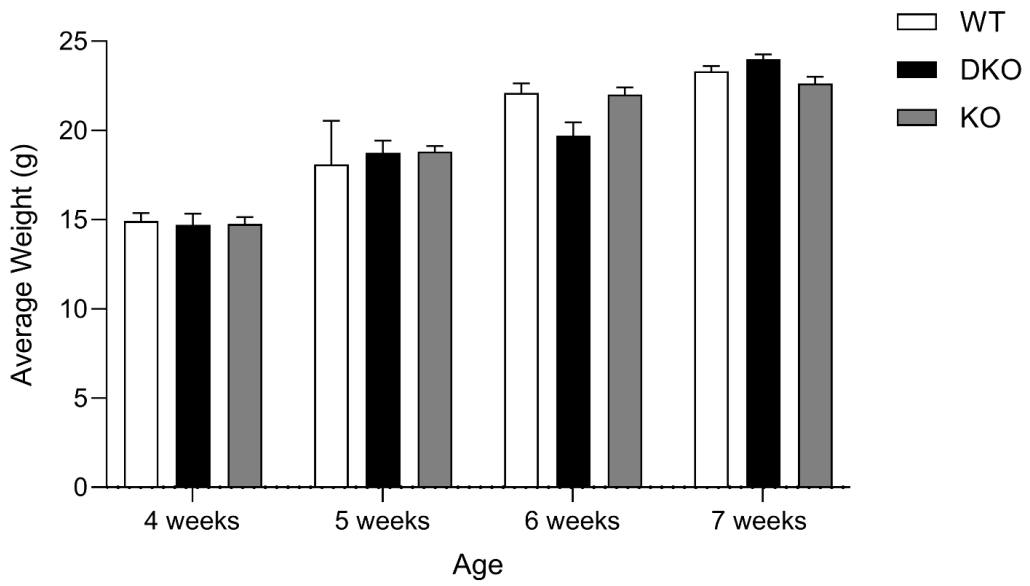

Figure 4.7. Average weight of WT, DKO and T-cad KO (KO) mice at 4-, 5-, 6- and 7-weeks of age compiled from all mouse experiments (mean ± SEM, n ≥ 4). Tukey's test for multiple comparisons revealed no significant difference between any of the genotypes at each timepoint.

4.4.3 Investigating uninjured control muscle fibres

During the regeneration studies, the right-hand side TA muscles were used as a control and isolated from the uninjured hindlimb of each of the mice. These muscles were cross sectioned and stained to measure area, quiescent SC populations and fibre type for all three genotypes[xxii].

Representative H&E-stained images of each genotype can be seen in (**Figure 4.8** A-C). Visually, the DKO fibres appeared larger than the other genotypes. This is consistent with the results of the laminin staining that outlines each of the muscle fibres and allows for a streamlined analysis (**Figure 4.8** D-F). Analyses revealed that the average myofiber size is 1401 μm^2, 1605 μm^2, and 1513 μm^2 for WT, DKO and T-cad KO, respectively. Significantly, the DKO fibres are 1.15-fold larger than WT fibres and 1.06-fold larger than T-cad KO fibres. Furthermore, the T-cad KO fibres are significantly larger than WT (1.08-fold). The frequency distribution plot shows a similar distribution between each of the genotypes but illustrated a larger number of DKO myofibers with an area greater than 3000 μm^2. Taken together, the data show that the uninjured DKO fibres are larger.

[xxii] The WT control muscle sections for these analyses were taken from the control muscles isolated during the WT versus T-cadherin KO study only.

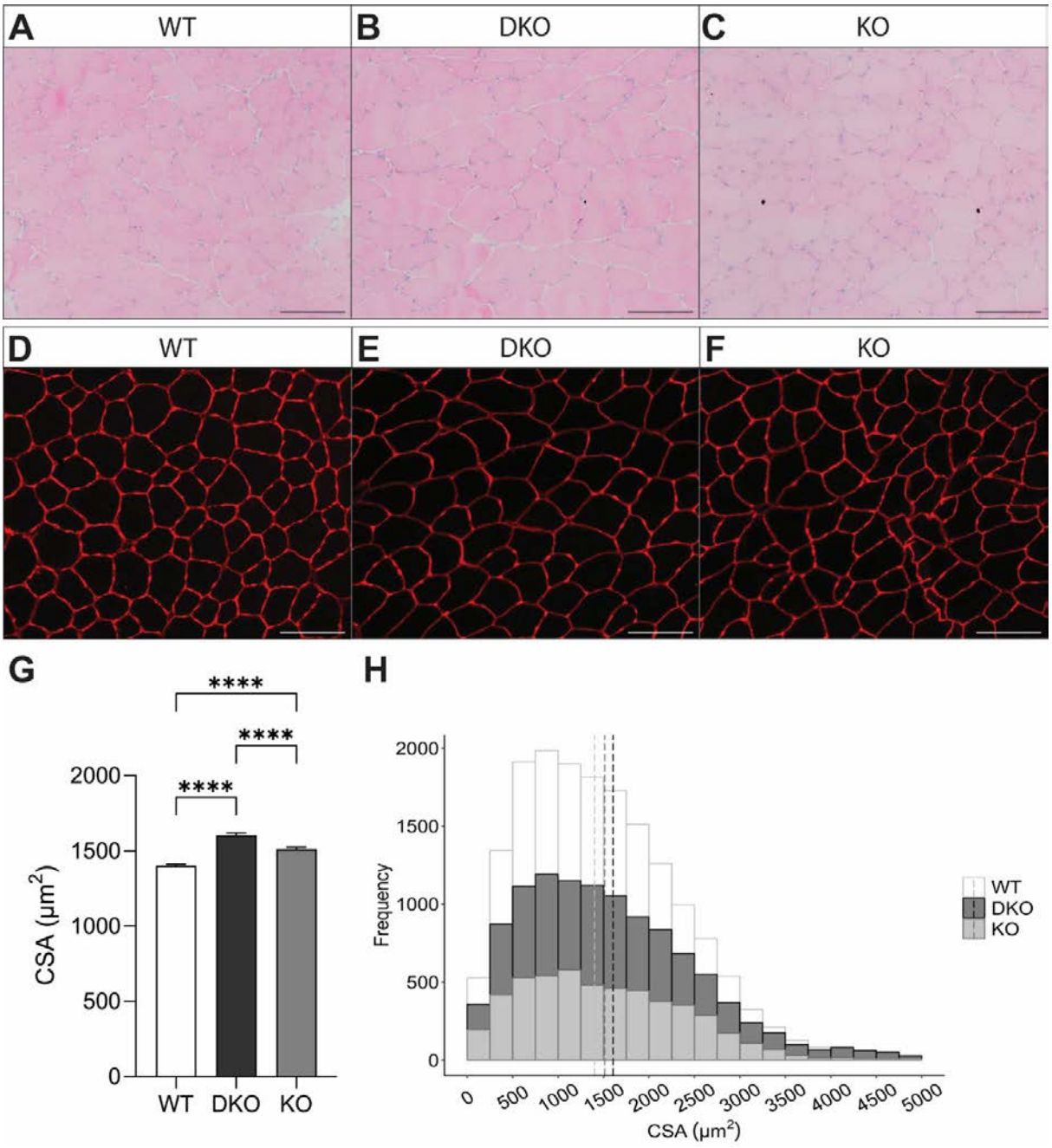

Figure 4.8. Cross sections of uninjured control TA muscle fibres. Representative H&E-stained sections from **A.** WT, **B.** DKO, and **C.** T-cad KO (KO) and images of fluorescent laminin-stained (red) sections from **D.** WT, **E.** DKO, and **F.** KO TA muscles. Scale bars 100 µm. **G.** Cross sectional area analysis (mean ± SEM, n=3). **H**. Stacked frequency distribution of myofiber area for all genotypes. Dashed lines represent mean values. **** = p<0.0001

Consecutive sections from the muscle fibres were stained with an antibody against PAX7 to identify populations of quiescent SCs. These positive nuclei were quantified as a percentage of the total number of nuclei present (**Figure 4.9**). According to these results SCs accounted for less than 3% of all nuclei present in uninjured muscle. There was an average of 1.7% PAX7 positive nuclei in WT, 2% in DKO and 2.3% in T-cad KO muscles. Although there was a slight increase in the number of positive nuclei in the DKO and T-cad KO cells, the difference between the genotypes was not significant.

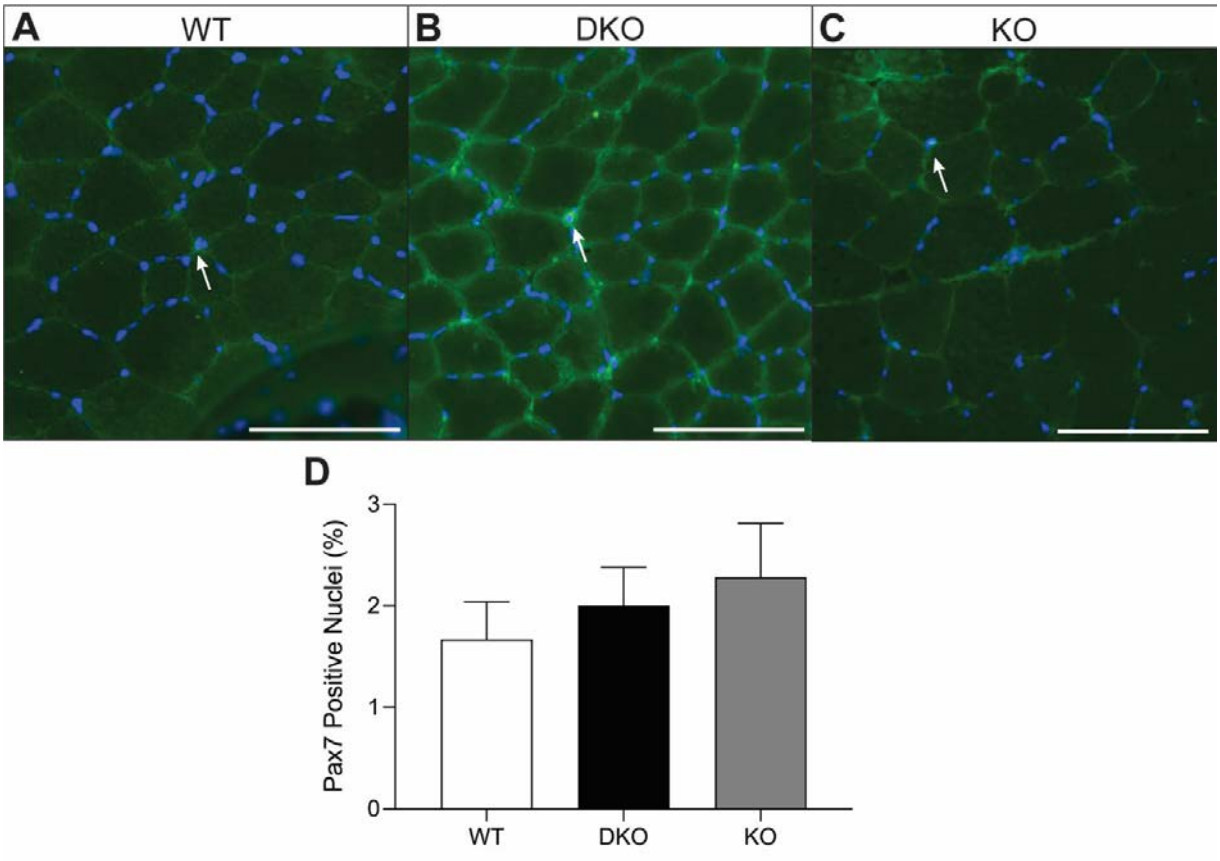

Figure 4.9. PAX7 (green) and DAPI (blue) staining of whole cross sections of uninjured muscle fibres. **A-C**. Representative images of positive PAX7 staining within **A.** WT, **B.** DKO, and **C.** T-cad KO (KO) myofibers. White arrows represent $PAX7^{+}$ satellite cells. Scale bar 100 µm. **D.** Comparison of average number of PAX7 positive nuclei for each genotype (mean ± SEM, n=4). Values are calculated as a percent of total number of nuclei present in each section. Multiple t-tests indicate no significant difference between the genotypes.

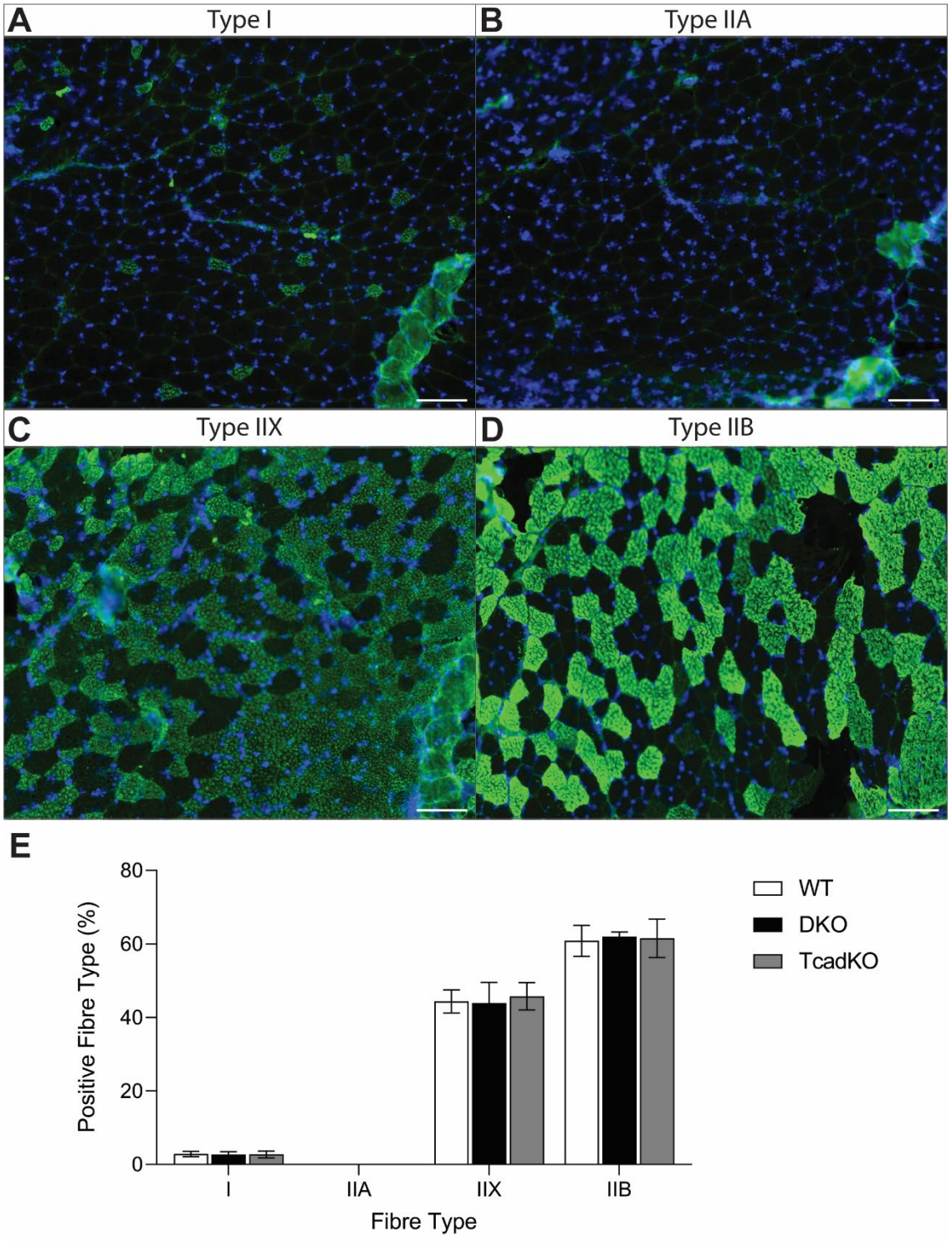

Figure 4.10. Immunofluorescent staining of WT, DKO and T-cad KO for different muscle fibre types (green) and DAPI (blue). **A-D.** Representative images for the immunofluorescent staining of muscle fibre type I, IIA, IIX and IIB, respectively. Where possible, consecutive sections were used for each fibre. Scale bar 100 µm. **E.** Fibre type present in each genotype represented by positive fluorescent staining as a percent of the muscle section (mean ± SEM, n = 4). Tukey's multiple comparison tests indicate no significant differences.

Consecutive muscle fibres from the area analysis were additionally probed with antibodies for different murine muscle types (**Figure 4.10** A-D). These antibodies identify different isoforms of myosin heavy chain that are associated with fast/slow twitch muscle fibres. No difference in muscle fibre type between any of the genotypes was found (**Figure 4.10** E). There was less than 3% of type I fibres present in all genotypes and no type IIA fibres present. Most of the muscle fibres were type IIB (60-63%), followed by type IIX (43-46%). The percentage of total fibres represented 108-110%, demonstrating most of the muscle fibres were counted in these analyses.

4.4.4 In vivo comparison of muscle regeneration in WT and DKO mice

For the regeneration studies, the left-hand side TA muscles of the WT and DKO mice were injured and allowed to regenerate for 2-, 3-, 7- and 10-days. These muscles were sectioned and examined for the presence of newly formed muscle fibres, activated SCs, macrophages and fibrotic tissue.

Muscle sections from the 10-day regeneration group were stained with H&E to visualise regeneration via quantification of centrally located nuclei (central nuclei), a hallmark feature of regenerating muscle fibres (**Figure 4.11** A-B). The results indicate that although the WT sections contained more myofibers with only one nucleus (70% versus 59%), the DKO sections had a greater number of myofibers with more than 2 nuclei present following 10 days of regeneration[xxiii]. Furthermore, there was a significant difference in the number of myofibers containing three centrally located nuclei with 3% in WT and 8% in DKO sections, equating to 2.7-fold more (**Figure 4.11**).

Muscle sections after three days of regeneration were used to identify the number of activated SCs and macrophages. Activated SCs were identified by the expression of MYOD and DAPI (**Figure 4.11** D-E, also see supplementary **Figure 9.1** in section 9.2.1 for individually stained images). There was 2-fold more activated SCs in the DKO (4%) versus the WT (2%) ($p<0.001$) (**Figure 4.11** F).

[xxiii] The analysis for number of centrally located nuclei in the WT versus DKO comparison was performed by Dr. Craig McFarlane.

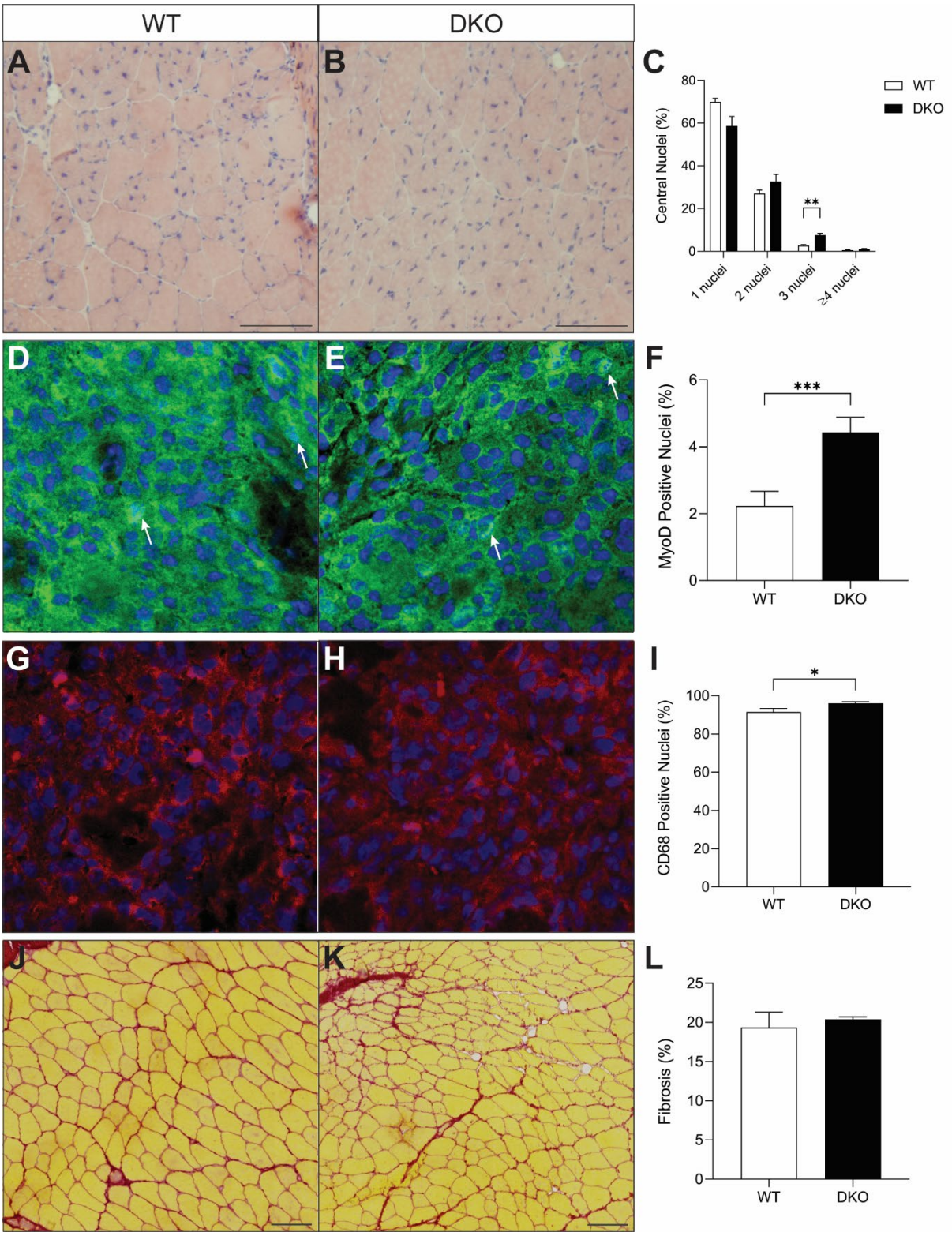
WT
DKO
A
B
C
WT
DKO
Central Nuclei (%)
80
60
40
20
0
**
1 nuclei
2 nuclei
3 nuclei
≥4 nuclei
D
E
F
MyoD Positive Nuclei (%)
6
4
2
0
***
WT
DKO
G
H
I
CD68 Positive Nuclei (%)
100
80
60
40
20
0
*
WT
DKO
J
K
L
Fibrosis (%)
25
20
15
10
5
0
WT
DKO

Figure 4.11. Comparison of the *in vivo* regenerative properties of skeletal muscles from WT and DKO mice. **A-B.** Representative images of H&E after 10 days regeneration. **C.** Number of myofibers, as a percent of total, that possess 1, 2, 3, or ≥4 centrally located nuclei (mean ± SEM, n=5). **D-E.** Representative images of immunofluorescent stained MYOD (green) and DAPI (blue) after three days of regeneration. Individually stained images can be seen in the supplementary figures in appendix two (section 9.2.1, **Figure 9.1**). White arrows indicate MYOD positive nuclei. **F.** Number of MYOD positive nuclei present as a percentage of total muscle nuclei (mean ± SEM, n=6). **G-H.** Representative images of immunofluorescent stained CD68 (red) and DAPI (blue) after three days of regeneration. Individually stained images can be seen in the supplementary figures in appendix two (section 9.2.1, **Figure 9.2**). **I.** Number of CD68 positive nuclei as a percentage of total number of nuclei (mean ± SEM, n=6). **J-K.** Representative images of picrosirius red staining after 10 days regeneration. **L.** Amount of fibrotic tissue present as a percentage of total muscle area (mean ± SEM, n=6). Scale bars 100 μm. Statistical significance was calculated using a student's t-test and significance values are denoted by * = $p<0.05$, ** = $p<0.01$, *** = $p<0.001$.

CD68 was used to identify macrophages (**Figure 4.11** G-H, also see supplementary **Figure 9.2** in section 9.2.1 for individually stained images). Although statistically significant, there was just a 1.05-fold increase in the number of CD68 positive cells in the DKO (96%) versus WT (92%). This value was higher than expected for the number of macrophages after 3 days of regeneration. This is likely due to the method of capturing and analysing positive cells in 10 random images of the injured region. Furthermore, given the bright fluorescence of CD68 surrounding the nucleus, it was often difficult to differentiate between positive and negative cells. This may have led to a higher-than-expected number of CD68 positive cells.

Finally, the day 10 sections were stained with picrosirius red - a collagen stain (**Figure 4.11** J-L). There were similar levels of collagen deposits in the WT (19%) and DKO sections (20%), indicating no difference in fibrosis following regeneration.

4.4.5 In vivo comparison *of muscle regeneration in WT and T-cad KO mice*

Given the T-cad KO primary myoblasts show limited differentiation changes we next considered T-cad KO versus WT genotype in the injury model. As previously, regenerating muscles were isolated from WT and T-cad KO mice at 2-, 3-, 7-, and 10-days post injury. Histology of these muscles was used to examine for differences in muscle fibre formation, SC activation, macrophage number and fibrosis. There were no significant differences observed between the WT and T-cad KO muscles for any of these parameters.

Central nuclei were identified from day 10 of injury through H&E staining (**Figure 4.12** A-B). In WT, 59% of the myofibers had one centrally located nucleus, 29% with two, 9% with three and 3% with four or more nuclei. In the T-cad KO, 64% of the myofibers had one centrally located nuclei, 25% had two, 8% had three and 2% had four or more (**Figure 4.12** C). The WT values are like the WT values seen in the WT versus DKO comparison, highlighting consistency between the two experiments and there was no significant difference between WT and T-cad KO muscles.

Immunofluorescent staining of day three injured muscles for MYOD and CD68 identified the percentage of activated SCs and macrophages, respectively (**Figure 4.12** D-I, also see supplementary **Figure 9.3** and **Figure 9.4** in section 9.2.2 for individually stained images). The T-cad KO muscle sections (5%) had 1.5-fold more activated SCs than the WT (3.3%), but this was not statistically significant. Analysis of CD68 positive macrophages showed that 80% of the total WT and 76% of the KO nuclei were macrophages and this was not statistically different. The issues encountered in the staining and counting of the CD68 positive cells in the WT versus DKO comparison were improved during this experiment and clearer images were taken for the entire cross section. For this reason, the WT values calculated for this analysis were not consistent with the WT values in the previous analysis and were thus considered separately. For day 10 injury picrosirius red staining, 27% of the WT and 30% of the T-cad KO muscle stained positive, and there was no significant difference between the groups (**Figure 4.12** J-L).

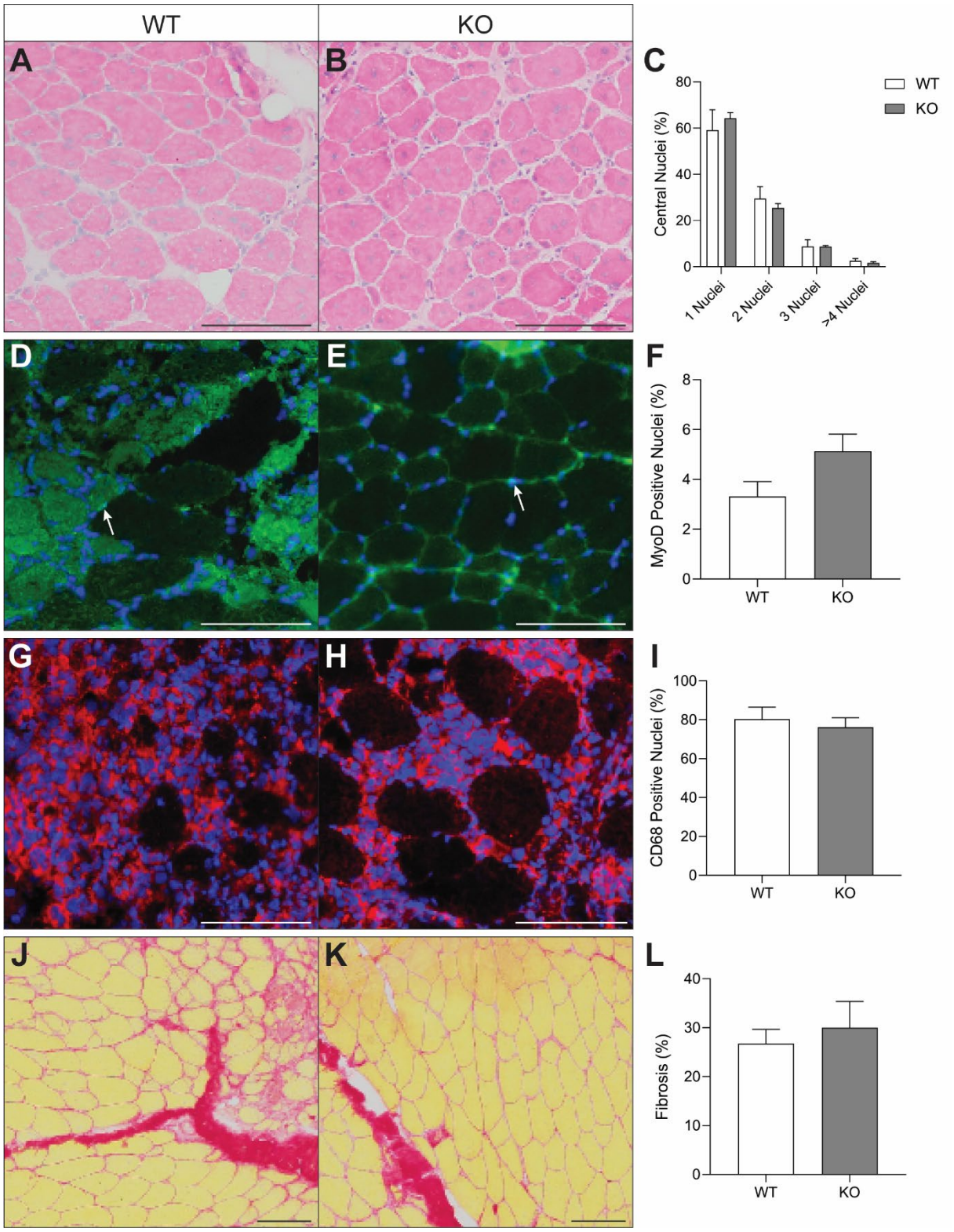
WT
KO
A
B
C
WT
KO
Central Nuclei (%)
80
60
40
20
0
1 Nuclei
2 Nuclei
3 Nuclei
>4 Nuclei
D
E
F
MyoD Positive Nuclei (%)
8
6
4
2
0
WT
KO
G
H
I
CD68 Positive Nuclei (%)
100
80
60
40
20
0
WT
KO
J
K
L
Fibrosis (%)
40
30
20
10
0
WT
KO

Figure 4.12. Comparison of *in vivo* regeneration of skeletal muscle from WT and T-cad KO (KO) mice **A-B.** Representative images of hematoxylin and eosin staining after 10 days regeneration. **C.** Number of myofibers, as a percent of total, that possess 1, 2, 3, or ≥4 centrally located nuclei (mean ± SEM, n=4). **D-E.** Representative images of immunofluorescent stained MYOD (green) and DAPI (blue) after three days regeneration. Individually stained images can be seen in the supplementary figures in appendix two (section 9.2.2, **Figure 9.3**). White arrows indicate MYOD positive nuclei. **F.** Number of MYOD positive nuclei present as a percentage of total muscle nuclei (mean ± SEM, n=4). **G-H.** Representative images of immunofluorescent stained CD68 (red) and DAPI (blue) after three days regeneration. Individually stained images can be seen in the supplementary figures in appendix two (section 9.2.2, **Figure 9.4**). **I.** Number of CD68 positive nuclei as a percentage of total number of nuclei (mean ± SEM, n=4). **J-K.** Representative images of picrosirius red staining after 10 days regeneration. **L.** The area occupied by fibrotic tissue present as a percent of total muscle section (mean ± SEM, n=4). Scale bars 100 μm. Statistical significance was calculated using the student's t-test.

4.5 Discussion

Preliminary data illustrated that DKO versus WT myoblasts have accelerated differentiation, but the mice show no differences in muscle development, and T-cadherin overexpression inhibits C2C12 myogenesis *in vitro*. Understanding of the role of T-cadherin in myogenesis is incomplete and knowledge of its function in skeletal muscle regeneration and repair is limited. To determine how T-cadherin may contribute to myogenesis, this chapter assesses the differentiation ability of T-cad KO versus WT myoblasts and evaluated the uninjured and injured muscle phenotype of the WT, T-cad KO and DKO mice. Together the chapter revealed that DKO mice have, after injury, accelerated muscle repair and suggests that T-cadherin has an important role in conjunction with its ligand APN, in muscle repair. Importantly, it was also shown that T-cadherin colocalised with Pax7, suggesting its presence on SCs. The implications of this chapter's findings are discussed below.

4.5.1 T-cadherin loss alone does not impact muscle regeneration

Using established protocols, primary myoblasts were isolated from WT and T-cad KO mice. Unlike the WT versus DKO myoblasts, there were no significant differences between WT versus T-cad KO in fusion index, average myotube size or expression of myogenin and MHC throughout the differentiation time course. Importantly, these data align with the results from the RNA sequencing of primary myoblasts in chapter 3 that showed many differentially expressed genes between the WT and DKO myoblasts, but only a small number of differentially expressed genes between the WT and T-cad KO myoblasts. Moreover, in the injury model of WT versus T-cad KO, we saw no change in macrophages, activated SCs, central nuclei, fibrosis, and fibre size between the genotypes. In contrast, between WT and DKO, the regeneration phenotype was pronounced with the DKO injured muscle having more macrophages, activated SCs and central nuclei than WT muscle during muscle regeneration, revealing accelerated muscle repair in the DKO mice, which was absent in the T-cad KO mice.

The data show that differences in skeletal muscle phenotype between WT, T-cad KO and DKO mice is most pronounced after injury and not during development. In the

uninjured muscles there was no change in the average total body weight, muscle fibre type and SC number between the DKO versus WT and T-cad KO versus WT. Interestingly, there were no type IIA fibres present in the muscle sections, which could be due to issues with the antibody during staining or a lack of type IIA fibres. As well, the number of Pax7 positive SCs ranged from 1.6% to 2.3% and was within the published range [60].

The only recognisable and significant difference was that the uninjured DKO myofibers were 15% larger than WT, and the T-cad KO 6% larger than WT. This could be due to enhanced regeneration following everyday wear and tear of the DKO and T-cad KO fibres, inherent differences between myofibers at development, or uneven sectioning of the muscles.

The expression of both T-cadherin and APN decrease at the beginning of regeneration but increase at day three, suggesting an important role for these proteins in muscle repair [212]. Hence, how could T-cadherin and APN expression enhance muscle regeneration *in vivo*? One likely mechanism involves inflammation. The injured DKO muscle had a slight increase in the number of macrophages as well as MYOD expression during regeneration. These two events may be interconnected and encourage SCs to activate sooner and progress through regeneration more efficiently than WT. The observations also imply that T-cadherin and APN loss *in vivo* are intertwined and improve regeneration in the DKO mice.

Macrophages and neutrophils are involved in the clearing out of muscle fibre debris, with infiltration peaking for the former at day three post injury [54]. There was a small but statistically significant increase in macrophage number in the DKO muscle post injury, and this may parallel accelerated clearing of the DKO TA muscle after injury. However, the bright CD68 staining and unclear images made it difficult to identify positive macrophages. As a result, the macrophage number was higher than expected and will require further validation before proceeding with the investigation of other macrophage markers. This is discussed below.

Significantly, APN regulates the immune response and is protective against inflammation, obesity, insulin resistance, and cardiovascular diseases (reviewed Luo, et al. [319]) and APN downregulation correlates with elevated inflammation and metabolic disease states [320-322]. Depending on the stimulus, macrophages can

polarize towards two different phenotypes, namely pro-inflammatory M1 macrophages and anti-inflammatory M2 macrophages [323]. All three APN receptors are expressed by macrophages and have roles in macrophage polarisation [319, 324, 325]. AdipoR1 binds gAPN and mediates pro-inflammatory cytokine expression, and AdipoR2 binds fAPN and mediates M2 polarization [324, 326]. Furthermore, in adaptive thermogenesis T-cadherin is increased by cold exposure, and promotes M2 proliferation [325]. Thus, it is plausible that decreased APN and T-cadherin expression during the first stage of regeneration, and their increase after day three, participate in a switch from M1 to M2 macrophages during muscle myogenesis.

M1 macrophages remove the debris, attract SCs to the injured area, stimulate their proliferation and prevent differentiation. This is associated with the secretion of inflammatory factors such as TNFα, IL-6, and IL1β. The blocking or loss of their function can downregulate MYOD, myogenin and myosin [327]. M2 macrophages accelerate SC differentiation, and this is promoted through the secretion of anti-inflammatory cytokines such as IL-4, IL-10, and IL-13. M2 macrophage absence delays muscle growth and limits differentiation and regeneration [327, 328].

In this light, a recent study using the APN receptor agonist AdipoRon during myogenesis down-regulated myogenin and MYOD [329]. Thus, the increased MYOD in the DKO injured muscles could be due to the increased number of macrophages that in turn activate downstream myogenic factors. It is possible that in T-cad KO mice, where the serum APN is 4-fold higher than in WT that MYOD expression is down-regulated through AdipoR1 and AdipoR2. This model is visualised in **Figure 4.13**. and it is important that future studies determine the M1 and M2 status of the injured muscle in the three genotypes.

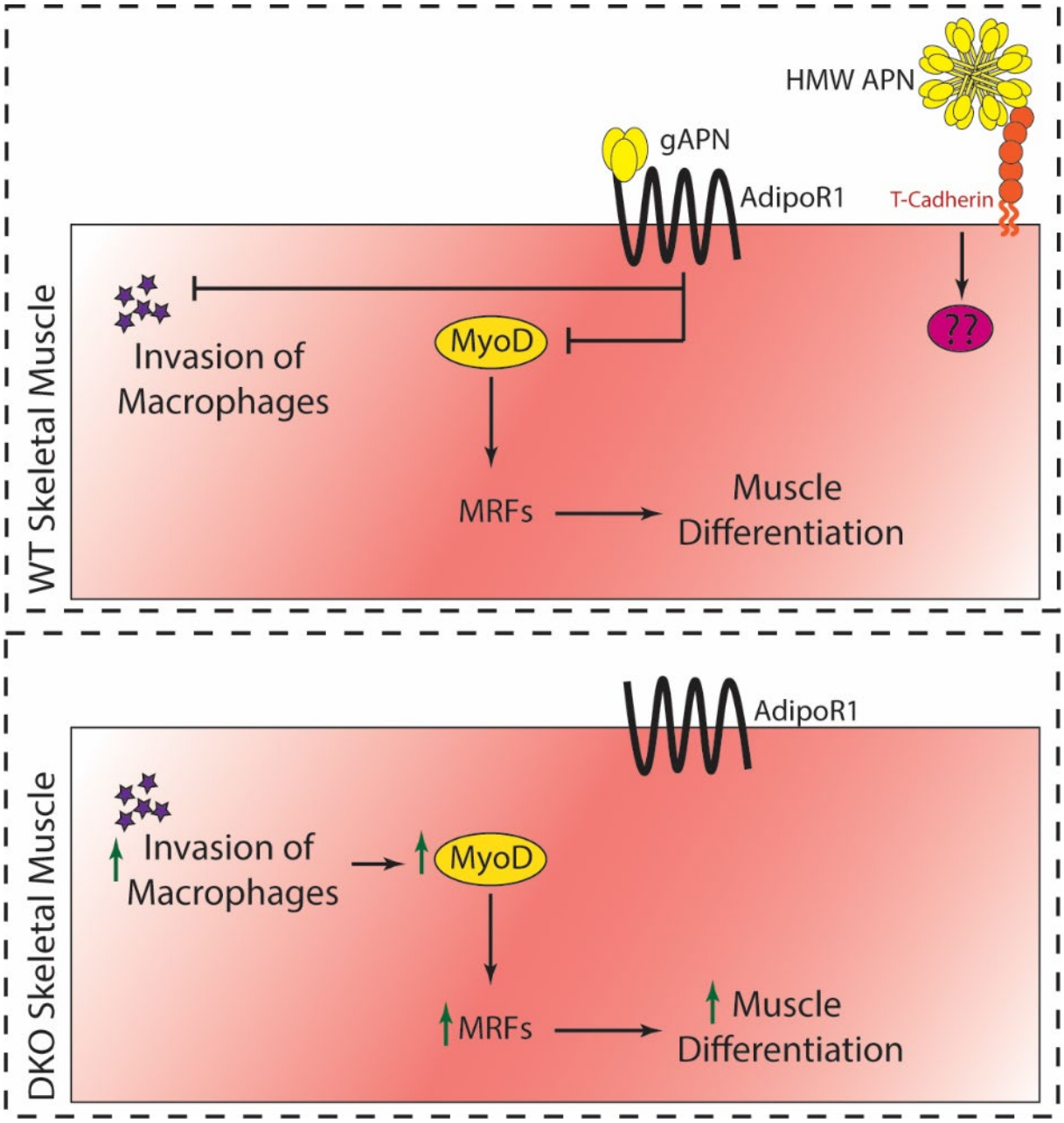

Figure 4.13. Control of MYOD signalling during myogenesis in WT and DKO skeletal muscle. In WT muscle, APN signals through AdipoR1 to mediate macrophage infiltration. APN also inhibits the expression of MYOD, thus delaying muscle differentiation. In DKO muscle, the lack of APN leads to increased macrophages and MYOD, overall increasing muscle differentiation. The function of T-cadherin in myogenesis independent of APN binding is explored in later chapters.

4.5.2 Controversy surrounding T-cadherin and adiponectin

The limited differences seen between WT and T-cad KO primary myoblast growth and *in vivo* regeneration in this chapter are in agreement with the results of Tanaka, et al. [212], who found no differences in muscle regeneration between WT and T-cad KO mice. Furthermore, Tanaka found no differences in regeneration between WT and APN KO muscles. It was only through adenoviral over expression of fAPN leading to supranormal serum levels, that muscle regeneration improved in aged WT and APN KO mice. No effect of fAPN was noted in young WT and aged T-cad KO mice [212]. This study did not investigate DKO mice.

Nonetheless, there are published inconsistencies regarding APN's role in muscle regeneration. Accordant with this thesis, a study that showed that activation of APN receptors by AdipoRon, repressed myotube formation and the expression of MYOD and myogenin [329]. Nonetheless, other studies suggest APN enhances myoblast differentiation. The addition of gAPN can promote myoblast differentiation through inhibiting the cell cycle and committing cells to terminal differentiation [109].

The limitation of these studies includes the background and age of the mice, and the form of APN that was measured or administered. By example, Liu, et al. examined the effects of a high fat diet administered for 9-weeks on APN induction from the gastrocnemius muscle. Although there were no changes in total APN concentration, the amount of mRNA and HMW isoforms present decreased [330]. In experiments with *db/db* mice (a mouse model of type 2 diabetes), the APN profiles were considered, and it was observed that in the soleus muscle total APN and HMW APN decreased, and MMW APN increased. In contrast, the EDL muscle from the same mice showed only significant increases in the LMW isoforms [330].

Apart from the different APN isoforms, the activation of APN receptors and myoblast differentiation is dependent on the age of the mice. The activation of AdipoR1 and R2 by AdipoRon promotes adipogenesis and suppresses MRFs in young SCs, but has the opposite effect in aged SCs [329]. These results parallel that of Tanaka et al. where APN overexpression enhances muscle regeneration in an ageing mouse model, but not in young C57BL6 mice [212]. This thesis used young adult mice and it remains to be determined if aged DKO mice have better SCs and repair than WT. In addition,

further research is required to understand the individual roles of APN isoforms in muscle regeneration.

Importantly, this chapter highlights the benefits of using both primary myoblasts and an *in vivo* injury model to determine the interactions of adhesion proteins during myogenesis. Tanaka et al. did not use DKO mice, which is unfortunate as the phenotype of T-cadherin in primary myoblasts was not described by them. The DKO phenotype described in this chapter is striking, especially compared to the effects seen in other cadherin knockout mice. For example, M-cadherin KO mice had no difference in myotube formation [205]. N-cadherin KO mice die due to developmental complications prior to skeletal muscle formation and the KO murine cell lines can form fully functional myotubes [200]. Our complementary approach of primary myoblasts and injury models is a better research strategy.

4.5.3 Recommendations and future directions

The results from this chapter illustrate a role for T-cadherin and APN in myogenesis and skeletal muscle regeneration. The data suggests that it is a combination of APN's anti-inflammatory effects and downstream signalling through AdipoR1 and -R2 that modulate MYOD expression. To aid our understanding, it is important to establish the differences between the different APN isoforms on primary myoblast differentiation and muscle regeneration. The bright fluorescence of the CD68 staining led to difficulties in differentiating between positive and negative macrophages. This staining should be repeated to improve visibility of positive cells. Additionally, using available tissues, each genotype should be probed for M1 and M2 macrophage markers to examine for an inflammatory switch in the DKO muscles. Finally, the experiments described above could be supported with APN KO mice to confirm the importance of T-cadherin and APN in regulating post-natal myogenesis.

4.6 Conclusion

This chapter focussed on understanding the role of T-cadherin and APN in post-natal myogenesis. Our results reveal that T-cadherin and APN are important in the regulation of muscle regeneration. Not only do DKO primary myoblasts differentiate sooner than WT myoblasts, but DKO myofibers regenerate more efficiently *in vivo* than WT mice. As there are no differences in the growth of T-cad KO myoblasts and injured myofibers compared to WT, it is apparent that high serum APN (as noted in the T-cad KO mice) can restrict myogenesis *in vivo.* Nonetheless, T-cadherin is a signalling molecule and can interact with other cadherins independently of APN and studies should be pursued to examine its role in myogenesis in more detail. This we have begun in chapters 5 and 6.

5 T-cadherin in Skeletal Muscle Metabolism

5.1 Introduction

Energy availability is crucial for the function of skeletal muscles in everyday movement and strength. Energy for muscle function is provided through multiple pathways and depends on the muscle fibre type and energy requirements. To meet these demands, the muscles will first utilize ATP stores and activate anaerobic respiratory pathways. If muscle contraction continues, the muscles will turn to aerobic respiration and begin utilising blood glucose, stored intramuscular glycogen and free fatty acids [76]. Energy production is particularly important during exercise and muscle regeneration where the mitochondria serve as the primary source of energy. In proliferating myoblasts oxidative phosphorylation accounts for only 30% of the required ATP, increasing to approximately 60% in myotubes [331]. Myoblast differentiation is also accompanied by an increase in mitochondrial biogenesis, protein synthesis and protein activity [332]. If mitochondrial health is compromised, ATP regeneration, through oxidative pathways, is reduced, which can limit muscle regeneration and repair.

Adiponectin can regulate metabolic homeostasis by activating AMP-activated protein kinase (AMPK). Through AMPK, APN increases glucose uptake, mitochondrial biogenesis, and fatty acid oxidation. In addition, the expression of serum APN is linked to increased insulin sensitivity, and reduced serum APN inversely correlates with metabolic syndromes such as obesity and type 2 diabetes.

Studies show that APN can mediate mitochondrial DNA content, and this is limited in AdipoR1 KO mice. AdipoR1 KO mice show decreased AMPK pathway activity, muscle endurance and the expression of molecules involved in mitochondrial biogenesis, even following the administration of APN [333]. In addition, APN binding through T-cadherin is critical for AMPK-signalling in cardiac tissue [224].

Here we find that DKO TA muscles have improved regenerative capacity after injury and the primary myoblasts show accelerated differentiation, which is perplexing while APN is absent and not increasing energy uptake. Thus, the focus of this chapter was to test if T-cadherin modulates energy use in myoblasts.

5.2 Preliminary data and aims

Initial studies showed significant increases in growth and differentiation of DKO versus WT myoblasts (see chapter one, section 1.10). These results show that the DKO myoblasts are committing to myogenesis sooner, fusing faster and forming myotubes earlier than WT myoblasts. Furthermore, the gene ontology analysis of the DKO differentiating myoblasts revealed the up regulation of genes involved in metabolic pathways.

Given the significant differences seen in the differentiation of the DKO versus WT primary myoblasts, this chapter examined mitochondrial function as a measure of metabolic capacity. Therefore, the studies described in this chapter aimed to:

1. Examine differences in mitochondrial function in T-cadherin over expressing C2C12 myoblasts.
2. Examine differences in mitochondrial function between primary WT and DKO myoblasts.

5.3 Methods

For complete materials and methods please see chapter 2 section 2.3 and 2.7.

Seahorse cell culture microplates were prepared as per the Agilent ‘Seahorse XFp Mito Stress Test’ or ‘Seahorse XF Palmitate-BSA FAO Substrate’ protocol and were either used for proliferating myoblasts or differentiating myoblasts at 24 or 48 hours. The Seahorse microplate was then inserted into the analyser and set to run as per Agilent Technologies standard ‘Mitochondrial Stress test Protocol’ for the XFp device. For the fatty acid oxidation assay, the cells were supplied with either BSA-conjugated palmitate or BSA just prior to the assay. At least three oxygen consumption rate (OCR) measurements were recorded prior to any injections and then after each subsequent injection of 1 µM Oligomycin, 1.5 µM FCCP and 0.5 µM antimycin/rotenone. Following the assay, the cells were stained with methylene blue to allow for normalisation of the assay to cell mass. Both C2C12 (pLN1 and pLTcad) and primary myoblasts were used for this analysis.

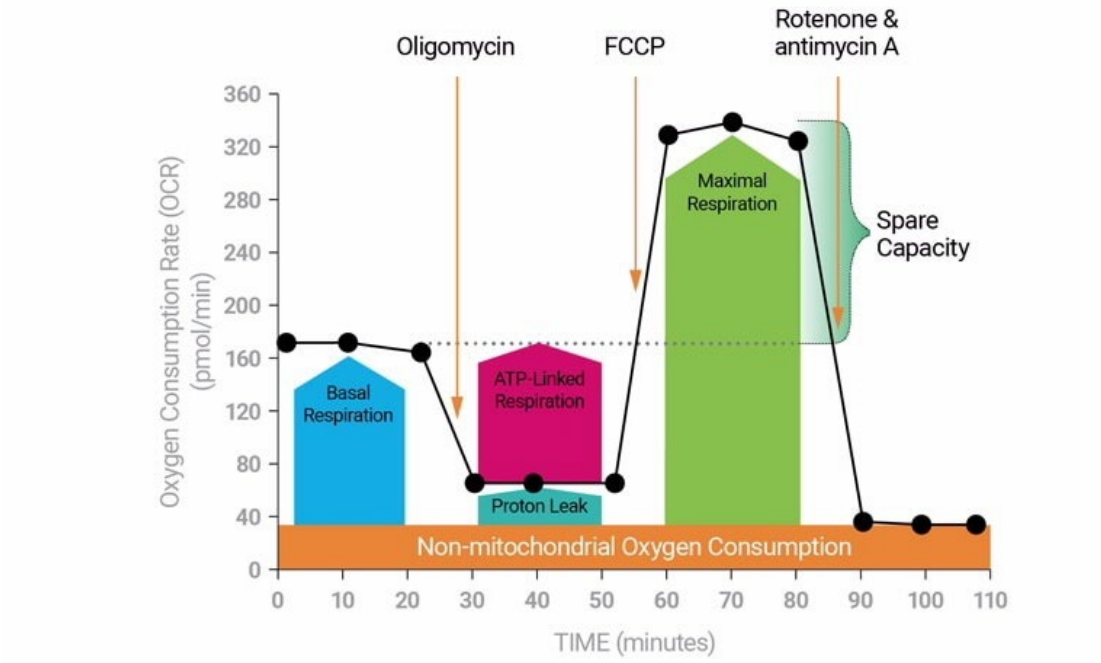

Figure 5.1. Agilent seahorse XFp Cell Mito Stress Test profile of the key parameters of mitochondrial respiration. Sequential compound injections allow for the quantification of basal respiration, ATP production, proton leak, maximal respiration, spare respiratory capacity, and non-mitochondrial respiration. Image taken from ‘Seahorse XF Cell Mito Stress Test Kit User Guide’ [3].

A schematic representation of real time OCR measurements following inhibitor injection in the 'Mito Stress Test' assay is depicted in **Figure 5.1**. These values are used to calculate basal respiration, ATP production, proton leak, non-mitochondrial respiration, maximal respiration, spare respiratory capacity, and coupling efficiency. The basal respiration is the oxygen consumption under baseline conditions minus the non-mitochondrial OCR. The OCR linked to ATP production and proton leak is measured after ATP synthase is inhibited. It is used to calculate the mitochondrial coupling efficiency, which measures the proportion of basal oxygen consumption that contributed to ATP synthesis versus proton leak. The maximal respiration and spare respiratory capacity are calculated following the addition of the mitochondrial uncoupler and measure how efficiently the cells can respond to stress. The spare respiratory capacity measures differences in OCR between basal and maximal respiration and is a measure of cellular fitness [3]. The non-mitochondrial respiration is the amount of oxygen consumed independent of the electron transport chain.

An OXPHOS antibody cocktail (abcam, cat: 110413) was used to assess mitochondrial content. Briefly, mitochondria were purified, lysates prepared from differentiating pLN1 and pLTcad C2C12 cells, subjected to SDS-PAGE electrophoresis, western blotting and probed with the OXPHOS cocktail for complex I – NADH dehydrogenase (NDUFB8), complex II – succinate dehydrogenase (SDHB), complex III – cytochrome c reductase (MTCOI), complex IV – cytochrome c oxidase (UQCRC2), and complex V – ATP synthase (ATP5A).

To determine mitochondrial content, C2C12 myoblasts and murine myoblasts were stained with MitoTracker Green FM for 20 minutes at 37 °C in the dark. Trypsinised cells were resuspended in PBS and FACS performed using the FITC channel of a FACS Fortessa flow cytometry system (BD Biosciences). 10,000 events from each of the three biological replicates were recorded and the background signal obtained from unstained cells was deducted. Median fluorescence intensity was averaged and represented as mean fluorescence intensity (MFI).

Analysis was performed using ImageJ software and statistical analysis using GraphPad Prism. Error bars represent standard error of the mean (SEM) unless otherwise stated. * = $p<0.05$, ** = $p<0.01$, *** = $p<0.001$, **** = $p<0.0001$ denote the significance values used throughout this chapter.

5.4 Results

5.4.1 T-cadherin overexpression in C2C12 cells impairs mitochondrial function

Control (pLN1) and T-cadherin overexpressing (pLTcad) C2C12 cell lysates were collected, separated, and probed for T-cadherin expression. pLTcad cells expressed substantially more T-cadherin than pLN1 cells and were used for further experiments (**Figure 5.2** A). To investigate the effects of T-cadherin on mitochondrial function, OCR in differentiating pLN1 and pLTcad C2C12 cells was measured using the Seahorse Extracellular XFp flux analyser. After cell mass normalisation, there were no substantial differences in the OCR at any point during the mitochondrial stress test. Following the addition of multiple electron transport chain inhibitors, both cell types responded similarly but the pLTcad cells' maximum OCR (recorded between 40-60 mins) was lower than that of the pLN1 cells (**Figure 5.2** B). There was no difference in basal respiration, proton leak, non-mitochondrial respiration, or ATP-linked respiration (**Figure 5.2** C). Oxygen consumption increased 3.4-fold in pLN1 cells and only 3.3-fold in pLTcad cells following the addition of the uncoupler (FCCP), and while a decrease in the maximal respiration of the pLTcad cells was noted, this was not significant (**Figure 5.2** B-C). The mitochondrial coupling efficiency was between 82-84% with less than 1% difference between the cell types. To ascertain mitochondrial content of pLN1 and pLTcad myoblasts, they were stained with MitoTracker Green FM and subjected to FACS to determine mean fluorescence intensity. The results show that there was a significant decrease in MitoTracker Green FM in pLTcad cells, suggesting that a reduced mitochondrial mass correlates with T-cadherin overexpression (**Figure 5.2** D).

Given the importance of fatty acid oxidation in myoblasts, the mitochondrial stress test was repeated with substrate-starved C2C12 cells at 48-hours differentiation, supplied with BSA conjugated palmitate (**Figure 5.3**). The normalised data shows that pLN1 C2C12 cells supplied with palmitate had the highest baseline OCR, followed by the pLN1 cells treated with BSA, the pLTcad cells treated with palmitate and the BSA pLTcad cells. Following mitochondrial uncoupling with the addition of FCCP, the palmitate treated cells could not reach the same maximum OCR as the BSA treated cells and the pLN1 cells treated with BSA had the highest OCR at this timepoint (**Figure 5.3** A).

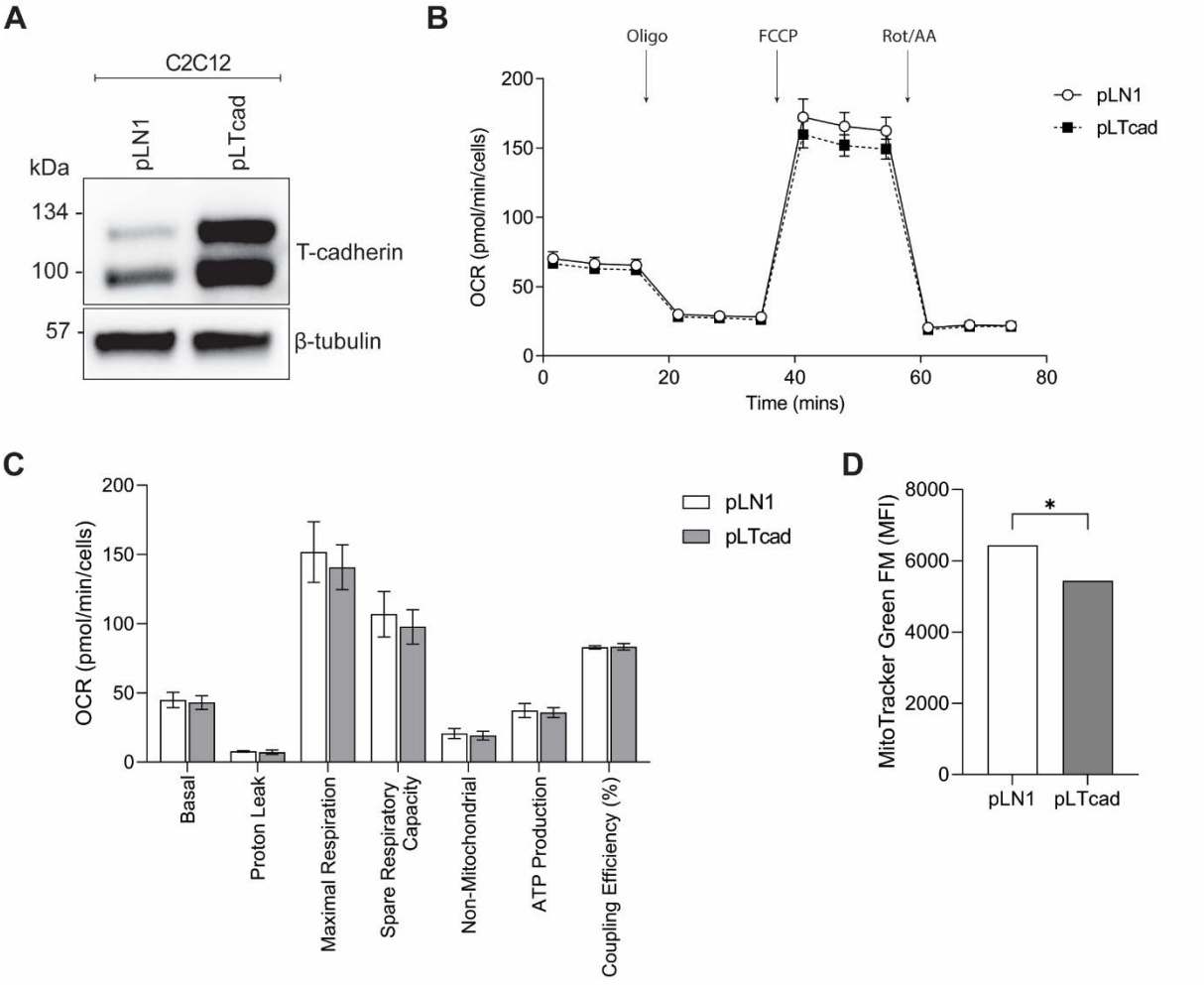

Figure 5.2. Mitochondrial function of pLN1 C2C12 cells and pLTcad cells after 24 hours differentiation. **A.** Western blot showing T-cadherin expression in pLN1 C2C12 and pLTcad C2C12 cells. **B.** Real time oxygen consumption rate (OCR) of pLN1 and pLTcad C2C12 cells during the Agilent Seahorse mitochondrial stress test, normalized to methylene blue concentration (n=3). 'Oligo', FCCP' and 'Rot/AA' represent the injection of oligomycin, FCCP, and rotenone/antimycin A, respectively. **C.** Quantification of basal respiration, respiration linked to proton leak, maximal respiration, spare respiratory capacity, non-mitochondrial linked respiration, respiration linked to ATP production and coupling efficiency (%) of pLN1 and pLTcad C2C12 cells as determined by the Agilent Seahorse 'mitochondrial stress test' normalised to methylene blue concentration (mean ± SEM, n=3). **D.** Proliferating cells. Median FITC fluorescence of pLN1 (6436 ± 134) and pLTcad (5440 ± 206.6) cells stained with MitoTracker Green FM represented as mean fluorescence intensity (MFI) (mean, n=2). Statistical significance determined with Tukey's test for multiple comparisons or a t-test. * = $p<0.05$.

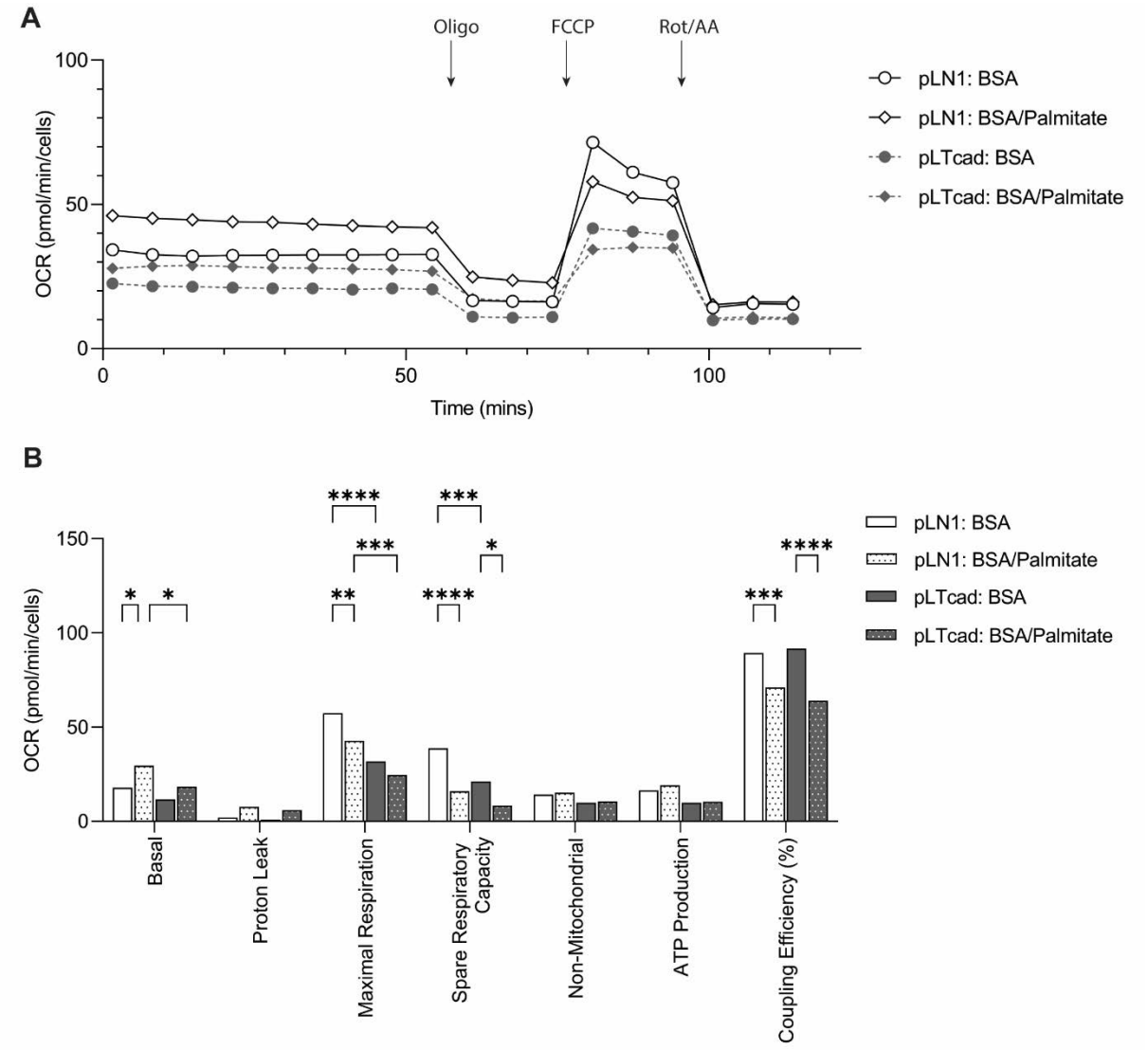

Figure 5.3. Fatty acid oxidation of pLN1 C2C12 cells and pLTcad C2C12 cells at 48 hours differentiation. **A.** Real time oxygen consumption rate (OCR) of pLN1 and pLTcad C2C12 cells during the mitochondrial stress test, normalized to methylene blue concentration. Prior to beginning the assay, the cells were given substrate-limited medium and then supplemented with either BSA or BSA-conjugated palmitate (n=2). 'Oligo', FCCP' and 'Rot/AA' represents the injection of oligomycin, FCCP, and rotenone/antimycin A, respectively. **B.** Quantification of basal respiration, respiration linked to proton leak, maximal respiration, spare respiratory capacity, non-mitochondrial linked respiration, and respiration linked to ATP production of pLN1 and pLTcad C2C12 cells based on results from the Seahorse 'mitochondrial stress test' assay with and without palmitate normalised to methylene blue concentration (mean, n=2). Statistical significance determined with Tukey's test for multiple comparisons. * = $p<0.05$, ** = $p<0.01$, *** = $p<0.001$, **** = $p<0.0001$.

Considering the outputs, the pLN1 cells with or without palmitate had a higher basal OCR than the pLTcad cells and the addition of palmitate significantly increased the basal OCR in pLN1 compared to pLTcad cells. There was no significant change in proton leakage between the cell types, and the proton leak OCR increased in the presence of palmitate. There was a significant reduction in maximal respiration of pLTcad versus pLN1 cells with and without palmitate. For spare respiratory capacity, there was a significant decrease in both cell types in the presence of palmitate, and this was significantly less in pLTcad versus pLN1 cells without palmitate. The non-mitochondrial and ATP-linked OCR with and without palmitate was less in pLTcad versus pLN1 (not significant). The coupling efficiency of pLN1 and pLTcad cells were of similar levels without palmitate and in its presence decreased to alike levels (**Figure 5.3** B). Taken together, the data suggest that while pLTcad cells have fewer mitochondria, they also have reduced basal respiration, maximum respiration, spare respiratory capacity, and ability to respond to stress in the presence of palmitate.

Next, mitochondrial proteins were purified from pLN1 and pLTcad C2C12 cells differentiated for 0-, 24-, 48-, and 72-hours, separated by gel electrophoresis and probed for five mitochondrial complexes: complex I – NADH dehydrogenase (NDUFB8), complex II – succinate dehydrogenase (SDHB), complex III – cytochrome c reductase (MTCOI), complex IV – cytochrome c oxidase (UQCRC2), and complex V – ATP synthase (ATP5A) (**Figure 5.4** A).

Complex IV was not detected in any of the samples at any timepoint, and pLN1 and pLTcad samples had higher concentrations of complex I and III when compared to the expression of complexes II and IV. To gauge differences, densitometry was used. Following the commencement of differentiation, pLTcad cells had, in all instances, lower concentrations of complex I, II, III and V, compared to pLN1 cells. In pLTcad cells, the expression of the mitochondrial proteins increased over the time course except for complex II, which increased after 48 hours but then decreased at 72 hours differentiation. The expression of each of the complexes was similar at 0 hours in pLN1 and pLTcad cells except for complex I that showed increased expression in pLTcad cells. Complex V had the smallest decrease in expression in pLTcad cells versus pLN1 cells (**Figure 5.4** B-E). Taken together, the Seahorse, mitochondrial staining and western blotting suggest that the increased T-cadherin expression in C2C12 cells equates with reduced mitochondrial content and respiratory potential.

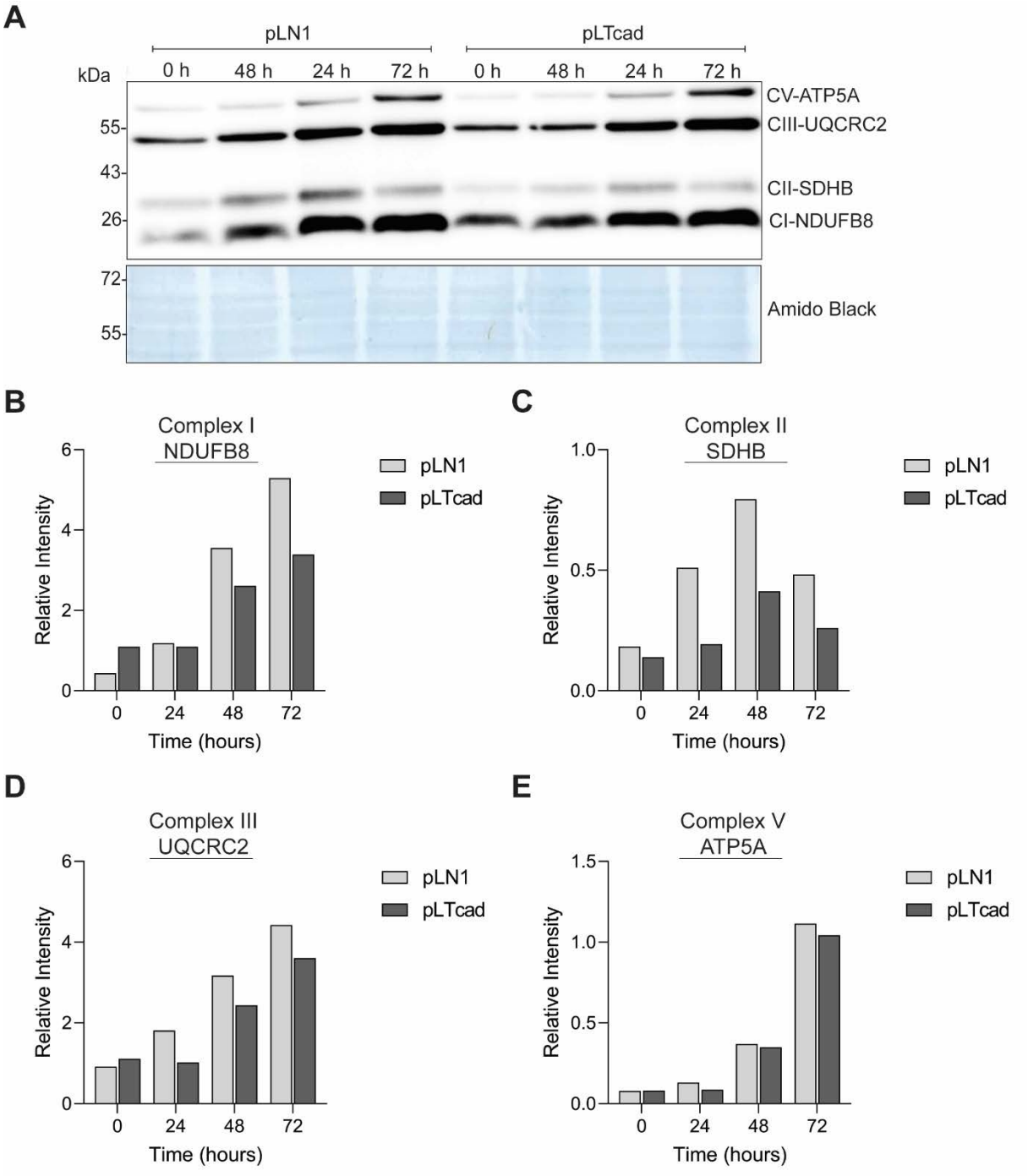

Figure 5.4. **A.** Western blot analysis of OXPHOS subunit (ATP5A, UQCRC2, MTCOI, SDHB and NDUFB8) protein levels in differentiating pLN1 and pLTcad C2C12 myoblasts at 0, 24, 48 and 72 hours. Each sample represents a pool of 15+ plates of differentiating cells and MTCOI (complex IV) was not detected. Densitometry graphs showing proteins levels of **B.** complex I – NADH dehydrogenase, **C.** complex II – succinate dehydrogenase, **D.** complex III – cytochrome c reductase and **E.** complex V – ATP synthase normalized to amido black staining, in arbitrary units.

5.4.2 T-cadherin and adiponectin loss improves mitochondrial function in differentiating primary myoblasts

Following the results of the study on mitochondrial function using C2C12 cells, the experiments were repeated with primary myoblasts. Firstly, the number of mitochondria were examined in the primary myoblasts using MitoTracker Green FM staining and analysed by flow cytometry (**Figure 5.5**). There was a significant but small increase (1.03-fold) in the mitochondrial staining intensity in DKO myoblasts versus WT myoblasts, indicating an increase in mitochondrial mass associated with T-cadherin and APN loss.

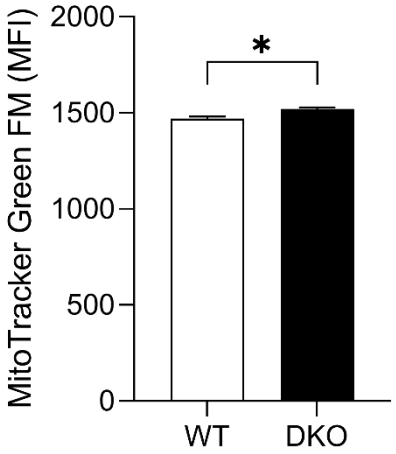

Figure 5.5. MitoTracker Green FM staining of WT and DKO primary myoblasts. Median FITC fluorescence of primary WT (1470 ± 10.02) and DKO (1521 ± 7.89) myoblasts stained with MitoTracker Green FM represented as mean fluorescence intensity (MFI) (mean ± SEM, n=5). A t-test was used to test for significance. * = $p<0.05$.

The OCR rate of the primary proliferating myoblasts was then examined. There were no differences in the OCR of proliferating WT versus DKO myoblasts and the myoblasts were affected similarly by the addition of the different electron transport chain inhibitors (**Figure 5.6** A). On cell normalisation, there were no apparent changes in basal respiration, proton leak, maximal respiration, non-mitochondrial respiration, or ATP-linked respiration in the DKO myoblasts. The coupling efficiency was 3.7% higher in the DKO myoblasts than in the WT, but the differences were not significant. Interestingly, there was no spare respiratory capacity in either cell type (**Figure 5.6** B).

At 24 hours differentiation, the DKO myotubes consistently consumed more oxygen than the WT myotubes (**Figure 5.6** C). The basal respiration of the DKO myotubes was approximately 1.5-fold greater than the WT myotubes. Comparing **Figure 5.6** B and D, the DKO myotubes consumed 2.8-fold more oxygen than as myoblasts, and the WT myotubes consumed 1.6-fold more oxygen than as myoblasts, which suggests an enhanced metabolic rate in the DKO myotubes. The DKO myotubes also showed increased trends in proton leak, maximal respiration, non-mitochondrial respiration, and ATP-linked respiration (**Figure 5.6** D). There was no difference in coupling efficiency between the genotypes, which remained at similar levels to that of the proliferating myoblasts (81% for WT myotubes versus 80% for DKO myotubes). Similar to proliferating myoblasts, there was no measurable spare respiratory capacity.

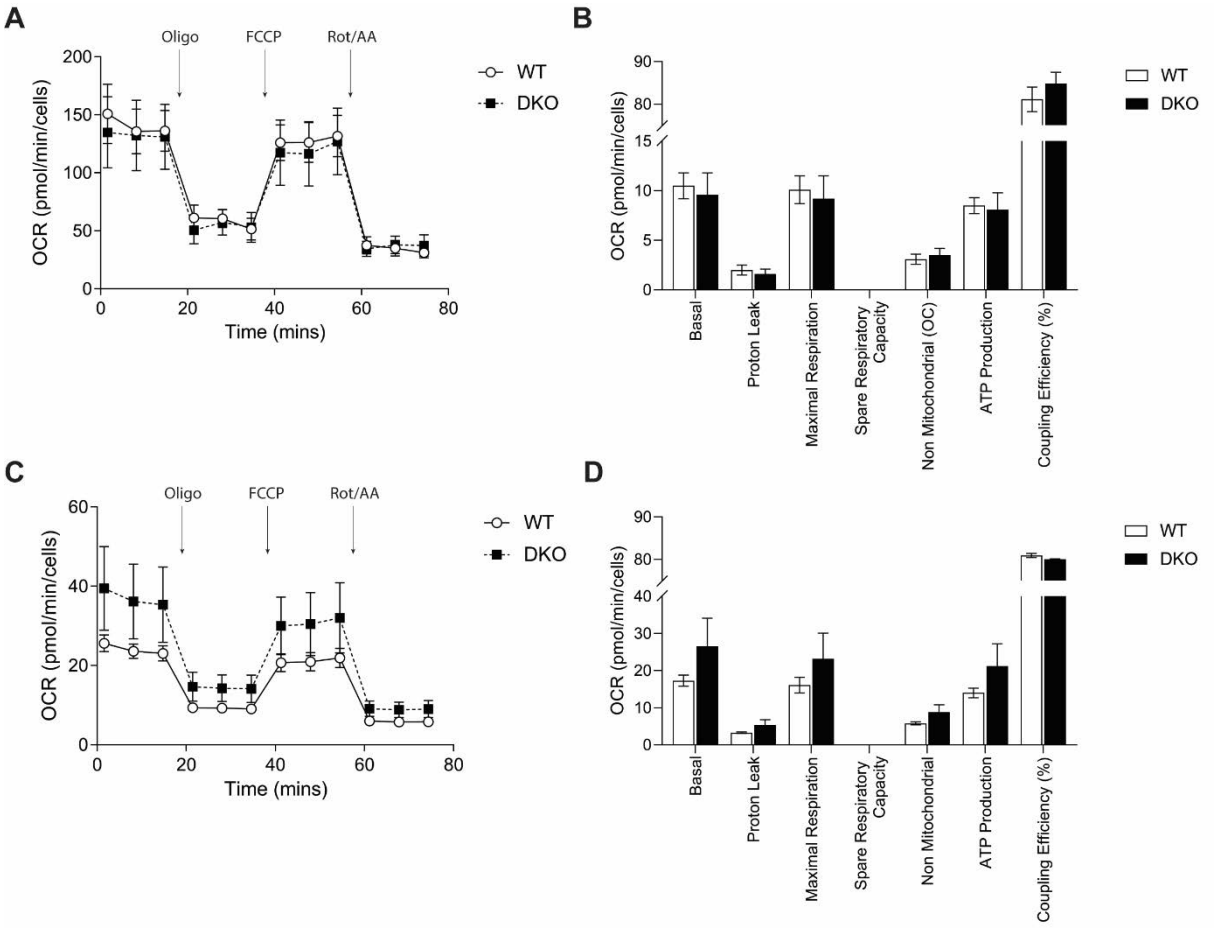

Figure 5.6: Mitochondrial function of proliferating and differentiating primary myoblasts from WT and DKO mice. Proliferating: **A.** Real time oxygen consumption rate (OCR) of WT and DKO primary myoblasts during the Agilent Seahorse mitochondrial stress test, normalized to methylene blue concentration at 0 hours differentiation (n=3). 'Oligo', FCCP' and 'Rot/AA' represents the injection of oligomycin, FCCP, and rotenone/antimycin A, respectively. **B.** Quantification of basal respiration, respiration linked to proton leak, maximal respiration, spare respiratory capacity, non-mitochondrial linked respiration, respiration linked to ATP production and coupling efficiency (%) (mean ± SEM, n=3). Differentiating 24 hours: **C.** Real time oxygen consumption rate (OCR) during the Agilent Seahorse mitochondrial stress test, normalized to methylene blue concentration (n=3). 'Oligo', FCCP' and 'Rot/AA' represents the injection of oligomycin, FCCP, and rotenone/antimycin A, respectively. **D.** Quantification of basal respiration, respiration linked to proton leak, maximal respiration, spare respiratory capacity, non-mitochondrial linked respiration, respiration linked to ATP production and coupling efficiency (%) (mean ± SEM, n=3). Multiple t-tests were used to determine significance.

5.5 Discussion

APN is known for its role as a positive effector of mitochondrial biogenesis. Although these effects occur primarily through an interaction with AdipoR1, this chapter examined T-cadherin as a receptor for APN's metabolic effects. In chapter 4, we observed that the loss of T-cadherin and APN leads to enhanced regenerative properties *in vivo* and primary myoblasts with accelerated differentiation properties *ex vivo*. To explain these observations, we examined energy use of C2C12 myoblasts overexpressing T-cadherin and primary DKO myoblasts. Interestingly, we find that compared to control pLN1 myoblasts, pLTcad myoblasts had impaired mitochondrial function and compared to WT primary myoblasts, DKO myoblasts had enhanced mitochondrial function. Paradoxically, APN is established to have a positive effect on mitochondrial biogenesis and energy production, yet here we find that APN absence in the DKO mouse muscle is associated with enhanced mitochondrial function and content. Thus, these data suggest that T-cadherin expression affects mitochondrial content and energy production to support myogenesis. These concepts are discussed below.

5.5.1 T-cadherin a regulator of mitochondrial biogenesis?

During myogenic regeneration, as myoblasts form myotubes, mitochondrial biogenesis and enzyme activity increases and there is a shift from glycolysis to oxidative phosphorylation. We observed in pLTcad myoblasts reduced mitochondrial number, in myotubes decreased expression of complex I, II, III and V and reduced OCR output after palmitate treatment. In DKO myoblasts we observed increased mitochondrial content and in myotubes higher OCRs throughout the mitochondrial stress test assay. The observations of reduced mitochondrial number in pLTcad cells and increased mitochondrial number in DKO cells, suggest T-cadherin expression is a regulator of mitochondrial biogenesis. However, in the stress test assays of the proliferating myoblasts no major differences were recorded, suggesting it is not an impediment on cellular function at this stage. Only when undergoing differentiation is respiration inhibited in pLTcad cells, with palmitate as the fuel source and increased in DKO cells in the presence of glucose. Future studies using a paraformaldehyde fixative compatible MitoTracker stain will be required to validate the mitochondrial number in

the pLTcad and DKO cells during differentiation, and the ability of the DKO cells to respire and produce ATP when palmitate is the energy source. Additionally, as the DKO cells developed in the absence of APN, whose application promotes fatty acid oxidation, studies using the Seahorse, DKO differentiating myoblasts, palmitate and recombinant fAPN should be undertaken to consider the influence of APN.

5.5.2 An alternative to mitochondrial biogenesis in the absence of adiponectin

The inhibition of mitochondrial complex synthesis leads to poor muscle regeneration, reduced expression of myogenin in C2C12 myoblasts and the formation of small myofibers and increased connective tissue [334]. Our findings are the reverse of APN's known mitochondrial biogenic action, as the expectation was that APN loss in the DKO should equate with reduced mitochondrial number and function. Additionally, in our *in vitro* models we can largely preclude the role of APN as the myoblasts were grown and differentiated in heat inactivated serums, and not treated with recombinant APN. During regeneration *in vivo*, it is likely that indirect events that emanate from APN loss and/or direct events pertaining to T-cadherin signalling, are responsible for modulating mitochondrial content. These concepts are discussed below.

5.5.3 A model of T-cadherin regulating mitochondrial biogenesis?

An important regulator of mitochondrial content is the family of PGC-1 (PPARγ co-activator 1) coactivators [333]. PGC-1α and PGC-1β regulate mitochondrial biogenesis, PGC-1α acts in response to energy needs and PGC-1β in the maintenance of basal respiration [335].

APN signalling normally increases mitochondrial biogenesis through PGC-1α. However, as APN is absent, the increased mitochondrial content observed in the DKO cells suggests that there are alternative mechanisms through which mitochondrial biogenesis is stimulated. A possible scenario, as presented in chapter 4 is the increased inflammation that parallels increased MYOD expression in the DKO muscles.

ChIP (chromatin immunoprecipitation)-sequencing data demonstrates that MYOD, along with enhancing genes important for differentiation and contraction, can also activate genes that regulate metabolism [336]. Subsequent gene ontology studies show that many of these genes are related to oxidative metabolic pathways including mitochondrial biogenesis, fatty acid metabolism and the Krebs cycle [336]. Notably, C2C12 myotubes with a doxycycline induced shRNA (small hairpin RNA) targeting MYOD and muscles from $MYOD^{-/-}$ mice have reduced basal OCR, lower maximal respiratory capacity, and reduced ATP content [336]. MYOD can regulate the expression of the mRNA and protein levels of PGC-1β by interacting with binding sites within the gene promoter region [336]. The overexpression of PGC-1β in C2C12 cells increases mitochondrial biogenesis and OCR, and PGC-1β transgenic mice show increased mtDNA, mitochondrial content and activity [337, 338]. Thus, given we observed in chapter 4 that DKO muscles induce the expression of MYOD earlier than WT cells, MYOD may in turn increase PGC1-β expression to induce mitochondrial biogenesis *in vivo*. Additional assays are required to confirm the role of these proteins in DKO cells.

Nonetheless, pLTcad cells *in vitro* are proliferating and differentiating without APN and inflammation, suggesting that T-cadherin itself is regulating mitochondrial biogenesis or the increased mitochondrial biogenesis is a by-product of regulating myoblast fusion. pLTcad proliferating cells have fewer mitochondria, thus it is feasible that T-cadherin can modulate mitochondrial content. However, T-cadherin can engage in homophilic and heterophilic interactions with other cadherins, and it is possible that these can regulate myoblast fusion.

In chapter 6, we find that T-cadherin can bind M-cadherin, which in turn interacts with β-catenin, an important myogenic transcriptional regulator. Active β-catenin interacts with MYOD and enhances its ability to activate target genes, such as PGC-1β [226] (**Figure 5.7**). Thus, if T-cadherin inhibits the formation of the M-cadherin-β-catenin adhesion complex, leading to β-catenin degradation (as explored in the next chapter), it could decrease mitochondrial biogenesis and activity through limiting MYOD activity and subsequent PGC-1β expression. Alternatively, when T-cadherin is absent, β-catenin is active and not degraded, MYOD is induced and PGC-1β is expressed. It is likely that in DKO mice APN loss enhances inflammation and increases MYOD, T-

cadherin absence on myoblasts promotes β-catenin, MYOD and PGC-1β, and they together promote mitochondrial biogenesis (this model is presented in **Figure 5.7**).

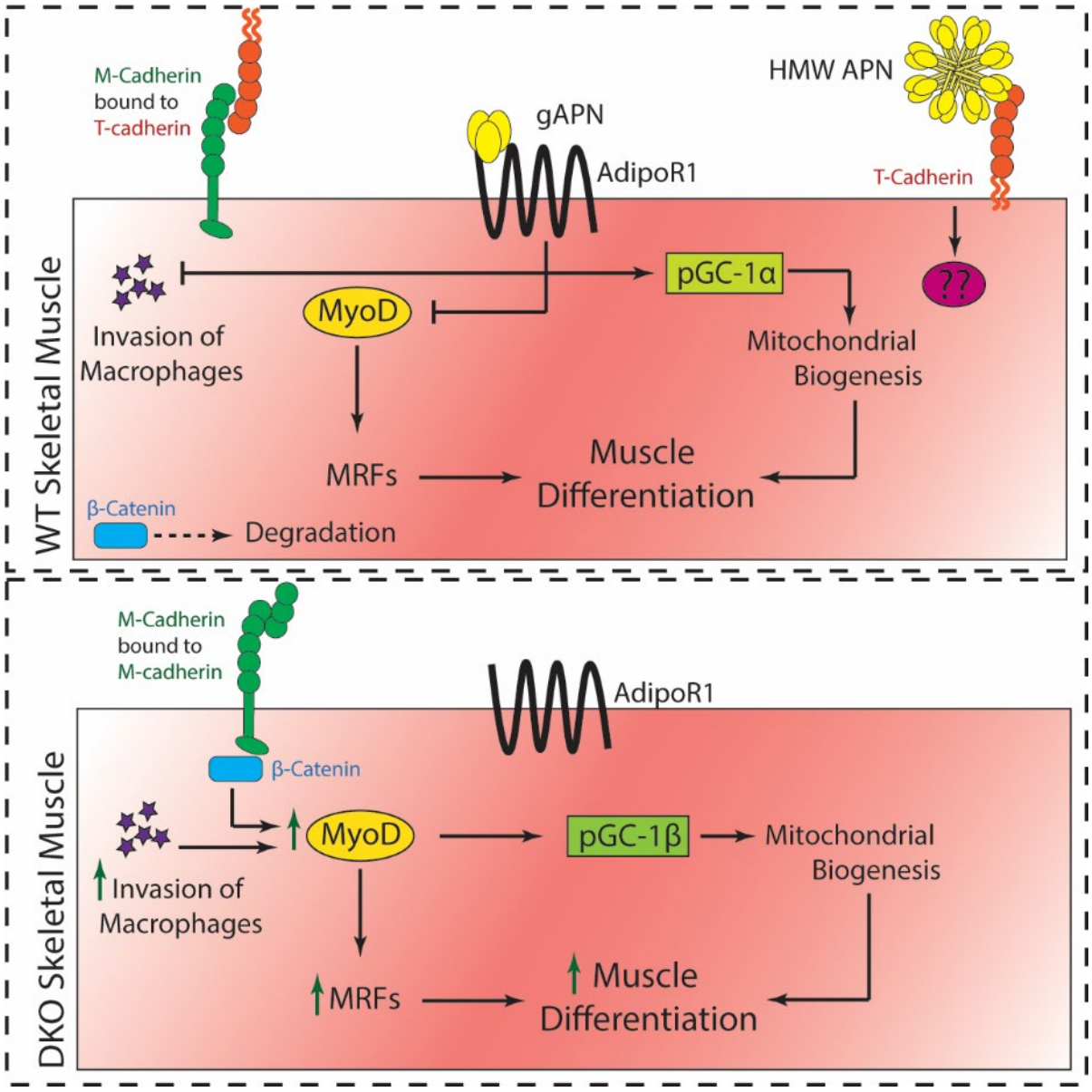

Figure 5.7. Control of MYOD signalling during myogenesis in WT and DKO skeletal muscle. In WT muscle, APN signals through AdipoR1 to mediate macrophage infiltration and inhibits the expression of MYOD. APN also increases mitochondrial biogenesis through PGC-1α. T-cadherin interacts with M-cadherin and inhibits further interactions with β-catenin. In DKO muscle, the lack of APN increases inflammatory macrophages and MYOD expression, to increase muscle differentiation. M-cadherin can freely bind β-catenin, limiting its degradation, which further increases MYOD expression. Increased MYOD, through stimulating pGC-1β can subsequently increase mitochondrial biogenesis.

5.5.4 Palmitate increases basal respiration but reduces maximal respiratory capacity

C2C12 cells treated with palmitate prior to the 'Mito Stress Test' assay displayed increased basal respiration but decreased maximal respiratory capacity. Palmitate is a common saturated free fatty acid and is known to have an apoptotic effect on cells. Myoblasts and myotubes can undergo mtDNA damage following exposure to palmitate [339]. In addition, the long-term exposure to saturated fatty acids can lead to mitochondrial dysfunction and metabolic diseases [340, 341]. The increase in basal respiration seen in the C2C12 cells is consistent with previous studies [339], and decrease in maximum OCR suggests the palmitate exposure reduces the cells' ability to respond to stress. Furthermore, there is a slight increase in proton leak and decrease in coupling efficiency following short term palmitate exposure. Thus, it may be useful to perform fatty acid oxidation assays with long-term exposure to palmitate to determine if there are viability differences between pLN1 and pLTcad C2C12 cells. In addition, the DKO myoblasts and myofibers were not treated with palmitate in this chapter, hence, to support a role for T-cadherin in our model, these studies should be undertaken over a short and long-term time frame.

5.5.5 Limitations and future recommendations

The data presented in this chapter suggest that T-cadherin can regulate mitochondrial number. To support a model by which T-cadherin regulates mitochondrial biogenesis, analyses of proliferating and differentiating pLN1 and pLTcad cells should be examined for the expression of both MYOD and PGC-1β. On establishing this pathway, this could then be repeated with WT and DKO myoblasts.

In this chapter, MitoTracker Green followed by FACS was used to examine mitochondrial content. As myotubes are not suitable for FACS analysis, it is imperative that a fixative compatible stain like MitoTracker Red FM is used to conduct a mitochondrial content analysis. Additionally, the examination of the content of other mitochondrial proteins, e.g. citrate synthase, could provide an indication of mitochondrial content during myotube differentiation. To determine whether altered mitochondrial content is a feature in the DKO uninjured and injured muscles versus WT, staining could be performed for succinate dehydrogenase activity.

In terms of respiration, these assays were performed using the Seahorse XFp, or ‘mini’ analyser. The microplates used for this machine only have 6 experimental wells available per assay and require two of these wells for calculating background signals. As a result, the number of replicates was often limited to perform both control and experimental cells on the same plate, at the same time.

Furthermore, normalisation to cell mass had to be performed externally. Unfortunately, the process of normalisation for these assays was not ideal as primary myotubes often came away from the plate following the assay. This could be improved using the fluorescent capabilities of the larger Seahorse XF analyser.

The size of the Seahorse XFp microplates also made it difficult to efficiently perform the fatty acid oxidation assay as this requires wells for both cell types as well as a BSA control versus fatty acid treatment. Furthermore, given the known interactions between T-cadherin and APN, and APN’s mitochondrial biogenesis properties and ability to promote fatty acid oxidation, the mitochondrial stress test assay should be performed with cells treated with mouse recombinant fAPN.

Finally, although C2C12 myoblasts provide an ideal *in vitro* model for assessing muscle growth, there are known limitations to using engineered cell lines and some differences between C2C12 cells and primary myoblasts are to be expected. Unlike C2C12 cells, neither the WT nor the DKO primary myoblasts possessed spare respiratory capacity, as their basal respiration was higher than their maximal respiration. This usually indicates a hindered capacity to respond to mitochondrial stress. During the experiment, the primary cells may have already been operating at maximal capacity due to the stressful conditions of the experiment. The cells were plated on a small surface area with multiple media changes to facilitate the optimal assay conditions and were likely stressed prior to beginning the assay. Repeat studies of the primary cells are suggested, using less handling to avoid the inherent cellular stress of the current models.

5.6 Conclusion

This chapter examined the metabolic consequences of T-cadherin and APN loss in skeletal muscle cells. The results suggest that T-cadherin and APN loss increases mitochondrial biogenesis in muscle cells undergoing injury and proliferation. Adiponectin loss most likely has an indirect inflammatory role in regulating MYOD, and T-cadherin loss plays a role through a yet to be completely characterised signalling pathway involving M-cadherin, β-catenin, MYOD and PGC-1β. The beginning of this pathway is explored in chapter 6.

6 T-cadherin's Interaction with the Myogenic Adhesion Complex

6.1 Introduction

During muscle regeneration, cell adhesion molecules (CAMs) play a major role in facilitating the fusion of opposing myoblasts. CAMs are located on the cell surface and are important for promoting the binding of cells to one another and to the extracellular matrix (ECM). These CAMs play an essential role in the extensive cell membrane and cytoskeletal reorganizations that occur during myoblast fusion. There are four families of CAMs involved in myogenic adhesion including IgCAMs, cadherins, integrins and selectins (reviewed in chapter one, section 1.6). Research surrounding the promyogenic role of these adhesion molecules illustrates the presence of a muscle adhesion complex that modulates myoblast fusion (**Figure 6.1**)[xxiv].

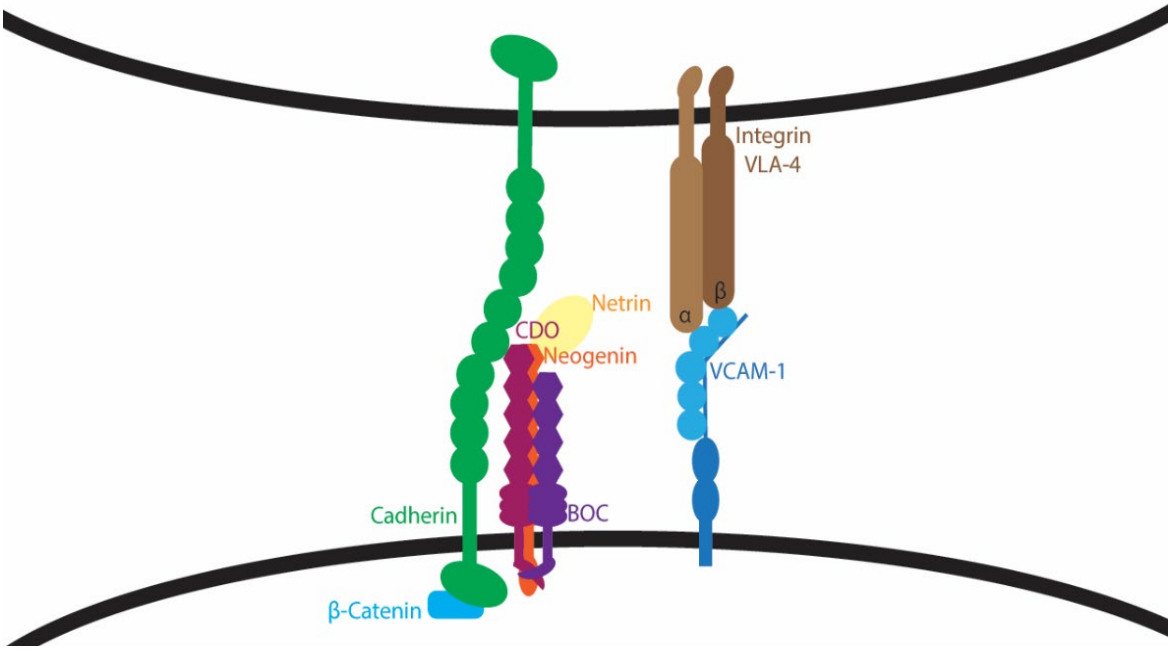

Figure 6.1. Cell adhesion molecules shown to play a role in the promyogenic cell adhesion complex. Research has shown the presence and interactions amongst N- and M-cadherin (green), CDO (rouge), Neogenin (orange), and BOC (purple), and neogenin binds netrins. VCAM-1 (blue) and VLA-4 (brown) bind independently of the other CAMs. Diagram taken from Taylor, et al. (2022) [2].

[xxiv] **Figure 6.1** is identical to **Figure 1.6** in section 1.6.4 and has been duplicated here for convenience.

Within this complex CDO and BOC interact and signal to cytoplasmic catenins bound to cadherins on the cell surface to elicit their promyogenic effects [164]. Furthermore, neogenin interacts with this complex and mediates its promyogenic role through selective binding to CDO [175]. Important to this chapter is the homophilic binding of the cadherins on opposing cells and their subsequent interactions with intercellular catenins.

Muscle cadherin (M-cadherin) is a member of the cadherin family that is found abundantly on developing skeletal muscles and at low levels on SCs [202, 203]. M-cadherin expression is transcriptionally activated by MRFs and reduced M-cadherin levels lead to reduced myoblast adhesion and differentiation [204]. Although muscle development is unaffected in M-cadherin knockout mice, likely due to the presence of compensatory cadherins, M-cadherin is still thought to play a crucial role in establishing correct alignment during fusion [205, 225]. During myogenesis, M-cadherin accumulates at areas of cell-cell contact between myoblasts and co-localises with β-catenin [225].

β-catenin is a member of the armadillo family of proteins and plays a major role in both Wnt signalling and cell adhesion. β-catenin acts as a transcription cofactor that can modify the activity of the TCF/LEF family of DNA binding proteins [342]. β-catenin mediated Wnt signalling is crucial for the induction of the bHLH MRFs MYF5 and MYOD, as well as the differentiation of multipotent cells into myogenic cells [30, 343-345]. However, some studies have demonstrated that this activation likely occurs in a TCF/LEF independent manner and instead β-catenin enhances the transcriptional activation of downstream MRFs via a direct interaction with MYOD [226]. This has recently been shown to also activate key fusion proteins myomaker and myomixer [20]. Against this background, the interaction with TCF/LEF binding proteins may still be important for the regulation of the Wnt pathway and the proliferation of MYOD negative SCs [20, 346]. Both β-catenin gain- and loss- of function studies in mice show impaired myogenesis and highlight the significance of β-catenin during this process [226, 227].

In the absence of Wnt signalling, casein kinase 1 alpha (CK1α) phosphorylates β-catenin at serine 45, priming the cofactor for further phosphorylation by glycogen synthase kinase-3β (GSK-3β) at serine 33/37 and threonine 41, respectively. β-catenin phosphorylated at residues 33 and 37 is recognized by the beta-transducin repeats-

containing proteins (β-TrCP) E3 complex resulting in ubiquitylation and rapid degradation by the 26S proteosome [347]. The removal of β-catenin exposes the TCF/LEF DNA complex to corepressors that suppress the transcription of Wnt signalling target proteins [348]. Mutations in both the degradation complex and within the phosphorylation sites have been linked to cancers following increased β-catenin levels and Wnt signalling [349-351]. Phosphorylation of β-catenin is not only important for its degradation but also for mediating Wnt signalling. Following the activation of the Wnt pathway, a cytoplasmic protein dishevelled (DVL) inactivates GSK-3β leading to the accumulation of stabilized β-catenin in the cytoplasm [352]. Non-phosphorylated β-catenin at Ser 37 and Thr 41 appears to have enhanced transcriptional activity and is often referred to as active β-catenin [353, 354]. Wnt signalling is mediated by this stable unphosphorylated β-catenin and can translocate to the nucleus to associate with TCF/LEF and regulate gene expression [353, 354]. Unphosphorylated β-catenin can also accumulate at sites of cell-to-cell contact during myogenesis [355].

The exact role of β-catenin at the myoblast membrane remains unclear but it is likely that it is involved in cadherin-mediated interactions with the actin cytoskeleton. Both M-cadherin and β-catenin have been shown to colocalize to sites of cell-to-cell contact during myoblast fusion and although there are only low levels of each present on SCs, the protein levels rapidly increase during myogenesis until myotubes are formed [225]. M-cadherin is known to form a complex with α-catenin/β-catenin in proliferating and differentiating C2C12 cells [356]. As α-catenin is known to associate with actin filaments, this interaction likely links the cadherin to the actin cytoskeleton to provide stability during reorganization. M-cadherin signalling within the cell also appears to regulate β-catenin availability. M-cadherin knockdown studies show a significant increase in both TCF/LEF transcription activity and β-catenin phosphorylation, leading to degradation [357]. Overall, the formation of the M-cadherin/β-catenin complex is an important step in myoblast fusion, but further research is required to elucidate the exact mechanism by which this occurs.

6.2 Preliminary data and aims

The Hebbard lab has previously shown that both T-cadherin and M-cadherin colocalize on murine C2C12 myoblasts and immunoprecipitation studies confirm the interaction between β-catenin and M-cadherin (**Figure 6.2**). Interestingly, the interaction between β-catenin and M-cadherin was reduced in the presence of T-cadherin. Together, these data suggest that T-cadherin could interfere with the formation of the M-cadherin/β-catenin complex *in vitro*.

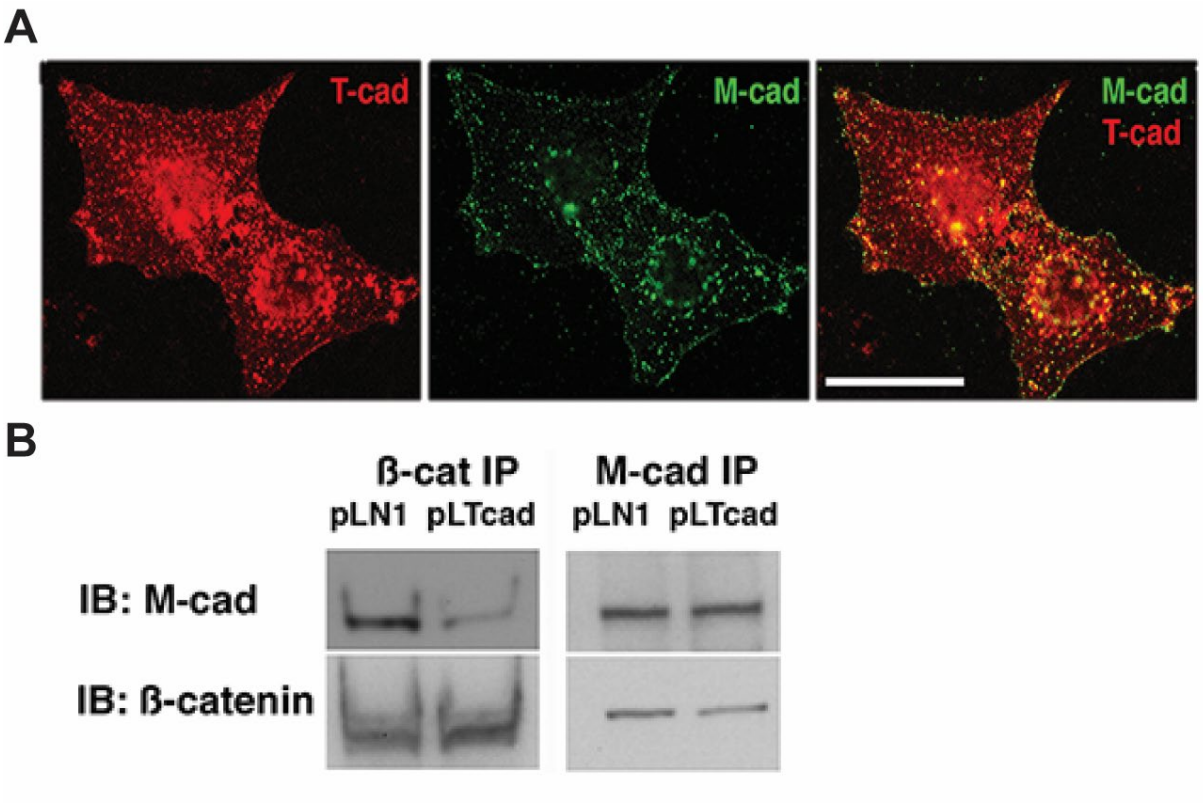

Figure 6.2. Unpublished results from the Hebbard Lab. **A.** Expression of T-cadherin and M-cadherin on murine C2C12 myoblasts. Scale bar 50 μm. **B.** M-cadherin and β-catenin immunoprecipitates using pLN1 and pLTcad C2C12 cells. Western blots probed with both M-cadherin and β-catenin antibodies.

Given the importance of M-cadherin and β-catenin in myogenesis, a section of my Honours thesis aimed to investigate the role of T-cadherin in regulating this complex. Co-immunoprecipitation experiments conducted during my honours research with a Brij 97 lysis buffer illustrated in-part the physical interaction between T-cadherin and M-cadherin (**Figure 6.3**).

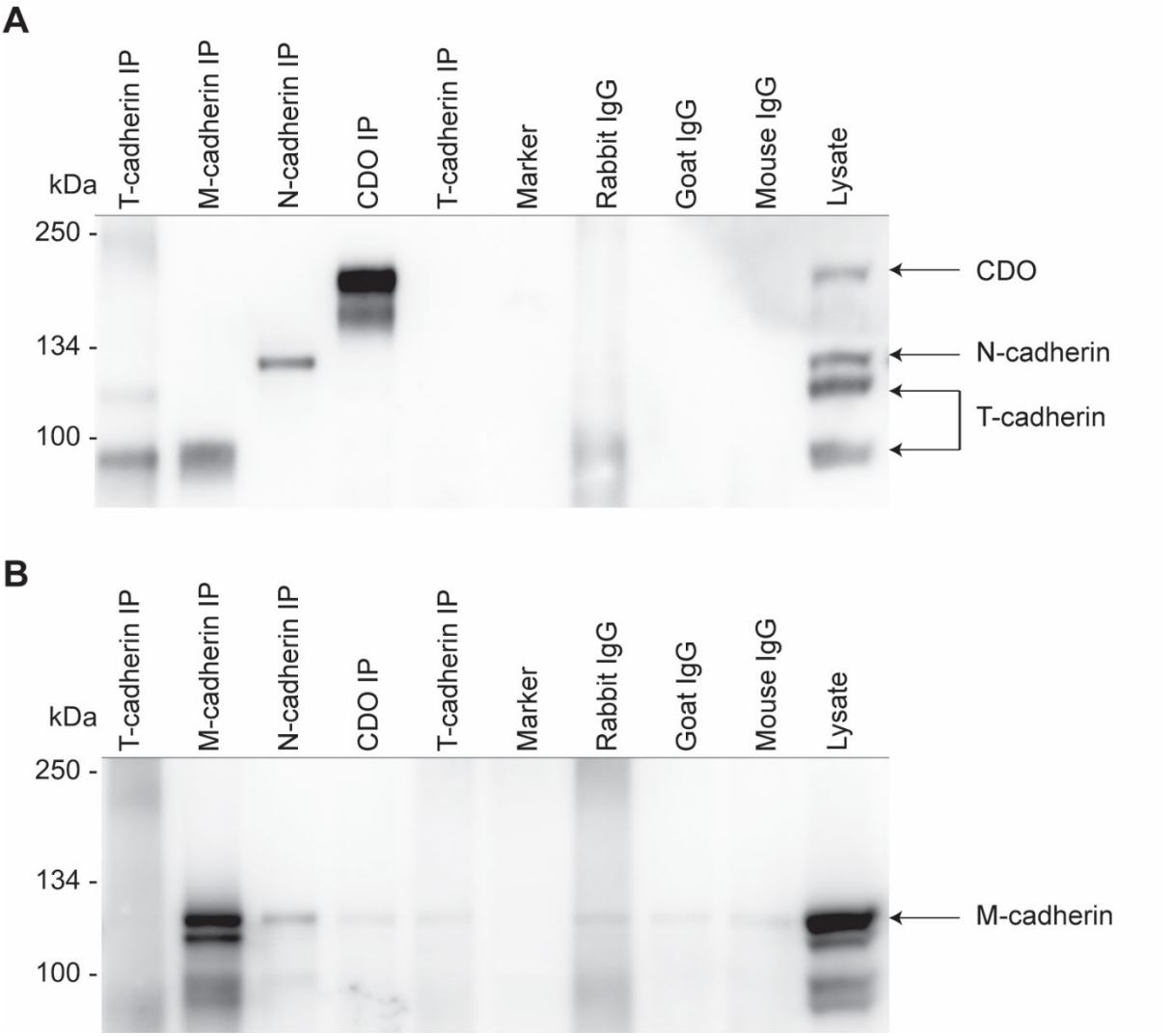

Figure 6.3: Co-immunoprecipitation of myogenic signalling molecules using a Brij 97 lysis buffer. Immunoprecipitates (IP) were formed using protein G beads prepared with antibodies against T-cadherin (Ranscht antibody [1]), M-cadherin, N-cadherin, CDO, and an alternate T-cadherin (anti-peptide created by the Hebbard lab) and includes immunoglobulin controls for rabbit, goat and mouse IgGs. The illustrated blots show western blots using specific antibodies against **A.** CDO, N-cadherin and T-cadherin, and **B.** M-cadherin.

T-cadherin antibodies detected both the mature T-cadherin isoform (90 kDa) and the unprocessed precursor isoform (120 kDa) in the whole cell lysates and in T-cadherin and only the mature isoform in the M-cadherin immunoprecipitates. Nonetheless and in contrast, M-cadherin was only detected in the lysate and in the M- and N-cadherin immunoprecipitates and not in the T-cadherin immunoprecipitates. CDO was only present in the lysate and the CDO immunoprecipitates lanes.

A possible explanation for the lack of M-cadherin in the T-cadherin immunoprecipitates is poor affinity or lack of quality of the T-cadherin antibodies versus M-cadherin antibodies, and that T-cadherin's interactions with itself as a negative regulator and other cadherins is weak [358].

Considering that T- and M-cadherin could interact, T-cadherin has APN-independent adhesion functions, and that the overexpression and loss of T-cadherin can affect myogenesis, it was hypothesized that T-cadherin can negatively regulate skeletal muscle growth through interacting with M-cadherin on myoblasts. Hence, this chapter further explored the interaction between T- and M-cadherin, as well as M-cadherin's effect on β-catenin activity. To do this, immunoprecipitations, cell-based adhesion models and signalling evaluations with primary myoblasts were employed to address the following aims:

1. Examine T-cadherin's interactions with M-cadherin *in vitro*.
2. Investigate the effects of T-cadherin on β-catenin activity.

6.3 Methods

For complete materials and methods see chapter 2 section 2.6.

6.3.1 Co-Immunoprecipitation

Total lysates were generated from differentiated C2C12 cells, both with and without treatment with DTSSP (3,3'-Dithiobis[sulfosuccinimidylpropionate]) crosslinking reagent, in either Brij 97 lysis buffer or Triton X-114 lysis buffer. Lysates were incubated with protein G-Sepharose beads bound to appropriate antibodies for two hours. Following incubation, the beads were washed, resuspended in loading buffer, heated at 95 °C for 5 minutes, and the proteins were separated using SDS-PAGE electrophoresis.

6.3.2 Overexpression constructs

The following overexpressing constructs were stably transfected into Chinese hamster ovary (CHO) cells that do not express any cadherins. Throughout this chapter the cells will be referred to by their construct name as listed below (**Table 6.1**).

Table 6.1. List of overexpression constructs transfected into CHO cells.

Name	**Overexpression**
pLN1	pLEGFP-N1 vector backbone with the GFP removed
pLTcad	pLN1 with murine T-cadherin cDNA insert
pEMcad.GFP	pLEGFP-N1 with murine M-cadherin cDNA insert

6.3.3 Short term aggregation assay

Cadherins were stably transfected into CHO cells using lipofectamine 3000 and stable clones were generated through G-418 antibiotic selection. A suspension of single cell CHO cells was plated into 24-well plates coated with 5% BSA in PBS in the following combinations: (i) pLN1 alone, (ii) pLTcad alone, (iii) pEMcad.GFP alone, (iv) pLN1 and pEMcad.GFP, and (v) pLTcad and pEMcad.GFP and supplied with calcium chloride to enable cadherin function. The plates were then placed on a gyrating shaker

at 80 rpm for 20 minutes at 37 °C. Following aggregation, an equal volume of 8% paraformaldehyde (PFA) was added to each well and kept at 4 °C for imaging. Images of the entire well were captured, and aggregates were counted as small (<5 cell aggregates), medium (5-10 cell aggregates) and large (> 10 cell aggregates).

Analysis was performed using ImageJ and QUPath software and statistical analysis used GraphPad Prism. Error bars represent standard error of the mean (SEM) unless otherwise stated. * = $p<0.05$, ** = $p<0.01$, **** = $p<0.0001$ denote the significance values used throughout this chapter.

6.4 Results

6.4.1 Immunoprecipitation of cadherins in C2C12 myoblasts

To extend the interaction studies, immunoprecipitations were repeated with Brij 97 lysis buffer and the cross-linking reagent DTSSP. These experiments were performed with wildtype C2C12 cells and pLTcad C2C12 cells (**Figure 6.4**). Immunoprecipitation using C2C12 cells showed results in agreement with the preliminary studies. Using specific T-cadherin antibodies, T-cadherin was strongly expressed as two forms (125 and 105 kDa) in the lysates, T-cadherin immunoprecipitates, and as a 105 kDa form in the M-cadherin immunoprecipitates (**Figure 6.4** A). Probing with the M-cadherin antibody revealed strong antigen recognition in the lysates and in the M-cadherin immunoprecipitates but was absent in the T-cadherin immunoprecipitates (**Figure 6.4** B).

Given that T-cadherin is present in M-cadherin immunoprecipitates and implies a real interaction, the experiment was then repeated with T-cadherin overexpressing pLTcad cells and a DTSSP cross-linker to stabilise interactions between proteins during the assay.

The T-cadherin antibody showed a strong signal in the cell lysates and T-cadherin immunoprecipitates (**Figure 6.4** C). There was weak T-cadherin binding to the M-cadherin immunoprecipitates, but not above background levels. The addition of the cross-linker reduced the amount of T-cadherin protein in the cell lysate and increased the background within the T-cadherin immunoprecipitates (**Figure 6.4** D). On probing the experiment performed with pLTcad cells, M-cadherin protein was present in the M-cadherin immunoprecipitates, and in the T-cadherin immunoprecipitates (**Figure 6.4** E). In the case of pLTcad cells and in the presence of DTSSP cross-linker, the M-cadherin antibody recognised antigen in the pLTcad lysates, M-cadherin immunoprecipitates, and in the T-cadherin immunoprecipitates (**Figure 6.4** F). No M-cadherin protein was observed in the rabbit IgG controls.

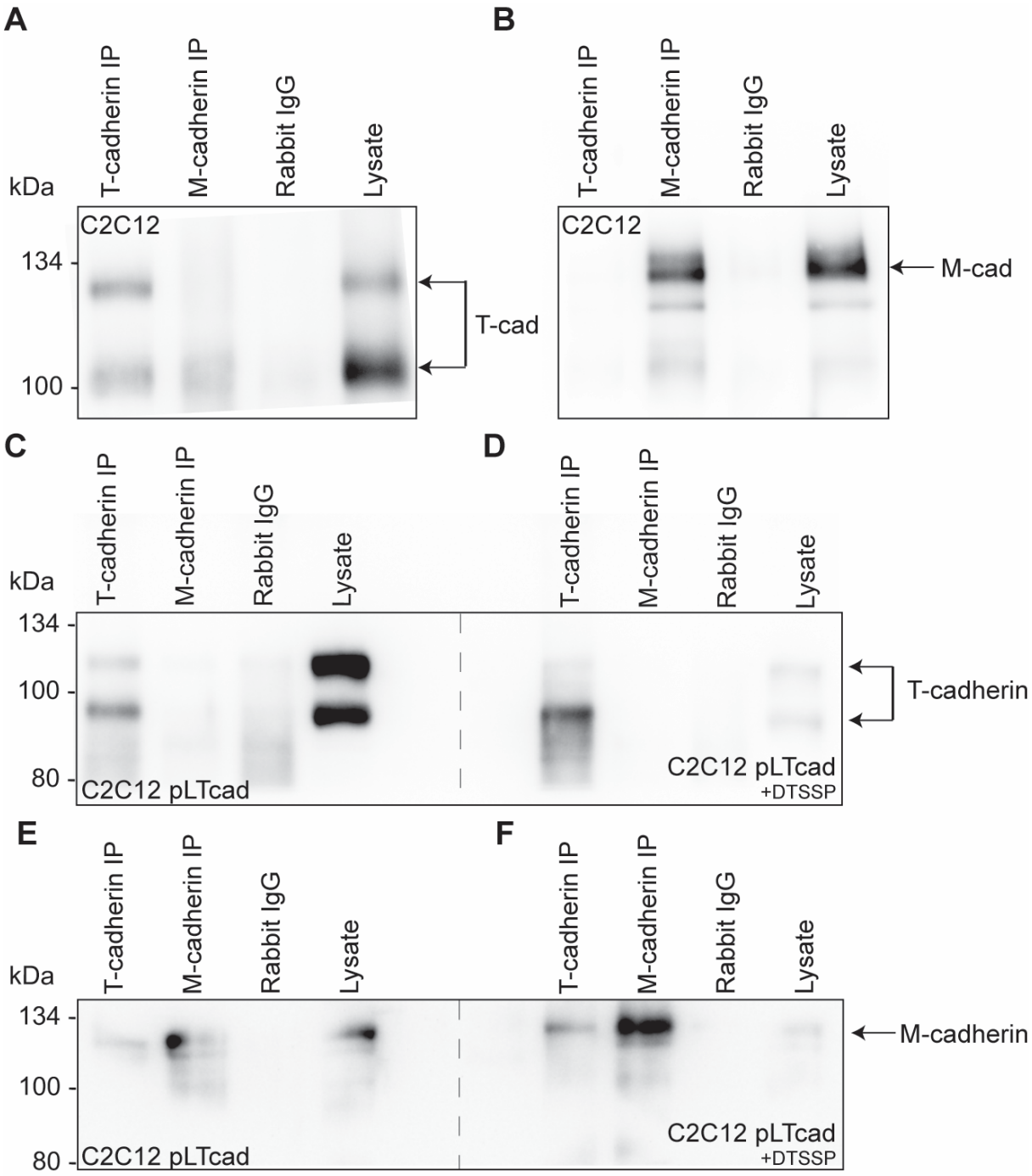

Figure 6.4. Immunoprecipitations of myogenic cadherins using a Brij97 lysis buffer. Immunoprecipitates were generated from Brij97 lysed C2C12 and pLTcad C2C12 cells with protein G beads prepared with rabbit antibodies against T-cadherin, M-cadherin, and rabbit immunoglobulin (IgG). C2C12 immunoprecipitates probed with **A.** T-cadherin and **B.** M-cadherin. pLTcad C2C12 immunoprecipitates probed with **C-D** T-cadherin, and **E-F.** M-cadherin. **D** and **F.** Treated with DTSSP crosslinker prior to lysis.

The immunoprecipitation assay was then undertaken with pLTcad C2C12 cells, DTSSP and a Triton X-114 lysis buffer. The blot was first probed with T-cadherin and showed strong binding in the lysate and T-cadherin immunoprecipitates (**Figure 6.5** A). The blot was then reprobed with M-cadherin antibodies and showed strong binding in the M-cadherin immunoprecipitates, weak binding in the cell lysates and none in the T-cadherin immunoprecipitates (**Figure 6.5** B).

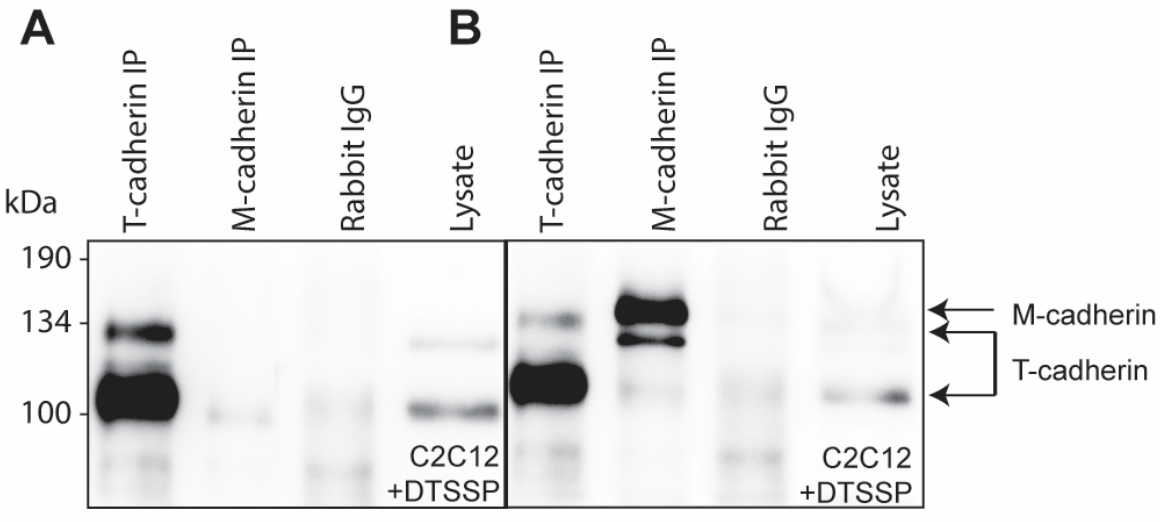

Figure 6.5. Immunoprecipitations of myogenic cadherins using a Triton X-114 lysis buffer. Immunoprecipitates generated from DTSSP treated Triton X-114 lysed C2C12 cells with protein G beads prepared with rabbit antibodies against T-cadherin, M-cadherin, and rabbit immunoglobulin (IgG). C2C12 immunoprecipitates probed with **A.** T-cadherin and **B.** M-cadherin.

6.4.2 Expression of β-catenin in differentiating primary myoblasts

Given M-cadherin is known to interact with β-catenin during myoblast fusion and β-catenin is a positive regulator of myogenesis, WT and DKO myoblasts were isolated, differentiated over a time course, lysed and then probed with antibodies against β-catenin and β-catenin that has been phosphorylated at serine 45 (p-β-catenin) (**Figure 6.6**). This phosphorylation is performed by CK1α and primes β-catenin for further phosphorylation by GSK-3β and subsequent degradation. As myogenesis progresses from 6 hours to 12 hours, the levels of total β-catenin and phosphorylated β-catenin increased (**Figure 6.6** A-B). Nonetheless, the proportion of total β-catenin versus p-β-catenin was unaltered between 6- and 12-hours in both WT (25% and 27% p-β-catenin

at 6- and 12- hours respectively) and DKO lysates (27% and 28% p-β-catenin at 6- and 12-hours respectively) (**Figure 6.6** C). Furthermore, there was no difference in the level of either form of β-catenin between the two genotypes (**Figure 6.6** C). Further studies are required to determine changes in β-catenin, and these include examining other β-catenin phosphorylated forms, β-catenin degradation, and β-catenin sub-cellular localization during myogenesis.

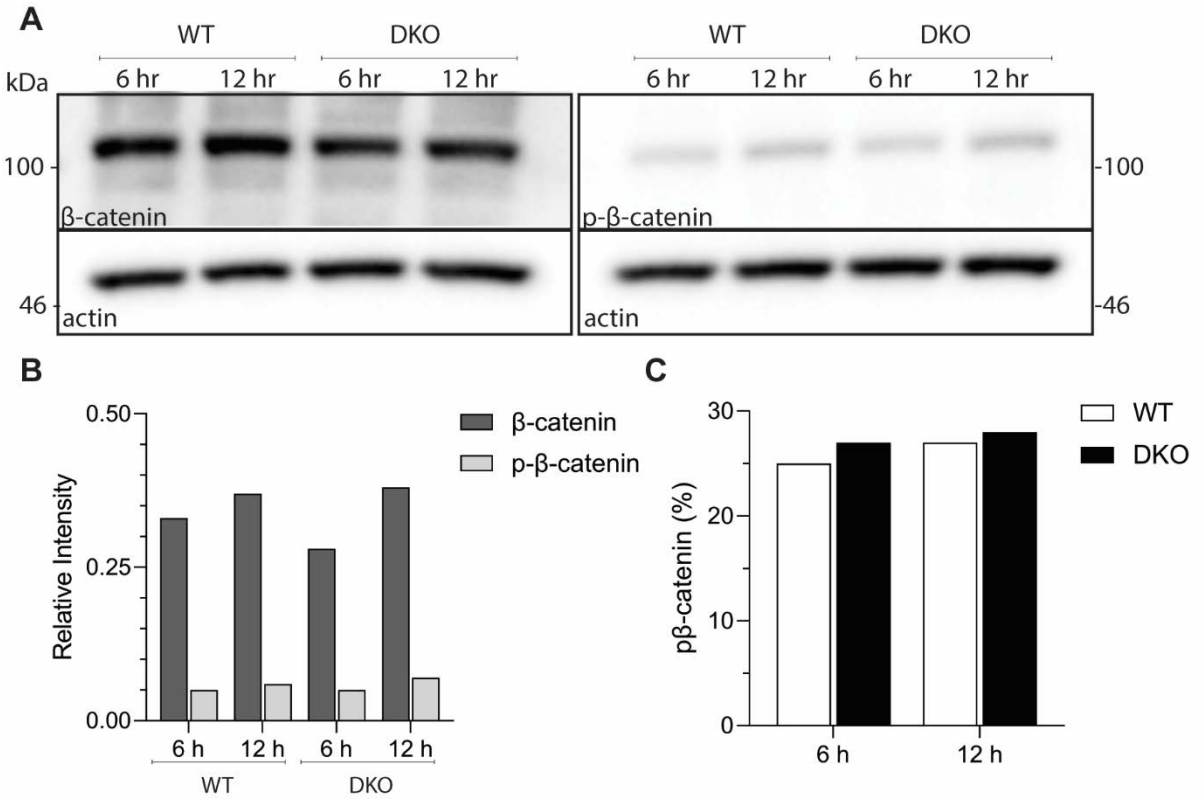

Figure 6.6. β-catenin expression in differentiating WT and DKO primary myoblasts at 6- and 12-hours. **A.** Western blots were probed for the expression of total and serine 45 phosphorylated β-catenin (p-β-catenin). **B.** Relative intensity of phosphorylated and dephosphorylated β-catenin in western blot analysis. **C.** Percentage of serine 45 phosphorylated β-catenin in differentiating primary myoblasts.

6.4.3 Overexpression of different cadherins in CHO cells

The immunoprecipitation assays suggested that M- and T-cadherin interact in C2C12 cells. To further examine this interaction, CHO cells were transfected with M- and T-cadherin and cadherin-dependent cell-cell aggregation assays were performed [359]. CHO cells do not express cadherins and are thus ideal for studying the effects of cadherin binding. CHO cells were individually and stably transfected with T- and M-

cadherins and dissociated into a single cell suspension in low concentrations of trypsin to maintain cadherin cell surface expression. The M-cadherin construct also contained a GFP-tag to assist with identification of the transfected cells during assay analyses. Cell lysates were also generated from each cell line and probed for the expression of each cadherin (**Figure 6.7**).

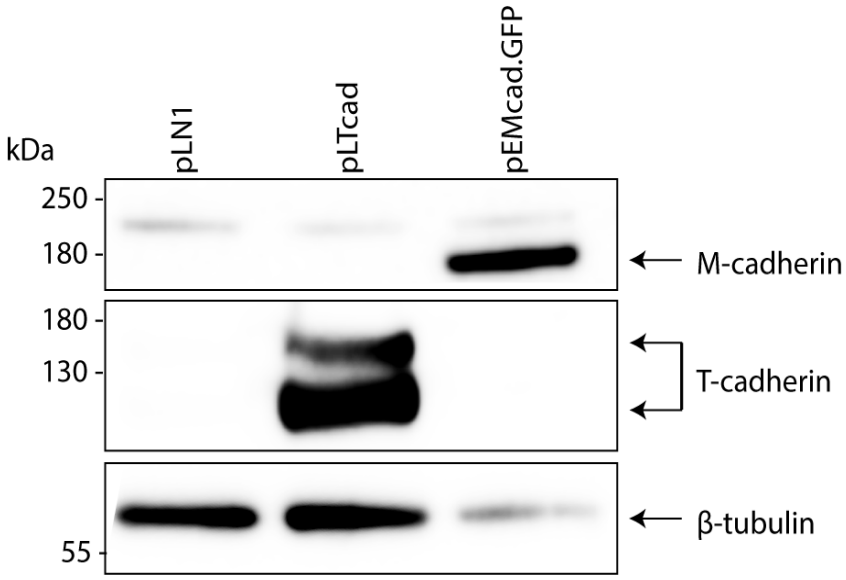

Figure 6.7. Cadherin expression in transfected CHO cells. Lysates from control pLN1 cells, T-cadherin (pLTcad) and M-cadherin (pEMcad.GFP) cells were probed for T- and M-cadherin, and β-tubulin as a loading control.

Cells transfected with the pLN1 empty vector showed no expression of either T-cadherin or M-cadherin. The T- and M-cadherin overexpressing cells showed strong expression of T- and M-cadherin, respectively.

6.4.4 Aggregation of cadherin expressing CHO cells

The aggregation assay was performed with the CHO cells expressing different cadherins to determine the interactions between these two cadherins. Cells were incubated together in the following combinations: (i) pLN1 alone, (ii) pLTcad alone, (iii) pEMcad.GFP alone, (iv) pLN1 and pEMcad.GFP, and (v) pLTcad and pEMcad.GFP and calcium chloride was supplied to maintain cadherin function. Both brightfield and fluorescence microscopy were used to visualise the cells, and aggregates were

categorised into small (less than 5 cells), medium (5-10 cells) and large (more than 10 cells).

6.4.4.1 Aggregation of CHO cells with single cadherin

The control wells were plated with only one cell type and all aggregates with more than 3 cells were counted and categorised (**Figure 6.8**). The pLN1 cells formed a similar number of aggregates as the pLTcad cells (**Figure 6.8** A and B), and the pEMcad.GFP cells formed fewer aggregates (**Figure 6.8** C). An average of 309 aggregates were counted for three pLN1 wells, 140 aggregates for pEMcad.GFP wells and 344 for pLTcad wells and there was a significant difference in the number of aggregates counted in the pEMcad.GFP wells compared to the other cell types (**Figure 6.8** D). Hence analyses showed significantly fewer small and medium aggregates for the pEMcad.GFP (90 small and 37 medium) wells versus pLN1 (182 small and 101 medium) and pLTcad (213 small and 105 medium) wells (**Figure 6.8** E). Unfortunately, the cells remained suspended following the assay, and it was difficult to count the total number of cells present for normalisation. There were no statistically significant differences between the total average number of aggregates counted in the pLN1 and pLTcad wells or between the average number of large aggregates (27, 13 and 26 for pLN1, pEMcad.GFP and pLTcad, respectively) of any cell type. The differences observed for the pEMcad.GFP cells were unexpected and is likely due to a reduced number of cells. For this reason and to allow comparison, the data was converted to a proportion of total aggregates counted per cell type (**Figure 6.9**).

These data show that the majority (between 59% and 65%) of the aggregates were small aggregates followed by approximately 27% - 33% medium aggregates and between 7% - 9% large aggregates (**Figure 6.9**). These results suggest that there is no relationship between the size of the aggregates formed and the cell type used in the assay.

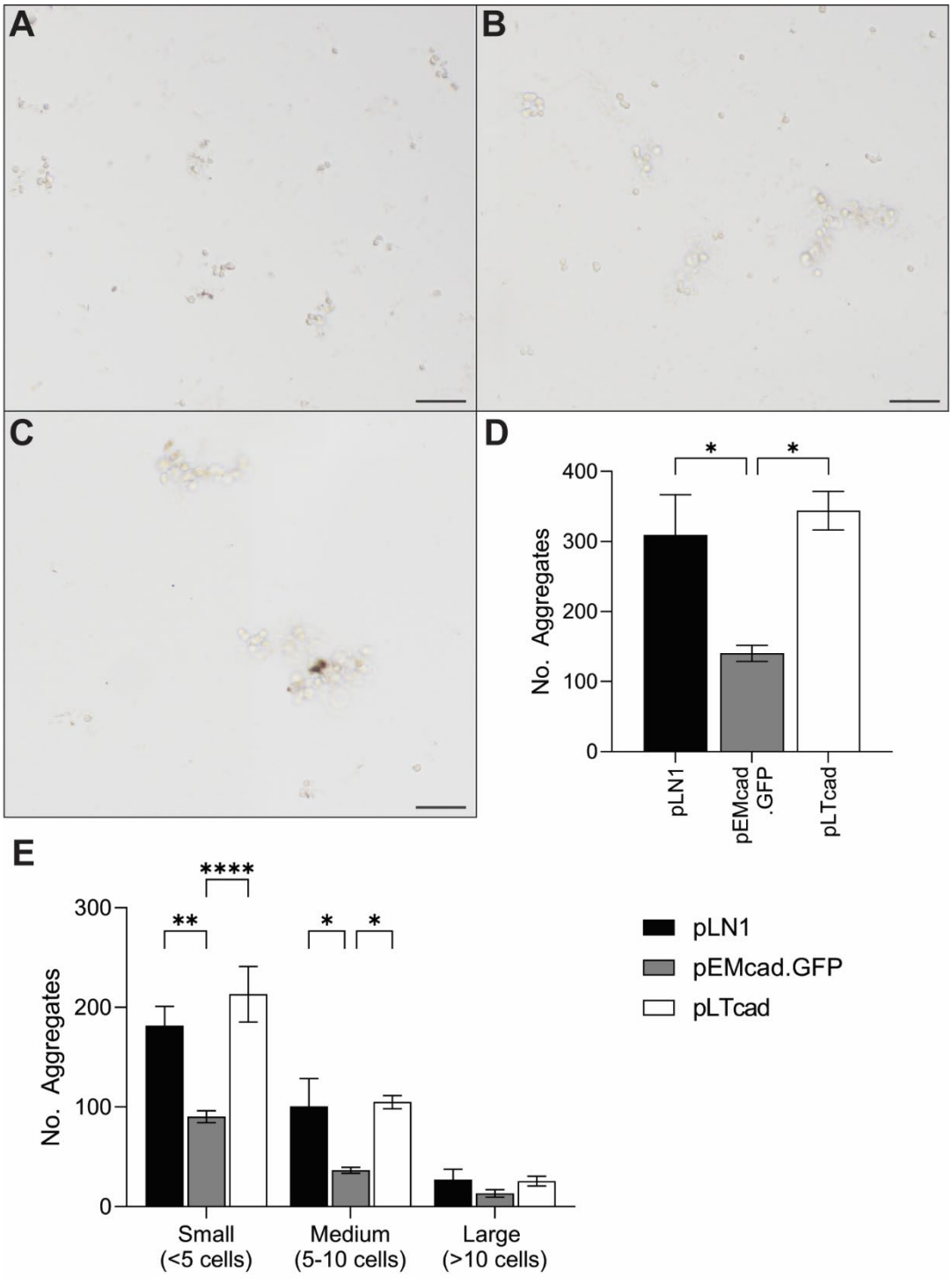

Figure 6.8. Aggregates formed between individual cadherin expressing CHO cells. Representative images of aggregate formation between CHO cells expressing **A.** pLN1, **B.** pLTcad, and **C.** pEMcad.GFP. Scale bars 100 µm. **D.** Average of total number of aggregates formed in the wells (mean ± SEM, n=3). **E.** Number of aggregates formed between cells categorised into small (less than 5 cells total), medium (5-10 cells total) and large (more than 10 cells) (mean ± SEM, n=3). * = $p<0.05$, ** = $p<0.01$, **** = $p<0.0001$.

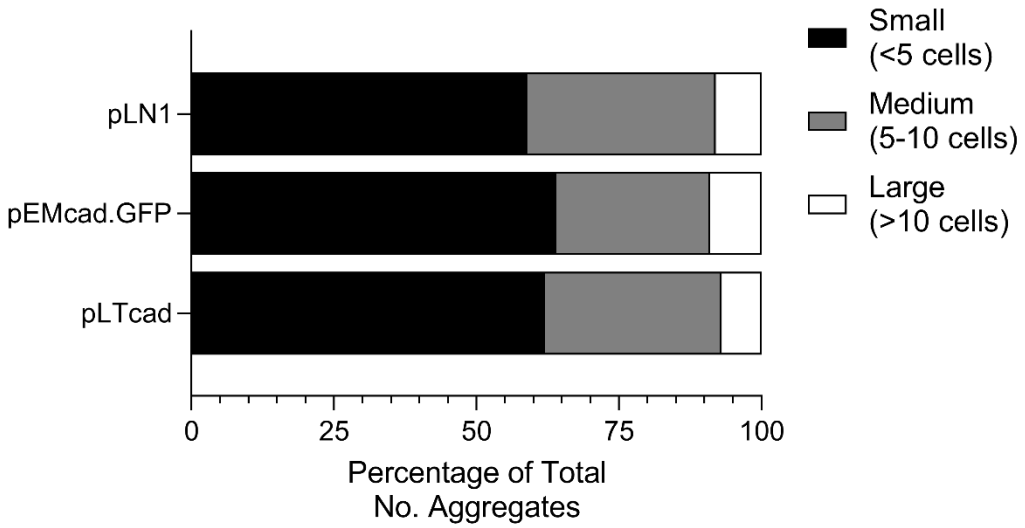

Figure 6.9. Percent of aggregates formed between individual pLN1, pEMcad.GFP and pLTcad expressing CHO cells as a proportion of the average total number of aggregates per cell type. Aggregates were separated into small (less than 5 cells total), medium (5-10 cells total) and large (more than 10 cells).

6.4.4.2 Aggregation of two CHO cells expressing different cadherins

To determine interaction between T- and M-cadherins, the aggregation assay was performed with two CHO cell types per well, (i) pLN1 and pEMcad.GFP (**Figure 6.10** A), and (ii) pLTcad and pEMcad.GFP (**Figure 6.10** B). The GFP tag on the pEMcad.GFP CHO cells, in combination with brightfield microscopy, was used to visualize the cells. The aggregates were categorized into small (less than 5 cells), medium (5-10 cells), or large (more than 10 cells) and whether they contained one cell type or a combination of two cell types ('combination aggregates'). An average of 190 combination aggregates were counted across three wells. For pLN1 plus pEMcad.GFP 70% (133) of the aggregates were small, followed by 28% (54) medium aggregates and 2% (4) large aggregates (**Figure 6.10** C). In contrast, for pLTcad plus pEMcad.GFP there was an average of 175 aggregates counted per cell: 52% (91) small, 36% (63) medium and 12% (22) large aggregates (**Figure 6.10** C). Analysis of single cell type aggregates showed for pLN1 and pEMcad.GFP an average of 15 pLN1 and 18 pEMcad.GFP small aggregates and 2 pLN1 and 1 pEMcad.GFP medium aggregates (**Figure 6.10** D). For pLTcad and pEMcad.GFP an average of 12 pEMcad.GFP and 55 pLTcad small aggregates, and 1 pEMcad.GFP and 20 pLTcad medium aggregates were observed (**Figure 6.10** D).

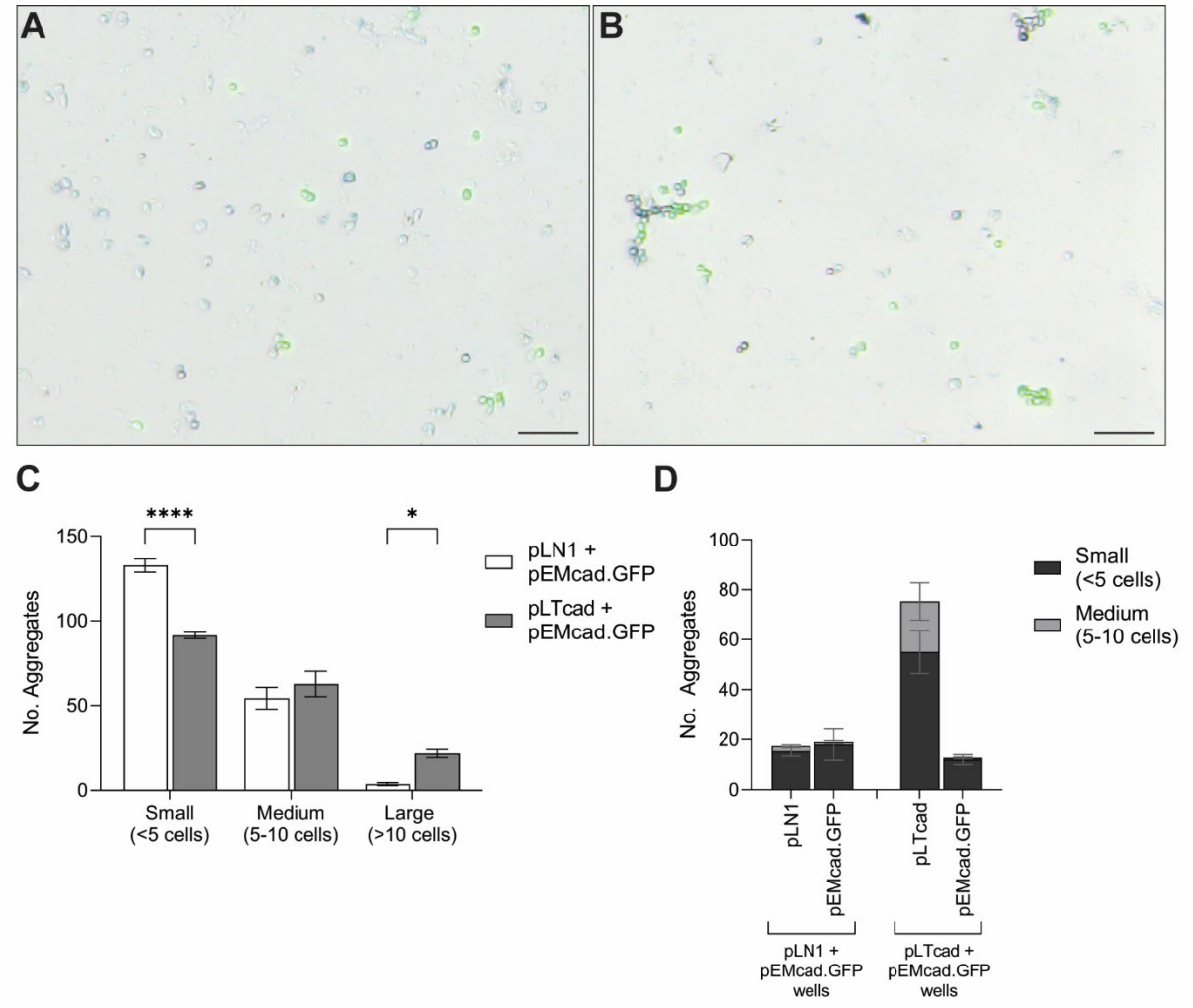

Figure 6.10. Aggregates formed between cadherin expressing CHO cells. Representative images of aggregate formation and GFP visualisation of **A.** pLN1 and pEMcad.GFP and **B.** pLTcad and pEMcad.GFP. Scale bars 100 μm. **C.** Number of aggregates with two cell types compared to aggregate size (mean ± SEM, n=3). **D.** Number of aggregates with one cell type, stacked by size of aggregates (mean ± SEM, n=3). Aggregates were categorised as small (less than 5 cells), medium (5-10 cells) and large (more than 10 cells) (n=3). * = $p<0.05$, **** = $p<0.0001$.

Unfortunately, the total cell number could not be obtained for this assay, so to allow comparison, the results were reconfigured and displayed as a proportion of the total number of combination aggregates counted per group (**Figure 6.11**). These proportions showed a clear difference in the size of aggregates formed between the two experimental groups. There were more small aggregates and fewer large aggregates present in the pLN1 plus pEMcad.GFP group when compared to the pLTcad plus pEMcad.GFP combination.

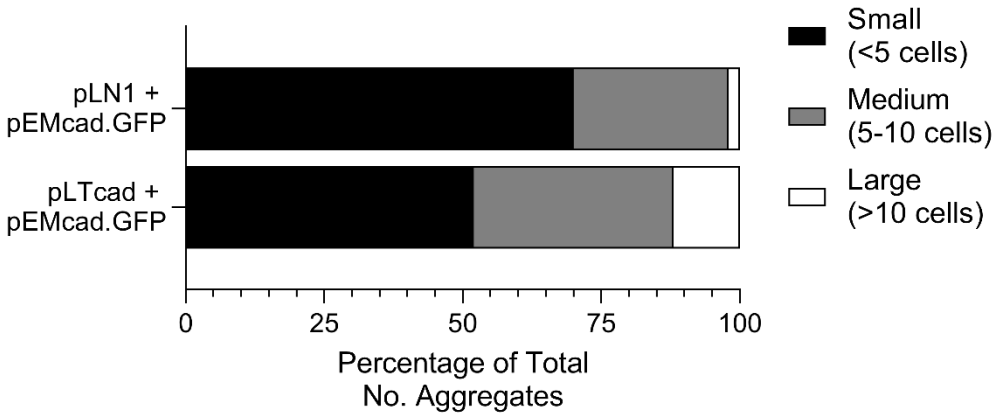

Figure 6.11. Percentage of combination aggregates formed between cadherin expressing CHO cells as a proportion of the average total number of aggregates per group. Aggregates were separated into small (less than 5 cells total), medium (5-10 cells total) and large (more than 10 cells).

To allow for a total comparison between the single cadherin assays and the combination cadherin assays, the data in **Figure 6.9** and **Figure 6.11** were combined to generate **Figure 6.12**. This figure displays the ratio of small, medium, and large aggregates as a percentage of the total number of aggregates for each experimental group. This analysis showed that most of the aggregates in these experiments were small. Of note, the pLTcad plus pEMcad.GFP combination had slightly fewer small aggregates than the other experimental wells (57% versus 59% for pLN1) and slightly more large aggregates than the other experimental cell types (10% versus 9% for the pEMcad.GFP) (**Figure 6.12**). Overall, these differences, although minimal, may indicate an interaction between the two cadherins due to the greater number of large aggregates formed by the other combination cell types.

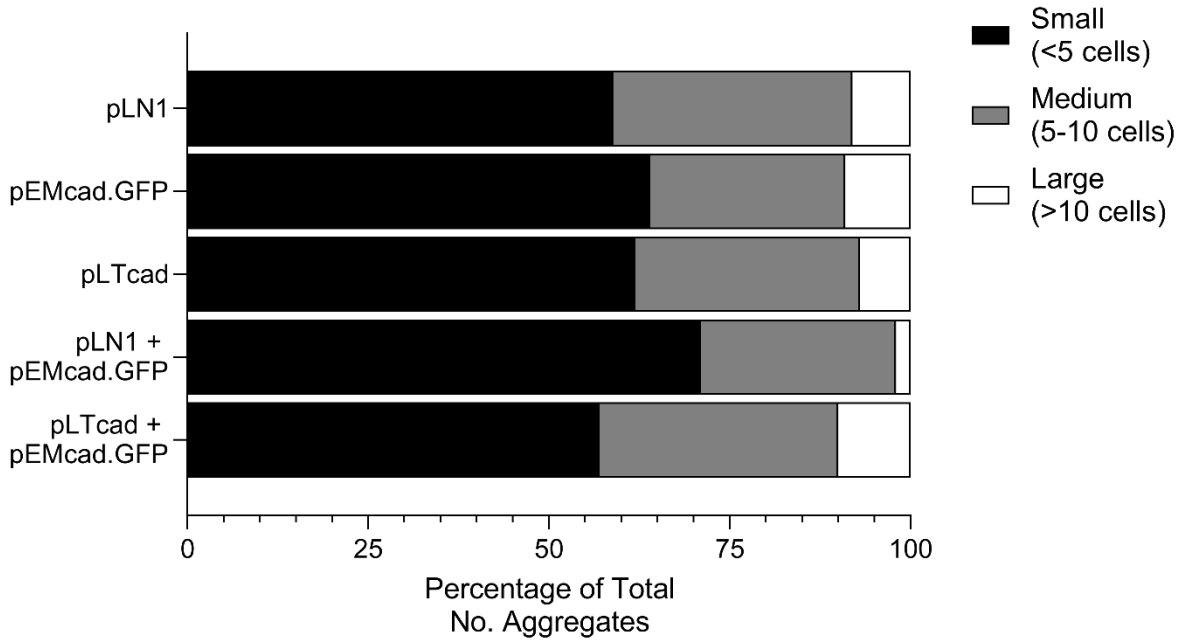

Figure 6.12. Percentage of aggregates formed between cadherin expression CHO cells as a proportion of the average total number of aggregates per group. Figure combines data from single cell and combination cell assays. Data for wells containing two cell types include both single cell and combination aggregates in the total number. Aggregates were separated into small (less than 5 cells total), medium (5-10 cells total) and large (more than 10 cells).

6.5 Discussion

The M-cadherin/β-catenin complex has been established as an important precursor for the formation of cell-to-cell junctions in myoblasts. However, there is still much research required to understand the regulation of this complex and how it affects myoblast fusion. This chapter aimed to explore the effects of T-cadherin on this adhesion complex. These results confirmed the interaction of T- and M-cadherin, and preliminary experiments suggest that this does not affect the phosphorylation of β-catenin. The implications of this work are discussed below.

6.5.1 T-cadherin interacts with M-cadherin in vitro

Preliminary studies suggested T- and M-cadherin interact. This chapter aimed to confirm this interaction using immunoprecipitation and aggregation assays. T-cadherin is a GPI-anchored protein and as such is associated with detergent resistant membrane domains [360]. This study used two non-denaturing, non-ionic detergents including Birj97, a detergent known to dissolve detergent resistant membranes, and Triton X-114, a phase separating detergent.

Beginning with Brij97, immunoprecipitates were prepared with lysates from C2C12 and pLTcad C2C12 cells. Consistent with results obtained during my Honours studies on C2C12 cells, T-cadherin antibodies recognized antigen in the T-cadherin immunoprecipitates, cell lysates and the M-cadherin immunoprecipitates. M-cadherin was only detected in the M-cadherin immunoprecipitates and lysates. The lack of M-cadherin in the T-cadherin immunoprecipitates is possibly a result of poorer affinity or reduced quality of the T-cadherin antibody compared to the M-cadherin antibody. It is also possible that the interaction between the cadherins inhibits epitope access for this antibody. Various T-cadherin antibodies were trialled for this assay and showed either a lower affinity for T-cadherin or increased background staining (data not shown).

To enhance the immunoprecipitation assay, pLTcad cells and a protein cross-linker (DTSSP) were used. In pLTcad immunoprecipitates, with and without DTSSP, T-cadherin was detected in the T-cadherin immunoprecipitates and lysates, and not in the M-cadherin immunoprecipitates. Subsequent probing with M-cadherin antibodies revealed M-cadherin in T- and M-cadherin immunoprecipitates and lysates from

pLTcad cells. The addition of DTSSP to pLTcad cells increased the M-cadherin signal in T- and M-cadherin immunoprecipitates but reduced protein signal in the lysates.

The absence of T-cadherin in the M-cadherin immunoprecipitates from pLTcad lysates was unexpected as a strong signal is observed in C2C12 lysates. A possible explanation is that the bound M-cadherin antibody sterically inhibits interactions with T-cadherin, limiting T-cadherin binding and presence in M-cadherin immunoprecipitates from pLTcad cells. Taken together, these experiments using C2C12 and pLTcad cells together show that M- and T-cadherin interact.

Another consideration is that although DTSSP increased the detection of M-cadherin in T-cadherin immunoprecipitates, there were also reduced levels of T- and M-cadherin in the immunoprecipitates and whole cell lysates. Although DTSSP stabilised the binding of T- and M-cadherin, it is possible that the concentration of DTSSP was too high or that the excess cross linker was not effectively removed prior to lysate preparation. Excess DTSSP can lead to non-specific cross-linking and can increase western blot background. In future assays, the DTSSP concentration could be optimised for cell number and excess DTSSP effectively quenched and removed.

Immunoprecipitation experiments were also performed with Triton X-114 detergent, C2C12 cells and the DTSSP crosslinker. This assay detected cadherins only in their respective immunoprecipitates and lysates. Although Triton X-114 was not suitable for this assay, perhaps due to its inability to reach detergent resistant membranes, Triton X-114 can also be used for temperature dependent phase separation of proteins during immunoprecipitation. Triton X-114 is homogenous at 0 °C but separates into an aqueous and detergent phase above 20 °C, which can be used to concentrate certain proteins [361]. If repeated, a temperature dependent separation could be used to optimize the pull down and study of the interacting cadherins.

6.5.2 T-cadherin's influence on the M-cadherin-β-catenin complex

The M-cadherin-β-catenin complex is important for forming cell-to-cell junctions and providing strength and stability for actin reorganisation during myoblast fusion. Preliminary data shows that M-cadherin interacts with β-catenin in C2C12 myoblasts and in pLTcad differentiating cells the interaction is reduced. The overexpressing pLTcad cells show reduced myogenesis and decreased fusion (see preliminary results,

section 1.10). A possible explanation and model for the reduced myogenesis is that the interaction between T- and M-cadherin inhibits M-cadherin-β-catenin complex formation and thus muscle differentiation (**Figure 6.13**).

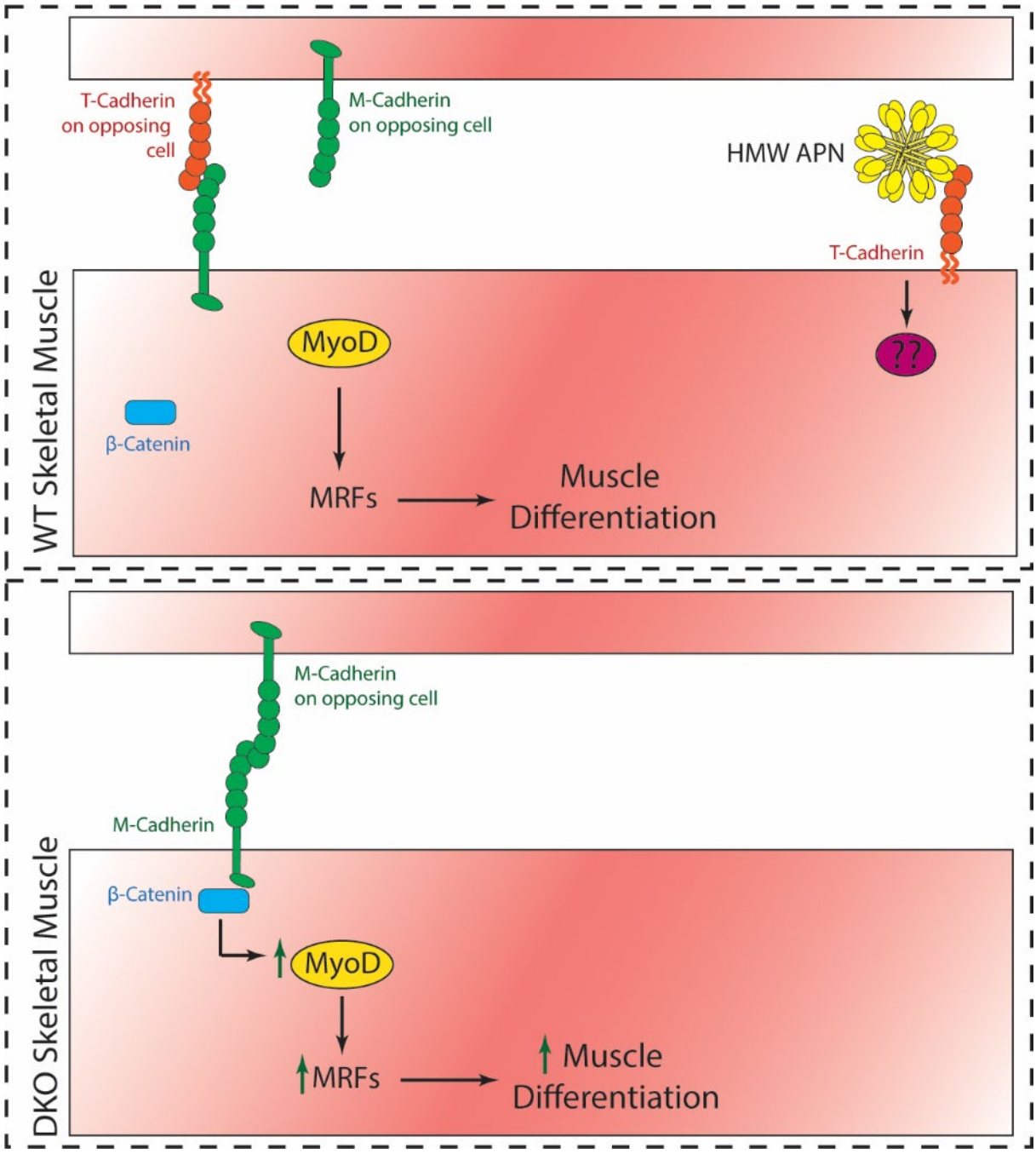

Figure 6.13. Effects of T-cadherin interacting with M-cadherin on skeletal muscle differentiation. In WT muscle, T-cadherin interacts with M-cadherin and inhibits the formation of the M-cadherin-β-catenin complex in myoblasts. In the absence of T-cadherin in DKO muscle, M-cadherin interacts with β-catenin and enhances muscle differentiation.

Given β-catenin can be degraded or localise to the nucleus to modify TCF/LEF activity, preliminary western blot analyses were conducted to determine the levels of total and serine 45 phosphorylated β-catenin in differentiating primary WT and DKO myoblasts.

The phosphorylation of serine 45 occurs via CK1α and acts as a priming step before GSK-3β phosphorylation and subsequent degradation, and illustrates the proportion of β-catenin that has been primed for degradation [357]. There was an increase in the levels of total β-catenin from 6 to 12 hours differentiation, but there was no difference between the WT and DKO myoblasts. This is consistent with the current literature that shows β-catenin protein levels increase in line with myoblast differentiation, and suggests that T-cadherin loss has no effect on the level of total β-catenin [225]. Although there was an increase in serine 45 phosphorylated β-catenin from 6- to 12-hours, there was no difference between the genotypes and suggests T-cadherin does not affect the phosphorylation of β-catenin at serine 45. Future studies to determine if T-cadherin expression influences β-catenin phosphorylation and activity could include antibodies against other phosphorylated forms of β-catenin, such as active β-catenin. Apart from whole lysate studies, cellular fractionation studies should be included with pLN1 and pLTcad cells over a differentiation time course to see where in myotubes the different β-catenin forms are located.

6.5.3 T-cadherin and M-cadherin interact on opposing CHO cells

This interaction of T- and M-cadherin was confirmed by immunoprecipitation and further examined by the CHO cell aggregation assay. The assay showed that a greater number of large aggregates were formed between pLTcad and pEMcad.GFP CHO cells compared to the combination of pLN1 and pEMcad.GFP CHO cells. Although there were similar numbers of total aggregates, more of the pLTcad and pEMcad.GFP cells were involved in large cell aggregates, suggesting increased affinity due to the presence of both T-cadherin and M-cadherin.

However, there were also aggregates of all sizes formed by CHO cells expressing a single cadherin. This was expected as pLTcad and pEMcad.GFP cells can aggregate through homophilic interaction of these cadherins. Notwithstanding, it was surprising that pLN1 cells formed aggregates while they do not express cadherins and were expected to remain as single cells. Given that CHO cells lack cadherins, the

aggregates may be due to the presence of residual DNA or cell debris that can cause increased background aggregation. To eliminate this suspected problem, future assays could include DNase to minimise this. Furthermore, there were more aggregates formed in the control wells than in the experimental wells and this suggests that there was uneven plating or total cell numbers. The increased total cell number could also account for the greater number of larger aggregations formed because of closer cell proximity. If performed again, these experiments would be optimised at a specific cell number to ensure minimal aggregation of the pLN1 cells. Overall, the experiment with the immunoprecipitation data suggests that T- and M-cadherin interact.

6.5.4 Limitations and Future Recommendations

This chapter tested for an interaction between T- and M-cadherin. Immunoprecipitation studies illustrated this, but the aggregation assays require further fine tuning to confidently confirm this interaction by this method. To replace the aggregation assay, a proximity ligation assay could be conducted with C2C12 cells or primary myoblasts. This assay allows for the detection of protein-protein interactions *in situ* and uses the amplification of fluorescent probes bound to specific antibodies to visualize areas of proximity [362]. In addition, β-catenin activity and subcellular localisation is important to determine its functionality in pLTcad cells and in response to loss of T-cadherin in DKO cells.

6.6 Conclusion

This chapter confirms that T-cadherin can bind M-cadherin in differentiating C2C12 myoblasts. It is possible that this interaction is one of the mechanisms behind T-cadherin's negative regulation of muscle regeneration. If this interaction inhibits M-cadherin from binding with the actin cytoskeleton and forming cellular junctions, this will inhibit myoblast fusion during differentiation. Further work is required to determine whether this interaction is affecting M-cadherin's ability to bind β-catenin and form cell junctions during differentiation and whether this affects the concentration of active β-catenin in the cell. Studies also need to be conducted to determine if a signalling axis of T-cadherin regulation of β-catenin, MYOD and PGC-1β is functional and regulates mitochondrial biogenesis. Understanding these mechanisms, particularly in primary myogenic cells, is important in furthering our understanding of how skeletal muscle myogenesis is regulated during regeneration and could assist in the improvement of muscle repair following severe muscular injury.

7 Discussion and Conclusion

Skeletal muscles are the largest tissue in the body and are essential for building strength, maintaining posture, and allowing everyday movements. Muscles are formed early during embryonic development and maintain a population of self-renewing SCs to facilitate regeneration throughout life. During muscle formation, myoblasts fuse together to form multinucleated myofibers in a process known as myogenesis, which is tightly controlled by myogenic regulatory factors. Muscle regeneration and repair that occurs postnatally recapitulates this process of myogenesis and importantly any dysregulation of post-natal myogenesis or of the self-renewing cells involved can lead to muscle loss (atrophy) that is associated with chronic illness and ageing. Thus, the search to better understand factors that can improve muscle function and regenerative ability is critical for improving muscle health in human disease. In this light, the focus of this thesis concerns the role of a cell adhesion molecule, T-cadherin, in regulating and facilitating muscle differentiation. Despite T-cadherin being abundantly expressed on skeletal muscles and binding APN, its role in regulating muscle differentiation is still poorly understood. Preliminary results from the Hebbard lab show that C2C12 muscle cells overexpressing T-cadherin show delayed differentiation and reduced myoblast fusion. The T-cadherin overexpressing cells also have reduced M-cadherin-β-catenin complex formation, a process thought to be important in facilitating fusion. Furthermore, findings from my Honours research show enhanced differentiation of primary DKO myoblasts. Thus, these data lead to the overarching question of this thesis, what is T-cadherin's role in regulating muscle regeneration?

In answering this question, this thesis contains several important and relevant findings. The RNA sequencing results from Chapter 3 identify several differentially expressed genes between WT and DKO primary myotubes, but not between the WT and T-cadherin KO cells, suggesting that the loss of APN and T-cadherin affects *ex vivo* myogenesis. In Chapter 4, improved muscle repair is observed in DKO regenerating muscle tissue, but not T-cadherin KO muscles where serum APN levels are supranormal. Additionally, no observable differences in myogenic differentiation were noted between T-cadherin KO and WT myoblasts. In Chapter 5, it was found that T-cadherin can regulate mitochondrial content and activity. T-cadherin overexpression reduces mitochondrial complex expression and activity and, in contrast, DKO

proliferating myoblasts have increased mitochondrial content and differentiated myotubes have greater mitochondrial activity. In Chapter 6, the data show that T-cadherin and M-cadherin interact in C2C12 cells, and this may impact downstream signalling. Taken together, the data suggests that T-cadherin and APN play an important role in regulating myogenesis and that T-cadherin has APN-independent myogenic cell adhesion functions. The implication of these findings with regards to the literature on myogenesis and muscle repair, and a potential model of T-cadherin's functions in myogenesis are presented below.

7.1 T-cadherin and adiponectin negatively regulate muscle regeneration

An important finding of this thesis is that DKO, but not T-cadherin knockout (T-cad KO), myoblasts undergo enhanced regeneration both *ex vivo* and *in vivo.* The results show that DKO primary myoblasts commit to differentiation and fuse more rapidly than WT myoblasts. Moreover, there are no changes in myogenesis between T-cad KO and WT myoblasts. These results were confirmed in the injury regeneration study where DKO muscle displayed enhanced differentiation compared to WT murine muscle. At day three regeneration, the DKO muscle had increased macrophage infiltration and an increased number of activated SCs. After 7 days of regeneration, there was an increased number of central nuclei within the newly formed muscle fibres, indicating enhanced regeneration and formation of new muscle fibres.

Despite APN having roles in many different tissues, it is nonetheless difficult to pinpoint the exact mechanism through which APN mediates myogenesis. Moreover, controversy surrounds APN functions in muscle regeneration as it has been shown to enhance *in vitro* myogenesis [109], reduce damage in a muscular dystrophy model [242], and inhibit C2C12 and SC proliferation, and C2C12 differentiation [329]. Furthermore, an APN receptor agonist can promote muscle atrophy [363], and genetic loss of APN has no impact on muscle repair [212]. Hence, the findings of this thesis are an important inflection point that improves our understanding of both APN and T-cadherin's role in muscle repair.

A point that can be further explored concerns the potential reasons for the accelerated muscle repair and *ex vivo* myogenesis noted for cells on the DKO background. An increase in activated SC numbers is likely responsible for the enhanced differentiation

of DKO primary myoblasts and the faster rate of muscle regeneration in the DKO muscle. MYOD expression was increased in DKO injured muscle after 3 days regeneration and not in T-cadherin KO mice. This suggests that T-cadherin and APN signalling influences the expression of MYOD and the DKO SCs are activated sooner. This could explain why DKO myoblasts commit to differentiation sooner, as MYOD stimulates the expression of myogenin. Together, this would explain the overall increase in muscle regeneration, but does not explain the mechanism behind MYOD's increased expression. A possible scenario for this is the absence of APN signalling. When APN receptors are activated by an APN agonist in regenerating muscles fibres, MYOD and myogenin expression are reduced [329]. Furthermore, given the absence of any notable difference in myogenic differentiation between T-cad KO, that have elevated serum APN, and WT myofibers, it is likely that APN signalling in T-cad KO mice occurs through AdipoR1 to restrict differentiation and repair. Whereas in the DKO muscle, where APN is absent, increased MYOD expression and enhanced repair is noted upon injury.

Another plausible explanation for the increase in MYOD is the increase in macrophages seen in DKO muscle fibres at day three of regeneration. Macrophage infiltration is an essential first step of regeneration that clears necrotic tissue, increases SC proliferation and assists in initiating differentiation [53]. Thus, the increased number of macrophages in the DKO tissue during regeneration could promote SC activation and proliferation.

Interestingly, APN has been shown to have anti-inflammatory properties and stimulates macrophage polarization to an anti-inflammatory M2 state. These macrophages are better known for being reparative, rather than inflammatory, and encourage muscle cell fusion by limiting migration [364]. Therefore, a lack of APN may prolong the M1 inflammatory state and encourage SC proliferation rather than fusion. Unfortunately, observing this switch between M1 and M2 macrophages was outside the scope of this thesis, and it is not clear if this switch to 'reparative' macrophages is affected in the absence of APN or if it is maintained by the expression of other cytokines. Additional studies could investigate this in WT, T-cad KO and DKO regenerating muscle tissue.

Apart from these observations, the results also show that DKO primary myotubes have increased mitochondrial function. The DKO differentiating myotubes have increased basal and maximal respiration and an increased number of mitochondria in proliferating primary cells. Consistent with this, the T-cadherin overexpressing pLTcad C2C12 cells have reduced expression of the mitochondrial complexes and maximal respiration at 24 hours differentiation. It is possible that MYOD is also responsible for the differences in metabolism. C2C12 myotubes with a doxycycline induced shRNA (small hairpin RNA) targeting MYOD have reduced basal OCRs and lower maximal respiratory capacity compared to a doxycycline induced scrambled shRNA (control) [336]. This is likely a result of MYOD binding to the PGC-1β promoter and increasing PGC-1β expression which, in turn, increases mitochondrial biogenesis and OCR. Therefore, the increased expression of MYOD not only influences differentiation but also the expression of metabolic genes. This concept would help explain the increased mitochondrial biogenesis even in the absence of APN. Examination of PGC-1 levels in the differentiating primary myoblasts and pLTcad cells would contribute towards our understanding of this process. Furthermore, although there were no differences in muscle fibre types between the different mouse genotypes, it would be interesting to examine if changes in metabolic genes altered the muscle fibre type over time.

7.2 T-cadherin interacts with M-cadherin to inhibit adhesion complex formation

There is much research surrounding the roles of APN in metabolic diseases and muscle regeneration and while some of these studies highlight the importance of T-cadherin as a receptor, very few examine its role individually. Although the findings of this thesis suggest that T-cadherin alone is not responsible for the improvement in DKO mouse muscle regeneration, it is possible that it also plays a more significant role other than as a receptor for APN. By example, earlier work by Ranscht and Dours-Zimmermann on T-cadherin illustrated that T-cadherin is a negative regulator of neurite out-growth, independent of APN [187]. In line with this, preliminary results show that overexpressing T-cadherin in C2C12 myoblasts impairs muscle differentiation and interferes with the formation of the M-cadherin-β-catenin complex. The results of this thesis confirmed that T-cadherin does interact with M-cadherin in C2C12 cells but have yet to show the potential effects of this in muscle. Importantly, M-cadherin in muscle

cells has many different functions. It can engage in homophilic binding to regulate differentiation [204], interact with microtubules [365], inhibit β-catenin phosphorylation [206], and regulate glucose transport [207] and SC quiescence [119].

Thus, in view of this thesis' findings as well as published data, T-cadherin may control muscle regeneration by negatively regulating the fusion of myoblasts. It is possible that it achieves this through homophilic binding, or by binding M-cadherin to restrict M-cadherin homophilic binding and limiting M-cadherin-β-catenin interactions in myoblasts. This would also diminish the downstream effects of β-catenin, including the upregulation of MYOD and the functionality of M-cadherin in myogenesis as listed in the above studies. Thus, T-cadherin inhibition of M-cadherin could contribute to a swathe of myogenic cellular changes that are the subject of ongoing studies. In this light and based on the data presented in this thesis, **Figure 7.1** proposes the action of T-cadherin and APN on regenerating WT and DKO skeletal muscle.

7.3 Conflicting findings on adiponectin's role in regenerating muscle

A review of the literature has revealed that our findings differ from those published by others. By example, a recent report by Tanaka et. al. shows that APN binding to T-cadherin enhances rather than inhibits regeneration [212]. Although these findings contrast to our results, there are a few key points that could contribute to these differences. Firstly, muscle regeneration only improved when APN was delivered by adenovirus to supraphysiological levels, along with angiotensin II treatment to partially mimic muscle ageing [212]. In addition to the high levels of APN, another important difference between this study and that of this thesis are the different ages of the mice, a critical consideration, as the activation of the APN receptors can have opposite effects in young versus aged SCs. In young SCs, APN signalling inhibits proliferation and downregulates the expression of myogenic regulatory factors. In contrast, the myogenic regulatory factors are promoted in aged SCs and proliferation remains unaffected [329]. These differences illustrates that there are still large gaps in our understanding of how SC regulation changes over time, specifically, how does APN contribute to myogenesis and repair at normal serum concentrations, and where does T-cadherin fit into these processes?

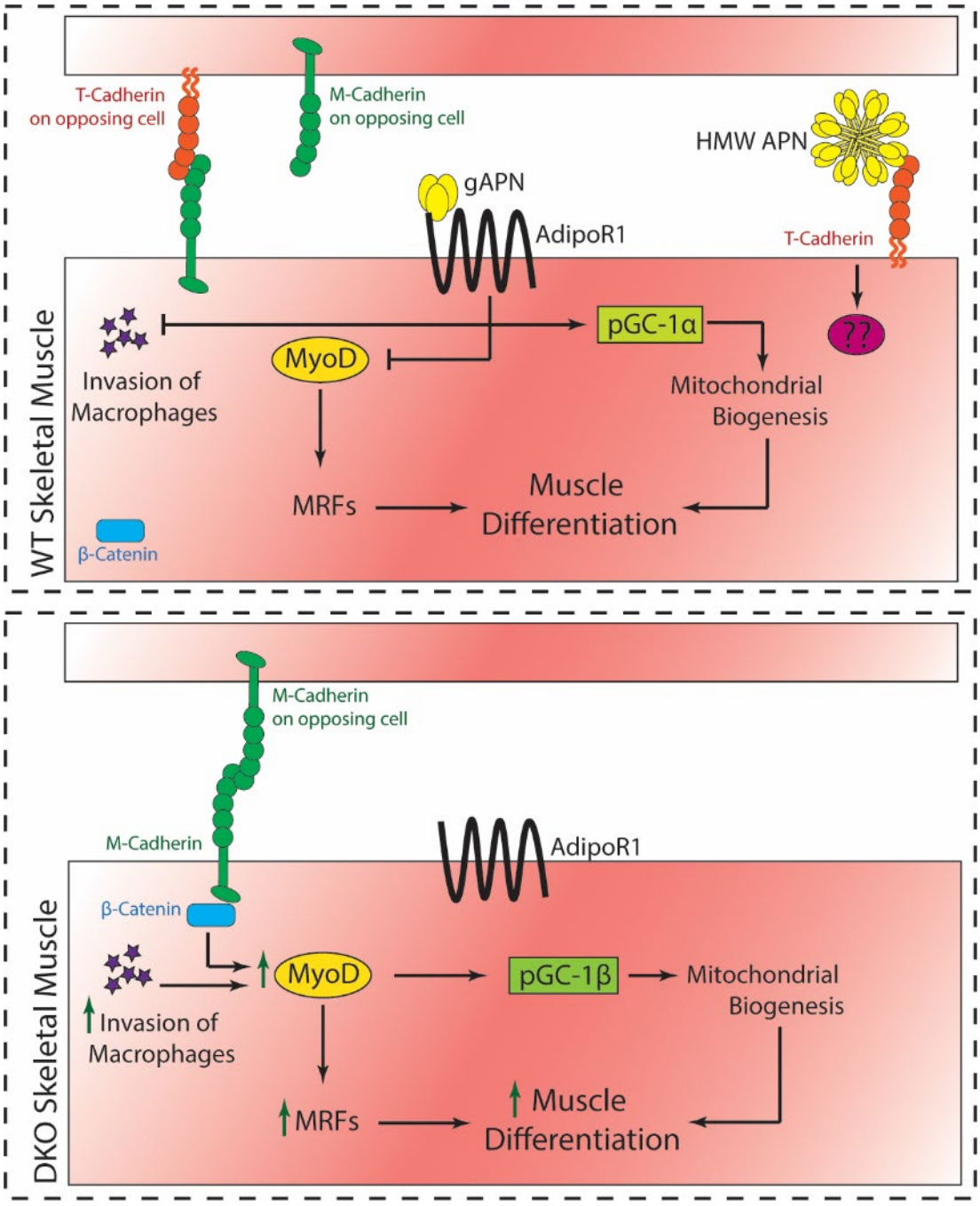

Figure 7.1. Proposed effects of T-cadherin and APN on regeneration in WT and DKO muscle. In WT muscle T-cadherin interacts with M-cadherin and inhibits the formation of the M-cadherin-β-catenin complex. APN binds AdipoR1, which restricts MYOD expression in young SCs, and limits macrophage inflammation. Mitochondrial biogenesis through PGC-1α is restricted. In DKO muscle M-cadherin freely interacts with β-catenin, and together with the increased macrophage infiltration enhances the expression of MYOD. The increased expression of MYOD promotes MRFs and enhances muscle differentiation. MYOD also promotes mitochondrial biogenesis through PGC-1β, which can in turn promote muscle differentiation.

7.4 Implications for this research

Understanding the importance of T-cadherin in post-natal muscle regeneration may have significant implications for improving human health. Muscle atrophy is a common comorbidity associated with both chronic illnesses and ageing and yet there is no effective treatment. Through understanding how T-cadherin negatively regulates skeletal muscle regeneration, we could identify downstream pathways and subsequent targets to limit muscle mass loss in patients.

7.5 Limitations of this research

There are many exciting implications for this research, but it is important to recognise the limitations of these studies to help guide further experimentation. One of the major limitations of this study was the limited sample size and lack of statistical power within the RNA sequencing assay. Unfortunately, the RNA sequencing assay only included two replicate samples. Each of these samples was pooled from 4-6 mice but could not be sequenced individually due to difficulties in obtaining enough SC numbers for analysis from one mouse. Furthermore, due to the differences in expression of common metabolic housekeeping genes, qPCR failed to validate gene expression. Moving forward, qPCR validation should be performed with alternate housekeeping genes. Fortunately, gene ontology assays provided a way to visualise the broader scope of these genes.

There are also concerns around the immunofluorescence staining of the macrophages (CD68) and activated satellite cells (MYOD) in the injury regeneration assays. Unfortunately, the staining of the muscle sections was particularly bright and caused difficulties in the identification of positive cells. Moving forward, these experiments should be repeated with a lower concentration or alternate antibody to confirm the differences observed between the genotypes.

Another limitation of this research was the use of engineered cell lines in place of primary myoblasts. Although primary myoblasts were used where possible, it was often difficult to obtain enough satellite cells from the pool of mice to conduct experiments and so murine C2C12 cells were used in these cases. Although C2C12 cells mimic the

differentiation process of myoblasts, they been shown to express higher levels of adhesion proteins and assays should be repeated with primary satellite cells where possible to confirm findings [366].

The investigation into mitochondrial function in WT and DKO cells was hindered by the limited sample capacity of the Seahorse XFp instrument. There were limited wells available in the microplate for each assay and this often led to experiments being conducted on different plates at different times. In particular, the fatty acid oxidation assay is usually performed on a 24-well plate to ensure consistency between samples, but these experiments had to be conducted over multiple microplates and may have resulted in some unavoidable errors within the analysis. Furthermore, this instrument is not capable of performing normalisation methods, so this had to be conducted externally. Although great care was taken to preserve myotubes during the washing stages of normalisation, this may have affected the overall results. Repeating these experiments in a 24-well plate with the Seahorse XF analyser would ensure consistency between samples and allow for fluorescent normalisation during the assay.

Finally, although the aggregation assay hinted at the interaction between T- and M-cadherin, there were many weaknesses that limited the outcome of this experiment. Unexpectedly, there were many aggregates formed between pLN1 CHO cells indicating cadherin independent aggregation was occurring, potentially due to the presence of ‘sticky’ residual DNA. Furthermore, as the cells remained suspended following the termination of the assay, it is possible that many aggregates were missed as they were not in focus during analysis. These factors could be improved in future studies.

7.6 Recommendations for additional research

The results from this thesis present compelling evidence regarding the role of T-cadherin and APN in regulating skeletal muscle myogenesis. However, there is still much to be done to uncover the mechanism behind this regulation. First and foremost, western blots of WT and DKO differentiating myoblasts should be probed for the expression of MYOD, PGC-1α and PGC-1β. This would assist in explaining the enhanced regeneration seen in the DKO cells. Secondly, although we have shown that

the loss of T-cadherin and APN are necessary to increase myoblast fusion, we have yet to show if there is a change in myogenic differentiation between single APN KO and WT mice. In line with this, assays using T-cadherin overexpressing C2C12 cells should be re-examined with the addition of recombinant APN. Furthermore, it may be worthwhile to examine the polarisation of macrophages during the regeneration process to help understand how APN affects macrophage infiltration following injury.

Although the RNA sequencing from this thesis lacked statistical power, future analyses could benefit from repeating these assays with WT and DKO primary myoblasts at earlier time points of differentiation. Genes could then be validated by qPCR, and this may help in our understanding of how the DKO cells differ from the WT. Furthermore, following the validation of the differentially expressed genes, individual genes, such as myomaker and myomixer, could be selected and targeted to closely examine their relationship with T-cadherin and their overall role in muscle differentiation.

Given the importance of ageing on SC activity in regeneration, these studies could be repeated in an ageing mouse model to help understand the inconsistencies between this study and existing literature. Based on the studies performed on uninjured skeletal muscle sections, there does not appear to be any differences in the morphology, number of SCs present, or muscle fibre type, suggesting that although T-cadherin and APN may play an important role in myogenesis, they do not affect the development of muscles. Many issues with SCs arise gradually over time and as such future studies could benefit from an analysis between WT and DKO muscle tissue following repeated cycles of injury and regeneration. This would provide insight into whether this research could lead to improved treatment for muscle wasting and would allow for the exploration of changes in fibrosis over time.

Although the immunoprecipitations show that T-cadherin interacts with M-cadherin, this could be further supported by a proximity ligation assay in differentiating muscles cells. It is also not clear how T- and M-cadherin binding effects the expression or degradation of β-catenin. β-catenin is phosphorylated at many sites, thus in conjunction with examining the subcellular localisation of β-catenin, the identification of different phosphorylated forms of β-catenin would assist in determining β-catenin activity in the presence or absence of T-cadherin in differentiating myoblasts.

The findings from these recommendations should improve our understanding of the myogenic adhesion complex that forms during myogenesis and how it interacts with APN to regulate muscle regeneration. Understanding this process is paramount to finding an improved treatment for muscle wasting. It is hoped that the findings presented in this thesis will assist in the identification of suitable proteins that can be targeted within the muscle to improve muscle regeneration and satellite cell function throughout life. Future experiments should focus on identifying these targets and modifying them in murine models of atrophy, sarcopenia, and muscular dystrophy. Together with repeated injury regeneration studies, this research will provide valuable insight into the treatment and prevention of muscle wasting and disease.

7.7 Conclusion

This study investigated the role of T-cadherin in skeletal muscle myogenesis and regeneration. Our results reveal that both T-cadherin and adiponectin play an important role in regulating skeletal muscle myogenesis. The exact role of T-cadherin and adiponectin in regeneration is likely a very complex interaction between adhesion proteins and adiponectin signalling and there is still much to be understood. Our results show that mice lacking T-cadherin and adiponectin have enhanced muscle regeneration, indicated by the increased expression of activated SCs and macrophages at day three regeneration and the increased number of centrally located nuclei at day 7 regeneration. The increase in expression of MYOD at day three regeneration parallels increases in mitochondrial content and function in the DKO primary myotubes. Finally, although T-cadherin acts as a receptor for adiponectin, the results show that T-cadherin can interact with M-cadherin to inhibit the formation of the M-cadherin-β-catenin adhesion complex. Taken together, this shows a clear role for both T-cadherin and adiponectin in regulating myogenesis. These findings will have significant ramifications for understanding human health and may lead to improved treatment strategies for muscle atrophy that is often associated with chronic conditions.

8 References

1. Hebbard, L., et al., *T-cadherin supports angiogenesis and adiponectin association with the vasculature in a mouse mammary tumor model.* Cancer Research, 2008. **68**(5): p. 1407-16.
2. Taylor, L., et al., *Cell adhesion an important determinant of myogenesis and satellite cell activity.* Biochim Biophys Acta Mol Cell Res, 2022. **1869**(2): p. 119170.
3. Agilent Technologies, I. *Seahorse XF Cell Mito Stress Test Kit User Guide* [User Guide] 2019 [cited 2023 16/06/2023]; Second Edition:[Available from: https://www.agilent.com/cs/library/usermanuals/public/XF_Cell_Mito_Stress_Test_Kit_User_Guide.pdf.
4. Frontera, W.R. and J. Ochala, *Skeletal muscle: A brief review of structure and function.* Calcified Tissue International, 2014. **96**(3): p. 183-195.
5. Manhart, A., et al., *Mechanical positioning of multiple nuclei in muscle cells.* PLoS Comput Biol, 2018. **14**(6): p. e1006208.
6. Fitts, R.H., *The cross-bridge cycle and skeletal muscle fatigue.* J Appl Physiol (1985), 2008. **104**(2): p. 551-8.
7. Geeves, M.A., R. Fedorov, and D.J. Manstein, *Molecular mechanism of actomyosin-based motility.* Cell Mol Life Sci, 2005. **62**(13): p. 1462-77.
8. Pette, D. and R. Staron, *Myosin isoforms, muscle fiber types, and transitions.* Microscopy Research and Technique, 2000. **50**(6): p. 500-509.
9. Westerblad, H., J. Bruton, and A. Katz, *Skeletal muscle: Energy metabolism, fiber types, fatigue and adaptability.* Experimental Cell Research, 2010. **316**(18): p. 3093-3099.
10. Knudsen, A.B., et al., *The human myotendinous junction: An ultrastructural and 3D analysis study.* Scandinavian Journal of Medicine & Science in Sports, 2015. **25**(1): p. e116-e123.
11. Talbot, J. and L. Maves, *Skeletal muscle fiber type: using insights from muscle developmental biology to dissect targets for susceptibility and resistance to muscle disease.* Wiley Interdiscip Rev Dev Biol, 2016. **5**(4): p. 518-34.
12. Robertson, E.J. and S.J. Arnold, *Making a commitment: cell lineage allocation and axis patterning in the early mouse embryo.* Nature Reviews Molecular Cell Biology, 2009. **10**(2): p. 91-103.
13. Christ, B. and C.P. Ordahl, *Early stages of chick somite development.* Anatomy and Embryology, 1995. **191**(5): p. 381-396.
14. Buckingham, M., et al., *The formation of skeletal muscle: from somite to limb.* The Journal of Anatomy, 2003. **202**(1): p. 59-68.
15. von Maltzahn, J., et al., *Wnt signaling in myogenesis.* Trends in Cell Biology, 2012. **22**(11): p. 602-609.
16. Cisternas, P., et al., *Wnt Signaling in Skeletal Muscle Dynamics: Myogenesis, Neuromuscular Synapse and Fibrosis.* Molecular Neurobiology, 2014. **49**(1): p. 574-589.
17. MacDonald, B.T., K. Tamai, and X. He, *Wnt/β-Catenin Signaling: Components, Mechanisms, and Diseases.* Developmental Cell, 2009. **17**(1): p. 9-26.
18. Armstrong, D.D. and K.A. Esser, *Wnt/β-catenin signaling activates growth-control genes during overload-induced skeletal muscle hypertrophy.* American Journal of Physiology - Cell Physiology, 2005. **289**(4): p. 853-859.

19. Münsterberg, A.E., et al., *Combinatorial signaling by Sonic hedgehog and Wnt family members induces myogenic bHLH gene expression in the somite.* Genes & development, 1995. **9**(23): p. 2911-2922.
20. Cui, S., et al., *β-Catenin is essential for differentiation of primary myoblasts via cooperation with MyoD and α-catenin.* Development (Cambridge, England), 2019. **146**(6): p. dev167080.
21. Takada, S., et al., *Wnt-3a regulates somite and tailbud formation in the mouse embryo.* Genes and Development, 1994. **8**(2): p. 174-189.
22. Kassar-Duchossoy, L., et al., *Pax3/Pax7 mark a novel population of primitive myogenic cells during development.* Genes and Development, 2005. **19**(12): p. 1426-1431.
23. Kahane, N., et al., *The third wave of myotome colonization by mitotically competent progenitors: regulating the balance between differentiation and proliferation during muscle development.* Development, 2001. **128**(12): p. 2187-2198.
24. Petropoulos, H. and I.S. Skerjanc, *Beta-catenin is essential and sufficient for skeletal myogenesis in P19 cells.* The Journal of biological chemistry, 2002. **277**(18): p. 15393-15399.
25. Birchmeier, C. and H. Brohmann, *Genes that control the development of migrating muscle precursor cells.* Curr Opin Cell Biol, 2000. **12**(6): p. 725-30.
26. Olson, E.N., *MyoD family: a paradigm for development?* Genes Dev, 1990. **4**(9): p. 1454-61.
27. Berkes, C.A. and S.J. Tapscott, *MyoD and the transcriptional control of myogenesis.* Semin Cell Dev Biol, 2005. **16**(4-5): p. 585-95.
28. Ott, M.O., et al., *Early expression of the myogenic regulatory gene, myf-5, in precursor cells of skeletal muscle in the mouse embryo.* Development, 1991. **111**(4): p. 1097-1107.
29. Davis, R.L., H. Weintraub, and A.B. Lassar, *Expression of a single transfected cDNA converts fibroblasts to myoblasts.* Cell, 1987. **51**(6): p. 987-1000.
30. Tajbakhsh, S., et al., *Differential activation of Myf5 and MyoD by different Wnts in explants of mouse paraxial mesoderm and the later activation of myogenesis in the absence of Myf5.* Development, 1998. **125**(21): p. 4155-4162.
31. Gustafsson, M.K., et al., *Myf5 is a direct target of long-range Shh signaling and Gli regulation for muscle specification.* Genes Dev, 2002. **16**(1): p. 114-26.
32. Bajard, L., et al., *A novel genetic hierarchy functions during hypaxial myogenesis: Pax3 directly activates Myf5 in muscle progenitor cells in the limb.* Genes Dev, 2006. **20**(17): p. 2450-64.
33. Cossu, G., et al., *Determination, diversification and multipotency of mammalian myogenic cells.* Int J Dev Biol, 2000. **44**(6): p. 699-706.
34. Rudnicki, M., et al., *Inactivation of MyoD in mice leads to up-regulation of the myogenic HLH gene Myf-5 and results in apparently normal muscle development.* Cell, 1992. **71**(3): p. 383-390.
35. Rudnicki, M., et al., *MyoD or Myf-5 is required for the formation of skeletal muscle.* Cell, 1993. **75**(7): p. 1351-1359.
36. Braun, T., et al., *Targeted inactivation of the muscle regulatory gene Myf-5 results in abnormal rib development and perinatal death.* Cell, 1992. **71**(3): p. 369-382.
37. Yun, K. and B. Wold, *Skeletal muscle determination and differentiation: story of a core regulatory network and its context.* Current Opinion in Cell Biology, 1996. **8**(6): p. 877-889.

38. Hasty, P., et al., *Muscle deficiency and neonatal death in mice with a targeted mutation in the myogenin gene.* Nature, 1993. **364**(6437): p. 501-6.
39. Nabeshima, Y.-i., et al., *Myogenin gene disruption results in perinatal lethality because of severe muscle defect.* Nature, 1993. **364**(6437): p. 532-535.
40. Kassar-Duchossoy, L., et al., *Mrf4 determines skeletal muscle identity in Myf5:Myod double-mutant mice.* Nature, 2004. **431**(7007): p. 466-71.
41. Kim, J., et al., *Mechanisms of myoblast fusion during muscle development.* Current Opinion in Genetics and Development, 2015. **32**: p. 162-70.
42. Millay, D.P., et al., *Myomaker is a membrane activator of myoblast fusion and muscle formation.* Nature, 2013. **499**(7458): p. 301-5.
43. Quinn, M.E., et al., *Myomerger induces fusion of non-fusogenic cells and is required for skeletal muscle development.* Nat Commun, 2017. **8**: p. 15665.
44. Zhang, Q., et al., *The microprotein Minion controls cell fusion and muscle formation.* Nat Commun, 2017. **8**: p. 15664.
45. Bi, P., et al., *Control of muscle formation by the fusogenic micropeptide myomixer.* Science, 2017. **356**(6335): p. 323-327.
46. Sampath, S.C. and D.P. Millay, *Myoblast fusion confusion: the resolution begins.* Skelet Muscle, 2018. **8**(1): p. 3.
47. Millay, D.P., et al., *Myomaker is essential for muscle regeneration.* Genes Dev, 2014. **28**(15): p. 1641-6.
48. Fu, X., H. Wang, and P. Hu, *Stem cell activation in skeletal muscle regeneration.* Cellular and Molecular Life Sciences, 2015. **72**(9): p. 1663-1677.
49. Yin, H., F. Price, and M. Rudnicki, *Satellite cells and the muscle stem cell niche.* Physiological Reviews, 2013. **93**(1): p. 23-67.
50. Allam Ali, M., *Myotube formation in skeletal muscle regeneration.* Journal of Anatomy, 1979. **128**(3): p. 553-562.
51. Alderton, J.M. and R.A. Steinhardt, *Calcium influx through calcium leak channels is responsible for the elevated levels of calcium-dependent proteolysis in dystrophic myotubes.* J Biol Chem, 2000. **275**(13): p. 9452-60.
52. Orimo, S., et al., *Analysis of inflammatory cells and complement C3 in bupivacaine-induced myonecrosis.* Muscle Nerve, 1991. **14**(6): p. 515-20.
53. Wang, X. and L. Zhou, *The Many Roles of Macrophages in Skeletal Muscle Injury and Repair.* Front Cell Dev Biol, 2022. **10**: p. 952249.
54. Arnold, L., et al., *Inflammatory monocytes recruited after skeletal muscle injury switch into antiinflammatory macrophages to support myogenesis.* J Exp Med, 2007. **204**(5): p. 1057-69.
55. Bencze, M., et al., *Proinflammatory macrophages enhance the regenerative capacity of human myoblasts by modifying their kinetics of proliferation and differentiation.* Mol Ther, 2012. **20**(11): p. 2168-79.
56. Wang, X., et al., *Infiltrating macrophages are broadly activated at the early stage to support acute skeletal muscle injury repair.* J Neuroimmunol, 2018. **317**: p. 55-66.
57. Zammit, P., T. Partridge, and Z. Yablonka-Reuveni, *The skeletal muscle satellite cell: the stem cell that came in from the cold.* Journal of Histochemistry & Cytochemistry, 2006. **54**(11): p. 1177-91.
58. Mauro, A., *Satellite cell of skeletal muscle fibres.* Journal of Cell Biology, 1961. **9**(2): p. 493.
59. Bentzinger, C.F., et al., *Cellular dynamics in the muscle satellite cell niche.* EMBO Rep, 2013. **14**(12): p. 1062-72.

60. Cheng, W., et al., *Self-renewal and differentiation of muscle satellite cells are regulated by the Fas-associated death domain.* J Biol Chem, 2014. **289**(8): p. 5040-50.
61. Le Grand, F. and M. Rudnicki, *Skeletal muscle satellite cells and adult myogenesis.* Current Opionins in Cell Biology, 2007. **19**(6): p. 628-33.
62. Gibson, M.C. and E. Schultz, *The distribution of satellite cells and their relationship to specific fiber types in soleus and extensor digitorum longus muscles.* Anat Rec, 1982. **202**(3): p. 329-37.
63. Mackey, A.L., et al., *Assessment of satellite cell number and activity status in human skeletal muscle biopsies.* Muscle Nerve, 2009. **40**(3): p. 455-65.
64. Seale, P., et al., *Pax7 is required for specification of myogenic satellite cells.* Cell, 2000. **102**(6): p. 777-786.
65. Crist, C.G., D. Montarras, and M. Buckingham, *Muscle satellite cells are primed for myogenesis but maintain quiescence with sequestration of Myf5 mRNA targeted by microRNA-31 in mRNP granules.* Cell Stem Cell, 2012. **11**(1): p. 118-26.
66. Feige, P., et al., *Orienting Muscle Stem Cells for Regeneration in Homeostasis, Aging, and Disease.* Cell Stem Cell, 2018. **23**(5): p. 653-664.
67. Schultz, E., *Satellite cell proliferative compartments in growing skeletal muscles.* Dev Biol, 1996. **175**(1): p. 84-94.
68. Kuang, S., et al., *Asymmetric self-renewal and commitment of satellite stem cells in muscle.* Cell, 2007. **129**(5): p. 999-1010.
69. Collins, C.A., et al., *Stem cell function, self-renewal, and behavioral heterogeneity of cells from the adult muscle satellite cell niche.* Cell, 2005. **122**(2): p. 289-301.
70. Rantanen, J., et al., *Satellite cell proliferation and the expression of myogenin and desmin in regenerating skeletal muscle: evidence for two different populations of satellite cells.* Lab Invest, 1995. **72**(3): p. 341-7.
71. Cooper, R.N., et al., *In vivo satellite cell activation via Myf5 and MyoD in regenerating mouse skeletal muscle.* J Cell Sci, 1999. **112 (Pt 17)**: p. 2895-901.
72. Megeney, L.A., et al., *MyoD is required for myogenic stem cell function in adult skeletal muscle.* Genes Dev, 1996. **10**(10): p. 1173-83.
73. Gayraud-Morel, B., et al., *A role for the myogenic determination gene Myf5 in adult regenerative myogenesis.* Dev Biol, 2007. **312**(1): p. 13-28.
74. Ishibashi, J., et al., *MyoD induces myogenic differentiation through cooperation of its NH2- and COOH-terminal regions.* J Cell Biol, 2005. **171**(3): p. 471-82.
75. Hargreaves, M. and L.L. Spriet, *Skeletal muscle energy metabolism during exercise.* Nat Metab, 2020. **2**(9): p. 817-828.
76. Hargreaves, M., *Skeletal muscle metabolism during exercise in humans.* Clinical and Experimental Pharmacology and Physiology, 2000. **27**: p. 225-228.
77. Joseph, J. and J.D. Doles, *Disease-associated metabolic alterations that impact satellite cells and muscle regeneration: perspectives and therapeutic outlook.* Nutr Metab (Lond), 2021. **18**(1): p. 33.
78. Ryall, J.G., et al., *The NAD(+)-dependent SIRT1 deacetylase translates a metabolic switch into regulatory epigenetics in skeletal muscle stem cells.* Cell Stem Cell, 2015. **16**(2): p. 171-83.
79. Moyes, C.D., et al., *Mitochondrial biogenesis during cellular differentiation.* Am J Physiol, 1997. **272**(4 Pt 1): p. C1345-51.

80. Wagatsuma, A., N. Kotake, and S. Yamada, *Muscle regeneration occurs to coincide with mitochondrial biogenesis.* Mol Cell Biochem, 2011. **349**(1-2): p. 139-47.
81. Lee, B. and J. Shao, *Adiponectin and lipid metabolism in skeletal muscle.* Acta Pharmaceutica Sinica B, 2012. **2**(4): p. 335-340.
82. Zhou, H., et al., *Adiponectin represses gluconeogenesis independent of insulin in hepatocytes.* Biochemical and Biophysical Research Communications, 2005. **338**(2): p. 793-9.
83. Pajvani, U.B., et al., *Complex distribution, not absolute amount of adiponectin, correlates with thiazolidinedione-mediated improvement in insulin sensitivity.* J Biol Chem, 2004. **279**(13): p. 12152-62.
84. Fruebis, J., et al., *Proteolytic cleavage product of 30-kDa adipocyte complement-related protein increases fatty acid oxidation in muscle and causes weight loss in mice.* Proceedings of the National Academy of Sciences, 2001. **98**(4): p. 2005-2010.
85. Combs, T.P. and E.B. Marliss, *Adiponectin signaling in the liver.* Reviews in Endocrine and Metabolic Disorders, 2014. **15**(2): p. 137-47.
86. Takeuchi, T., et al., *Adiponectin receptors, with special focus on the role of the third receptor, T-cadherin, in vascular disease.* Medical Molecular Morphology, 2007. **40**(3): p. 115-20.
87. Yamauchi, T., et al., *Cloning of adiponectin receptors that mediate antidiabetic metabolic effects.* Nature, 2003. **423**(6941): p. 762-769.
88. Wang, Z. and P. Scherer, *Adiponectin, the past two decades.* Journal of Molecular Cell Biology, 2016. **8**(2): p. 93-100.
89. Yamauchi, T., et al., *Adiponectin receptors: a review of their structure, function and how they work.* Best Pract Res Clin Endocrinol Metab, 2014. **28**(1): p. 15-23.
90. Yamauchi, T., et al., *Targeted disruption of AdipoR1 and AdipoR2 causes abrogation of adiponectin binding and metabolic actions.* Nature Medicine, 2007. **13**(3): p. 332-9.
91. Hebbard, L. and B. Ranscht, *Multifaceted roles of adiponectin in cancer.* Best Practice & Research: Clinical Endocrinology Metabolism, 2014. **28**(1): p. 59-69.
92. Arita, Y., et al., *Paradoxical decrease of an adipose-specific protein, adiponectin. in obesity.* Biochemical and Biophysical Research Communication, 1999. **257**(1): p. 79-83.
93. Stumvoll, M., et al., *Association of the T-G polymorphism in adiponectin (exon 2) with obesity and insulin sensitivity: interaction with family history of type 2 diabetes.* Diabetes, 2002. **51**(1): p. 37-41.
94. Hivert, M.F., et al., *Common variants in the adiponectin gene (ADIPOQ) associated with plasma adiponectin levels, type 2 diabetes, and diabetes-related quantitative traits: the Framingham Offspring Study.* Diabetes, 2008. **57**(12): p. 3353-9.
95. Vionnet, N., et al., *Genomewide search for type 2 diabetes-susceptibility genes in French whites: evidence for a novel susceptibility locus for early-onset diabetes on chromosome 3q27-qter and independent replication of a type 2-diabetes locus on chromosome 1q21-q24.* Am J Hum Genet, 2000. **67**(6): p. 1470-80.
96. Civitarese, A.E., et al., *Role of adiponectin in human skeletal muscle bioenergetics.* Cell Metabolism, 2006. **4**(1): p. 75-87.

97. Yamauchi, T., et al., *The fat-derived hormone adiponectin reverses insulin resistance associated with both lipoatrophy and obesity.* Nature Medicine, 2001. **7**(8): p. 941-946.
98. Yamauchi, T., et al., *Adiponectin stimulates glucose utilization and fatty-acid oxidation by activating AMP-activated protein kinase.* Nature Medicine, 2002. **8**(11): p. 1288-95.
99. Ryu, J., et al., *APPL1 potentiates insulin sensitivity by facilitating the binding of IRS1/2 to the insulin receptor.* Cell Rep, 2014. **7**(4): p. 1227-38.
100. Mao, X., et al., *APPL1 binds to adiponectin receptors and mediates adiponectin signalling and function.* Nat Cell Biol, 2006. **8**(5): p. 516-23.
101. Zhou, L., et al., *Adiponectin activates AMP-activated protein kinase in muscle cells via APPL1/LKB1-dependent and phospholipase C/Ca2+/Ca2+/calmodulin-dependent protein kinase kinase-dependent pathways.* J Biol Chem, 2009. **284**(33): p. 22426-22435.
102. Ventura-Clapier, R., A. Garnier, and V. Veksler, *Transcriptional control of mitochondrial biogenesis: the central role of PGC-1alpha.* Cardiovasc Res, 2008. **79**(2): p. 208-17.
103. Yoon, M., et al., *Adiponectin increases fatty acid oxidation in skeletal muscle cells by sequential activation of AMP-activated protein kinase, p38 mitogen-activated protein kinase, and peroxisome proliferator-activated receptor alpha.* Diabetes, 2006. **55**(9): p. 2562-70.
104. Ceddia, R.B., et al., *Globular adiponectin increases GLUT4 translocation and glucose uptake but reduces glycogen synthesis in rat skeletal muscle cells.* Diabetologia, 2005. **48**(1): p. 132-9.
105. Ruan, H. and L. Dong, *Adiponectin signaling and function in insulin target tissues.* Journal of Molecular Cell Biology, 2016. **8**(2): p. 101-109.
106. Krause, M., et al., *Adiponectin is expressed by skeletal muscle fibers and influences muscle phenotype and function.* American Journal of Physiology - Cell Physiology, 2008. **295**(1): p. C203-12.
107. Yamauchi, T. and T. Kadowaki, *Adiponectin receptor as a key player in healthy longevity and obesity-related diseases.* Cell Metabolism, 2013. **17**(2): p. 185-96.
108. Berg, A.H., T.P. Combs, and P.E. Scherer, *ACRP30/adiponectin: an adipokine regulating glucose and lipid metabolism.* Trends in Endocrinology and Metabolism, 2002. **13**(2): p. 84-89.
109. Fiaschi, T., et al., *Globular adiponectin induces differentiation and fusion of skeletal muscle cells.* Cell Research, 2009. **19**(5): p. 584-97.
110. Fiaschi, T., et al., *Globular adiponectin activates motility and regenerative traits of muscle satellite cells.* PLoS One, 2012. **7**(5): p. e34782.
111. Jones, N.C., et al., *The p38alpha/beta MAPK functions as a molecular switch to activate the quiescent satellite cell.* J Cell Biol, 2005. **169**(1): p. 105-16.
112. Asfour, H.A., M.Z. Allouh, and R.S. Said, *Myogenic regulatory factors: The orchestrators of myogenesis after 30 years of discovery.* Experimental biology and medicine (Maywood, N.J.), 2018. **243**(2): p. 118-128.
113. Chen, H., et al., *Adiponectin activates the AMPK signaling pathway to regulate lipid metabolism in bovine hepatocytes.* Journal of Steroid Biochemistry and Molecular Biology, 2013. **138**: p. 445-54.
114. Zhang, M. and I.S. McLennan, *During secondary myotube formation, primary myotubes preferentially absorb new nuclei at their ends.* Dev Dyn, 1995. **204**(2): p. 168-77.

115. Zammit, P., et al., *Pax7 and myogenic progression in skeletal muscle satellite cells.* Journal of Cell Science, 2006. **119**(Pt 9): p. 1824-32.
116. Schultz, E., M.C. Gibson, and T. Champion, *Satellite cells are mitotically quiescent in mature mouse muscle: An EM and radioautographic study.* The Journal of experimental zoology, 1978. **206**(3): p. 451-456.
117. Alway, S.E., M.J. Myers, and J.S. Mohamed, *Regulation of satellite cell function in sarcopenia.* Frontiers in aging neuroscience, 2014. **6**: p. 246-246.
118. Furuichi, Y., et al., *Excess Glucose Impedes the Proliferation of Skeletal Muscle Satellite Cells Under Adherent Culture Conditions.* Frontiers in cell and developmental biology, 2021. **9**: p. 640399-640399.
119. Goel, A.J., et al., *Niche Cadherins Control the Quiescence-to-Activation Transition in Muscle Stem Cells.* Cell Reports, 2017. **21**(8): p. 2236-2250.
120. Marti, M., et al., *M-cadherin-mediated intercellular interactions activate satellite cell division.* Journal of Cell Science, 2013. **126**(22): p. 5116-5131.
121. McEver, R.P., *Selectins: initiators of leucocyte adhesion and signalling at the vascular wall.* Cardiovascular research, 2015. **107**(3): p. 331-339.
122. Baker, W., et al., *P-selectin inhibition suppresses muscle regeneration following injury.* Journal of leukocyte biology, 2004. **76**(2): p. 352-358.
123. Costa, M.L., *Cytoskeleton and Adhesion in Myogenesis.* ISRN Developmental Biology, 2014. **2014**: p. 1-15.
124. Hynes, R.O., *Integrins: Versatility, modulation, and signaling in cell adhesion.* Cell (Cambridge), 1992. **69**(1): p. 11-25.
125. Mayer, U., *Integrins: Redundant or Important Players in Skeletal Muscle?* The Journal of biological chemistry, 2003. **278**(17): p. 14587-14590.
126. Thorsteinsdóttir, S., et al., *The extracellular matrix dimension of skeletal muscle development.* Dev Biol, 2011. **354**(2): p. 191-207.
127. Lowell, C.A. and T.N. Mayadas, *Overview: studying integrins in vivo.* Methods Mol Biol, 2012. **757**: p. 369-97.
128. Campbell, K.P., et al., *Primary structure of dystrophin-associated glycoproteins linking dystrophin to the extracellular matrix.* Nature (London), 1992. **355**(6362): p. 696-702.
129. Song, W.K., et al., *H36-alpha 7 is a novel integrin alpha chain that is developmentally regulated during skeletal myogenesis.* The Journal of cell biology, 1992. **117**(3): p. 643-657.
130. Gao, Q.Q. and E.M. McNally, *The Dystrophin Complex: Structure, Function, and Implications for Therapy.* Comprehensive Physiology, 2011: p. 1223-1239.
131. George-Weinstein, M., et al., *In Vitro and in Vivo Expression α7 Integrin and Desmin Define the Primary and Secondary Myogenic Lineages.* Developmental biology, 1993. **156**(1): p. 209-229.
132. Ziober, B.L., et al., *Mutations in the integrin α7 gene cause congenital myopathy.* Nature genetics, 1998. **19**(1): p. 94-97.
133. Mayer, U., et al., *Absence of integrin alpha 7 causes a novel form of muscular dystrophy.* Nature genetics, 1997. **17**(3): p. 318.
134. Burkin, D.J., et al., *Enhanced expression of the alpha 7 beta 1 integrin reduces muscular dystrophy and restores viability in dystrophic mice.* The Journal of cell biology, 2001. **152**(6): p. 1207-1218.
135. Hodges, B.L., et al., *Altered expression of the alpha7beta1 integrin in human and murine muscular dystrophies.* Journal of cell science, 1997. **110 (Pt 22)**: p. 2873-2881.

136. Burkin, D.J., et al., *Transgenic expression of {alpha}7{beta}1 integrin maintains muscle integrity, increases regenerative capacity, promotes hypertrophy, and reduces cardiomyopathy in dystrophic mice.* Am J Pathol, 2005. **166**(1): p. 253-63.
137. Guo, C., et al., *Absence of α7 integrin in dystrophin-deficient mice causes a myopathy similar to Duchenne muscular dystrophy.* Human molecular genetics, 2006. **15**(6): p. 989-998.
138. Heller, K.N., et al., *Human α7 Integrin Gene (ITGA7) Delivered by Adeno-Associated Virus Extends Survival of Severely Affected Dystrophin/Utrophin-Deficient Mice.* Human gene therapy, 2015. **26**(10): p. 647-656.
139. Heller, K.N., et al., *AAV-mediated overexpression of human α7 integrin leads to histological and functional improvement in dystrophic mice.* Mol Ther, 2013. **21**(3): p. 520-5.
140. Sarathy, A., et al., *SU9516 Increases α7β1 Integrin and Ameliorates Disease Progression in the mdx Mouse Model of Duchenne Muscular Dystrophy.* Mol Ther, 2017. **25**(6): p. 1395-1407.
141. Menko, A.S. and D. Boettiger, *Occupation of the extracellular matrix receptor, integrin, is a control point for myogenic differentiation.* Cell (Cambridge), 1987. **51**(1): p. 51-57.
142. Schwander, M., et al., *β1 Integrins Regulate Myoblast Fusion and Sarcomere Assembly.* Developmental cell, 2003. **4**(5): p. 673-685.
143. Luo, W., et al., *TMEM182 interacts with integrin beta 1 and regulates myoblast differentiation and muscle regeneration.* J Cachexia Sarcopenia Muscle, 2021. **12**(6): p. 1704-1723.
144. Rozo, M., L. Li, and C.M. Fan, *Targeting β1-integrin signaling enhances regeneration in aged and dystrophic muscle in mice.* Nat Med, 2016. **22**(8): p. 889-96.
145. Liu, H., et al., *Beta3-integrin mediates satellite cell differentiation in regenerating mouse muscle.* FASEB J, 2011. **25**(6): p. 1914-21.
146. Rosen, G.D., et al., *Roles for the integrin VLA-4 and its counter receptor VCAM-1 in myogenesis.* Cell (Cambridge), 1992. **69**(7): p. 1107-1119.
147. Yang, J.T., et al., *Genetic analysis of alpha 4 integrin functions in the development of mouse skeletal muscle.* The Journal of cell biology, 1996. **135**(3): p. 829-835.
148. Taverna, D., et al., *Dystrophic muscle in mice chimeric for expression of alpha5 integrin.* The Journal of cell biology, 1998. **143**(3): p. 849.
149. Georges-Labouesse, E., et al., *Absence of integrin alpha 6 leads to epidermolysis bullosa and neonatal death in mice.* Nature genetics, 1996. **13**(3): p. 370.
150. Wilschut, K.J., et al., *Alpha 6 integrin is important for myogenic stem cell differentiation.* Stem Cell Res, 2011. **7**(2): p. 112-23.
151. Bajanca, F., et al., *Integrin alpha6beta1-laminin interactions regulate early myotome formation in the mouse embryo.* Development, 2006. **133**(9): p. 1635-44.
152. Lyons, G.E., et al., *Expression of NCAM isoforms during skeletal myogenesis in the mouse embryo.* Developmental Dynamics, 1992. **194**(2): p. 94-104.
153. Dickson, G., et al., *Enhanced myogenesis in NCAM-transfected mouse myoblasts.* Nature, 1990. **344**(6264): p. 348-351.

154. Peck, D. and F.S. Walsh, *Differential Effects of Over-Expressed Neural Cell Adhesion Molecule Isoforms on Myoblast Fusion.* The Journal of cell biology, 1993. **123**(6): p. 1587-1595.
155. Tassin, A.M., et al., *MODULATION OF EXPRESSION AND CELL-SURFACE DISTRIBUTION OF N-CAM DURING MYOGENESIS INVITRO.* Neurochemistry International, 1991. **18**(1): p. 97-106.
156. Moore, S.E., et al., *Skeletal muscle neural cell adhesion molecule (N-CAM): changes in protein and mRNA species during myogenesis of muscle cell lines.* The Journal of cell biology, 1987. **105**(3): p. 1377-1386.
157. O'Reilly, C., et al., *Hepatocyte growth factor (HGF) and the satellite cell response following muscle lengthening contractions in humans.* Muscle Nerve, 2008. **38**(5): p. 1434-1442.
158. Charlton, C.A., W.A. Mohler, and H.M. Blau, *Neural cell adhesion molecule (NCAM) and myoblast fusion.* Dev Biol, 2000. **221**(1): p. 112-9.
159. Choo, H.-J., et al., *A tale of two niches: differential functions for VCAM-1 in satellite cells under basal and injured conditions.* American Journal of Physiology: Cell Physiology, 2017. **313**(4): p. C392-C404.
160. Kang, J.-S., et al., *CDO: An oncogene-, serum-, and anchorage-regulated member of the Ig/fibronectin type III repeat family.* The Journal of Cell Biology, 1997. **138**(1): p. 203-213.
161. Mulieri, P.J., et al., *Developmental expression pattern of the cdo gene.* Developmental dynamics, 2000. **219**(1): p. 40-49.
162. Kang, J.-S., et al., *CDO, A robo-related cell surface protein that mediates myogenic differentiation.* The Journal of Cell Biology, 1998. **143**(2): p. 403-413.
163. Cole, F., et al., *Positive regulation of myogenic bHLH factors and skeletal muscle development by the cell surface receptor CDO.* Developmental Cell, 2004. **7**(6): p. 843-854.
164. Kang, J.-S., et al., *Promyogenic members of the Ig and cadherin families associate to positively regulate differentiation.* Proceedings of the National Academy of Sciences of the United States of America, 2003. **100**(7): p. 3989-3994.
165. Bae, G.U., et al., *Cdo interacts with APPL1 and activates Akt in myoblast differentiation.* Mol Biol Cell, 2010. **21**(14): p. 2399-411.
166. Perdiguero, E., et al., *Genetic analysis of p38 MAP kinases in myogenesis: fundamental role of p38alpha in abrogating myoblast proliferation.* The EMBO journal, 2007. **26**(5): p. 1245.
167. Tran, P., et al., *TGF-beta-activated Kinase 1 (TAK1) and Apoptosis Signal-regulating Kinase 1 (ASK1) Interact with the Promyogenic Receptor Cdo to Promote Myogenic Differentiation via Activation of p38MAPK Pathway.* Journal of Biological Chemistry, 2012. **287**(15): p. 11602-11615.
168. Bae, J.H., et al., *Satellite cell-specific ablation of Cdon impairs integrin activation, FGF signalling, and muscle regeneration.* Journal of cachexia, sarcopenia and muscle, 2020. **11**(4): p. 1089-1103.
169. Kang, J.-S., et al., *BOC, an Ig superfamily member, associates with CDO to positively regulate myogenic differentiation.* The EMBO Journal, 2002. **21**(1/2): p. 114-124.
170. Mulieri, P.J., et al., *Expression of the boc gene during murine embryogenesis.* Developmental Dynamics, 2002. **223**(3): p. 379-388.
171. Wegorzewska, M., R.S. Krauss, and J.S. Kang, *Overexpression of the immunoglobulin superfamily members CDO and BOC enhances differentiation*

of the human rhabdomyosarcoma cell line RD. Molecular carcinogenesis, 2003. **37**(1): p. 1-4.
172. Round, J. and E. Stein, *Netrin signaling leading to directed growth cone steering.* Current opinion in neurobiology, 2007. **17**(1): p. 15-21.
173. Huber, A.B., et al., *Signaling at the growth cone: ligand-receptor complexes and the control of axon growth and guidance.* Annual review of neuroscience, 2003. **26**: p. 509.
174. Kang, J.-S., et al., *Netrins and neogenin promote myotube formation.* The Journal of Cell Biology, 2004. **167**(3): p. 493-504.
175. Bae, G.-U., et al., *Neogenin regulates skeletal myofiber size and focal adhesion kinase and extracellular signal-regulated kinase activities in vivo and in vitro.* Molecular biology of the cell, 2009. **20**(23): p. 4920-4931.
176. Delling, U., et al., *A calcineurin-NFATc3-dependent pathway regulates skeletal muscle differentiation and slow myosin heavy-chain expression.* Mol Cell Biol, 2000. **20**(17): p. 6600-11.
177. Tamura, K., et al., *Structure-function analysis of cell adhesion by neural (N-) cadherin.* Neuron, 1998. **20**(6): p. 1153-1163.
178. Nagar, B., et al., *Structural basis of calcium-induced E-cadherin rigidification and dimerization.* Nature, 1996. **380**(6572): p. 360-364.
179. Kim, S.A., et al., *Calcium-dependent dynamics of cadherin interactions at cell—cell junctions.* Proceedings of the National Academy of Sciences of the United States of America, 2011. **108**(24): p. 9857-9862.
180. Tariq, H., et al., *Cadherin flexibility provides a key difference between desmosomes and adherens junctions.* Proceedings of the National Academy of Sciences of the United States of America, 2015. **112**(17): p. 5395-5400.
181. Goodwin, M. and A.S. Yap, *Classical cadherin adhesion molecules: coordinating cell adhesion, signaling and the cytoskeleton.* Journal of Molecular Histology, 2004. **35**(8): p. 839-844.
182. Harrison, O.J., E.M. Corps, and P.J. Kilshaw, *Cadherin adhesion depends on a salt bridge at the N-terminus.* Journal of Cell Science, 2005. **118**(18): p. 4123-4130.
183. Cifuentes-Diaz, C., et al., *Distinct location and prevalence of alpha-, beta-catenins and gamma-catenin/plakoglobin in developing and denervated skeletal muscle.* Cell adhesion and communication, 1998. **5**(2): p. 161.
184. Moore, R. and F. Walsh, *The cell adhesion molecule M-cadherin is specifically expressed in developing and regenerating, but not denervated skeletal muscle.* Development, 1993. **117**(4): p. 1409-1420.
185. Hahn, C.G. and J. Covault, *Neural regulation of N-cadherin gene expression in developing and adult skeletal muscle.* Journal of Neuroscience, 1992. **12**(12): p. 4677-4687.
186. Inuzuka, H., C. Redies, and M. Takeichi, *Differential expression of R- and N-cadherin in neural and mesodermal tissues during early chicken development.* Development, 1991. **113**(3): p. 959-967.
187. Ranscht, B. and M. Dours-Zimmermann, *T-Cadherin, a novel cadherin cell adhesion molecule in the nervous sysrem lacks the conserved cytoplasmic region.* Neuron, 1991. **7**(3): p. 391-402.
188. Charrasse, S., et al., *Rho GTPases and cadherin-based cell adhesion in skeletal muscle development.* Journal of Muscle Research and Cell Motility, 2003. **24**(4): p. 311-315.

189. Jaffe, A.B. and A. Hall, *Rho GTPases: biochemistry and biology.* Annual review of cell and developmental biology, 2005. **21**(1): p. 247-269.
190. Aspenström, P., et al., *Taking Rho GTPases to the next level: The cellular functions of atypical Rho GTPases.* Experimental Cell Research, 2007. **313**(17): p. 3673-3679.
191. Carnac, G., et al., *RhoA GTPase and serum response factor control selectively the expression of MyoD without affecting Myf5 in mouse myoblasts.* Molecular biology of the cell, 1998. **9**(7): p. 1891-1902.
192. Elena, V., et al., *The Small G-Proteins Rac1 and Cdc42 Are Essential for Myoblast Fusion in the Mouse.* Proceedings of the National Academy of Sciences - PNAS, 2009. **106**(22): p. 8935-8940.
193. Charrasse, S., et al., *N-Cadherin-Dependent Cell-Cell Contact Regulates Rho GTPases and β-Catenin Localization in Mouse C2C12 Myoblasts.* The Journal of Cell Biology, 2002. **158**(5): p. 953-965.
194. Duband, J.-L., et al., *Adhesion Molecules during Somitogenesis in the Avian Embryo.* The Journal of Cell Biology, 1987. **104**(5): p. 1361-1374.
195. Cifuentes-Diaz, C., et al., *M-cadherin localization in developing adult and regenerating mouse skeletal muscle: possible involvement in secondary myogenesis.* Mechanisms of Development, 1995. **50**(1): p. 85-97.
196. Cifuentes-Diaz, C., et al., *N-cadherin and N-CAM-mediated adhesion in development and regeneration of skeletal muscle.* Neuromuscular Disorders, 1993. **3**(5): p. 361-365.
197. Radice, G.L., et al., *Developmental Defects in Mouse Embryos Lacking N-Cadherin.* Developmental Biology, 1997. **181**(1): p. 64-78.
198. Mege, R.M., et al., *N-cadherin and N-CAM in myoblast fusion: compared localisation and effect of blockade by peptides and antibodies.* Journal of cell science, 1992. **103 (Pt 4)**: p. 897.
199. Knudsen, K.A., L. Myers, and S.A. McElwee, *A role for the Ca 2+-dependent adhesion molecule, N-cadherin, in myoblast interaction during myogenesis.* Experimental Cell Research, 1990. **188**(2): p. 175-184.
200. Charlton, C., et al., *Fusion Competence of Myoblasts Rendered Genetically Null for N-Cadherin in Culture.* The Journal of Cell Biology, 1997. **138**(2): p. 331-336.
201. Lu, M. and R.S. Krauss, *N-cadherin ligation, but not Sonic hedgehog binding, initiates Cdo-dependent p38alpha/beta MAPK signaling in skeletal myoblasts.* Proc Natl Acad Sci U S A, 2010. **107**(9): p. 4212-7.
202. Irintchev, A., et al., *Expression pattern of M-cadherin in normal, denervated, and regenerating mouse muscles.* Developmental Dynamics, 1994. **199**(4): p. 326-337.
203. Donalies, M., et al., *Expression of M-cadherin, a member of the cadherin multigene family, correlates with differentiation of skeletal muscle cells.* Proceedings of the National Academy of Sciences of the United States of America, 1991. **88**(18): p. 8024-8028.
204. Zeschnigk, M., et al., *Involvement of M-cadherin in terminal differentiation of skeletal muscle cells.* Journal of Cell Science, 1995. **108**(9): p. 2973.
205. Hollnagel, A., et al., *The cell adhesion molecule M-cadherin is not sssential for muscle development and regeneration.* Molecular and Cellular Biology, 2002. **22**(13): p. 4760-4770.

206. Wang, Y., J.S. Mohamed, and S.E. Alway, *M-cadherin-inhibited phosphorylation of ß-catenin augments differentiation of mouse myoblasts.* Cell Tissue Res, 2013. **351**(1): p. 183-200.
207. Masson, S.W.C., et al., *β-catenin regulates muscle glucose transport via actin remodelling and M-cadherin binding.* Mol Metab, 2020. **42**: p. 101091.
208. Kucharczak, J., et al., *R-Cadherin expression inhibits myogenesis and induces myoblast transformation via Rac1 GTPase.* Cancer research, 2008. **68**(16): p. 6559-6568.
209. Niitsuma, K., et al., *Localization and Expression of R-Cadherin in Skeletal Muscle following Nerve Injury.* European Surgical Research, 2005. **37**(2): p. 79-84.
210. Johnson, E., et al., *R-cadherin Influences Cell Motility via Rho Family GTPases.* Journal of Biological Chemistry, 2004. **279**(30): p. 31041-31049.
211. Ciatto, C., et al., *T-cadherin structures reveal a novel adhesive binding mechanism.* Nature Structural & Molecular Biology, 2010. **17**(3): p. 339-47.
212. Tanaka, Y., et al., *Adiponectin promotes muscle regeneration through binding to T-cadherin.* Scientific Reports, 2019. **9**(1).
213. Krauss, R., et al., *Close encounters: regulation of vertebrate skeletal myogenesis by cell-cell contact.* Journal of Cell Science, 2005. **118**(Pt 11): p. 2355-62.
214. Krauss, R.S., *Regulation of promyogenic signal transduction by cell-cell contact and adhesion.* Exp Cell Res, 2010. **316**(18): p. 3042-9.
215. Chang, N.C., et al., *The Dystrophin Glycoprotein Complex Regulates the Epigenetic Activation of Muscle Stem Cell Commitment.* Cell Stem Cell, 2018. **22**(5): p. 755-+.
216. Dumont, N.A., et al., *Dystrophin expression in muscle stem cells regulates their polarity and asymmetric division.* Nature medicine, 2015. **21**(12): p. 1455-1463.
217. Chang, N.C., F.P. Chevalier, and M.A. Rudnicki, *Satellite Cells in Muscular Dystrophy – Lost in Polarity.* Trends in molecular medicine, 2016. **22**(6): p. 479-496.
218. Philippova, M., et al., *A guide and guard: The many faces of T-cadherin.* Cellular Signalling, 2009. **21**(7): p. 1035-1044.
219. Philippova, M., et al., *RhoA and Rac mediate endothelial cell polarization and detachment induced by T-cadherin.* FASEB J, 2005. **19**(6): p. 588-90.
220. Hug, C., et al., *T-cadherin is a receptor for hexameric and high-molecular-weight forms of Acrp30/adiponectin.* Proceedings of the National Academy of Sciences of the United States of America, 2004. **101**(28): p. 10308-10313.
221. Niermann, T., et al., *The glycosyl phosphatidylinositol anchor of human T-cadherin binds lipoproteins.* Biochem Biophys Res Commun, 2000. **276**(3): p. 1240-7.
222. Kita, S., et al., *Native adiponectin in serum binds to mammalian cells expressing T-cadherin, but not AdipoRs or calreticulin.* Elife, 2019. **8**.
223. Parker-Duffen, J., et al., *T-cadherin is essential for adiponectin-mediated revascularization.* Journal of Biological Chemistry, 2013. **288**(34): p. 24886-24897.
224. Denzel, M., et al., *T-cadherin is critical for adiponectin-mediated cardioprotection in mice.* The Journal Clinical Investigation, 2010. **120**(12): p. 4342-4352.

225. Wrobel, E., E. Brzoska, and J. Moraczewski, *M-cadherin and beta-catenin participate in differentiation of rat satellite cells.* European Journal of Cell Biology, 2007. **86**(2): p. 99-109.
226. Kim, C.-H., et al., *β-Catenin Interacts with MyoD and Regulates Its Transcription Activity.* Molecular and Cellular Biology, 2008. **28**(9): p. 2941-2951.
227. Goichberg, P., et al., *Recruitment of β-catenin to cadherin-mediated intercellular adhesions is involved in myogenic induction.* Journal of Cell Science, 2001. **114**(7): p. 1309-1319.
228. Aberle, H., et al., *beta-catenin is a target for the ubiquitin-proteasome pathway.* EMBO J, 1997. **16**(13): p. 3797-804.
229. Lovering, R.M., N.C. Porter, and R.J. Bloch, *The muscular dystrophies: from genes to therapies.* Phys Ther, 2005. **85**(12): p. 1372-88.
230. Walter, M. and P. Reilich, *Recent developments in Duchenne muscular dystrophy: facts and numbers.* Journal of Cachexia, Sarcopenia and Muscle, 2017. **8**(5): p. 681-685.
231. Szűcs, Z., et al., *An Ultra-Rare Manifestation of an X-Linked Recessive Disorder: Duchenne Muscular Dystrophy in a Female Patient.* Int J Mol Sci, 2022. **23**(21).
232. Yablonka-Reuveni, Z. and J. Anderson, *Satellite cells from dystrophic (mdx) mice display accelerated differentiation in primary cultures and in isolated myofibers.* Developmental Dynamics, 2006. **235**(1): p. 203-12.
233. Cohn, R.D. and K.P. Campbell, *Molecular basis of muscular dystrophies.* Muscle & Nerve, 2000. **23**(10): p. 1456-1471.
234. Morgan, J. and P.S. Zammit, *Direct effects of the pathogenic mutation on satellite cell function in muscular dystrophy.* Experimental Cell Research, 2010. **316**(18): p. 3100-3108.
235. Webster, C. and H. Blau, *Accelerated age-related decline in replicative life-span of Duchenne muscular dystrophy myoblasts: implications for cell and gene therapy.* Somatic cell and molecular genetics, 1990. **16**(6): p. 557-565.
236. Boldrin, L., P.S. Zammit, and J.E. Morgan, *Satellite cells from dystrophic muscle retain regenerative capacity.* Stem Cell Research, 2015. **14**(1): p. 20-9.
237. Kottlors, M. and J. Kirschner, *Elevated satellite cell number in Duchenne muscular dystrophy.* Cell Tissue Res, 2010. **340**(3): p. 541-8.
238. Bankolé, L.C., et al., *Fibre type-specific satellite cell content in two models of muscle disease.* Histopathology, 2013. **63**(6): p. 826-32.
239. Vila, M.C., et al., *Mitochondria mediate cell membrane repair and contribute to Duchenne muscular dystrophy.* Cell Death Differ, 2017. **24**(2): p. 330-342.
240. Hughes, M.C., et al., *Early myopathy in Duchenne muscular dystrophy is associated with elevated mitochondrial H.* J Cachexia Sarcopenia Muscle, 2019. **10**(3): p. 643-661.
241. Allen, D.G., N.P. Whitehead, and S.C. Froehner, *Absence of Dystrophin Disrupts Skeletal Muscle Signaling: Roles of Ca2+, Reactive Oxygen Species, and Nitric Oxide in the Development of Muscular Dystrophy.* Physiol Rev, 2016. **96**(1): p. 253-305.
242. Abou-Samra, M., et al., *Involvement of adiponectin in the pathogenesis of dystrophinopathy.* Skelet Muscle, 2015. **5**: p. 25.
243. Erkut, E. and T. Yokota, *CRISPR Therapeutics for Duchenne Muscular Dystrophy.* Int J Mol Sci, 2022. **23**(3).

244. Meola, G. and R. Cardani, *Myotonic dystrophies: An update on clinical aspects, genetic, pathology, and molecular pathomechanisms.* Biochim Biophys Acta, 2015. **1852**(4): p. 594-606.
245. Vihola, A., et al., *Histopathological differences of myotonic dystrophy type 1 (DM1) and PROMM/DM2.* Neurology, 2003. **60**(11): p. 1854-7.
246. Pisani, V., et al., *Preferential central nucleation of type 2 myofibers is an invariable feature of myotonic dystrophy type 2.* Muscle Nerve, 2008. **38**(5): p. 1405-1411.
247. Merlini, L., A. Vagheggini, and D. Cocchi, *Sarcopenia and sarcopenic obesity in patients with muscular dystrophy.* Frontiers in Aging Neuroscience, 2014. **6**: p. 274.
248. Cruz-Jentoft, A.J., et al., *Sarcopenia: European consensus on definition and diagnosis: Report of the European Working Group on Sarcopenia in Older People.* Age Ageing, 2010. **39**(4): p. 412-23.
249. Cruz-Jentoft, A.J., et al., *Sarcopenia: revised European consensus on definition and diagnosis.* Age Ageing, 2019. **48**(4): p. 601.
250. Nilwik, R., et al., *The decline in skeletal muscle mass with aging is mainly attributed to a reduction in type II muscle fiber size.* Exp Gerontol, 2013. **48**(5): p. 492-8.
251. Roth, S.M., et al., *Skeletal muscle satellite cell populations in healthy young and older men and women.* The Anatomical Record, 2000. **260**(4): p. 351-358.
252. Shefer, G., et al., *Satellite-cell pool size does matter: Defining the myogenic potency of aging skeletal muscle.* Developmental Biology, 2006. **294**(1): p. 50-66.
253. Lin, J., et al., *Transcriptional co-activator PGC-1 alpha drives the formation of slow-twitch muscle fibres.* Nature, 2002. **418**(6899): p. 797-801.
254. Krämer, D.K., et al., *Human skeletal muscle fibre type variations correlate with PPAR alpha, PPAR delta and PGC-1 alpha mRNA.* Acta Physiol (Oxf), 2006. **188**(3-4): p. 207-16.
255. Sandri, M., et al., *PGC-1alpha protects skeletal muscle from atrophy by suppressing FoxO3 action and atrophy-specific gene transcription.* Proc Natl Acad Sci U S A, 2006. **103**(44): p. 16260-5.
256. Tisdale, M.J., *Cachexia in cancer patients.* Nature Reviews Cancer, 2002. **2**(11): p. 862-871.
257. Srikanthan, P., A.L. Hevener, and A.S. Karlamangla, *Sarcopenia exacerbates obesity-associated insulin resistance and dysglycemia: findings from the National Health and Nutrition Examination Survey III.* PLoS One, 2010. **5**(5): p. e10805.
258. Can, B., et al., *Serum markers of inflammation and oxidative stress in sarcopenia.* Aging Clin Exp Res, 2017. **29**(4): p. 745-752.
259. Australian Bureau of Statistics, *National Health Survey: First results 2017-18*, A. Government, Editor. 2018.
260. Tanner, C.J., et al., *Muscle fiber type is associated with obesity and weight loss.* Am J Physiol Endocrinol Metab, 2002. **282**(6): p. E1191-6.
261. Stuart, C.A., et al., *Slow-twitch fiber proportion in skeletal muscle correlates with insulin responsiveness.* J Clin Endocrinol Metab, 2013. **98**(5): p. 2027-36.
262. Patti, M.E., et al., *Coordinated reduction of genes of oxidative metabolism in humans with insulin resistance and diabetes: Potential role of PGC1 and NRF1.* Proc Natl Acad Sci U S A, 2003. **100**(14): p. 8466-71.

263. Mootha, V.K., et al., *PGC-1alpha-responsive genes involved in oxidative phosphorylation are coordinately downregulated in human diabetes.* Nat Genet, 2003. **34**(3): p. 267-73.
264. Fu, X., et al., *Obesity impairs skeletal muscle regeneration through inhibition of AMPK.* Diabetes, 2016. **65**(1): p. 188-200.
265. Nguyen, M.-H., M. Cheng, and T.J. Koh, *Impaired muscle regeneration in Ob/ob and Db/db mice.* TheScientificWorldJournal, 2011. **11**: p. 1525-1535.
266. Garcia, P. and A. Sood, *Adiponectin in pulmonary disease and critically ill patients.* Curr Med Chem, 2012. **19**(32): p. 5493-500.
267. Sente, T., et al., *Adiponectin resistance in skeletal muscle: pathophysiological implications in chronic heart failure.* J Cachexia Sarcopenia Muscle, 2016. **7**(3): p. 261-74.
268. Putku, M., et al., *CDH13 promoter SNPs with pleiotropic effect on cardiometabolic parameters represent methylation QTLs.* Hum Genet, 2015. **134**(3): p. 291-303.
269. Jee, S.H., et al., *Adiponectin concentrations: a genome-wide association study.* Am J Hum Genet, 2010. **87**(4): p. 545-52.
270. Nicolas, A., et al., *T-cadherin gene variants are associated with type 2 diabetes and the Fatty Liver Index in the French population.* Diabetes Metab, 2017. **43**(1): p. 33-39.
271. Kitamoto, A., et al., *CDH13 Polymorphisms are Associated with Adiponectin Levels and Metabolic Syndrome Traits Independently of Visceral Fat Mass.* Journal of Atherosclerosis and Thrombosis, 2016. **23**(3): p. 309-319.
272. Wu, Y., et al., *Genome-wide association study for adiponectin levels in Filipino women identifies CDH13 and a novel uncommon haplotype at KNG1-ADIPOQ.* Hum Mol Genet, 2010. **19**(24): p. 4955-64.
273. Yuan, G., et al., *Reduced circulating oxytocin and High-Molecular-Weight adiponectin are risk factors for metabolic syndrome.* Endocr J, 2016. **63**(7): p. 655-62.
274. Chung, C.M., et al., *A genome-wide association study reveals a quantitative trait locus of adiponectin on CDH13 that predicts cardiometabolic outcomes.* Diabetes, 2011. **60**(9): p. 2417-23.
275. Li, X., et al., *Associations between serum adipocytokines and glycemic tolerance biomarkers in a rural Chinese population.* PLoS One, 2017. **12**(8): p. e0182273.
276. Haan, C. and I. Behrmann, *A cost effective non-commercial ECL-solution for Western blot detections yielding strong signals and low background.* Journal of Immunological Methods, 2007. **318**(1): p. 11-19.
277. Hindi, L., et al., *Isolation, Culturing, and Differentiation of Primary Myoblasts from Skeletal Muscle of Adult Mice.* Bio Protoc, 2017. **7**(9).
278. Andrews, S., *FastQC: a quality control tool for high throughput sequence data*. 2010: http://www.bioinformatics.babraham.ac.uk/projects/fastqc.
279. Ewels, P., et al., *MultiQC: summarize analysis results for multiple tools and samples in a single report.* Bioinformatics, 2016. **32**(19): p. 3047-8.
280. Li, B. and C.N. Dewey, *RSEM: accurate transcript quantification from RNA-Seq data with or without a reference genome.* BMC Bioinformatics, 2011. **12**: p. 323.
281. Love, M.I., W. Huber, and S. Anders, *Moderated estimation of fold change and dispersion for RNA-seq data with DESeq2.* Genome Biol, 2014. **15**(12): p. 550.
282. Eden, E., et al., *GOrilla: a tool for discovery and visualization of enriched GO terms in ranked gene lists.* BMC Bioinformatics, 2009. **10**: p. 48.

283. Supek, F., et al., *REVIGO summarizes and visualizes long lists of gene ontology terms.* PLoS One, 2011. **6**(7): p. e21800.
284. Danecek, P., et al., *The variant call format and VCFtools.* Bioinformatics, 2011. **27**(15): p. 2156-8.
285. Purcell, S., et al., *PLINK: a tool set for whole-genome association and population-based linkage analyses.* Am J Hum Genet, 2007. **81**(3): p. 559-75.
286. Noble, W.S., *How does multiple testing correction work?* Nat Biotechnol, 2009. **27**(12): p. 1135-7.
287. Chamberlain, L.H., *Inhibition of isoprenoid biosynthesis causes insulin resistance in 3T3-L1 adipocytes.* FEBS Lett, 2001. **507**(3): p. 357-61.
288. Yeh, Y.S., et al., *The Mevalonate Pathway Is Indispensable for Adipocyte Survival.* iScience, 2018. **9**: p. 175-191.
289. Buhaescu, I. and H. Izzedine, *Mevalonate pathway: a review of clinical and therapeutical implications.* Clin Biochem, 2007. **40**(9-10): p. 575-84.
290. Peng, H.B., et al., *The relationship between perlecan and dystroglycan and its implication in the formation of the neuromuscular junction.* Cell Adhes Commun, 1998. **5**(6): p. 475-89.
291. Yamagata, M., et al., *Selective distributions of proteoglycans and their ligands in pericellular matrix of cultured fibroblasts. Implications for their roles in cell-substratum adhesion.* J Cell Sci, 1993. **106 (Pt 1)**: p. 55-65.
292. Larraín, J., et al., *Expression of perlecan, a proteoglycan that binds myogenic inhibitory basic fibroblast growth factor, is down regulated during skeletal muscle differentiation.* Exp Cell Res, 1997. **234**(2): p. 405-12.
293. Casar, J.C., et al., *Heparan sulfate proteoglycans are increased during skeletal muscle regeneration: requirement of syndecan-3 for successful fiber formation.* J Cell Sci, 2004. **117**(Pt 1): p. 73-84.
294. Croze, M.L. and C.O. Soulage, *Potential role and therapeutic interests of myo-inositol in metabolic diseases.* Biochimie, 2013. **95**(10): p. 1811-27.
295. Dilworth, L.L., et al., *The effect of phytic acid on the levels of blood glucose and some enzymes of carbohydrate and lipid metabolism.* West Indian Med J, 2005. **54**(2): p. 102-6.
296. Sun, Z., et al., *Zyxin is involved in regulation of mechanotransduction in arteriole smooth muscle cells.* Front Physiol, 2012. **3**: p. 472.
297. Taylor, A., et al., *Adaptations to excess choline in insulin resistant and Pcyt2 deficient skeletal muscle.* Biochem Cell Biol, 2017. **95**(2): p. 223-231.
298. Cánovas, V., et al., *The role of prostate tumor overexpressed 1 in cancer progression.* Oncotarget, 2017. **8**(7): p. 12451-12471.
299. Pedrotti, S., et al., *The RNA-binding protein Rbfox1 regulates splicing required for skeletal muscle structure and function.* Hum Mol Genet, 2015. **24**(8): p. 2360-74.
300. Orlandini, M., et al., *The characterization of a novel monoclonal antibody against CD93 unveils a new antiangiogenic target.* Oncotarget, 2014. **5**(9): p. 2750-60.
301. Mofarrahi, M. and S.N. Hussain, *Expression and functional roles of angiopoietin-2 in skeletal muscles.* PLoS One, 2011. **6**(7): p. e22882.
302. Park-Windhol, C., et al., *Endomucin inhibits VEGF-induced endothelial cell migration, growth, and morphogenesis by modulating VEGFR2 signaling.* Sci Rep, 2017. **7**(1): p. 17138.
303. Knowles, J., M. Loizidou, and I. Taylor, *Endothelin-1 and angiogenesis in cancer.* Curr Vasc Pharmacol, 2005. **3**(4): p. 309-14.

304. Chang, T.K., et al., *Apelin Promotes Endothelial Progenitor Cell Angiogenesis in Rheumatoid Arthritis Disease.* Front Immunol, 2021. **12**: p. 737990.
305. Niaudet, C., et al., *Adgrf5 contributes to patterning of the endothelial deep layer in retina.* Angiogenesis, 2019. **22**(4): p. 491-505.
306. Lee, Y.S., et al., *Fatty acid-binding protein 4 regulates fatty infiltration after rotator cuff tear by hypoxia-inducible factor 1 in mice.* J Cachexia Sarcopenia Muscle, 2017. **8**(5): p. 839-850.
307. Chen, Y., et al., *The role of CEMIP in tumors: An update based on cellular and molecular insights.* Biomed Pharmacother, 2022. **146**: p. 112504.
308. Hernandez-Carretero, A., et al., *Cysteine- and glycine-rich protein 3 regulates glucose homeostasis in skeletal muscle.* Am J Physiol Endocrinol Metab, 2018. **315**(2): p. E267-E278.
309. Rossi, D., et al., *A novel FLNC frameshift and an OBSCN variant in a family with distal muscular dystrophy.* PLoS One, 2017. **12**(10): p. e0186642.
310. Lee, H., et al., *A Phosphoproteomic Screen Identifies a Guanine Nucleotide Exchange Factor for Rab3A Protein as a Mitogen-activated Protein (MAP) Kinase Phosphatase-5-regulated MAP Kinase Target in Interleukin 6 (IL-6) Secretion and Myogenesis.* J Biol Chem, 2017. **292**(9): p. 3581-3590.
311. Luo, H.R., et al., *GRAB: a physiologic guanine nucleotide exchange factor for Rab3A, which interacts with inositol hexakisphosphate kinase.* Neuron, 2001. **31**(3): p. 439-51.
312. Gioftsidi, S., F. Relaix, and P. Mourikis, *The Notch signaling network in muscle stem cells during development, homeostasis, and disease.* Skelet Muscle, 2022. **12**(1): p. 9.
313. Meadows, E., et al., *Myogenin regulates a distinct genetic program in adult muscle stem cells.* Dev Biol, 2008. **322**(2): p. 406-14.
314. Peng, Y., et al., *Mechano-signaling via Piezo1 prevents activation and p53-mediated senescence of muscle stem cells.* Redox Biol, 2022. **52**: p. 102309.
315. Pradhan, B.S. and T.J. Prószyński, *A Role for Caveolin-3 in the Pathogenesis of Muscular Dystrophies.* Int J Mol Sci, 2020. **21**(22).
316. Posey, A.D., et al., *EHD1 mediates vesicle trafficking required for normal muscle growth and transverse tubule development.* Dev Biol, 2014. **387**(2): p. 179-90.
317. Safi, A., et al., *Role for the pleckstrin homology domain-containing protein CKIP-1 in phosphatidylinositol 3-kinase-regulated muscle differentiation.* Mol Cell Biol, 2004. **24**(3): p. 1245-55.
318. Hawke, T.J. and D.J. Garry, *Myogenic satellite cells: physiology to molecular biology.* J Appl Physiol (1985), 2001. **91**(2): p. 534-51.
319. Luo, Y. and M. Liu, *Adiponectin: a versatile player of innate immunity.* J Mol Cell Biol, 2016. **8**(2): p. 120-8.
320. Ouchi, N., et al., *Obesity, adiponectin and vascular inflammatory disease.* Curr Opin Lipidol, 2003. **14**(6): p. 561-6.
321. Pischon, T., et al., *Plasma adiponectin levels and risk of myocardial infarction in men.* JAMA, 2004. **291**(14): p. 1730-7.
322. Gil-Campos, M., R.R. Cañete, and A. Gil, *Adiponectin, the missing link in insulin resistance and obesity.* Clin Nutr, 2004. **23**(5): p. 963-74.
323. Scala, P., et al., *Stem Cell and Macrophage Roles in Skeletal Muscle Regenerative Medicine.* Int J Mol Sci, 2021. **22**(19).
324. Yamaguchi, N., et al., *Adiponectin inhibits Toll-like receptor family-induced signaling.* FEBS Lett, 2005. **579**(30): p. 6821-6.

325. Hui, X., et al., *Adiponectin Enhances Cold-Induced Browning of Subcutaneous Adipose Tissue via Promoting M2 Macrophage Proliferation.* Cell Metab, 2015. **22**(2): p. 279-90.
326. Mandal, P., et al., *Molecular mechanism for adiponectin-dependent M2 macrophage polarization: link between the metabolic and innate immune activity of full-length adiponectin.* J Biol Chem, 2011. **286**(15): p. 13460-9.
327. Yang, W. and P. Hu, *Skeletal muscle regeneration is modulated by inflammation.* J Orthop Translat, 2018. **13**: p. 25-32.
328. Saclier, M., et al., *Differentially activated macrophages orchestrate myogenic precursor cell fate during human skeletal muscle regeneration.* Stem Cells, 2013. **31**(2): p. 384-96.
329. Liu, S., et al., *Adiponectin receptors activation performs dual effects on regulating myogenesis and adipogenesis of young and aged muscle satellite cells.* Cell Prolif, 2023. **56**(3): p. e13370.
330. Liu, Y., et al., *Functional significance of skeletal muscle adiponectin production, changes in animal models of obesity and diabetes, and regulation by rosiglitazone treatment.* Am J Physiol Endocrinol Metab, 2009. **297**(3): p. E657-64.
331. Leary, S.C., et al., *Interactions between bioenergetics and mitochondrial biogenesis.* Biochim Biophys Acta, 1998. **1365**(3): p. 522-30.
332. Remels, A.H., et al., *Regulation of mitochondrial biogenesis during myogenesis.* Mol Cell Endocrinol, 2010. **315**(1-2): p. 113-20.
333. Iwabu, M., et al., *Adiponectin and AdipoR1 regulate PGC-1alpha and mitochondria by Ca(2+) and AMPK/SIRT1.* Nature, 2010. **464**(7293): p. 1313-9.
334. Rochard, P., et al., *Mitochondrial activity is involved in the regulation of myoblast differentiation through myogenin expression and activity of myogenic factors.* J Biol Chem, 2000. **275**(4): p. 2733-44.
335. Dillon, L.M., A.P. Rebelo, and C.T. Moraes, *The role of PGC-1 coactivators in aging skeletal muscle and heart.* IUBMB Life, 2012. **64**(3): p. 231-41.
336. Shintaku, J., et al., *MyoD Regulates Skeletal Muscle Oxidative Metabolism Cooperatively with Alternative NF-κB.* Cell Rep, 2016. **17**(2): p. 514-526.
337. St-Pierre, J., et al., *Bioenergetic analysis of peroxisome proliferator-activated receptor gamma coactivators 1alpha and 1beta (PGC-1alpha and PGC-1beta) in muscle cells.* J Biol Chem, 2003. **278**(29): p. 26597-603.
338. Arany, Z., et al., *The transcriptional coactivator PGC-1beta drives the formation of oxidative type IIX fibers in skeletal muscle.* Cell Metab, 2007. **5**(1): p. 35-46.
339. Patková, J., M. Anděl, and J. Trnka, *Palmitate-induced cell death and mitochondrial respiratory dysfunction in myoblasts are not prevented by mitochondria-targeted antioxidants.* Cell Physiol Biochem, 2014. **33**(5): p. 1439-51.
340. Coll, T., et al., *Oleate reverses palmitate-induced insulin resistance and inflammation in skeletal muscle cells.* J Biol Chem, 2008. **283**(17): p. 11107-16.
341. Hirabara, S.M., R. Curi, and P. Maechler, *Saturated fatty acid-induced insulin resistance is associated with mitochondrial dysfunction in skeletal muscle cells.* J Cell Physiol, 2010. **222**(1): p. 187-94.
342. Gottardi, C.J. and B.M. Gumbiner, *Adhesion signaling: how beta-catenin interacts with its partners.* Curr Biol, 2001. **11**(19): p. R792-4.

343. Cossu, G., et al., *Activation of different myogenic pathways: myf-5 is induced by the neural tube and MyoD by the dorsal ectoderm in mouse paraxial mesoderm.* Development, 1996. **122**(2): p. 429-37.
344. Rochat, A., et al., *Insulin and wnt1 pathways cooperate to induce reserve cell activation in differentiation and myotube hypertrophy.* Mol Biol Cell, 2004. **15**(10): p. 4544-55.
345. Pan, W., et al., *Beta-catenin regulates myogenesis by relieving I-mfa-mediated suppression of myogenic regulatory factors in P19 cells.* Proc Natl Acad Sci U S A, 2005. **102**(48): p. 17378-83.
346. Otto, A., et al., *Canonical Wnt signalling induces satellite-cell proliferation during adult skeletal muscle regeneration.* J Cell Sci, 2008. **121**(Pt 17): p. 2939-50.
347. Hart, M., et al., *The F-box protein beta-TrCP associates with phosphorylated beta-catenin and regulates its activity in the cell.* Curr Biol, 1999. **9**(4): p. 207-10.
348. Cavallo, R.A., et al., *Drosophila Tcf and Groucho interact to repress Wingless signalling activity.* Nature, 1998. **395**(6702): p. 604-8.
349. Korinek, V., et al., *Constitutive transcriptional activation by a beta-catenin-Tcf complex in APC-/- colon carcinoma.* Science, 1997. **275**(5307): p. 1784-7.
350. Morin, P.J., et al., *Activation of beta-catenin-Tcf signaling in colon cancer by mutations in beta-catenin or APC.* Science, 1997. **275**(5307): p. 1787-90.
351. Rubinfeld, B., et al., *Stabilization of beta-catenin by genetic defects in melanoma cell lines.* Science, 1997. **275**(5307): p. 1790-2.
352. Miller, J.R. and R.T. Moon, *Signal transduction through beta-catenin and specification of cell fate during embryogenesis.* Genes Dev, 1996. **10**(20): p. 2527-39.
353. Staal, F.J., et al., *Wnt signals are transmitted through N-terminally dephosphorylated beta-catenin.* EMBO Rep, 2002. **3**(1): p. 63-8.
354. van Noort, M., et al., *Wnt signaling controls the phosphorylation status of beta-catenin.* J Biol Chem, 2002. **277**(20): p. 17901-5.
355. Hendriksen, J., et al., *Plasma membrane recruitment of dephosphorylated beta-catenin upon activation of the Wnt pathway.* J Cell Sci, 2008. **121**(11): p. 1793-802.
356. Kuch, C., et al., *M-Cadherin-Mediated Cell Adhesion and Complex Formation with the Catenins in Myogenic Mouse Cells.* Experimental Cell Research, 1997. **232**(2): p. 331-338.
357. Wang, Y., et al., *M-cadherin-inhibited phosphorylation of ß-catenin augments differentiation of mouse myoblasts.* Cell and tissue research, 2013. **351**(1): p. 183-200.
358. Vestal, D. and B. Ranscht, *Glycosyl phosphatidylinositol - anchored t-cadherin mediates calcium-dependent, homophilic cell adhesion.* The Journal of Cell Biology, 1992. **119**(2): p. 451-461.
359. Takeichi, M. and S. Nakagawa, *Cadherin-dependent cell-cell adhesion.* Current Protocols In Cell Biology, 2001.
360. Philippova, M., et al., *T-cadherin and signal-transducing molecules co-localize in caveolin-rich membrane domains of vascular smooth muscle cells.* FEBS Letters, 1998. **429**(2): p. 207-210.
361. Bordier, C., *Phase separation of integral membrane proteins in Triton X-114 solution.* J Biol Chem, 1981. **256**(4): p. 1604-7.
362. Alam, M.S., *Proximity Ligation Assay (PLA).* Curr Protoc Immunol, 2018. **123**(1): p. e58.

363. Ito, R., et al., *Activation of adiponectin receptors has negative impact on muscle mass in C2C12 myotubes and fast-type mouse skeletal muscle.* PLoS One, 2018. **13**(10): p. e0205645.
364. Dort, J., et al., *Macrophages Are Key Regulators of Stem Cells during Skeletal Muscle Regeneration and Diseases.* Stem Cells Int, 2019. **2019**: p. 4761427.
365. Kaufmann, U., et al., *The M-cadherin catenin complex interacts with microtubules in skeletal muscle cells- implications for the fusion of myoblasts.* Journal of Cell Science, 1999. **112**: p. 55-67.
366. Grabowska, I., et al., *Comparison of satellite cell-derived myoblasts and C2C12 differentiation in two- and three-dimensional cultures: changes in adhesion protein expression.* Cell Biol Int, 2011. **35**(2): p. 125-33.

9 Appendices

9.1 Appendix One – Published Literature Review

The following pages include the complete literature review published in Biochemica et Biophyscia Acta (BBA) in 2021, featured in Chapter 1, section 1.6.

BBA - Molecular Cell Research 1869 (2022) 119170

Contents lists available at ScienceDirect

BBA - Molecular Cell Research

journal homepage: www.elsevier.com/locate/bbamcr

Review

Cell adhesion an important determinant of myogenesis and satellite cell activity

Lauren Taylor [a], Miriam Wankell [a], Pankaj Saxena [b,c], Craig McFarlane [a,*,1], Lionel Hebbard [a,d,*,1]

[a] Department of Molecular and Cell Biology, College of Public Health, Medical and Veterinary Sciences, Centre for Molecular Therapeutics, Centre for Tropical Bioinformatics and Molecular Biology, Australian Institute of Tropical Medicine and Health, James Cook University, Townsville, Queensland, Australia
[b] Department of Cardiothoracic Surgery, The Townsville University Hospital, Townsville, Queensland, Australia
[c] College of Medicine, Dentistry, James Cook University, Townsville, Queensland, Australia
[d] Storr Liver Centre, Westmead Institute for Medical Research, Westmead Hospital and University of Sydney, Sydney, New South Wales, Australia

ARTICLE INFO

Keywords:
Myogenesis
Cell adhesion molecules
Satellite cells

ABSTRACT

Skeletal muscles represent a complex and highly organised tissue responsible for all voluntary body movements. Developed through an intricate and tightly controlled process known as myogenesis, muscles form early in development and are maintained throughout life. Due to the constant stresses that muscles are subjected to, skeletal muscles maintain a complex course of regeneration to both replace and repair damaged myofibers and to form new functional myofibers. This process, made possible by a pool of resident muscle stem cells, termed satellite cells, and controlled by an array of transcription factors, is additionally reliant on a diverse range of cell adhesion molecules and the numerous signaling cascades that they initiate. This article will review the literature surrounding adhesion molecules and their roles in skeletal muscle myogenesis and repair.

1. Introduction

The largest tissue type in the human body is the skeletal muscles. They make up approximately 40% of the total body weight and are responsible for imparting strength, stability and support to facilitate voluntary movement. Skeletal muscle development, or myogenesis, begins early during embryonic development and is made possible through the formation, growth, differentiation and fusion of committed myogenic progenitor cells present in the myotome compartment of somites [1,2]. Myogenesis is tightly controlled by a group of transcription factors known as myogenic regulatory factors (MRFs), which regulate myogenic commitment, muscle cell (myoblast) proliferation, fusion and eventual differentiation of myoblasts into multinucleated myotubes [3]. The MRF myogenic regulatory factor-5 (Myf5), which is initially expressed in the somite, together with myogenic determination factor (MyoD), commit cells to adopt a myogenic fate [4]. These MRFs act in concert with one another and can be overexpressed to compensate for each other in knockout cells and in mice [5,6]. Following the formation of a pool of myogenic progenitor cells, these cells give rise to myoblasts, or skeletal muscle cells, which during primary myogenesis differentiate and fuse together to form multinucleated myotubes. Myoblast fusion requires cell movement, the apposition of membranes and reorganisation of the cytoskeleton to form fusion pores and ultimately the merging of membranes. Recent research has shown critical roles for two muscle proteins, Myomaker and Myomixer in myoblast fusion, and a contemporary review has been published [7–9]. During secondary myogenesis, mononucleated myoblasts align along these primary myotubes, and through further fusion form secondary myotubes [10]. This fusion process, otherwise referred to as myogenic differentiation, is controlled by the expression of additional MRFs, known as myogenin and MRF-4 (muscle specific regulatory factor-4) [1,11].

Importantly, skeletal muscles are able to maintain their mass postnatally, and even build upon it, thanks to a resident population of muscle specific stem cells, termed satellite cells (SCs), that reside between the sarcolemma and basal lamina of muscle fibres [12,13]. SCs originate in the somites, similar to the precursor myoblasts, but adopt a quiescent state beneath the basal lamina [14]. However, in response to muscle injury or damage, SCs are able to activate, re-enter the cell cycle, and

* Corresponding authors at: Department of Molecular & Cell Biology, College of Public Health, Medical and Veterinary Sciences, James Cook University, 1 James Cook Drive, Townsville, QLD 4811, Australia.
E-mail addresses: craig.mcfarlane@jcu.edu.au (C. McFarlane), lionel.hebbard@jcu.edu.au (L. Hebbard).
[1] Equal corresponding authors.

https://doi.org/10.1016/j.bbamcr.2021.119170
Received 5 September 2021; Received in revised form 18 October 2021; Accepted 1 November 2021
Available online 8 November 2021

undertake myogenesis similar to what is observed during embryonic growth, fuse to form new multinucleated myotubes, and facilitate the replacement of damaged or defective muscle fibres. Consistent with their stem cell nature, sub-populations of SCs are then able to return to a quiescent state and have the ability to self-renew, so as to maintain their population throughout adult life [15].

Given the importance of SCs in maintaining skeletal muscle mass, any defects in SC function, and the associated regenerative processes of skeletal muscle can have detrimental downstream consequences on human health. Most notably, reduced SC numbers and defective SC function has been linked to the loss of muscle mass and impaired muscle function associated with chronic diseases, including type 2 diabetes and sarcopenia [16,17]. Recent evidence suggests that specific cell adhesion molecules (CAMs), including the calcium-dependent cadherins M-cadherin and N-cadherin, have pivotal roles in maintaining SC quiescence and activation [18,19], which suggests CAMs may have roles in muscle disease. Hence, the role of CAMs in skeletal muscle myogenesis is of particular interest to the field, with a better understanding of these complex processes providing a potential avenue for developing therapeutic approaches for improving muscle growth and chronic disease outcomes. Thus, this review will consider myogenic CAMs and will discuss their known function in skeletal muscle growth and maintenance, and highlight potential avenues for further research.

2. Cell adhesion molecules (CAMs)

The formation of myofibers during development not only depends on the complex expression of myogenic transcription factors, but also on the select expression of adhesion molecules. CAMs are proteins, located on the cell surface, that are involved in binding cells to one another or to the extracellular matrix (ECM). CAMs have diverse functions within the body and are not only important for adhesion but also for signaling in development, proliferation and in cancer progression. CAMs are often divided into four superfamilies: the immunoglobulin superfamily of adhesion molecules (IgCAMs), cadherins, integrins and selectins. The various groups of CAMs and their role in myogenesis will now be considered. Selectins are typically responsible for binding carbohydrates and are important for leukocyte trafficking to expose leukocytes to signaling molecules [20]. Although studies have revealed potential roles for selectins in facilitating skeletal muscle regeneration [21], selectins have not been shown to play a major role in myogenesis, as such will not be discussed in this review. The remaining groups of CAMs and their role in myogenesis will now be considered.

2.1. Integrins

Integrins are a family of cell adhesion molecules that are responsible for both cell-cell and cell-matrix interactions as well as acting as receptors for extracellular ligands and binding to the cytoskeleton. As these proteins are the principal tools used for binding and communicating with the ECM, they are abundantly present on the cell surface. These heterodimeric glycoproteins consist of noncovalently bound α and β subunits; forming up to 24 unique integrins based on the varying complexity of the subunits [22–24]. Integrins influence cell behaviour as bi-directional cell signaling molecules. In the resting state they exist in a bent-over inactive conformation and become activated through the binding of agonists such as chemokines and growth factors to G-protein receptors, and extracellular force. This in turn leads to molecules such as paxillin, talin and kindlin binding to the β subunit to promote an open and activated integrin, allowing binding to ECM components (collagen, laminin, fibronectin). Subsequently, this promotes integrin clustering and the recruitment of signaling molecules including, integrin linked tyrosine (ILK) and focal adhesion kinases (FAK), and the modulation of downstream signaling including Akt, extracellular signal-related kinase (ERK), Rho guanine nucleotide binding proteins (Rho GTPases) and mammalian target of rapamycin (mTOR). The nature of signaling is dependent on the integrin, cell type and ECM. During developmental myogenesis specific integrins are expressed and their presence coincides with that of their extracellular ligands laminin and fibronectin [25,26].

The dystrophin-glycoprotein complex (DGC) and integrin α7β1, serve as the two primary laminin receptors in skeletal muscle, binding the muscle fibres to the basal lamina [27,28]. Mutations in nearly all the DGC associated proteins result in skeletal muscle pathologies; with mutations in the major DGC protein, dystrophin, resulting in Duchenne and Becker muscle dystrophies (DMD and BMD), and in dystroglycans and sarcoglycans associating with a wide range of limb-girdle muscular dystrophies and other pathological changes [29]. Integrin α7 was postulated to play a major role in secondary myogenesis due to observations that α7 and its ligand laminin are expressed on primary myotubes following primary myogenesis [30]. In this regard, patients with congenital myopathy were observed to possess a mutated α7 gene, and this was supported by experiments showing that α7 null mice develop mild muscular dystrophy [31,32]. Significantly, endogenous α7β1 integrin mRNA and protein, is upregulated in DMD patients and in *mdx* mice (a mouse model of human DMD), and was suggested to be a compensatory action between the two laminin ligands [33,34]. In agreement, the over-expression of α7β1 in *mdx/utr*$^{-/-}$ mice that lack both dystrophin and utrophin, led to an extension in life, a reduction in muscular dystrophy pathology and an increase in satellite cell number [33,35]. These data suggested that α7 was protective, and as a consequence double knock-out mice lacking both α7 and dystrophin (*mdx* mice) had a much more severe and progressive muscular dystrophy than that observed in mice with the individual loss of each gene alone [36]. Together, these reports suggested that the re-expression of α7 could be a therapeutic strategy for treatment of DMD patients. Subsequent studies using adeno-associated virus (AAV) delivery methods in *mdx* and *mdx/utr*$^{-/-}$ mice resulted in improved muscle fibre size and lifespan [37,38]. Further studies using the small molecule SU9516 reduced the phosphorylation of pro-inflammatory p65-nuclear factor-κβ (NF-κβ) and activity of Ste20-related proline alanine rich kinase (SPAK) and oxidative stress response 1 (OSR1) kinase pathways, promoted α7β1 expression in myogenic cell lines, and reduced disease progression in *mdx* mice [39]. As a consequence, therapies targeting α7 could be an avenue to treat muscular dystrophies.

β1 integrin itself appears to be essential for the development of myofibers, as defects in myoblast fusion, observed through the accumulation of unfused cells and the formation of short muscle fibres, are observed in *in vitro* studies and in mice with muscle-specific inactivation of the β1 integrin. Importantly, the muscle-specific inactivation of the integrin β1 gene in mice leads to death at birth with non-inflated lungs, and poorly developed muscle fibres [40,41]. At the signaling level β1 can interact with transmembrane 182 (TMEM182) to regulate FAK, ERK and Akt myogenic signaling, and additionally co-operate with fibroblast growth factor (FGF) signaling to maintain SC proliferation and renewal [42,43]. Another β integrin, β3 has been found to be transiently expressed in activated SCs during mouse muscle regeneration, mediates myogenic gene expression and SC migration, and β3 integrin gene absence *in vivo* leads to impaired muscle regeneration. Mechanistically, it was found that β3 is required for maintaining Rac1 GTPase activity (a Rho GTPase family member), myogenic gene expression and focal adhesion complexes in differentiating myoblasts [44].

In addition to α7β1, *in vitro* studies in rodent and avian cells indicate that integrins α4β1, α4β7 and α5β1 which bind fibronectin, and α6β1 and laminin, respectively, may also play a role in cell adhesion and communication during skeletal muscle myogenesis. The α4 integrins, found on multinucleated myotubes, were as well thought to be of importance during secondary myogenesis through interactions with a counter receptor, vascular cell adhesion protein-1 (VCAM-1), found on the proliferating myoblasts [45]. However chimeric mice with a high percentage of α4-deficient embryonic stem cells developed normal muscle and displayed uninhibited myotube formation *in vitro* [46]. The exact role for α5β1 in muscle development is poorly understood,

notwithstanding studies have shown that α5 absence in chimeric mice results in changes in muscle structure resembling muscular dystrophy [47]. The loss of α6 in mice does not lead to a muscle phenotype [48]. However *in vitro* studies inhibiting α6 have presented unexpected results, as blocking antibodies and siRNA treatment limited differentiation of porcine primary muscle cells, whereas treatment with blocking antibodies in murine explants activated the myogenic programme in dermomyotomal cells [49,50]. These data suggest that α6β1 may have alternate functions during distinct myogenic stages.

3. Immunoglobulin superfamily of adhesion molecules

The cell adhesion molecules of the IgCAM family function in diverse cell types and are involved in a variety of biological processes. This family includes the neural cell adhesion molecule (NCAM), vascular adhesion protein-1 (VCAM-1), CAM-related/down-regulated by oncogenes (CDO), brother of CDO (BOC) and neogenin.

3.1. NCAM

NCAM was the first IgCAM implicated in myogenesis in the somites and the myotome compartment during development [51]. *In vitro* overexpression studies in murine C2C12 myoblasts, revealed that increased NCAM enhances myoblast fusion [52,53]. Further studies have revealed that myoblasts express transmembrane isoforms of NCAM, that then switch to an alternate GPI-anchored form in myotubes, which is suggested to be essential for the fusion of myoblasts to myotubes [51,54,55]. Additionally, NCAM is found expressed on both quiescent and activated satellite cells from the proliferative stages through to fusion, which suggest a role for NCAM in postnatal myogenesis [56,57]. Despite these studies, NCAM null mice do not have any apparent defects in skeletal muscle development, and NCAM knock-out primary myoblasts differentiate *in vitro* at the same rate as wild-type cells, suggesting that other cell adhesion molecules can compensate for NCAM loss [58].

3.2. VCAM-1

VCAM-1 is expressed by proliferating myoblasts and on SCs and has a high affinity for integrin α4β1 (also known as VLA-4), which is present on the surface of multinucleated myofibers [45]. The inhibition of VCAM-1, or its ligands, in C2C12 cells, results in a reduced number of nuclei within the myotubes, when compared to controls, suggesting an inhibition of myoblast fusion [59]. The selective deletion of VCAM-1 from SCs in mice, during regeneration resulted in SCs with premature lineage progression to a more differentiated state, a robust influx of immune cells expressing integrin α4β and apoptosis, leading to a transient delay in myofiber growth. However, 30 days post-injury no defects were noted in myofiber cross-sectional area, suggesting that VCAM-1 is not required at later stages of regeneration, or that perhaps there is compensation by other cell-cell adhesion molecules. Interestingly, in uninjured VCAM-1 null mice, the basal fusion of the SCs was reduced, and this corresponded with reduced myofiber cross-sectional area [60]. Taken together, these reports suggest that the role of VCAM in myogenesis and myofiber growth is contingent on the inflammatory state of the SC niche.

3.3. CDO

CAM-related/down-regulated by oncogenes (CDO), also known as CDON, is a further member of the Ig/FNIII (Fibronectin type III) family of cell surface receptors and possesses five Ig-like domains, with three FNIII like repeats in the extracellular region, a transmembrane domain and a cytoplasmic tail [61]. CDO is initially expressed in the central nervous system as early as E7.5, however expression is also seen in the skeletal muscle precursors, but is absent in the adult muscle [62,63]. CDO exhibits a promyogenic role *in vivo* and *in vitro* and appears to be an integral component of the link between the cell surface and nuclear transcription factors, that positively regulates myogenic differentiation. In this manner, CDO overexpression enhances differentiation and the expression of muscle-specific proteins, while the expression of anti-sense CDO limits myotube formation [63]. Moreover, CDO null mice show delayed muscle development, and knock-out primary myoblasts derived from the CDO null mice display defective differentiation in culture [64]. Mechanistically, CDO, through interactions with promyogenic cadherins, N-cadherin and M-cadherin, positively regulate the differentiation of myogenic cell lines by post-translationally activating MyoD [65]. Further intricate studies illustrated that CDO can complex to the scaffold proteins JLP (JNK-associated leucine zipper protein) and Bnip-2 (BCL2/adenovirus E1B 19 kDa protein-interacting protein 2), and the adaptor protein APPL1 (adaptor protein containing PH [pleckstrin homology]) domain, PTB [phosphotyrosine binding] domain, and leucine zipper motif to respectively activate p38 mitogen activated protein kinase (p38MAPK) and Akt, two key myogenic signaling pathways [66,67]. Studies by the same group then found that TGF-β-activated kinase 1 (TAK1) and apoptosis signal-regulating kinase 1 (ASK1) interacted with CDO to promote myogenesis through activation of p38MAPK [68]. Further placing CDO in an influential position in myogenesis, recent data shows that the specific deletion of CDO from muscle SCs impairs muscle regeneration, fibroblast growth factor (FGF) and integrin signaling. Specifically, the loss of CDO in SCs resulted in impaired muscle regeneration and increased fibrotic deposition. Further analysis showed that CDO loss decreased β1-integrin expression, reduced extracellular signal-regulated kinase (ERK) levels, and impaired SC response to FGF, resulting in reduced proliferation and self-renewal capacity of SCs [69].

3.4. BOC

Brother of CDO (BOC), is an additional member of the Ig/FNIII family of receptor proteins and has four Ig repeats and three FNIII structures in its ectodomain. The expression of BOC during both embryonic development and in C2C12 myoblasts overlap significantly with CDO [70,71]. Immunoprecipitation studies show strong binding between CDO and BOC and shows that the two CAMs function together as components of an adhesion complex that acts to regulate myogenic differentiation [70]. Notably, oncogenic forms of Ras, a family of GTPases that act as crucial members of a signaling network controlling cell cycle growth, migration and apoptosis, can block differentiation in C2C12 cells through transcriptional downregulation of MyoD, myogenin, CDO and BOC. Significantly, the forced re-expression of either CDO or BOC in Ras expressing C2C12 cells leads to the induction of endogenous MyoD and myogenin, and thus myogenesis [70]. Moreover, it was observed that the forced expression of BOC or CDO in the human rhabdomyosarcoma cell line RD promoted muscle-cell like differentiation [72]. Together, these data suggest a positive link for BOC and CDO between the cell surface and MRFs.

3.5. Neogenin

Neogenin is a multifunctional transmembrane receptor that is a part of the immunoglobulin superfamily and is composed of an extracellular domain containing four Ig-like loops and six FNIII repeats, a transmembrane region and a cytoplasmic tail. As a homologue of DCC (deleted in colorectal cancer), the primary function of neogenin was predicted to be similar to DCC to facilitate axon guidance through the binding of netrins, which represent a small family of laminin-related proteins, that associate with cell membranes and the ECM [73,74]. In C2C12 cells, neogenin overexpression enhanced myotube formation by promoting myoblast differentiation [75]. Subsequent studies revealed that despite normal myotome development, neogenin-null mice display smaller myofibers at E18.5 and postnatally from 3 weeks of age [76].

Mechanistically, it was found that neogenin can complex with CDO, and bind Netrin-3, a laminin related protein, which *via* CDO stimulated the Nuclear factor of activated T-cells (NFAT) pathway, to regulate muscle differentiation [75,77]. An interesting aspect of the binding of netrin and neogenin on myoblasts, is that it does not lead to alterations in muscle-specific gene products, including MyoD, myogenin, and MHC, suggesting an alternative pro-myogenic mechanism is in play.

4. Cadherins

Cadherins exist in multiple tissue-specific isoforms and promote both homophilic (binding between cells of the same type) and heterophilic (binding between cells of different types) interactions. Cadherins typically express a C-terminal cytoplasmic domain, a transmembrane domain, and an N-terminal variable extracellular domain, often used to classify the cadherin into subgroups. Each of these subgroups are responsible for a variety of functions between cells, and by example, the classic cadherins express 5 extracellular domains between which reside three calcium binding sites that are necessary for correct conformation and intercellular binding [78,79]. The binding of calcium brings rigidity to the ectodomain so that it adopts a crescent shape necessary for bonding between adjacent cells [80]. Cadherins are primarily located at adherens junctions, which are protein structures along the plasma membrane that mediate adhesion between cells [81]. The cadherins facilitate adhesion through the formation of trans bonds between the N-terminal β-strands of the EC1 domains, bridging the intermembrane space through their ectodomains [82,83]. Furthermore, cadherins, along with conferring adhesion between cells, are essential for intracellular and intercellular signaling and communication, which is achieved through the interaction of their cytoplasmic tails with catenin proteins [84].

The most abundant cadherins in skeletal muscle are muscle (M-), neuronal (N-), retinal (R-), and truncated (T-) cadherins [85–88]. M- and N-cadherin are best described in myogenesis, and cadherin control of the Rho family of guanine triphosphate hydrolases (GTPases) has been studied due to the dependence of fusion on the recognition, adherence and alignment between myoblasts [89]. Rho is a subgroup of the Ras superfamily of GTPases and are major contributors to morphogenic and migratory properties of cells [90,91]. Through the activation of muscle specific promoters, RhoA is expressed and is crucial for the accumulation of β-catenin at sites of cell-cell contact. Similarly, the GTPases Rac1 and Cdc42 are essential for myoblast fusion *in vivo* and *in vitro*, as their loss impairs muscle formation [92–94].

4.1. N-cadherin

The first cadherin to appear during myogenesis is N-cadherin, where it is expressed in the myotome compartment of somites and in embryonic muscle during development [95]. First described in neurons, N-cadherin plays a significant role in the development of many tissues within the body. N-cadherin signaling, which is important for cell cycle exit, occurs in-part through the regulation of RhoA and Rac1. N-cadherin negatively regulates Rac1 function and increases the activity of RhoA, thereby initiating myogenic progression [94]. N-cadherin is down-regulated in secondary myogenesis during the point in embryonic development where myoblasts switch the expression of their primary adhesion proteins from N- to M- cadherin [96,97]. Due to the vital role N-cadherin plays in heart muscle development, N-cadherin-null mice are embryonically lethal and are unable to be studied [98]. Studies blocking N-cadherin function in C2C12 myoblasts inhibited myogenesis [99,100]. Nevertheless, the subsequent isolation of N-cadherin null myoblasts revealed that their fusion competence was equivalent to wild-type, and suggested that other CAMs could compensate for N-cadherin myogenic function [101]. Despite these findings, subsequent signaling studies found that N-cadherin ligation between opposing myoblasts stimulated CDO-dependent activation of p38MAPK, that in turn promotes muscle differentiation [102]. In sum, these data suggest N-cadherin is a key signaling CAM in myogenesis.

4.2. M-cadherin

M-cadherin is abundantly expressed in the developing skeletal muscle but is downregulated in adult muscle fibres, where it is only found in muscle SCs at low levels [103,104]. M-cadherin expression is activated through the binding of MRFs to transcription sites close to the M-cadherin gene. Initial M-cadherin knockdown studies in muscle cell lines indicated that reduced M-cadherin leads to a reduction in myoblast adhesion and differentiation [105]. Nevertheless, M-cadherin knockout mice have normal muscle development with no obvious defects in growth or repair, suggesting that *in vivo* M-cadherin loss could be compensated by other cadherins like N- and R-cadherin [106]. Subsequent cell biology studies show M-cadherin stabilises β-catenin, and regulates β-catenin/Wnt signaling to promote myogenesis independent of T-cell specific transcription factor/lymphoid enhancer binding factor (TCF/LEF) [107].

Recent studies have shown that CAMs occupy an important role in readying SCs for activation. The study by Goel et al. [18] showed that M- and N-cadherin mediated adhesion between SCs and myofibers is necessary for promoting SC quiescence, while the genetic removal of both M-cadherin and N-cadherin diminishes cell-to-cell binding, leading to partial SC activation, without injury. A contemporary cell biology study has also linked M-cadherin to metabolism, where it was shown that insulin stimulated phosphorylation of β-catenin on Serine 552 was critical for GLUT4 translocation to the cell membrane, and subsequent binding of β-catenin to M-cadherin [108]. These studies suggest a plausible molecular link between insulin resistance and SC activity, *via* the interactions of M-cadherin and β-catenin.

4.3. R-cadherin

Retinal cadherin (R-cadherin) is another classical cadherin, originally discovered in the retina, but is also expressed in the heart, kidney, thymus and on the skeletal muscle [109,110]. R-cadherin is detected in the somites and localises to the cell-cell contacts of primary myoblasts but is diminished in normal adult muscle. Interestingly, R-cadherin is present in rhabdomyosarcomas (RMS), a cancer of the muscle tissue, but is absent in normal myoblasts. Moreover, it has been shown that R-cadherin can promote tumorigenesis in C2C12 myoblasts by inhibiting myogenic induction through impairing cell cycle exit, and promoting cell motility. Furthermore, R-cadherin can upregulate the activity of Rac1, leading to the inhibition of the cell cycle and hence muscle myogenesis, and additionally downregulate M- and N-cadherin function to disrupt muscle development [109,111].

4.4. T-cadherin

In contrast to the classical cadherins, T-cadherin does not express a transmembrane, or cytoplasmic domain, and is instead attached to the cell membrane through a glycosylphosphatidylinositol (GPI) moiety that localises to lipid rafts [88]. Another key difference between T-cadherin and the classical cadherins is that T-cadherin executes homophilic binding through a different mechanism. While classical cadherins bind one another through a strand-swapping mechanism, T-cadherin engages in intracellular recognition through a homophilic interface between the EC1 and EC2 domains – referred to as the X-dimer [112]. T-cadherin is expressed on developing and mature skeletal muscle, but limited studies have been performed to identify the role of this cadherin in skeletal muscle growth. Nonetheless, a recent study considering skeletal muscle regeneration in mice suggests T-cadherin may play a role by acting as a receptor for adiponectin [113]. Here the genetic loss of adiponectin or T-cadherin had no affect muscle regeneration. Muscle regeneration improved only when adiponectin was adenovirally expressed to supra

physiological levels (10- to 30-fold above normal) together with infused angiotensin II to partially mimic muscle aging. Thus, further studies are required to consider T-cadherin's molecular functions in myogenesis and SC activity.

5. The myogenic cell adhesion complex

The many years of study by numerous investigators has led to the development of an elegant model for myogenic cell adhesion molecules in how they communicate and interact with one another to regulate skeletal muscle myogenesis. Some of these molecules have been found to participate in the formation of an integrated promyogenic cell adhesion complex with other CAMs. CDO and BOC form a cis complex through an association of their ectodomains and cytoplasmic tails [114]. Both CDO and BOC can as well bind to cadherins, which can communicate with the cytoplasmic catenins, and importantly, studies indicate that this cadherin interaction is necessary for the promyogenic effects of CDO [115,116]. This cell adhesion complex also interacts with other members of the immunoglobulin superfamily, namely neogenin and netrin [75,114]. Data suggests that neogenin mediates most of its role through selective binding with CDO, which in turn regulates netrin signaling (Fig. 1 and Table 1). These reports indicate that there is a promyogenic effect associated with the formation of this complex. Nevertheless, there is still much to be understood about how they mediate these effects, and how this complex regulates muscle development, regeneration and SC activation. Moreover, in this light recent research by the Rudnicki group has shown that the DGC plays a necessary role in regulating SCs cell polarity and epigenetic activation of SC commitment. The absence of dystrophin causes a dramatic reduction in asymmetric division, and hence the number of myogenic progenitors to support regeneration [117–119]. Significantly, in regard to the information presented in this review concerning α7β1, VCAM-1, CDO, M- and N-cadherin, it is likely that other CAMs could regulate SCs division and differentiation. These

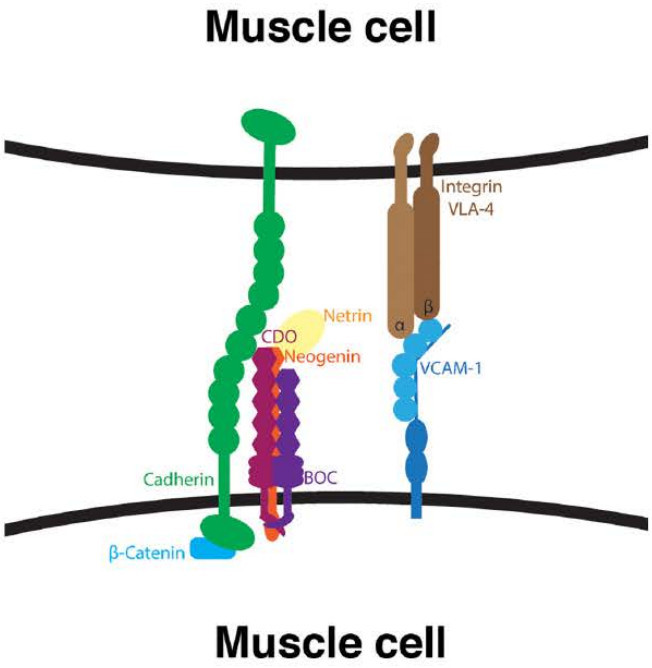

Fig. 1. Cartoon depicting the major cell adhesion molecules in the promyogenic cell adhesion complex. Research from the last 20 years shows the presence and interaction of N- and M-cadherin (green), CDO (rouge), Neogenin (orange), and BOC (purple) in the complex; and neogenin binds netrins. VCAM-1 (blue) and VLA-4 (brown; integrin α4β1) bind independently of the other CAMs. (For interpretation of the references to colour in this figure legend, the reader is referred to the web version of this article.)

Table 1
Lists the major myogenic CAMs, their function and expression.

Family	CAM	Function	Expression	Reference
Integrin	α7β1	Binding of the muscle fibres to the basal lamina to assist adhesion of myoblasts	Myoblasts and myotubes	[28]
	α4β1	Assists secondary myogenesis through adhesion with counter receptor VCAM-1	Myoblasts and myotubes	[24,45]
	α4β7	Assists secondary myogenesis through adhesion with counter receptor VCAM-1	Myoblasts and myotubes	[24,45]
	α5β1	Maintaining a proliferative state, and thus sustaining growth	Myoblasts and myotubes	[24,47]
	α6β1	Helps to facilitate the transition of myoblasts from proliferation to differentiation	Myoblasts and myotubes	[24]
IgCAM	NCAM	Enhances myoblast fusion	Myoblasts, myotubes, and satellite cells	[53]
	VCAM-1	Assists secondary myogenesis through adhesion to integrin subunit alpha 4	Myoblasts and satellite cells	[45]
	CDO	Enhances differentiation	Myoblasts and satellite cells	[64]
	BOC	Enhances differentiation	Myoblasts and satellite cells	[70]
	Neogenin	Enhances differentiation	Myoblasts and myotubes	[64,75]
Cadherins	N-cadherin	Initiates myogenic differentiation through cell cycle exit	Myoblasts and satellite cells	[94]
	M-cadherin	Enhances myoblast adhesion and differentiation	Myoblasts, myotubes and satellite cells	[85]
	R-cadherin	Enhances differentiation through cell cycle exit	Myoblasts	[109]
	T-cadherin	Binds adiponectin, role in myogenesis largely unknown	Myoblasts and myotubes	[88,113]

CAMs and/or their downstream signaling could possibly be used to counter the negative influence of a dysfunctional DGC in muscular dystrophy or muscle wasting diseases and provide a therapeutic approach.

6. Conclusion

In conclusion, cell adhesion molecules play a significant role in the formation and maintenance of skeletal muscle cells. The formation of an intricate 'adhesion complex' at cell-cell contacts throughout muscle development and regeneration signifies the importance of improving our understanding of this process. Publications suggest that SC phenotype and function is regulated through cell adhesion and offer a potential window to develop more cogent therapeutic strategies. Hence CAMs and their downstream signaling could become therapeutic targets to alleviate the effects of dystrophin loss or reduced expression, and to promote SC expansion and differentiation to treat muscle wasting diseases. Better understanding the mechanisms that regulate degeneration, and repair, could play a dynamic role in assisting patients to maintain muscle mass, increasing life expectancy and reducing disease morbidity.

Declaration of competing interest

The authors declare that they have no known competing financial

interests or personal relationships that could have appeared to influence the work reported in this paper.

Acknowledgements

The manuscript was prepared with support from a Townsville Hospital and Health Service (THHS) Study Education and Research Trust Account (SERTA) Research Grant 2021–14 to PS, CM, and LH, and a James Cook University Sandpit to Seed Grant to LH and CM. LT is funded by a James Cook University PhD Scholarship.

References

[1] M. Buckingham, L. Bajard, T. Chang, P. Daubes, J. Hadchouel, S. Meilhac, et al., The formation of skeletal muscle: from somite to limb, J. Anat. 202 (2003) 59–68.
[2] B. Christ, C.P. Ordahl, Early stages of chick somite development, Anat. Embryol. 191 (1995) 381–396.
[3] H.A. Asfour, M.Z. Allouh, R.S. Said, Myogenic regulatory factors: the orchestrators of myogenesis after 30 years of discovery, Exp. Biol. Med. (Maywood) 243 (2018) 118–128.
[4] M.O. Ott, E. Bober, G. Lyons, H. Arnold, M. Buckingham, Early expression of the myogenic regulatory gene, myf-5, in precursor cells of skeletal muscle in the mouse embryo, Development 111 (1991) 1097–1107.
[5] M. Rudnicki, T. Braun, S. Hinuma, R. Jaenisch, Inactivation of MyoD in mice leads to up-regulation of the myogenic HLH gene Myf-5 and results in apparently normal muscle development, Cell 71 (1992) 383–390.
[6] M. Rudnicki, P. Schnegelsberg, R. Stead, T. Braun, H.-H. Arnold, R. Jaenisch, MyoD or Myf-5 is required for the formation of skeletal muscle, Cell 75 (1993) 1351–1359.
[7] B. Chen, W. You, Y. Wang, T. Shan, The regulatory role of myomaker and myomixer-myomerger-minion in muscle development and regeneration, Cell. Mol. Life Sci. 77 (2020) 1551–1569.
[8] D.P. Millay, J.R. O'Rourke, L.B. Sutherland, S. Bezprozvannaya, J.M. Shelton, R. Bassel-Duby, et al., Myomaker is a membrane activator of myoblast fusion and muscle formation, Nature 499 (2013) 301–305.
[9] M.E. Quinn, Q. Goh, M. Kurosaka, D.G. Gamage, M.J. Petrany, V. Prasad, et al., Myomerger induces fusion of non-fusogenic cells and is required for skeletal muscle development, Nat. Commun. 8 (2017) 15665.
[10] M. Zhang, I.S. McLennan, During secondary myotube formation, primary myotubes preferentially absorb new nuclei at their ends, Dev. Dyn. 204 (1995) 168–177.
[11] K. Yun, B. Wold, Skeletal muscle determination and differentiation: story of a core regulatory network and its context, Curr. Opin. Cell Biol. 8 (1996) 877–889.
[12] P. Zammit, F. Relaix, Y. Nagata, A. Ruiz, C. Collins, T. Partridge, et al., Pax7 and myogenic progression in skeletal muscle satellite cells, J. Cell Sci. 119 (2006) 1824–1832.
[13] A. Mauro, Satellite cell of skeletal muscle fibres, J. Cell Biol. 9 (1961) 493.
[14] E. Schultz, M.C. Gibson, T. Champion, Satellite cells are mitotically quiescent in mature mouse muscle: an EM and radioautographic study, J. Exp. Zool. 206 (1978) 451–456.
[15] C.A. Collins, I. Olsen, P.S. Zammit, L. Heslop, A. Petrie, T.A. Partridge, et al., Stem cell function, self-renewal, and behavioral heterogeneity of cells from the adult muscle satellite cell niche, Cell 122 (2005) 289–301.
[16] S.E. Alway, M.J. Myers, J.S. Mohamed, Regulation of satellite cell function in sarcopenia, Front. Aging Neurosci. 6 (2014), 246-246.
[17] Y. Furuichi, Y. Kawabata, M. Aoki, Y. Mita, N.L. Fujii, Y. Manabe, Excess glucose impedes the proliferation of skeletal muscle satellite cells under adherent culture conditions, Front. Cell Dev. Biol. 9 (2021), 640399-640399.
[18] A.J. Goel, M.-K. Rieder, H.-H. Arnold, G.L. Radice, R.S. Krauss, Niche cadherins control the quiescence-to-activation transition in muscle stem cells, Cell Rep. 21 (2017) 2236–2250.
[19] M. Marti, N. Montserrat, C. Pardo, L. Mulero, L. Miquel-Serra, A.M.C. Rodrigues, et al., M-cadherin-mediated intercellular interactions activate satellite cell division, J. Cell Sci. 126 (2013) 5116–5131.
[20] R.P. McEver, Selectins: initiators of leucocyte adhesion and signalling at the vascular wall, Cardiovasc. Res. 107 (2015) 331–339.
[21] W. Baker, B.A.S.P. Schneider, A. Kulkarni, G. Sloan, R. Schaub, J. Sypek, et al., P-selectin inhibition suppresses muscle regeneration following injury, J. Leukoc. Biol. 76 (2004) 352–358.
[22] M.L. Costa, Cytoskeleton and adhesion in myogenesis, ISRN Dev. Biol. 2014 (2014) 1–15.
[23] R.O. Hynes, Integrins: versatility, modulation, and signaling in cell adhesion, Cell (Cambridge) 69 (1992) 11–25.
[24] U. Mayer, Integrins: redundant or important players in skeletal muscle? J. Biol. Chem. 278 (2003) 14587–14590.
[25] C.A. Lowell, T.N. Mayadas, Overview: studying integrins in vivo, Methods Mol. Biol. 757 (2012) 369–397.
[26] S. Thorsteinsdottir, M. Deries, A.S. Cachaco, F. Bajanca, The extracellular matrix dimension of skeletal muscle development, Dev. Biol. 354 (2011) 191–207.
[27] K.P. Campbell, C.J. Leveille, O. Ibraghimov-Beskrovnaya, C.A. Slaughter, J. M. Ervasti, S.W. Sernett, Primary structure of dystrophin-associated glycoproteins linking dystrophin to the extracellular matrix, Nature (London) 355 (1992) 696–702.
[28] W.K. Song, W. Wang, R.F. Foster, D.A. Bielser, S.J. Kaufman, H36-alpha 7 is a novel integrin alpha chain that is developmentally regulated during skeletal myogenesis, J. Cell Biol. 117 (1992) 643–657.
[29] Q.Q. Gao, E.M. McNally, The dystrophin complex: structure, function, and implications for therapy, Compr. Physiol. (2011) 1223–1239.
[30] M. George-Weinstein, R.F. Foster, J.V. Gerhart, S.J. Kaufman, In vitro and in vivo expression α7 integrin and desmin define the primary and secondary myogenic lineages, Dev. Biol. 156 (1993) 209–229.
[31] B.L. Ziober, T. Tsukahara, I. Nonaka, M. Ogawa, K. Arahata, C. Matsuda, et al., Mutations in the integrin α7 gene cause congenital myopathy, Nat. Genet. 19 (1998) 94–97.
[32] U. Mayer, G. Saher, R. Fässler, A. Bornemann, F. Echtermeyer, H. von der Mark, et al., Absence of integrin alpha 7 causes a novel form of muscular dystrophy, Nat. Genet. 17 (1997) 318.
[33] D.J. Burkin, G.Q. Wallace, K.J. Nicol, D.J. Kaufman, S.J. Kaufman, Enhanced expression of the alpha 7 beta 1 integrin reduces muscular dystrophy and restores viability in dystrophic mice, J. Cell Biol. 152 (2001) 1207–1218.
[34] B.L. Hodges, Y.K. Hayashi, I. Nonaka, W. Wang, K. Arahata, S.J. Kaufman, Altered expression of the alpha7beta1 integrin in human and murine muscular dystrophies, J. Cell Sci. 110 (Pt 22) (1997) 2873–2881.
[35] D.J. Burkin, G.Q. Wallace, D.J. Milner, E.J. Chaney, J.A. Mulligan, S.J. Kaufman, Transgenic expression of {alpha}7{beta}1 integrin maintains muscle integrity, increases regenerative capacity, promotes hypertrophy, and reduces cardiomyopathy in dystrophic mice, Am. J. Pathol. 166 (2005) 253–263.
[36] C. Guo, M. Willem, A. Werner, G. Raivich, M. Emerson, L. Neyses, et al., Absence of α7 integrin in dystrophin-deficient mice causes a myopathy similar to duchenne muscular dystrophy, Hum. Mol. Genet. 15 (2006) 989–998.
[37] K.N. Heller, C.L. Montgomery, P.M. Janssen, K.R. Clark, J.R. Mendell, L. R. Rodino-Klapac, AAV-mediated overexpression of human alpha7 integrin leads to histological and functional improvement in dystrophic mice, Mol. Ther. 21 (2013) 520–525.
[38] K.N. Heller, C.L. Montgomery, K.M. Shontz, K.R. Clark, J.R. Mendell, L.R. Rodino-Klapac, Human α7 integrin gene (ITGA7) delivered by adeno-associated virus extends survival of severely affected Dystrophin/Utrophin-deficient mice, Hum. Gene Ther. 26 (2015) 647–656.
[39] A. Sarathy, R.D. Wuebbles, T.M. Fontelonga, A.R. Tarchione, L.A. Mathews Griner, D.J. Heredia, et al., SU9516 increases alpha7beta1 integrin and ameliorates disease progression in the mdx mouse model of duchenne muscular dystrophy, Mol. Ther. 25 (2017) 1395–1407.
[40] A.S. Menko, D. Boettiger, Occupation of the extracellular matrix receptor, integrin, is a control point for myogenic differentiation, Cell (Cambridge) 51 (1987) 51–57.
[41] M. Schwander, M. Leu, M. Stumm, O.M. Dorchies, U.T. Ruegg, J. Schittny, et al., β1 integrins regulate myoblast fusion and sarcomere assembly, Dev. Cell 4 (2003) 673–685.
[42] W. Luo, Z. Lin, J. Chen, G. Chen, S. Zhang, M. Liu, et al., TMEM182 interacts with integrin beta 1 and regulates myoblast differentiation and muscle regeneration, J. Cachexia. Sarcopenia Muscle (2021) (In press).
[43] M. Rozo, L. Li, C.M. Fan, Targeting beta1-integrin signaling enhances regeneration in aged and dystrophic muscle in mice, Nat. Med. 22 (2016) 889–896.
[44] H. Liu, A. Niu, S.E. Chen, Y.P. Li, Beta3-integrin mediates satellite cell differentiation in regenerating mouse muscle, FASEB J. 25 (2011) 1914–1921.
[45] G.D. Rosen, J.R. Sanes, R. LaChance, J.M. Cunningham, J. Roman, D.C. Dean, Roles for the integrin VLA-4 and its counter receptor VCAM-1 in myogenesis, Cell (Cambridge) 69 (1992) 1107–1119.
[46] J.T. Yang, T.A. Rando, W.A. Mohler, H. Rayburn, H.M. Blau, R.O. Hynes, Genetic analysis of alpha 4 integrin functions in the development of mouse skeletal muscle, J. Cell Biol. 135 (1996) 829–835.
[47] D. Taverna, M.H. Disatnik, H. Rayburn, R.T. Bronson, J. Yang, T.A. Rando, et al., Dystrophic muscle in mice chimeric for expression of alpha5 integrin, J. Cell Biol. 143 (1998) 849.
[48] E. Georges-Labouesse, N. Messaddeq, G. Yehia, L. Cadalbert, A. Dierich, M. Le Meur, Absence of integrin alpha 6 leads to epidermolysis bullosa and neonatal death in mice, Nat. Genet. 13 (1996) 370.
[49] K.J. Wilschut, H.T. van Tol, G.J. Arkesteijn, H.P. Haagsman, B.A. Roelen, Alpha 6 integrin is important for myogenic stem cell differentiation, Stem Cell Res. 7 (2011) 112–123.
[50] F. Bajanca, M. Luz, K. Raymond, G.G. Martins, A. Sonnenberg, S. Tajbakhsh, et al., Integrin alpha6beta1-laminin interactions regulate early myotome formation in the mouse embryo, Development 133 (2006) 1635–1644.
[51] G.E. Lyons, R. Moore, O. Yahara, M.E. Buckingham, F.S. Walsh, Expression of ncam isoforms during skeletal myogenesis in the mouse embryo, Dev. Dyn. 194 (1992) 94–104.
[52] G. Dickson, D. Peck, C.H. Barton, F.S. Walsh, S.E. Moore, Enhanced myogenesis in NCAM-transfected mouse myoblasts, Nature 344 (1990) 348–351.
[53] D. Peck, F.S. Walsh, Differential effects of over-expressed neural cell adhesion molecule isoforms on myoblast fusion, J. Cell Biol. 123 (1993) 1587–1595.
[54] A.M. Tassin, R.M. Mege, D. Goudou, G.M. Edelman, F. Rieger, Modulation of expression and cell-surface distribution of n-cam during myogenesis invitro, Neurochem. Int. 18 (1991) 97–106.
[55] S.E. Moore, J. Thompson, V. Kirkness, J.G. Dickson, F.S. Walsh, Skeletal muscle neural cell adhesion molecule (N-CAM): changes in protein and mRNA species during myogenesis of muscle cell lines, J. Cell Biol. 105 (1987) 1377–1386.

[56] A.L. Mackey, M. Kjaer, N. Charifi, J. Henriksson, J. Bojsen-Moller, L. Holm, et al., Assessment of satellite cell number and activity status in human skeletal muscle biopsies, Muscle Nerve 40 (2009) 455–465.
[57] C. O'Reilly, B. McKay, S. Phillips, M. Tarnopolsky, G. Parise, Hepatocyte growth factor (HGF) and the satellite cell response following muscle lengthening contractions in humans, Muscle Nerve 38 (2008) 1434–1442.
[58] C.A. Charlton, W.A. Mohler, H.M. Blau, Neural cell adhesion molecule (NCAM) and myoblast fusion, Dev. Biol. 221 (2000) 112–119.
[59] G.D. Rosen, J.R. Sanes, R. Lachance, J.M. Cunningham, J. Roman, D.C. Dean, Roles for the integrin vla-4 and its counter receptor VCAM-1 in myogenesis, Cell 69 (1992) 1107–1119.
[60] H.-J. Choo, J.P. Canner, K.E. Vest, Z. Thompson, G.K. Pavlath, A tale of two niches: differential functions for VCAM-1 in satellite cells under basal and injured conditions, Am. J. Physiol. Cell Physiol. 313 (2017) C392–C404.
[61] J.-S. Kang, M. Gao, J. Feinleib, P. Cotter, S. Guadagno, R. Krauss, CDO: an oncogene-, serum-, and anchorage-regulated member of the Ig/fibronectin type III repeat family, J. Cell Biol. 138 (1997) 203–213.
[62] P.J. Mulieri, A. Okada, D.A. Sassoon, S.K. McConnell, R.S. Krauss, Developmental expression pattern of the cdo gene, Dev. Dyn. 219 (2000) 40–49.
[63] J.-S. Kang, P.J. Mulieri, C. Miller, D.A. Sassoon, R.S. Krauss, CDO, a robo-related cell surface protein that mediates myogenic differentiation, J. Cell Biol. 143 (1998) 403–413.
[64] F. Cole, W. Zhang, A. Geyra, J.-S. Kang, R.S. Krauss, Positive regulation of myogenic bHLH factors and skeletal muscle development by the cell surface receptor CDO, Dev. Cell 7 (2004) 843–854.
[65] J.-S. Kang, J.L. Feinleib, S. Knox, M.A. Ketteringham, R.S. Krauss, Promyogenic members of the Ig and cadherin families associate to positively regulate differentiation, Proc. Natl. Acad. Sci. 100 (2003) 3989–3994.
[66] G.U. Bae, J.R. Lee, B.G. Kim, J.W. Han, Y.E. Leem, H.J. Lee, et al., Cdo interacts with APPL1 and activates akt in myoblast differentiation, Mol. Biol. Cell 21 (2010) 2399–2411.
[67] E. Perdiguero, V. Ruiz-Bonilla, L. Gresh, L. Hui, E. Ballestar, P. Sousa-Victor, et al., Genetic analysis of p38 MAP kinases in myogenesis: fundamental role of p38alpha in abrogating myoblast proliferation, EMBO J. 26 (2007) 1245.
[68] P. Tran, S.M. Ho, B.G. Kim, T.A. Vuong, Y.E. Leem, G.U. Bae, et al., TGF-beta-activated kinase 1 (TAK1) and apoptosis signal-regulating kinase 1 (ASK1) interact with the promyogenic receptor cdo to promote myogenic differentiation via activation of p38MAPK pathway, J. Biol. Chem. 287 (2012) 11602–11615.
[69] J.H. Bae, M. Hong, H.J. Jeong, H. Kim, S.J. Lee, D. Ryu, et al., Satellite cell-specific ablation of Cdon impairs integrin activation, FGF signalling, and muscle regeneration, J. Cachexia. Sarcopenia Muscle 11 (2020) 1089–1103.
[70] J.-S. Kang, R. Krauss, P. Mulieri, L. Taliana, Y. Hu, BOC, an ig superfamily member, associates with CDO to positively regulate myogenic differentiation, EMBO J. 21 (2002) 114–124.
[71] P.J. Mulieri, J.S. Kang, D.A. Sassoon, R.S. Krauss, Expression of the boc gene during murine embryogenesis, Dev. Dyn. 223 (2002) 379–388.
[72] M. Wegorzewska, R.S. Krauss, J.S. Kang, Overexpression of the immunoglobulin superfamily members CDO and BOC enhances differentiation of the human rhabdomyosarcoma cell line RD, Mol. Carcinog. 37 (2003) 1–4.
[73] J. Round, E. Stein, Netrin signaling leading to directed growth cone steering, Curr. Opin. Neurobiol. 17 (2007) 15–21.
[74] A.B. Huber, A.L. Kolodkin, D.D. Ginty, J.-F. Cloutier, Signaling at the growth cone: ligand-receptor complexes and the control of axon growth and guidance, Annu. Rev. Neurosci. 26 (2003) 509.
[75] J.-S. Kang, M.-J. Yi, W. Zhang, J. Feinleib, F. Cole, R. Krauss, Netrins and neogenin promote myotube formation, J. Cell Biol. 167 (2004) 493–504.
[76] G.-U. Bae, Y.-J. Yang, G. Jiang, M. Hong, H.-J. Lee, M. Tessier-Lavigne, et al., Neogenin regulates skeletal myofiber size and focal adhesion kinase and extracellular signal-regulated kinase activities in vivo and in vitro, Mol. Biol. Cell 20 (2009) 4920–4931.
[77] U. Delling, J. Tureckova, H.W. Lim, L.J. De Windt, P. Rotwein, J.D. Molkentin, A calcineurin-NFATc3-dependent pathway regulates skeletal muscle differentiation and slow myosin heavy-chain expression, Mol. Cell. Biol. 20 (2000) 6600–6611.
[78] K. Tamura, W.S. Shan, W.A. Hendrickson, D.R. Colman, L. Shapiro, Structure-function analysis of cell adhesion by neural (N-) cadherin, Neuron 20 (1998) 1153–1163.
[79] B. Nagar, M. Ikura, J.M. Rini, M. Overduin, Structural basis of calcium-induced E-cadherin rigidification and dimerization, Nature 380 (1996) 360–364.
[80] S.A. Kim, C.-Y. Tai, L.-P. Mok, E.A. Mosser, E.M. Schuman, Calcium-dependent dynamics of cadherin interactions at cell—cell junctions, Proc. Natl. Acad. Sci. U. S. A. 108 (2011) 9857–9862.
[81] H. Tariq, J. Bella, T.A. Jowitt, D.F. Holmes, M. Rouhi, Z. Nie, et al., Cadherin flexibility provides a key difference between desmosomes and adherens junctions, Proc. Natl. Acad. Sci. U. S. A. 112 (2015) 5395–5400.
[82] M. Goodwin, A.S. Yap, Classical cadherin adhesion molecules: coordinating cell adhesion, signaling and the cytoskeleton, J. Mol. Histol. 35 (2004) 839–844.
[83] O.J. Harrison, E.M. Corps, P.J. Kilshaw, Cadherin adhesion depends on a salt bridge at the N-terminus, J. Cell Sci. 118 (2005) 4123–4130.
[84] C. Cifuentes-Diaz, D. Goudou, R.M. Mège, E. Velasco, M. Nicolet, K. Herrenknecht, et al., Distinct location and prevalence of alpha-, beta-catenins and gamma-catenin/plakoglobin in developing and denervated skeletal muscle, Cell Adhes. Commun. 5 (1998) 161.
[85] R. Moore, F. Walsh, The cell adhesion molecule M-cadherin is specifically expressed in developing and regenerating, but not denervated skeletal muscle, Development 117 (1993) 1409–1420.
[86] C.G. Hahn, J. Covault, Neural regulation of N-cadherin gene expression in developing and adult skeletal muscle, J. Neurosci. 12 (1992) 4677–4687.
[87] H. Inuzuka, C. Redies, M. Takeichi, Differential expression of R- and N-cadherin in neural and mesodermal tissues during early chicken development, Development 113 (1991) 959–967.
[88] B. Ranscht, M. Dours-Zimmermann, T-cadherin, a novel cadherin cell adhesion molecule in the nervous sysrem lacks the conserved cytoplasmic region, Neuron 7 (1991) 391–402.
[89] S. Charrasse, M. Causeret, F. Comunale, A. Bonet-Kerrache, C. Gauthier-Rouvière, Rho GTPases and cadherin-based cell adhesion in skeletal muscle development, J. Muscle Res. Cell Motil. 24 (2003) 311–315.
[90] A.B. Jaffe, A. Hall, Rho GTPases: biochemistry and biology, Annu. Rev. Cell Dev. Biol. 21 (2005) 247–269.
[91] P. Aspenström, A. Ruusala, D. Pacholsky, v. Medicinska och farmaceutiska, u. Uppsala, c.m. Medicinska och farmaceutiska vetenskapsområdet, Taking Rho GTPases to the next level: the cellular functions of atypical Rho GTPases, Exp. Cell Res. 313 (2007) 3673–3679.
[92] G. Carnac, M. Primig, M. Kitzmann, P. Chafey, D. Tuil, N. Lamb, et al., RhoA GTPase and serum response factor control selectively the expression of MyoD without affecting Myf5 in mouse myoblasts, Mol. Biol. Cell 9 (1998) 1891–1902.
[93] V. Elena, M. Benedetta, B. Cord, W. Hagen, B. Carmen, N.O. Eric, The small G-proteins Rac1 and Cdc42 are essential for myoblast fusion in the mouse, Proc. Natl. Acad. Sci. 106 (2009) 8935–8940.
[94] S. Charrasse, M. Meriane, F. Comunale, A. Blangy, C. Gauthier-Rouvière, N-cadherin-dependent cell-cell contact regulates rho GTPases and β-catenin localization in mouse C2C12 myoblasts, J. Cell Biol. 158 (2002) 953–965.
[95] J.-L. Duband, S. Dufour, K. Hatta, M. Takeichi, G.M. Edelman, J.P. Thiery, Adhesion molecules during somitogenesis in the avian embryo, J. Cell Biol. 104 (1987) 1361–1374.
[96] C. Cifuentes-Diaz, M. Nicolet, H. Alameddine, D. Goudou, M. Dehaupas, F. Rieger, et al., M-cadherin localization in developing adult and regenerating mouse skeletal muscle: possible involvement in secondary myogenesis, Mech. Dev. 50 (1995) 85–97.
[97] C. Cifuentes-Diaz, M. Nicolet, D. Goudou, F. Rieger, R.Marc Mège, N-cadherin and N-CAM-mediated adhesion in development and regeneration of skeletal muscle, Neuromuscul. Disord. 3 (1993) 361–365.
[98] G.L. Radice, H. Rayburn, H. Matsunami, K.A. Knudsen, M. Takeichi, R.O. Hynes, Developmental defects in mouse embryos lacking N-cadherin, Dev. Biol. 181 (1997) 64–78.
[99] R.M. Mege, D. Goudou, C. Diaz, M. Nicolet, L. Garcia, G. Geraud, et al., N-cadherin and N-CAM in myoblast fusion: compared localisation and effect of blockade by peptides and antibodies, J. Cell Sci. 103 (Pt 4) (1992) 897.
[100] K.A. Knudsen, L. Myers, S.A. McElwee, A role for the ca 2+-dependent adhesion molecule, N-cadherin, in myoblast interaction during myogenesis, Exp. Cell Res. 188 (1990) 175–184.
[101] C.A. Charlton, W.A. Mohler, G.L. Radice, R.O. Hynes, H.M. Blau, Fusion competence of myoblasts rendered genetically null for N-cadherin in culture, J. Cell Biol. 138 (1997) 331–336.
[102] M. Lu, R.S. Krauss, N-cadherin ligation, but not sonic hedgehog binding, initiates cdo-dependent p38alpha/beta MAPK signaling in skeletal myoblasts, Proc. Natl. Acad. Sci. U. S. A. 107 (2010) 4212–4217.
[103] A. Irintchev, M. Zeschnigk, A. Starzinskipowitz, A. Wernig, Expression pattern of m-cadherin in normal, denervated, and regenerating mouse muscles, Dev. Dyn. 199 (1994) 326–337.
[104] M. Donalies, M. Cramer, M. Ringwald, A. Starzinski-Powitz, Expression of M-cadherin, a member of the cadherin multigene family, correlates with differentiation of skeletal muscle cells, Proc. Natl. Acad. Sci. U. S. A. 88 (1991) 8024–8028.
[105] M. Zeschnigk, D. Kozian, C. Kuch, M. Schmoll, A. Starzinski-Powitz, Involvement of M-cadherin in terminal differentiation of skeletal muscle cells, J. Cell Sci. 108 (1995) 2973.
[106] A. Hollnagel, C. Grund, W.W. Franke, H.-H. Arnold, The cell adhesion molecule M-cadherin is not sssential for muscle development and regeneration, Mol. Cell. Biol. 22 (2002) 4760–4770.
[107] Y. Wang, Y. Wang, J.S. Mohamed, J.S. Mohamed, S.E. Alway, S.E. Alway, M-cadherin-inhibited phosphorylation of ß-catenin augments differentiation of mouse myoblasts, Cell Tissue Res. 351 (2013) 183–200.
[108] S.W.C. Masson, B. Sorrenson, P.R. Shepherd, T.L. Merry, Beta-catenin regulates muscle glucose transport via actin remodelling and M-cadherin binding, Mol. Metab. 42 (2020), 101091.
[109] J. Kucharczak, S. Charrasse, F. Comunale, J. Zappulla, B. Robert, I. Teulon-Navarro, et al., R-cadherin expression inhibits myogenesis and induces myoblast transformation via Rac1 GTPase, Cancer Res. 68 (2008) 6559–6568.
[110] K. Niitsuma, M. Hatoko, M. Kuwahara, A. Tanaka, S. Yurugi, H. Iioka, Localization and expression of R-cadherin in skeletal muscle following nerve injury, Eur. Surg. Res. 37 (2005) 79–84.
[111] E. Johnson, C.S. Theisen, K.R. Johnson, M.J. Wheelock, R-cadherin influences cell motility via rho family GTPases, J. Biol. Chem. 279 (2004) 31041–31049.
[112] C. Ciatto, F. Bahna, N. Zampieri, H.C. VanSteenhouse, P.S. Katsamba, G. Ahlsen, et al., T-cadherin structures reveal a novel adhesive binding mechanism, Nat. Struct. Mol. Biol. 17 (2010) 339–347.
[113] Y. Tanaka, S. Kita, H. Nishizawa, S. Fukuda, Y. Fujishima, Y. Obata, et al., Adiponectin promotes muscle regeneration through binding to T-cadherin, Sci. Rep. 9 (2019).

[114] R. Krauss, F. Cole, U. Gaio, G. Takaesu, W. Zhang, J. Kang, Close encounters: regulation of vertebrate skeletal myogenesis by cell-cell contact, J. Cell Sci. 118 (2005) 2355–2362.
[115] R.S. Krauss, Regulation of promyogenic signal transduction by cell-cell contact and adhesion, Exp. Cell Res. 316 (2010) 3042–3049.
[116] J.-S. Kang, J. Feinleib, S. Knox, M. Ketteringham, R. Krauss, Promyogenic members of the ig and cadherin families associate to positively regulate differentiation, Proc. Natl. Acad. Sci. U. S. A. 100 (2003) 3989–3994.
[117] N.C. Chang, M.C. Sincennes, F.P. Chevalier, C.E. Brun, M. Lacaria, J. Segales, et al., The dystrophin glycoprotein complex regulates the epigenetic activation of muscle stem cell commitment, Cell Stem Cell 22 (2018) 755–768 e756.
[118] N.A. Dumont, Y.X. Wang, J. von Maltzahn, A. Pasut, C.F. Bentzinger, C.E. Brun, et al., Dystrophin expression in muscle stem cells regulates their polarity and asymmetric division, Nat. Med. 21 (2015) 1455–1463.
[119] N.C. Chang, F.P. Chevalier, M.A. Rudnicki, Satellite cells in muscular dystrophy - lost in polarity, Trends Mol. Med. 22 (2016) 479–496.

9.2 Appendix Two – Supplementary Figures

The following pages contain supplementary figures for the data featured in chapter 4, section 4.4.4 and 4.4.5.

9.2.1 Immunofluorescence staining of WT and DKO injured muscle sections

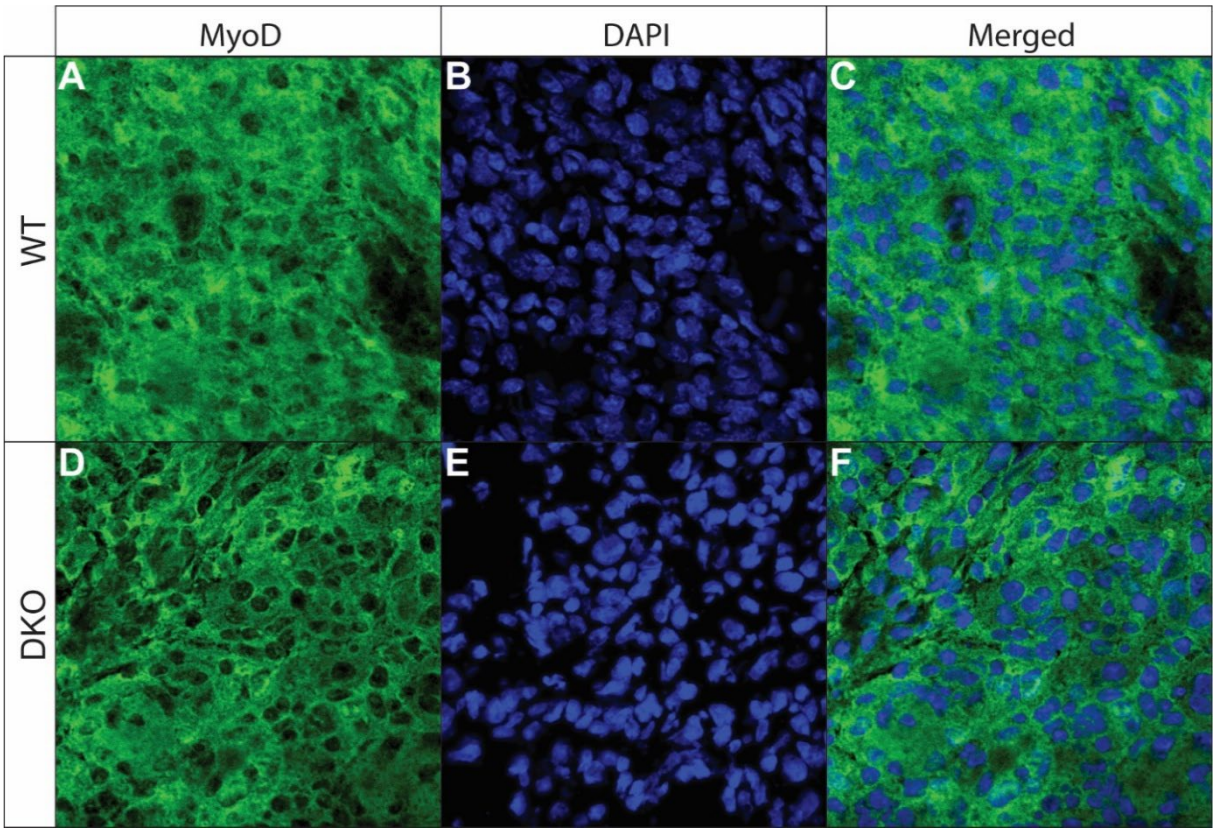

Figure 9.1. Immunofluorescence staining of MyoD positive nuclei from injured WT (**A-C**) and DKO (**D-F**) murine TA muscle sections following three days of regeneration. Sections were stained for **A+D**. MyoD (green), **B+E**. DAPI (blue) and **C+F.** Merged.

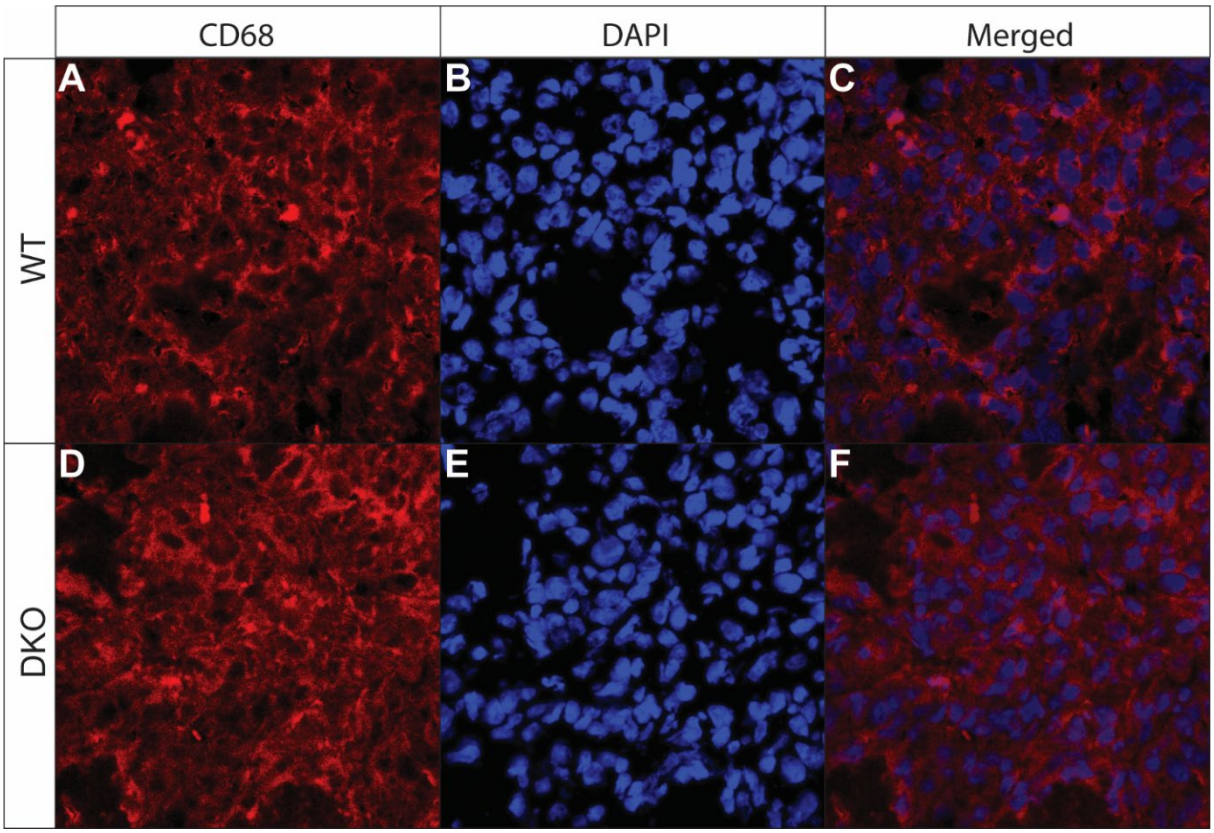

Figure 9.2. Immunofluorescence staining of CD68 positive cells from injured WT (**A-C**) and DKO (**D-F**) murine TA muscle sections following three days of regeneration. Sections were stained for **A+D**. CD68 (red), **B+E**. DAPI (blue) and **C+F.** Merged.

9.2.2 Immunofluorescence staining of WT and T-cad KO injured muscle sections

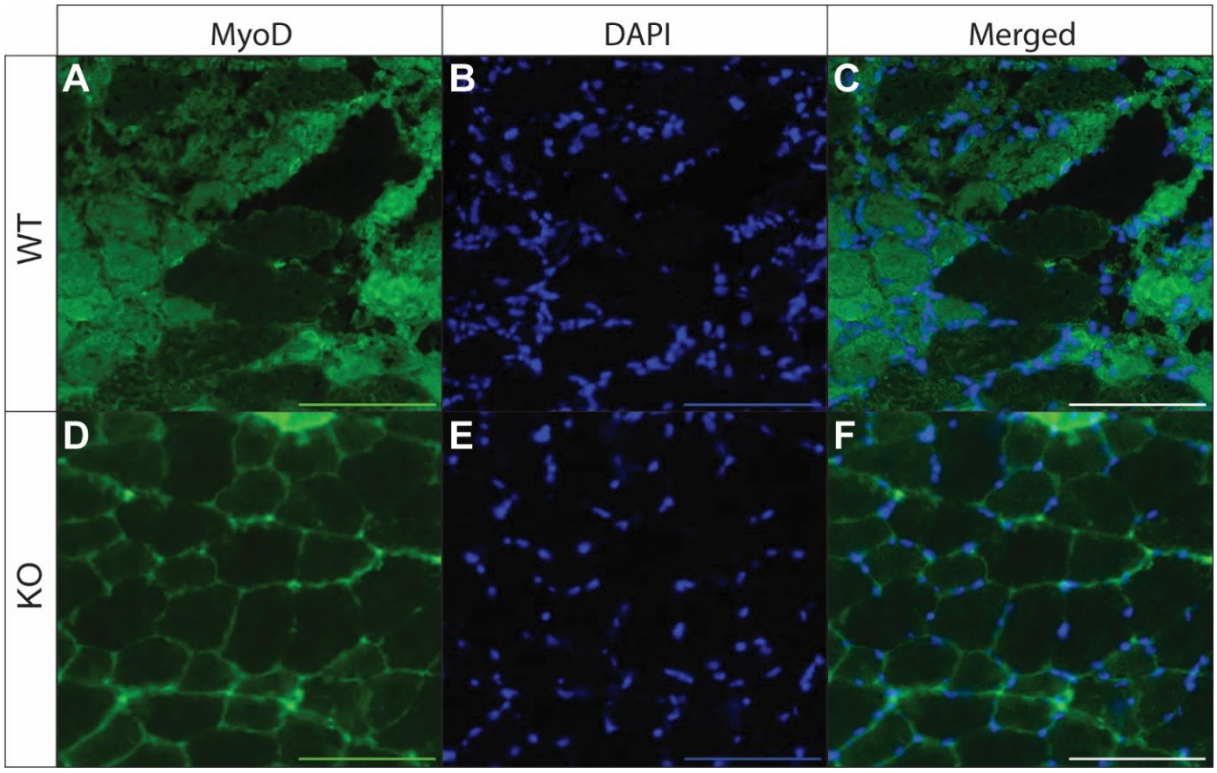

Figure 9.3. Immunofluorescence staining of MyoD positive nuclei from injured WT (**A-C**) and T-cad KO (KO) (**D-F**) murine TA muscle sections following three days of regeneration. Sections were stained for **A+D**. MyoD (green), **B+E**. DAPI (blue) and **C+F.** Merged.

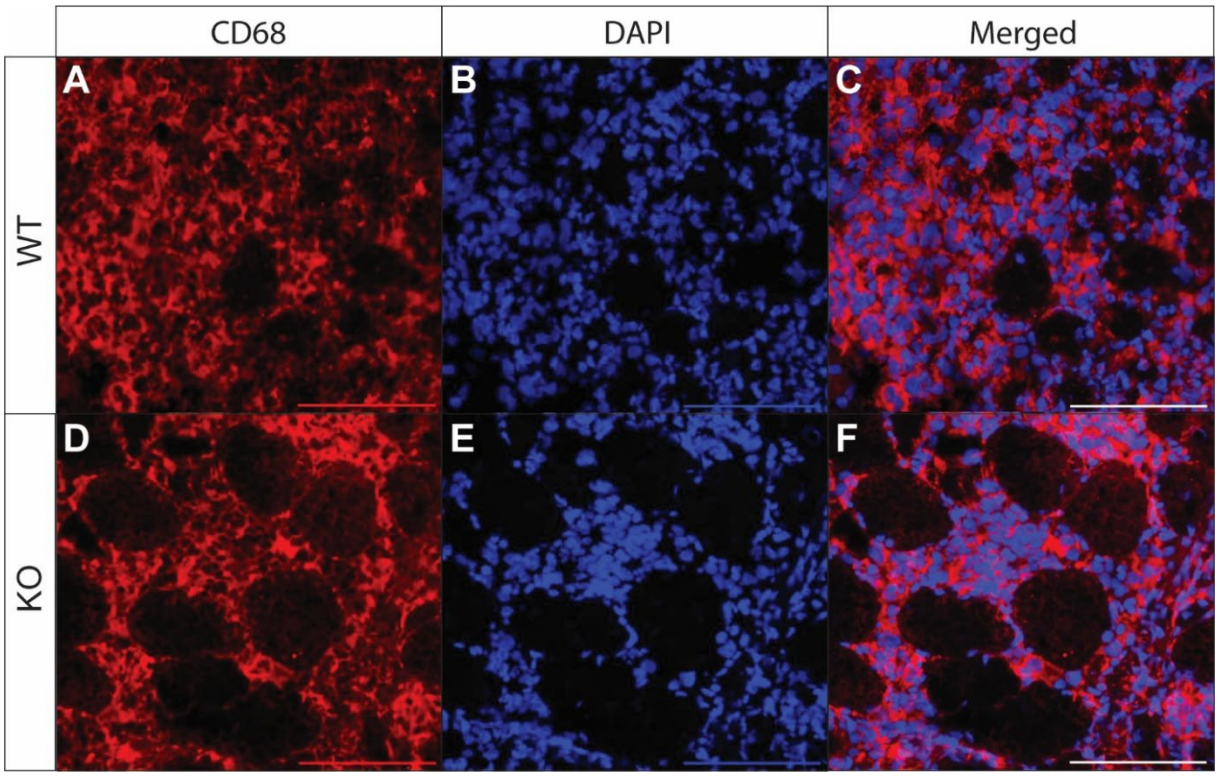

Figure 9.4. Immunofluorescence staining of CD68 positive cells from injured WT (**A-C**) and T-cad KO (KO) (**D-F**) murine TA muscle sections following three days of regeneration. Sections were stained for **A+D**. CD68 (red), **B+E**. DAPI (blue) and **C+F.** Merged.